UNIVERSIDAD NACIONAL AUTÓNOMA DE MÉXICO

POSGRADO EN CIENCIAS BIOLÓGICAS

FACULTAD DE MEDICINA

ANÁLISIS DE LA FIRMA GENÓMICA DE LNCRNAS DE CÉLULAS TRONCALES DE TEJIDO ADIPOSO CO-CULTIVADAS CON CÉLULAS DE CÁNCER

TESIS

QUE PARA OPTAR POR EL GRADO DE:

DOCTORA EN CIENCIAS

PRESENTA:

M. EN C. DE LA FUENTE HERNÁNDEZ MARCELA ANGÉLICA

TUTORA PRINCIPAL DE TESIS: DRA. VILMA ARACELI MALDONADO LAGUNAS
FACULTAD DE MEDICINA, UNAM
COMITÉ TUTOR: DR. FRANCISCO JESÚS ARENAS HUERTERO
FACULTAD DE MEDICINA, UNAM
COMITÉ TUTOR: DR. JULIO CÉSAR CARRERO SÁNCHEZ
INSTITUTO DE INVESTIGACIONES BIOMÉDICAS, UNAM

CIUDAD UNIVERSITARIA, CD. MX. SEPTIEMBRE, 2023

UNIVERSIDAD NACIONAL AUTÓNOMA DE MÉXICO

POSGRADO EN CIENCIAS BIOLÓGICAS

FACULTAD DE MEDICINA

ANÁLISIS DE LA FIRMA GENÓMICA DE LNCRNAS DE CÉLULAS TRONCALES DE TEJIDO ADIPOSO CO-CULTIVADAS CON CÉLULAS DE CÁNCER

TESIS

QUE PARA OPTAR POR EL GRADO DE:

DOCTORA EN CIENCIAS

PRESENTA:

M. EN C. DE LA FUENTE HERNÁNDEZ MARCELA ANGÉLICA

TUTORA PRINCIPAL DE TESIS: DRA. VILMA ARACELI MALDONADO LAGUNAS
FACULTAD DE MEDICINA, UNAM
COMITÉ TUTOR: DR. FRANCISCO JESÚS ARENAS HUERTERO
FACULTAD DE MEDICINA, UNAM
COMITÉ TUTOR: DR. JULIO CÉSAR CARRERO SÁNCHEZ
INSTITUTO DE INVESTIGACIONES BIOMÉDICAS, UNAM

CIUDAD UNIVERSITARIA, CD. MX. SEPTIEMBRE, 2023

COORDINACIÓN GENERAL DE ESTUDIOS DE POSGRADO
COORDINACIÓN DEL POSGRADO EN CIENCIAS BIOLÓGICAS
ENTIDAD (FACULTAD DE MEDICINA)
OFICIO: CGEP/CPCB/FMED/0550/2023
ASUNTO: Oficio de Jurado

M. en C. Ivonne Ramírez Wence
Directora General de Administración Escolar, UNAM
P r e s e n t e

Me permito informar a usted que en la reunión ordinaria del Comité Académico del Posgrado en Ciencias Biológicas, celebrada el día **22 de mayo de 2023** se aprobó el siguiente jurado para el examen de grado de **DOCTORA EN CIENCIAS** de la estudiante **DE LA FUENTE HERNÁNDEZ MARCELA ANGÉLICA** con número de cuenta **302032479** con la tesis titulada **"ANÁLISIS DE LA FIRMA GENÓMICA DE LNCRNAS DE CÉLULAS TRONCALES DE TEJIDO ADIPOSO CO-CULTIVADAS CON CÉLULAS DE CÁNCER",** realizada bajo la dirección de la **DRA. VILMA ARACELI MALDONADO LAGUNAS,** quedando integrado de la siguiente manera:

Presidente:	DR. ALEJANDRO ZENTELLA DEHESA
Vocal:	DRA. ALIESHA ARACELI GONZÁLEZ ARENAS
Vocal:	DRA. GISELA CEBALLOS CANCINO
Vocal:	DR. GONZALO CASTILLO ROJAS
Secretario:	DR. FRANCISCO JESÚS ARENAS HUERTERO

Sin otro particular, me es grato enviarle un cordial saludo.

A T E N T A M E N T E
"POR MI RAZA HABLARÁ EL ESPÍRITU"
Ciudad Universitaria, Cd. Mx., a 25 de julio de 2023

COORDINADOR DEL PROGRAMA

DR. ADOLFO GERARDO NAVARRO SIGÜENZA

POSGRADO EN CIENCIAS BIOLOGICAS
COORDINACIÓN

c. c. p. Expediente del alumno

AGNS/RCHT/EARR/rcht

Agradecimientos Institucionales

Al **Posgrado en Ciencias Biológicas, UNAM** sus docentes, especialistas, administrativos, personal en general, unidades, y recursos materiales que en su conjunto hacen posible la formación de estudiantes de Doctorado de calidad y con compromiso y responsabilidad social.

Al **Consejo Nacional de Ciencia y Tecnología**, **CONACyT** por el apoyo económico recibido a través de la beca **270150** que me permitió realizar mis estudios de posgrado.

A mi Tutora Principal la **Dra. Vilma Araceli Maldonado Lagunas**, por la oportunidad de formar parte de su grupo de investigación, por su acompañamiento y dirección durante el desarrollo de mi proyecto, así como compartir sus conocimientos y fomentar mi aprendizaje y crecimiento. Gracias por la confianza, paciencia y calidez humana.

A los miembros del Comité Tutor, el **Dr. Francisco Jesús Arenas Huertero** y el **Dr. Julio César Carrero Sánchez,** por el acompañamiento durante todo este tiempo, por su disponibilidad y su retroalimentación al proyecto y así como su entusiasmo y compromiso en mi formación.

Agradecimientos a título personal

Al **Instituto Nacional de Medicina Genómica** que, con sus unidades de alta tecnología, congresos, seminarios, simposios, talleres, actividades de esparcimiento, servicios académicos, grupos de investigación, personal administrativo y en general, fueron facilitadores en la realización de mi proyecto y participes de mi aprendizaje.

A los miembros de **Laboratorio de Epigenética** del INMEGEN, compañeros y colegas. Gracias por su disponibilidad en el compartir de conocimientos, tiempo, espacio y momentos.

A los miembros del jurado el **Dr. Arenas Huertero**, la **Dra. González Arenas**, la **Dra. Ceballos Cancino**, el **Dr. Castillo Rojas** y el **Dr. Zentella Dehesa** por su tiempo en la revisión y retroalimentación del escrito del presente trabajo.

Agradecimientos y dedicatorias a título personal

A Dios, por dar camino y abrir paso a mis sueños, por poner todos los elementos necesarios para hacerlo y estar en todos los tropiezos sosteniéndome. No solo agradezco sino también te lo dedico, todo es gracias a ti.

A mis padres, especialmente a mi mamá Carmen, ejemplo de constancia y entrega. Gracias por estar presente en todo momento, por la compañía, complicidad y apoyo infinito. Este trabajo también es tuyo.

A mis hermanos Mayra, Verónica y José por motivarme y ser mi ejemplo. Gracias por celebrar nuestras alegrías, estar presentes en las dificultades y por mis sobrinos que son mi inspiración constante.

A mi abuelita Carlotita, testigo fiel de mi aprendizaje y partícipe de mis sueños. Dios sabe mucho de mí gracias a tus oraciones. Te quiero muchísimo y te llevo en mi corazón.

A Mike, por ser colega, equipo, amigo, pareja y cumplir los múltiples roles en todo momento. Muchas gracias por compartir tus conocimientos, enseñanzas, colaboraciones, por escucharme, apoyarme, animarme y motivarme siempre a seguir esforzándome. Te amo y confió podamos seguir aprendiendo y creciendo juntos.

Y a un gran número de personas, difícil de mencionar a cada una, pero que de un modo particular han dado cause e impulso a mi vida durante el desarrollo de este proyecto y elaboración de esta tesis. A amigos, compañeros, colegas, hermanos y familia, gracias por ser parte, por estar y dar en el momento. Deseo actuar con reciprocidad a todo el bien recibido de ustedes.

Dedicado a los pacientes con cáncer que colaboran con la ciencia
confiando en que la investigación de su padecimiento genere conocimiento
para ayudar a otras personas.

"Poca ciencia aleja de Dios, mucha ciencia te acerca a Él"

Louis Pateur

“El conocimiento si no se comparte, no trasciende”

de un Ignoto

ÍNDICE

ÍNDICE DE FIGURAS

ÍNDICE DE TABLAS

RESUMEN

La obesidad es un factor que se asocia al desarrollo y peor pronóstico de al menos 13 tipos de cáncer. La relación entre la obesidad y el cáncer se establece en parte, por una comunicación intercelular entre las células tumorales y las células que conforman el tejido adiposo, entre las que se encuentran las células troncales derivadas de tejido adiposo (ADSC). Son diversos los reportes que han determinado cambios a nivel molecular en las células tumorales a consecuencia de esta comunicación intercelular, sin embargo, poco se sabe sobre los cambios en las ADSC. El cáncer cervical tiene una elevada tasa de incidencia y mortalidad de mujeres en países en vías de desarrollo, particularmente en aquellas que poseen un elevado índice de masa corporal. Es por ello que, en el presente trabajo, evaluamos el transcriptoma de ADSC, de pacientes con obesidad mórbida, en presencia de células HeLa, una línea celular proveniente de cáncer cervical.

Se realizaron ensayos de co-cultivo de ADSC con células HeLa en un formato "transwell". A las 24 horas se evaluaron los cambios en el transcriptoma de ADSC por secuenciación masiva RNAseq. El perfil de 761 RNAs fue diferencialmente expresado en ADSC y análisis de enriquecimiento de vías e inferencia de procesos biológicos reveló posibles cambios relevantes en ADSC posterior al co-cultivo, como son la migración, el ciclo celular y la muerte por apoptosis.

Por una parte, las ADSCs incrementaron su capacidad de migración y la población $ALDH^{high}$ en co-cultivo, un marcador característico de células troncales. Por otro lado, el inmunofenotipo troncal, la población en apoptosis y la proporción en etapas del ciclo celular no mostraron cambios significativos. El transcriptoma no codificante también presentó cambios en la expresión de miRNAs, pseudogenes y lncRNAs. El lnc-CXCL3, un lncRNA intragénico, demostró la capacidad de regular la expresión de genes cercanos, tales como CXCL2 y CXCL3. De manera interesante, se encontró que este lncRNA es importante para la migración de células tumorales y la formación de esferas en células semejantes a ADSC.

En conclusión, la comunicación de las ADSC con células de cáncer cervical lleva a cambios en el perfil de expresión de moléculas codificantes y no codificantes, las cuales regulan, de manera directa e indirecta, las características de ADSC, aproximándonos a comprender su papel en el proceso tumoral.

ABSTRACT

Obesity is a major factor in the development and worse prognosis of at least 13 types of cancer. The link between obesity and cancer is partly established by intercellular communication between tumour cells and the cells that make up adipose tissue, including adipose-derived stem cells (ADSC). The reports have showed that ADSC play a key role in the effect of obesity on cancer. Several studies have identified changes at the molecular level in tumour cells due to this intercellular communication, however, little is known about the changes in ADSC. Cervical cancer has a high incidence and mortality rate in women in developing countries, particularly in those with a high body mass index. For this reason, in the present work, we evaluated the transcriptome of ADSC, derived from morbidly obese patients, in the presence of HeLa, a cell line derived from cervical cancer.

Co-culture assays of ADSC with HeLa cells were performed in a transwell format. At 24 hours, changes in the ADSC transcriptome were assessed by massive RNAseq sequencing. The profile of 761 RNAs was differentially expressed in ADSC, and pathway enrichment analysis and inference of biological processes revealed possible relevant changes in ADSC following co-culture, such as migration, cell cycle and death by apoptosis.

On the one hand, ADSC increased their migration capacity and $ALDH^{high}$ population in co-culture, while the stem immunophenotype, apoptosis population and cell cycle stage ratio did not show significant changes. On the other hand, the non-coding transcriptome showed changes in the expression of miRNAs, pseudogenes and lncRNAs. The lnc-CXCL3, an intragenic lncRNA, showed the ability to regulate the expression of nearby genes, such as CXCL2 and CXCL3. Interestingly, this lncRNA was found to be important for tumour cell migration and sphere formation in ADSC-like cells.

In conclusion, the communication of ADSC with cervical cancer cells leads to changes in the expression profile of coding and non-coding molecules, which directly and indirectly, regulate ADSC characteristics, bringing us closer to understanding their role in the tumour process.

1. INTRODUCCIÓN

1.1 Obesidad

La obesidad se define como una acumulación anormal o excesiva de tejido adiposo en el cuerpo[1]. Existen diversas aproximaciones para determinar la acumulación de tejido adiposos en el cuerpo a partir de las mediciones antropométricas a través de la determinación de la circunferencia de la cintura, la relación cintura cadera o el grosor de los pliegues cutáneos[2]. También se emplean técnicas para la valoración de la composición corporal como densitometría hidrostática e impedancia bioeléctrica, limitando su uso a los centros que cuentan con la infraestructura y equipos[3].

El indicador más comúnmente utilizado para determinar la obesidad es el Índice de Masa Corporal (IMC), que relaciona la masa de la persona expresada en kilogramos entre el cuadrado de su talla en metros. Un IMC igual o superior a 30 kg/m^2 es un indicativo de obesidad[4].

Tabla 1 . Clasificación según el indicador de IMC
(Lambert Adolphe Quetelet, 1832)

CLASIFICACIÓN	IMC
Bajo de peso	<18.5
Normal	18.5-24.9
Sobrepeso	25-29.9
Obesidad	30-39.9
Obesidad mórbida	40

Las estimaciones realizadas por la Organización Mundial de la Salud (OMS) determinaron que, en las últimas 4 décadas los casos de obesidad casi se han triplicado en todo el mundo. Además, para el año 2016 cerca de 1900 millones de adultos mayores de 18 años presentaban un IMC superior al normal, de los cuales, más de 650 millones eran obesos[4].

De acuerdo con la Encuesta Nacional de Salud y Nutrición (ENSANUT) del 2018, en México, 39.1% de adultos mayores de 20 años presentaron sobrepeso y 36.1% obesidad, con lo que sumando estadas dos poblaciones es cerca del 75.2% de la población adulta[5]. En la Figura 1, se muestra el porcentaje de la población mexicana adulta que presentó esta condición de salud para el año 2018, según su distribución por sexos.

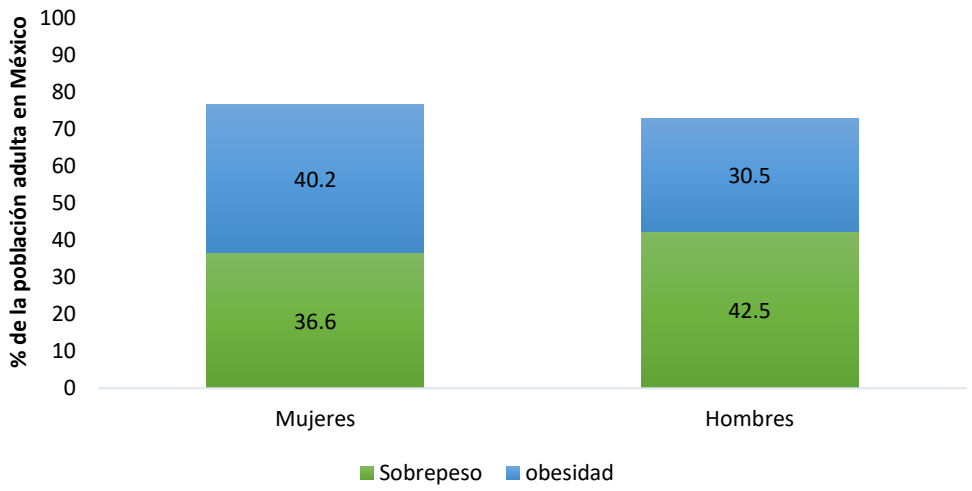

Figura 1. Porcentaje de población mayor de 20 años con sobrepeso y obesidad en México. De la población mexicana adulta (mayor a 20 años) se indica para cada sexo en verde el porcentaje % de la población que presentó sobrepeso y en azul el porcentaje % de la población con obesidad. Tomada y modificada de *ENSANUT 2018*[5]

La obesidad es un factor de riesgo importante para el desarrollo de múltiples patologías. Algunas de las comorbilidades más estudiadas de la obesidad son las metabólicas y las cardiovasculares. Sin embargo, un gran número de otras patologías se asocian a personas con sobrepeso y obesidad, dentro de las que están enfermedades del aparato digestivo, neurodegenerativas, alteraciones locomotoras y diversos tipos de neoplasias[6].

1.2 Obesidad y Cáncer

Estudios clínicos de cohorte, relacionan a la obesidad con un mayor riesgo de padecer algunos tipos de cáncer y a un peor pronóstico asociado a esta enfermedad[7]. La Agencia Internacional para la Investigación en Cáncer (IARC) en 2012 declaró que un elevado IMC es responsable del 3.6% de los nuevos casos de cáncer y un factor de riesgo en cerca del 28% en tumores localizados principalmente en la cavidad abdominal. Son el cáncer de mama con un 23.6%, y el de cuello uterino con 22.3%, los dos más representados, lo que demuestra su enorme repercusión en la población de sexo femenino (Figura 2)[8].

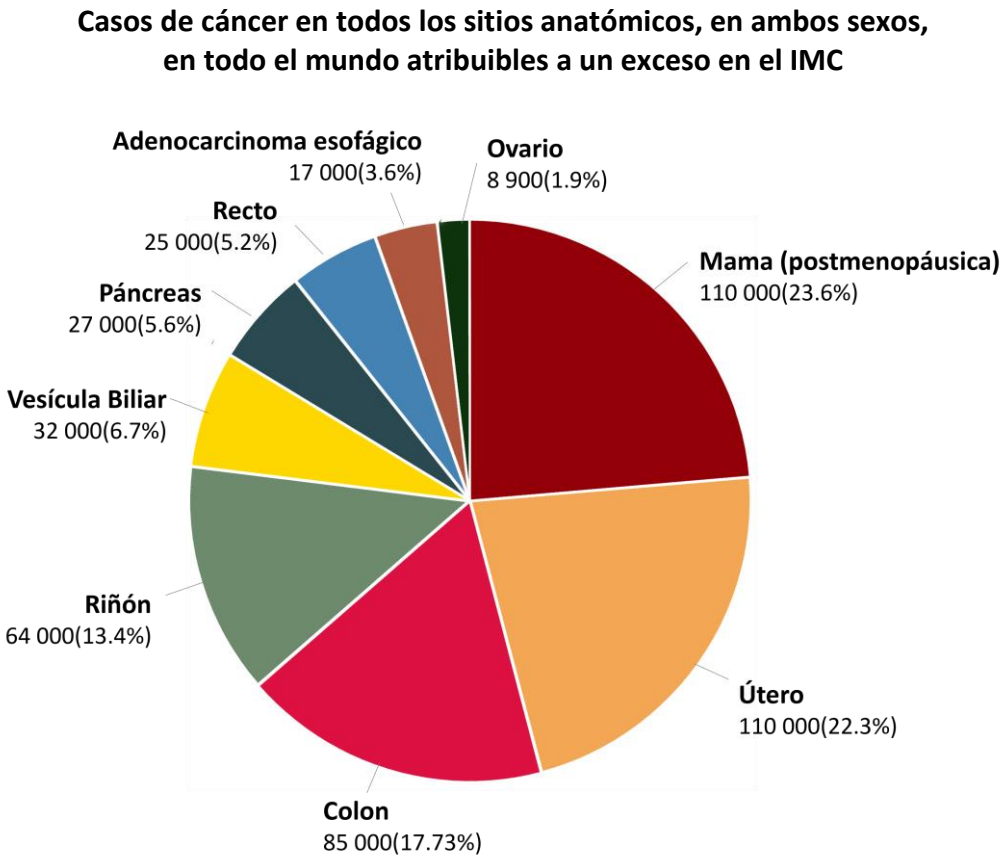

Figura 2. Porcentaje de casos de cáncer atribuibles al exceso de IMC por sitio anatómico, en ambos sexos, en el mundo. Se muestra por sitio anatómico como porcentaje del número total de todos los casos atribuibles en todos los sitios anatómicos. Tomada y modificada de *Global Cancer Observatory* [8].

En el año 2016 se identificaron 13 tipos distintos de cáncer con evidencia suficiente de estar relacionados con obesidad (Figura 3), ya sea favoreciendo su promoción, progresión o peor pronóstico, por lo que se les denomina Cánceres Asociados a Obesidad (CAO)[9].

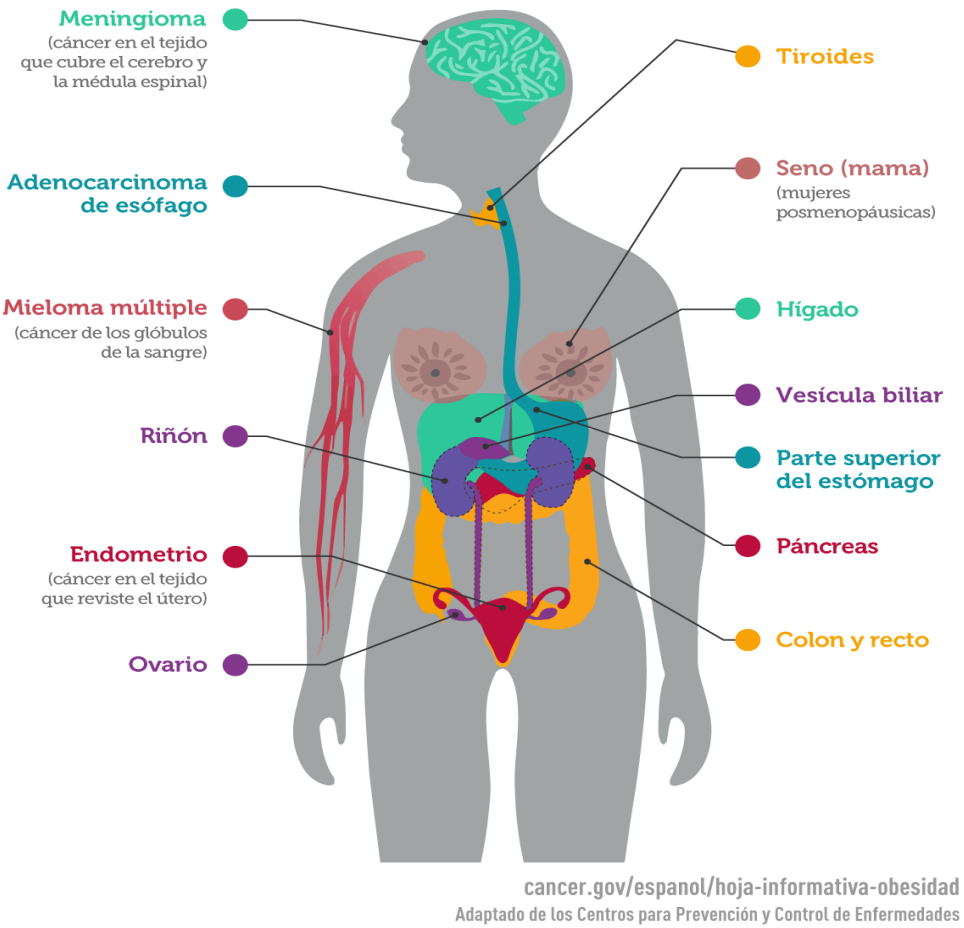

Figura 3. Cánceres asociados a sobrepeso y obesidad. Tomada y modificada de *Instituto Nacional del Cáncer.*[10]

Los mecanismos moleculares por los cuales la obesidad afecta la incidencia, la progresión, o la mortalidad en los diferentes tipos de cáncer se desconocen. No obstante, la producción de adipocinas, el microambiente proinflamatorio, la resistencia a insulina, los fenómenos de hipoxia y la infiltración de células del sistema inmune, entre otros, se sugieren que participan en esta asociación[11–14].

La obesidad conduce al desarrollo de tejido adiposo disfuncional, que produce abundantes niveles de citocinas proinflamatorias, hormonas sexuales y metabolitos lipídicos, junto con perfiles alterados de adipocinas. El tejido adiposo alterado se constituye de células troncales, adipocitos asociados al cáncer y progenitores de adipocitos. Cada uno de estos factores contribuye en el inicio y las distintas etapas de la progresión tumoral, como son el crecimiento y la recurrencia (Figura 4).

Las personas con obesidad, en comparación con los individuos de IMC normal, tienen una mayor probabilidad de presentar inflamación local crónica a causa de la presencia excesiva de tejido adiposos con una activación sostenida de vías que conllevan a la inducción de citoquinas inflamatorias[15,16]. Tiempos prolongados de exposición a mediadores inflamatorios, pueden favorecer la inestabilidad genómica de las células mediante diversos mecanismos, ya sea induciendo directamente daños en el DNA o afectando a los sistemas de reparación y alterando los puntos de control del ciclo celular, por tanto, puede conducir al desarrollo de cáncer[17] (Figura 4).

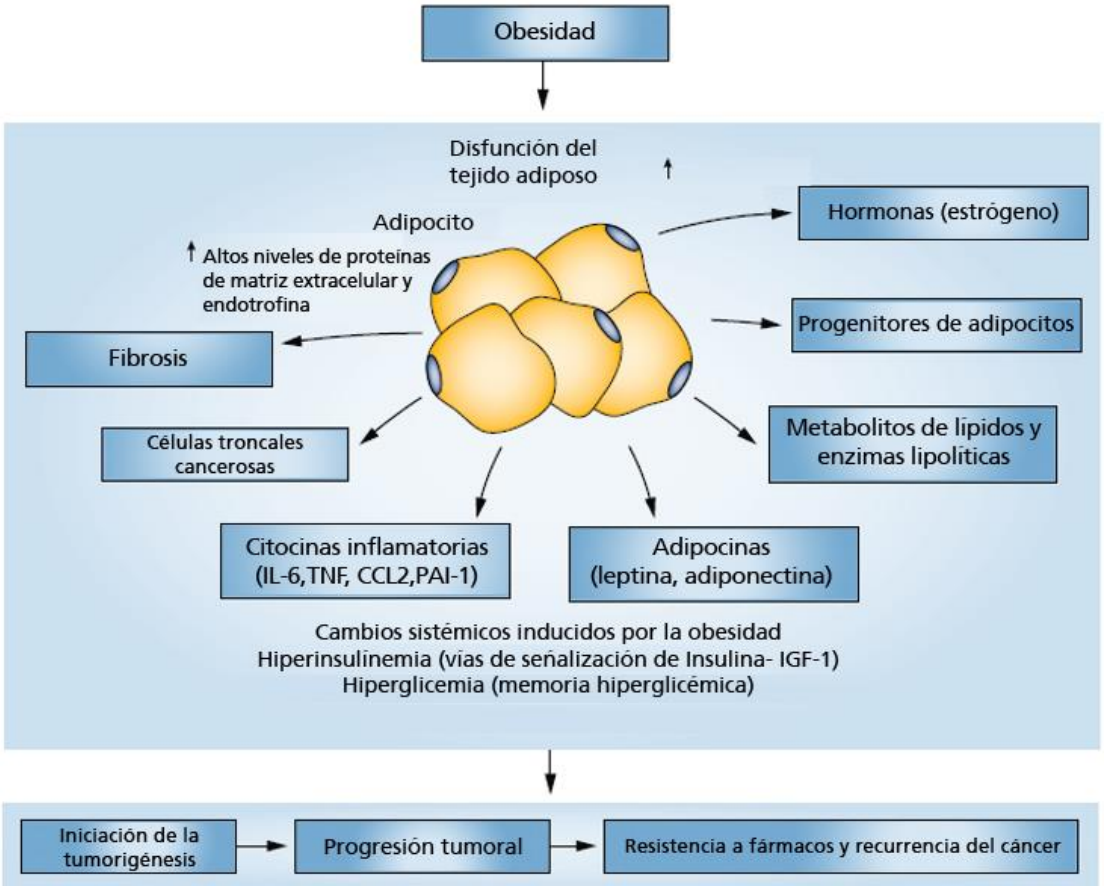

Figura 4. Posibles consecuencias de la disfunción del tejido adiposo inducida por la obesidad en el inicio, la progresión y la recurrencia de tumores. La obesidad conduce al desarrollo de tejido adiposo disfuncional, que produce niveles abundantes de citocinas proinflamatorias, hormonas sexuales, metabolitos lipídicos y perfiles alterados de adipocinas. El tejido adiposo alterado es fuente de diversas proteínas de matriz extracelular, adipocitos asociados al cáncer y progenitores. Cada uno de estos factores contribuye a diversas fases de la progresión tumoral, como el inicio, el crecimiento y la recurrencia. Los cambios metabólicos sistémicos asociados a la obesidad, como la hiperinsulinemia y la hiperglucemia, también contribuyen a crear un entorno favorable para los tumores. Tomada y modificada de *Park, J. et al* [14].

Los cambios metabólicos sistémicos asociados a la obesidad, como la hiperinsulinemia y la hiperglucemia, también participan en crear un entorno favorable tumoral[14]. Por un lado, la hiperinsulinemia favorece la activación de la vía IGF-1-insulina, que estimula la señalización a través de las proteínas cinasas activadas por mitógenos (MAPK) o la cascada PI3K-AKT[18] y por otro lado la hiperglucemia induce modificaciones epigenéticas en componentes de algunas vías oncogénicas, como las cascadas de señalización EGFR, HER2, HER3 y sus correspondientes ligandos, estimulando así el crecimiento tumoral[19].

Las personas con obesidad suelen tener mayores concentraciones de insulina en la sangre y del factor-1 de crecimiento semejante a la insulina (IGF-1). Las altas concentraciones de insulina y de IGF-1 pueden promover el desarrollo de cáncer de colon, riñón, próstata y endometrio[20]. Además, el tejido adiposo produce cantidades excesivas de estrógeno. Concentraciones altas de esta hormona se han asociado con riesgos mayores de desarrollar cáncer de mama, ovario y endometrio. La proliferación celular se incrementa en respuesta a la leptina, una hormona producida por el adipocito, mientras que se disminuye por la adiponectina, hormona que se encuentra en bajas concentraciones en personas con obesidad (Figura 5)[21].

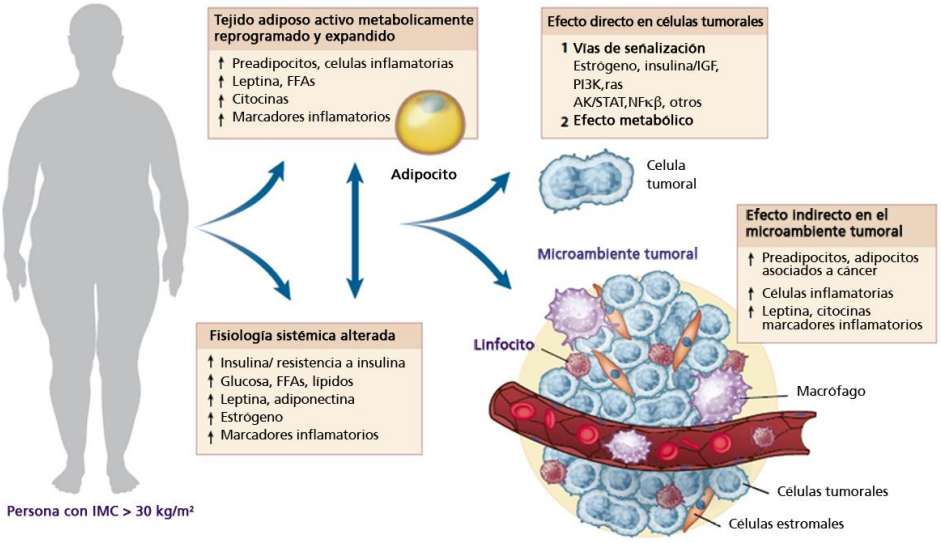

Figura 5. La compleja asociación entre obesidad y cáncer. La obesidad se asocia a un tejido adiposo expandido y reprogramado que es metabólicamente activo, lo que conduce a una inflamación localizada y a una secreción alterada de citocinas/adipocinas. El tejido adiposo puede afectar directamente al cáncer mediante la activación de vías de señalización clave o una alteración del metabolismo celular. También pueden actuar indirectamente en el microambiente tumoral para promover la proliferación, la angiogénesis, la invasión y la transición epitelio-mesénquima. Tomada y modificada de *Goodwin, PJ. Et al*[21].

Además, la obesidad puede influir en el diagnóstico, la administración y la toxicidad del tratamiento en pacientes con cáncer. Los individuos obesos pueden retrasar la búsqueda de atención médica y ser menos propensos que los no obesos a participar en programas de cribado[22]. La precisión en el diagnóstico también está limitada en los pacientes obesos, a causa de la hemodilución de los biomarcadores tumorales y en la adquisición y calidad de imágenes de exploración[23]. Un elevado IMC en la tomografía computarizada (TC) propicia una penetración de fotones inadecuada y un campo de visión limitado generando un menor contraste de la imagen. Por otro lado, la resonancia magnética (RM) se dificulta en pacientes con obesidad, creando una relación señal/ruido menor en la observación de órganos internos y disminuyendo la resolución de la imagen[23]. En cuanto al tratamiento, se pueden presentar dificultades técnicas en la administración de radioterapia y el manejo quirúrgico[24]. Finalmente, se reportó una mayor tasa de complicaciones posquirúrgicas e infecciones en heridas en pacientes con un IMC elevado, sometidos a cirugía mayor de cáncer abdominal[25].

1.3 Obesidad y cáncer cervical

El cáncer cervical, también llamado cáncer cervicouterino, es el cuarto más común en mujeres de todo el mundo, ya que en 2020 presentó una incidencia de 604 127 casos y 341 831 defunciones por año (Figura 6), siendo considerado un problema de salud en países en vías de desarrollo[26].

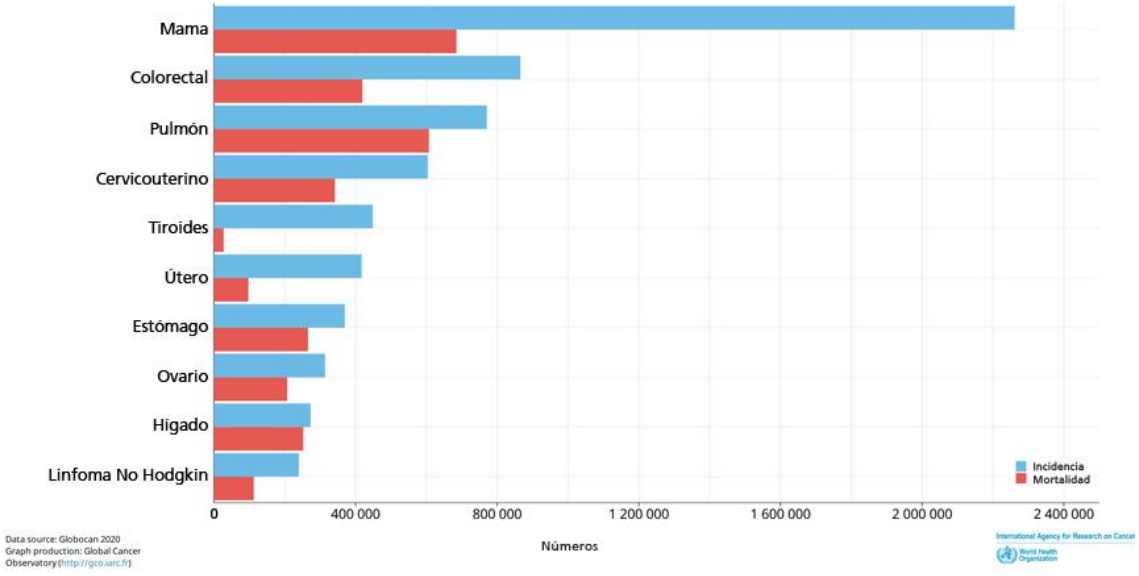

Figura 6. **Incidencia y mortalidad de cáncer en población femenina de todo el mundo.** Número de casos estimados en 2020 en mujeres de todas las edades. Tomado y modificado de *Global Cancer Observatory* [27].

En el 2020, en México el cáncer cervical fue el segundo más frecuente en mujeres con una incidencia del 12.6% y una mortalidad del 5.7% (Figura 7)[28].

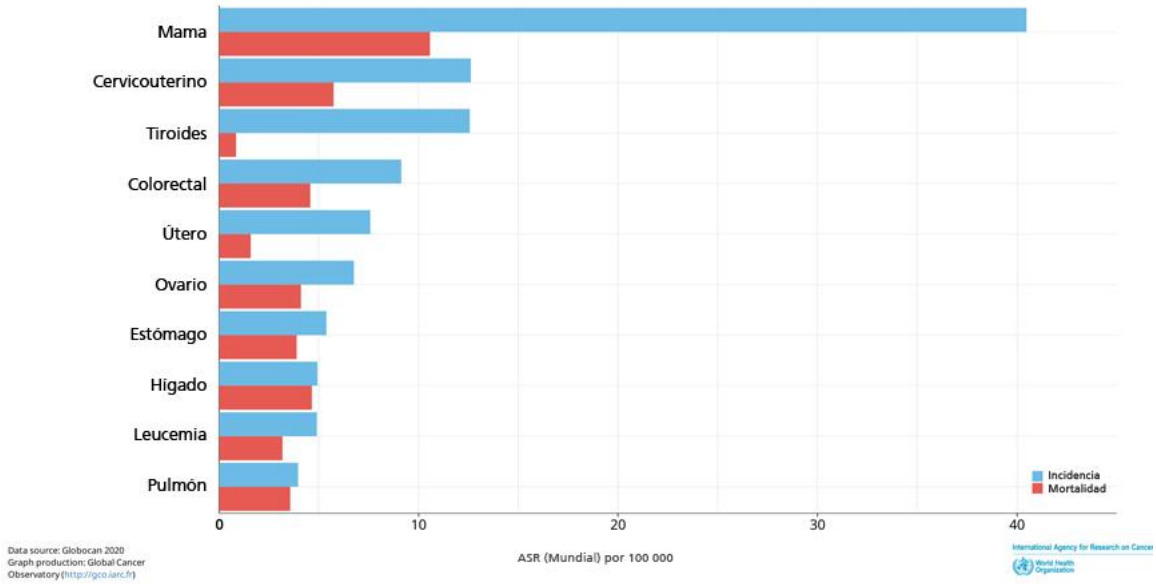

Figura 7. Incidencia y mortalidad de cáncer en población femenina de México. Tasas estimadas y estandarizadas por edad en 2020. Tomado y modificado de *Global Cancer Observatory* [28].

El agente etiológico asociado al desarrollo de cáncer cervical es el Virus del Papiloma Humano (VPH), detectado en casi el 99% de los pacientes con esta neoplasia. Sin embargo, no todos los pacientes infectados con este virus llegan a desarrollar la enfermedad, haciendo evidente la acumulación de otros factores y condiciones que favorecen la carcinogénesis cervical[29].

La obesidad es un factor que puede favorecer el desarrollo del cáncer cervical. Un estudio en Reino Unido reveló que el aumento de cada 5 kg/m² de IMC se asocia con una proporción de riesgo (HR) del 1.10 con cáncer de cérvix y del 1.62 con cáncer uterino[30]. Si bien, poco se conoce acerca de la relación de la obesidad y el cáncer cervical, estudios epidemiológicos en mujeres adultas norteamericanas señalan que un IMC ≥ 35 puede incrementar hasta en un 3.2 veces el riesgo relativo de muerte por este cáncer (Figura 8)[31].

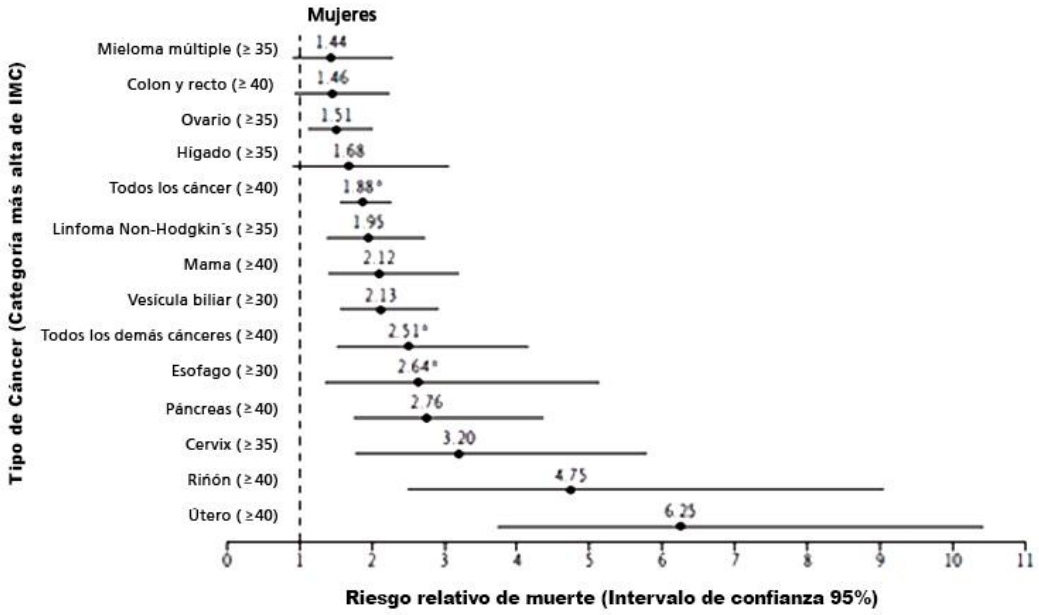

Figura 8. Mortalidad por cáncer en mujeres según su índice de masa corporal. Para cada riesgo relativo, la comparación se realizó entre el grupo de mujeres de IMC más alto y el grupo de mujeres de IMC 18.5 a 24.9. Los asteriscos indican riesgos relativos para mujeres que nunca fumaron. Tomada y modificada de *Calle EE., 2003*[31].

1.4 Tejido Adiposo

El tejido adiposo representa entre el 20% - 28% de la masa corporal de los individuos sanos, porcentaje que varía según el sexo y el estado energético, por lo que en individuos con obesidad, el tejido adiposo puede representar hasta el 80% de la masa corporal [32].

El tejido adiposo se clasifica en tejido adiposo marrón (TAM) y tejido adiposo blanco (TAB). El TAM, solo está presente en mamíferos y su función se relaciona con la capacidad de termorregulación[33] como resultado de la oxidación de lípidos para producir calor[34]. En los humanos, este tejido lo encontramos localizado en el feto y en el recién nacido a nivel axilar, cervical, perirrenal y periadrenal, pero su presencia disminuye rápidamente tras el nacimiento[35]. Por otra parte, el TAB es el principal tejido de almacenamiento de energía en forma de lípidos, además de la función de aislamiento y protección mecánica para algunos órganos vitales. En humanos, el TAB se distribuye en todo el cuerpo. A nivel intraabdominal, los mayores depósitos están alrededor del omento (omental), del intestino (mesentérico) y de las áreas perirrenales (retroperitoneal), y a nivel subcutáneo, el TAB se localiza sobre todo a nivel de los glúteos, los muslos y el abdomen[34].

El tejido adiposo es un órgano endócrino capaz de secretar sustancias de naturaleza lipídica y factores proteicos, de los cuales varios se relacionan con el sistema inmunitario, tales como: TNF-α, IL-1β, IL-6, IL-8, IL-10, IL-4, IL-13 y MCP-1, lo que establece una conexión entre la inflamación y la obesidad[36]. Otras moléculas sintetizadas por el tejido adiposo tienen funciones reguladoras importantes como: la leptina, en la sensación del apetito; el angiotensinógeno, para la regulación de la presión sanguínea; así como la adiponectina, resistina y visfatina que participan en la regulación del metabolismo energético y finalmente el factor de crecimiento de endotelio vascular (VEGF) y el factor de crecimiento transformante (TGFβ)[34].

El tejido adiposo se compone de dos fracciones celulares: los adipocitos, que representan aproximadamente el 80% del volumen y alrededor del 60% de la población celular total; y la fracción vascular estromal (SVF), compuesta principalmente por fibroblastos, células del sistema inmune, células vasculares y células precursoras de adipocitos (Figura 9)[37].

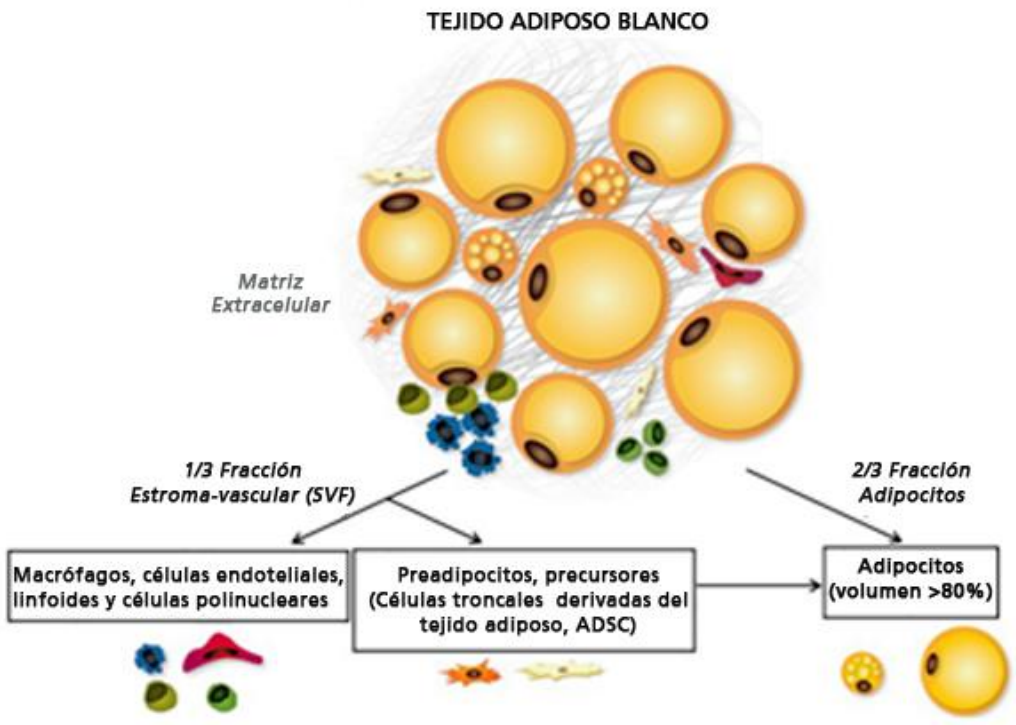

Figura 9. Composición celular del tejido adiposo blanco. Los adipocitos son el principal componente celular crucial tanto para el almacenamiento de energía como para la actividad endocrina. Otros tipos celulares presentes son precursores (como las células troncales derivadas del tejido adiposo – ADSC), fibroblastos, células vasculares y células del sistema inmune. Tomada y modificada de *Bourgeois et al.*[37].

1.5 Células Troncales Derivadas de Tejido Adiposo

El potencial de diferenciación celular es indispensable en el desarrollo de los seres vivos. Las células con capacidad de generar células diferenciadas se reconocen como células precursoras, quienes residen en múltiples tejidos. El tejido adiposo contiene una subpoblación de células troncales mesenquimales multipotentes (MSC, del inglés *Mesenchimal Stem Cells*) llamadas células troncales derivadas de tejido adiposo (ADSC, del inglés Adipose-Derivade Stem Cells) por residir en este tejido, que a través de la división asimétrica producen una célula multipotencial, con capacidad de autorrenovación, y otra célula con capacidad de diferenciación a linajes adipogénicos, osteogénicos, miogénicos y condrogénicos (Figura 10)[38,39].

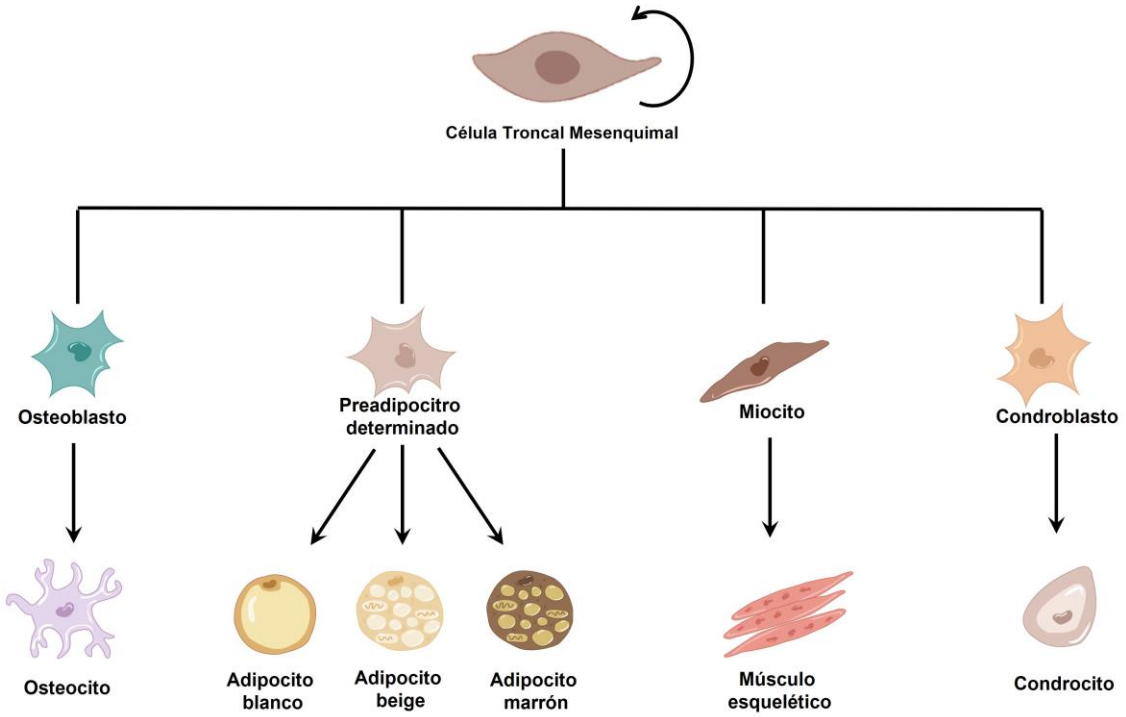

Figura 10. Células troncales derivadas de tejido adiposo y su capacidad de diferenciación. Las células troncales mesenquimales propias del tejido adiposo son conocidas como ADSC y presentan división asimétrica para su autorrenovación y capacidad de diferenciación.

Las ADSC tienen marcadores de superficie específicos que resultan útiles durante su identificación y aislamiento. El inmunofenotipo característico de las ADSC es: CD29+, CD73+, CD90+, CD105+, CD14-, CD31-, CD45-[40].

1.6 ADSC y cáncer

Los estudios *in vivo* sugieren que las células mesenquimales multipotentes tienen un papel clave en el efecto de la obesidad sobre el cáncer[41]. En específico, se describió que las ADSC son atraídas por las células tumorales a través de la señalización en respuesta a angiogenina, GM-CSF, IL-6, GRO-α y IL-8 (Figura11)[42]. Una vez instaladas en la periferia del tumor, las ADSC pueden favorecer la formación de endotelio vascular, la proliferación de células tumorales, la formación de tumores de mayor tamaño[43,44] la invasión y la metástasis[45,46].

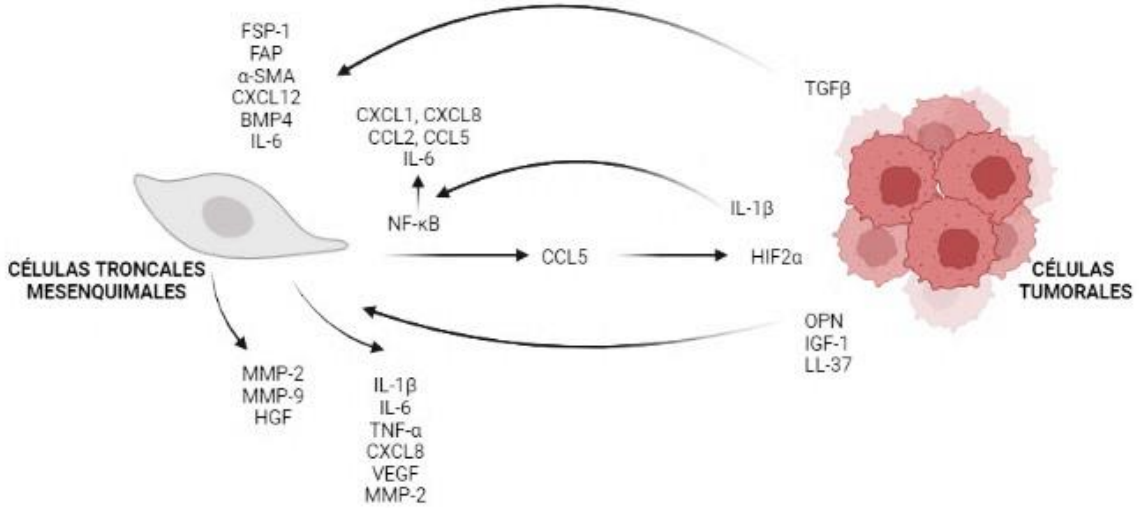

Figura 11. **Múltiples factores favorecen el crecimiento tumoral medido por las células troncales mesenquimales**. Las células tumorales pueden liberar IL-1β a través de vesículas que pueden potenciar la actividad NF-κB en las MSC y la liberación de múltiples citoquinas, en particular CXCL1, CXCL8, CCL2, CCL5 e IL-6. L Al interactuar con células tumorales, las MSCs adquieren un fenotipo de fibroblastos asociados a tumor (CAFs) que favorece la tumorigénesis con la producción de FSP-1, FAP, α-SMA, CXCL12, BMP4 e IL-6. Tomada y modificada de *Gwendal L. et al.*[41]. Creado con BioRender.com

Para comprender el mecanismo molecular mediante el cual las ADSC pueden participar en el desarrollo y mal pronóstico de algunos tipos de cáncer, es necesario reconocer que la comunicación y la señalización intercelular se regula a distintos niveles, como es el epigenético, a través de RNAs no codificantes (ncRNAs).

1.7 RNAs largos no codificantes

Actualmente, se sabe que el 75% del genoma humano se transcribe activamente, pero sólo el 2% se traduce a proteína, según la bases de datos Enciclopedia de Elementos de DNA (ENCODE)[47].

Se ha demostrado que los ncRNAs son reguladores epigenéticos, transcripcionales y postranscripcionales en un gran número de procesos celulares[48]. Dentro de los ncRNAs, los RNAs largos no codificantes (lncRNAs) junto con sus blancos moleculares representan un fascinante campo de estudio. El número estimado de lncRNAs en humanos reportados en la base de datos ENCODE es de 15 787[49], sin embargo en 2017 se informó la existencia de 27 919 lncRNAs[50].

Los lncRNAs son moléculas sintetizados por la RNA polimerasa II, con un rango de tamaño que va de 200 pb hasta 10Kb. Pueden sufrir modificaciones postranscripcionales como adición de poli A y CAP, así como presentar splicing alternativo e isoformas[51–54]. El nivel de metilación en el sitio de inicio transcripcional de los lncRNAs es generalmente mayor que el de los RNAs mensajeros, por lo tanto, son de expresividad baja y tejido específico[55].

Los lncRNAs pueden clasificarse según su localización en el genoma en relación con los genes codificantes (Figura 12). Los lncRNAs intrónicos se codifican en los intrones de los genes codificantes de proteínas, a diferencia de los lncRNAs intragénicos, que se sobrelapan con los exones de los genes. Algunos lncRNAs se localizan en el espacio genómico intergénico, entre los loci codificantes de proteínas, por lo que se les conoce como lncRNAs intergénicos, los cuales pueden derivar como producto alterno de la transcripción del gen codificante[56].

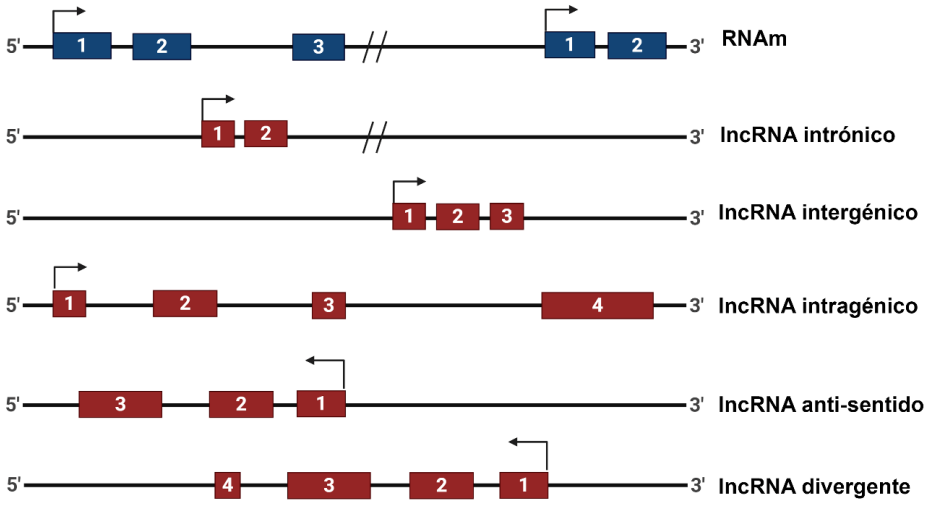

Figura 12. Clasificación de lncRNAs según su localización genómica con respecto a genes codificantes. La dirección localización y orientación de los lncRNA (recuadros rojos) en relación con los genes codificantes (recuadros azules) establece el tipo de lncRNA. Los exones están numerados y se indica la dirección de transcripción para cada caso. Tomada y modificada de *De la Fuente-Hernández MA. Et al.* [56].

Una forma adicional en la que los lncRNAs se pueden clasificar es la dirección de la transcripción. Los lncRNAs sentido son transcritos que se producen en la misma orientación que los genes codificantes de proteínas; mientras que los lncRNAs antisentido, se originan en la dirección inversa. En ocasiones, el mismo promotor puede mediar la transcripción tanto del gen codificante como del lncRNAs, a pesar de transcribirse en dirección opuesta, lo que justifica que estos lncRNAs se denominen lncRNAs divergentes (Figura 12)[57,58].

Los lncRNAs interactúan con otras moléculas de RNA, DNA e incluso proteínas, y como resultado de esta interacción múltiple, se ha demostrado que son capaces de regular la expresión génica a través de varios mecanismos (Figura 13). Uno de ellos, es actuar como guías moleculares al reclutar complejos modificadores de cromatina, favoreciendo su apertura (eucromatina) o cierre (heterocromatina). ANRIL (del inglés Antisense Noncoding RNA in the INK4 Locus) es un ejemplo de guía molecular que interactúa directamente con PRC1 y PRC2 (protein regulator of cytokines 1 and 2), dos miembros del complejo represivo de polycomb, para causar el silenciamiento de genes[59]. Los lncRNAs pueden actuar como RNAs señuelos de factores de transcripción y evitar la transcripción de sus genes blanco como sucede con PANDA (P21-associated noncoding RNA DNA damage-activated), un lncRNA que se asocia con el factor de transcripción NF-YA (Nuclear Transcription Factor Y Subunit Alpha) para prevenir la apoptosis mediada por p53[60]. A nivel post-transcripcional, los lncRNAs funcionan como esponjas de microRNAs (miRNAs), capturándolos por complementariedad de bases. Esto impide su función y favorece indirectamente la síntesis de la proteína cuyo RNA mensajero era blanco del miRNA[61,62]. Los lncRNAs también participan en el procesamiento de RNAs mensajeros, modulando su traducción, degradación, corte y empalme. Tal es el caso de MALAT1(Metastasis Associated Lung Adenocarcinoma Transcript 1), que afecta la expresión de genes del citoesqueleto y matriz extracelular, mediante el control del splicing alternativo al influir en la actividad y distribución de las proteínas SRs (SHI Related Sequence), componentes del complejo de corte y empalme[63]. Finalmente, los lncRNAs actúan como andamios para la formación de complejos multiprotéicos, facilitando la proximidad e interacción de diversas proteínas[61]. Un ejemplo de andamio se observa con HOTAIR (HOX transcript antisense intergenic RNA), que puede unirse simultáneamente tanto a PRC2 como al complejo LSD1-CoREST (Lysine specific

demethylase 1- co-repressor of REST), asegurando la metilación de la histona H3K27 y la desmetilación de la histona H3K4me2, necesarias en el silenciamiento de diversos genes[64].

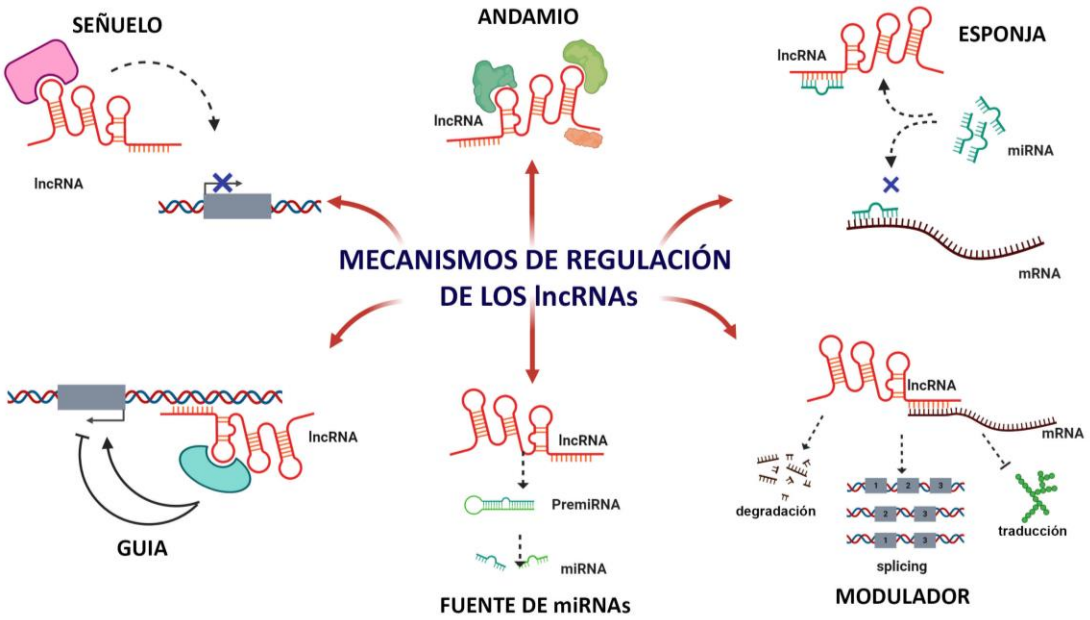

Figura 13. Mecanismos de regulación de los lncRNAs. Principales formas de acción de los lncRNAs, a través de la interacción con DNA, RNA y proteínas. La diversificación funcional de los lncRNAs les permite regular positiva o negativamente mecanismos transcripcionales o postranscripcionales. Tomada y modificada de *De la Fuente-Hernández MA. et al.* [56]

2. JUSTIFICACIÓN

La obesidad es un problema de salud pública latente y en aumento en México. La evidencia epidemiológica muestra que el exceso de peso se asocia con un mayor riesgo de promoción y desarrollo de varios tipos de cáncer resultando en un mal pronóstico de la enfermedad. Si bien, aún no se elucidan los mecanismos moleculares que subyacen a estas asociaciones, se ha observado que las células troncales derivadas de tejido adiposo (ADSC), tienen un papel importante. Las ADSC son quimioatraídas por las células tumorales, y una vez establecidas, promueven el crecimiento tumoral y un fenotipo más agresivo. La expresión de las moléculas que participan en esta comunicación intercelular se encuentra regulada a distintos niveles, dentro de los cuales participan los lncRNAs. El presente trabajo propone, a partir de los datos del transcriptoma, analizar la firma genómica de lncRNAs de células ADSC co-cultivadas con células HeLa, lo que permitirá definir el perfil asociado a los cambios en el fenotipo y función de las ADSC durante el co-cultivo con células de cáncer cervical.

3. HIPÓTESIS

Las ADSC, en presencia de células de cáncer cervical, presentarán cambios en su transcriptoma codificante y no codificante, mismos que se relacionarán con procesos celulares como la migración, la viabilidad, el fenotipo troncal y la formación de esferas.

4. OBJETIVOS

4.1 Objetivo general

Determinar la firma genómica de lncRNAs en ADSC co-cultivadas con células HeLa y analizar su importancia en el fenotipo de ADSC.

4.2 Objetivos particulares

1. Analizar el transcriptoma de ADSC durante el co-cultivo con células de cáncer cervicouterino obtenidos por secuenciación masiva.

2. Validar los cambios encontrados por secuenciación masiva en el transcriptoma de ADSC durante el co-cultivo con células de cáncer cervical.

3. Determinar si existen cambios en viabilidad celular, capacidad de migración, susceptibilidad a muerte, ciclo celular y fenotipo troncal de las células ADSC, posterior al co-cultivo con células de cáncer cervical.

4. Analizar la importancia de los lncRNAs en los cambios en el fenotipo de ADSC durante el co-cultivo con células de cáncer cervical.

5. ANTECEDENTES

Bajo la aprobación del Comité de Ética en Investigación del Instituto Nacional de Medicina Genómica No. 136 (Anexo 12.3) y con el respectivo consentimiento informado, se colectaron 3 muestras de tejido adiposo blanco visceral a partir de la derivación gástrica de mujeres con obesidad mórbida (IMC $\geq$ 40 kg/m^2). Las muestras fueron obtenidas por el Servicio de Gastrocirugía del Hospital de Especialidades del Centro Médico Nacional Siglo XXI del Instituto Mexicano del Seguro Social (IMSS). A través de una Tomografía por Emisión de Positrones (PET), se demostró que las pacientes donadoras de tejido adiposo no presentaron ningún tipo de cáncer asociado a obesidad al momento de la obtención del tejido. Las características antropométricas de las donadoras al momento de la obtención se resumen en la tabla 2.

Tabla 2. Características antropométricas de las pacientes donadoras de tejido adiposo blanco.

DONADOR	EDAD (años)	MASA (kg)	Talla (m)	IMC (kg/m^2)
1	26	96	1.55	40.5
2	47	140	1.70	48.5
3	39	130	1.57	52

A partir del tejido adiposo blanco, se obtuvo la fracción celular estromal utilizando la metodología propuesta por Zuk *et al.* [65] (Figura 14), para posteriormente aislar y caracterizar el cultivo primario de ADSCs.

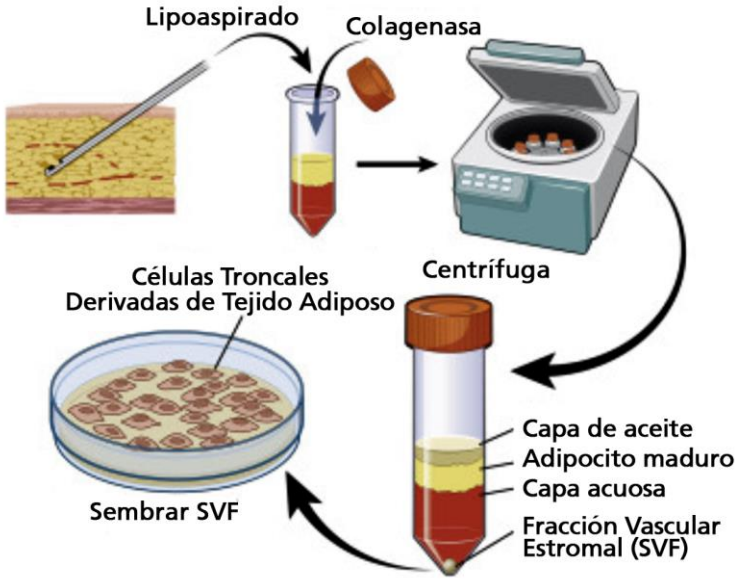

Figura 14. **Aislamiento de ADSC a partir de lipoaspirados de tejido adiposo blanco**. Principales etapas de la metodología empleada en la obtención del cultivo primario de ADSC. Tomada y modificada de *Thiagarajan PS., et al.* [66].

Todos los cultivos primarios obtenidos de ADSC fueron células con morfología fibroblastoide y capacidad adherente, características propias de células mesenquimales (Figura 15).

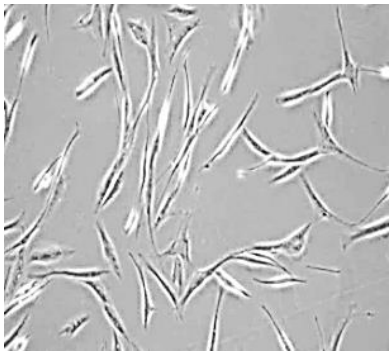

Figura 15. Morfología de las ADSC obtenidas de pacientes con obesidad mórbida. Fotografía representativa del cultivo primario a una confluencia de 50%. Microscopio óptico, microscopía de campo claro, objetivo 40x.

La caracterización del cultivo primario obtenido de cada paciente fue analizado por citometría de flujo para el inmunofenotipo de ADSC: $CD31^-$, $CD44^+$, $CD45^-$, $CD90^+$; de acuerdo con el Comité de Células Troncales Mesenquimatosas de la Sociedad Internacional de Terapia[40]. Todos las muestras presentaron una población positiva mayor al 96% del inmunofenotipo troncal CD44 y CD90 (Tabla 3), mientras que fueron negativos para CD45, propio de las células de origen hematopoyético, y CD31 ó PECAM-1, el cual es específico

de células endoteliales y sus progenitores. Por lo tanto, los resultados demostraron que los cultivos primarios cumplieron con los requisitos morfológicos e inmunofenotípicos atribuidos para ADSC (Tabla 3, Figura 16).

Tabla 3. Caracterización de las ADSC aisladas de pacientes a partir de la expresión de proteínas de membrana

DONADOR	Inmunofenotipo (%)			
	CD31-	CD44+	CD45-	CD90+
1	96	99.4	98.5	99.5
2	98.9	99.2	ND	99.2
3	98.1	99.2	99	99.7

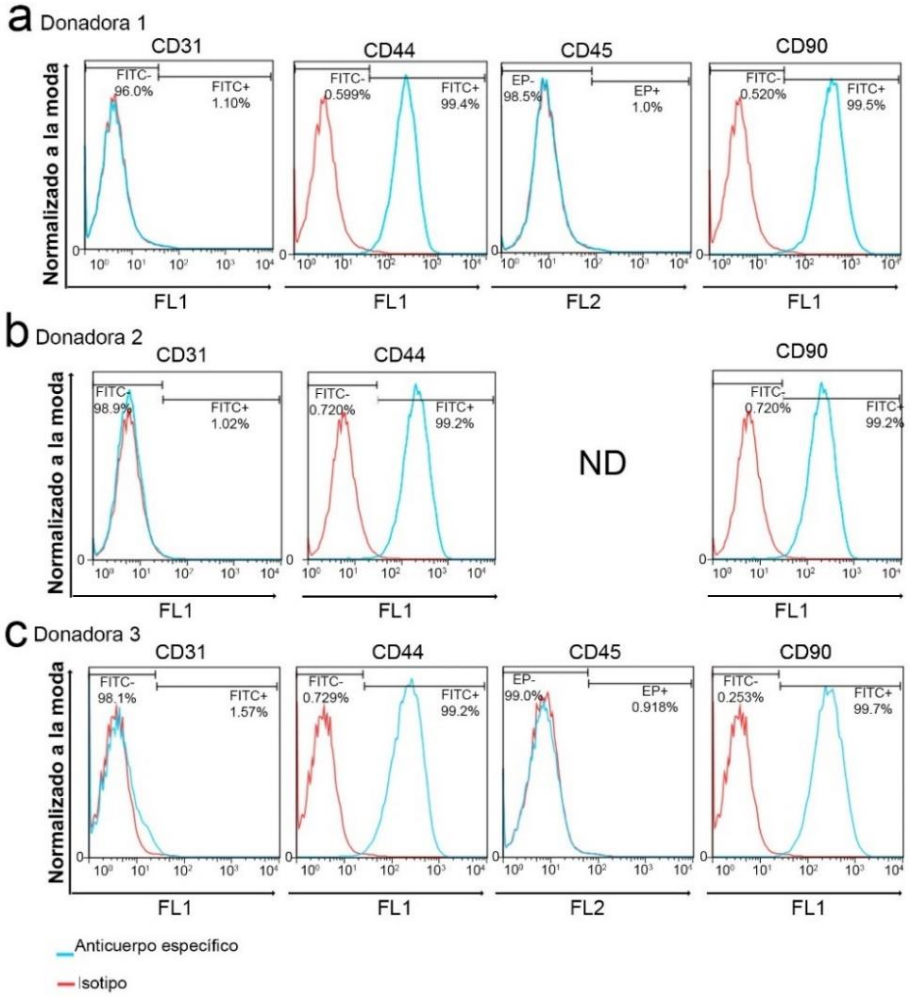

Figura 16. Caracterización del inmunofenotipo de la población estromal aislada del tejido adiposo blanco de mujeres con obesidad mórbida. Histogramas representativos del análisis por citometría de ADSC obtenidas de a) donador 1, b) donador 2, c) donador 3. En azul, células positivas CD31, CD44, CD45 y CD90. El isotipo se muestra en rojo. ND: no determinado.

Una vez caracterizados los cultivos primarios, las ADSC obtenidas de pacientes fueron co-cultivadas con células de cáncer cervical (HeLa) en un sistema “transwell”. Este sistema se compone de una membrana permeable de poro de 3.0 µm, la cual separa ambas poblaciones celulares, pero permite que exista una comunicación intercelular a través de factores solubles presentes en el medio de cultivo (Figura 17). El co-cultivo se mantuvo por 24 horas utilizando Dulbecco's Modified Eagle Medium (DMEM) en ausencia de suero fetal bovino (SFB), mientras que los monocultivos de las mismas líneas celulares se establecieron como grupos control.

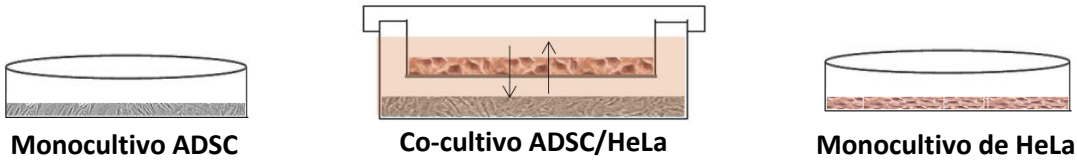

Figura 17. Ensayo de co-cultivo ADSC/HeLa. En la membrana del transwell se cultivaron las células HeLa y en la parte inferior las ADSC compartiendo el medio durante 24 h en ausencia de SFB. De manera simultanea ADSC y células HeLa permanecieron en monocapa con el mismo medio como grupos control.

Al término del ensayo, los 4 grupos de células correspondientes a cada condición (ADSC co-cultivo, ADSC monocultivo, células HeLa co-cultivo y células HeLa monocultivo) fueron lavadas con PBS (del inglés Phosphate-Buffered Saline) para la posterior extracción de RNA total y el análisis del transcriptoma por secuenciación masiva. En el presente trabajo, se analizó la expresión del transcriptoma de ADSC en presencia de células HeLa.

6. METODOLOGÍA

6.1 Análisis del inmunofenotipo de ADSC por citometría de flujo

Los cultivos primarios del pase 3 se trataron con la enzima Acutasa de American Type Culture Collection (ATCC), (cat. 30-2103) por 10 min a 37°C. Las células se concentraron por centrifugación y se lavaron dos veces con PBS 1X para teñirse con anticuerpos primarios acoplados a fluorocromos ($1x10^6$ células/10µL de anticuerpo). Los anticuerpos fueron anti-CD31-FITC (Millipore CBL468F), anti-CD44-FITC (MACS Miltenyi Biotec 130-095-195) anti-CD45-PE (Millipore FCMAB118F) y anti-CD90-FITC (Millipore, FCMAB211F). Para cada grupo se utilizó un isotipo a la misma concentración que los anticuerpos primarios, los cuales fueron Mouse IgG FITC (MACS Miltenyi Biotec, 130-092-213) y Mouse IgG1-PE (MACS Miltenyi Biotec, 103-092-212). Para la tinción se incubó a 4°C en ausencia de luz durante 30 min y se lavaron dos veces con PBS al 1% v/v de suero fetal bovino (SFB). Se fijaron con paraformaldehido al 4% durante 15 min a temperatura ambiente, se lavaron y se resuspendieron en 500 mL de PBS 1X. Para su análisis se registraron al menos 10 000 eventos para cada muestra, utilizando el citómetro FACSCalibur, (BD Biosciences) y el análisis de datos se realizó con el programa FlowJo v10 (Tree Star, BD Bioscences).

6.2 Diferenciación adipogénica

El kit de diferenciación de adipocitos para células troncales mesenquimales de tejido adiposo y preadipocitos (ATCC PCS-500-050), se utilizó para ensayos de diferenciación adipogénica de acuerdo con las instrucciones del fabricante. Las células se fijaron en paraformaldehido al 4% durante 15 min y la diferenciación adipogénica se detectó mediante la tinción de vacuolas de lípidos neutrales, con solución Rojo-oleoso al 0.5% en isopropanol (Sigma-Aldrich, O1391).

6.3 Cultivo celular

Las ADSC obtenidas de ATCC (Normal, Human “Pase Cero” Organismo: homo sapiens humano, PCS-500-011) se mantuvieron en Medio Basal de Células Mesenquimales (PCS-500-030, ATCC) suplementado con Mesenchymal Stem Cell Growth Kit for Adipose and Umbilical-derived MSCs–Low Serum (catálogo PCS-500-040, ATCC). El medio se

remplazó cada 4 o 5 días. Previo al ensayo, el medio óptimo de crecimiento se remplazó por Dulbecco's Modified Eagle Medium (DMEM) al 5% v/v de SFB. Esta línea celular comercial se utilizó para realizar los ensayos funcionales.

Las células HeLa (células epiteliales de adenocarcinoma de cuello uterino), Ca Ski (células epiteliales de carcinoma epidermoide de cuello uterino) y SiHa (línea celular de carcinoma de células escamosas de cuello uterino) de ATCC se mantuvieron en medio DMEM al 5% v/v de SFB. El medio de cultivo se remplazó cada 2 días.

Las células HaCat (línea celular inmortalizada de queratinocitos humanos) de ATCC se mantuvieron en medio DMEM/F-12 al 5% v/v de SFB. Previo al ensayó el medio se remplazó por DMEM 5% v/v de SFB o DMEM sin suplementar.

Las células 3T3-L1 (fibroblastos embrionarios de ratón) de ATCC se mantuvieron en medio DMEM al 5% v/v de SFB. El medio de cultivo se remplazó con medio fresco de 2 a 3 veces por semana.

Todas las células se mantuvieron a 37°C en una atmósfera con humedad que contenía 5% de CO_2.

6.4 Ensayo de co-cultivo ADSC/células de cáncer cervical

Para realizar el co-cultivo de ADSC con células HeLa, se usaron cajas transwell de 75 mm de diámetro, con insertos cuya membrana permeable de policarbonato presenta poros de 3.0 μm de diámetro (Corning Costar, cat.3420), la cual separa ambas poblaciones celulares, pero permite que el medio de cultivo se comparta. Entre el tercer y quinto pase, las ADSC se sembraron con una confluencia cercana al 90% ($5x10^5$ células) en el fondo de la placa con DMEM al 5% v/v de SFB. 12 h previas al ensayo, las células HeLa se sembraron a alta confluencia ($1x10^6$ células) sobre la membrana con DMEM 5% v/v de SFB. 4 h antes de iniciar el co-cultivo, se remplazó el medio de crecimiento por DMEM sin SFB en las tres condiciones: ADSC monocultivo (control), ADSC en transwell para co-cultivo y células HeLa en la membrana permeable. Al término de las 4 h, el medio se descartó, las células se lavaron dos veces con PBS 1X y el sistema transwell en co-cultivo ADSC/HeLa se colocó en DMEM sin SFB y se mantuvo durante 24 h. Al término del ensayo, los medios de crecimiento se colectaron y las células se lavaron con PBS 1X para la extracción de RNA.

6.5 Extracción de RNA

El RNA total del grupo ADSC co-cultivo y ADSC monocultivo se extrajo con el reactivo TRIZOL/cloroformo (Invitrogen) siguiendo las indicaciones del proveedor. El RNA de cada grupo se resuspendió en un volumen de 30 µL de agua Mili Q.A (Millipore) para su cuantificación a una absorbancia de 260 nm y 280 nm con NanoDrop.

6.6 Secuenciación del transcriptoma de ADSC co-cultivo y ADSC monocultivo

Para la secuenciación de los transcriptomas completos, se utilizaron RNAs con una calidad entre 8.8-10 de RIN (número de integridad del RNA) determinada por electroforesis capilar. Posterior a la extracción, el RNA ribosomal se eliminó con el kit Ribominus Eukaryoter RNA-seq (invitrogen Cat. A10837-8). Las bibliotecas de secuenciación se prepararon a partir del RNA total de acuerdo con el protocolo de la biblioteca TruSeq RNA Sample Prep de Illumina y se analizaron con la plataforma Illumina GAIIx machine. Las muestras se secuenciaron por triplicado biológico a partir de ensayos independientes con las ADSC de cada paciente y se obtuvieron aproximadamente 20 millones de lecturas (“reads”). Los datos de la secuenciación se analizaron con CLC genomics workbench (versión 7 CLC Bio Cambridge), determinando la expresión diferencial entre grupos por medio del EgdR y considerando una tasa de cambio ó Fold Change mayor o igual a 2 y menor o igual a -2 con una $p \leq 0.05$.

6.7 Transcripción reversa y análisis de expresión por RT-qPCR

Después del tratamiento del RNA con RQ1 Rnase-Free Dnase (Promega Cat. M6101), se retrotanscribió 2 µg de RNA de cada grupo de estudio utilizando el Maxima First Strand cDNA Synthesis Kit for RT-qPCR (Thermo Scientific Cat K1641).

Para validar los datos de expresión obtenidos a partir del análisis transcripcional, se analizó la expresión relativa de 10 genes en ADSC Co-cultivo y ADSC monocultivo por PCR cuantitativa (RT-qPCR). El nivel de transcripción de cada gen se determinó a partir de la reacción de cDNA con SYBR Selec Master Mix 2X (Applied Biosystems), con primers específicos diseñados con el programa Primer plus (http://primer3plus.com/cgi-bin/dev/primer3prefold.cgi). El análisis termodinámico de oligonucleótidos se realizó con Beacon Designer (http://www.premierbiosoft.com/qOligo/Oligo.jsp?PID=1), y para la

predicción de estructuras secundarias de los oligonucleótidos se usó UNAFold. (https://www.idtdna.com/UNAFold) (Anexo 12.4). El gen TBP se utilizó como control endógeno de expresión constitutiva para la cuantificación y normalización de los resultados. En todos los casos, se generaron curvas de disociación y se confirmó la especificidad de las reacciones de PCR. Se utilizó el método comparativo ΔΔCt para el análisis de datos[67]. El valor de expresión relativa representa el cálculo de $2^{-\Delta\Delta Ct}$.

6.8 Evaluación del transcriptoma codificante

Para el análisis integral del genoma codificante se utilizó el programa Ingenuity Pathway Analysis (IPA) (Ingenuity Systems, Redwood City, CA) de QIAGEN Bioinformatics. Las redes con la superposición de los genes regulados a la alta y a la baja (con base a su FCh) se construyeron a partir de la lista de moléculas diferencialmente expresadas en el co-cultivo. Dentro de las redes, los genes se representan como nodos y las relaciones biológicas entre dos nodos como líneas. Los resultados se compararon con los de Key Pathway (KP) de Metacore Clarivate Analitics para la misma lista de moléculas. Para el análisis de enriquecimiento de conjuntos de genes (GSEA) (Broad Institute, https://www.gsea-msigdb.org/gsea/index.jsp) se empleó para determina si el conjunto de genes en ADSC co-cultivo mostró diferencias estadísticamente significativas con respecto al monocultivo considerando el conjunto de datos con una tasa de descubrimiento falso (FDR) menor a 0.25 y un puntaje de enriquecimiento normalizado (NES) mayor a 2.

6.9 Ensayo de incorporación de BrdU y TUNEL

Posterior al ensayo de co-cultivo, se analizó la progresión del ciclo celular de ADSC co-cultivo y ADSC monocultivo a través de la incorporación de BrdU a la célula, utilizando el Kit de APO-BrdU TUNEL Assay Kit (Molecular Probes Cat. A23210), siguiendo las indicaciones del fabricante. El análisis se realizó por citometría de flujo en un citómetro FACSCalibur, (BD Biosciences) y los resultados se analizaron con el programa ModFit LT (Verity Software House) para evaluar la progresión del ciclo celular y FlowJo (Tree Star, BD Bioscences) para la muerte celular por apoptosis. Para el ensayo se realizaron tres replicas independientes con sus correspondientes triplicados técnicos.

6.10 Medio condicionado

El medio condicionado de células HeLa (M. HeLa), se colectó de una placa al 90% de confluencia después de la incubación con DMEM en ausencia de SFB durante 24 h a 37°C con 5% de CO_2. El medio condicionado de células HaCaT (M. HaCaT) se colectó de una placa al 90% de confluencia después de la incubación con DMEM sin SFB durante 24 h a 37°C, 5% de CO_2. El medio de co-cultivo (M. Co-cultivo) se obtuvo del sistema donde las ADSC crecieron en presencia de células HeLa durante 24 h. Este medio de co-cultivo se compone de DMEM sin SFB, con los factores solubles producidos por ADSC y células HeLa. Al finalizar el período de incubación, todos los medios se filtraron con poros de diámetro de 0.2 μm (Corning) para la eliminación de restos celulares y fueron utilizados inmediatamente o se almacenaron a -70ºC.

6.11 Ensayo de cierre de herida

Las ADSC de pase 4 o 5 se cultivaron a alta confluencia en placas de formato de 6 pozos (3.5 cm de diámetro). Previo al inicio del ensayo, las ADSC se mantuvieron en medio DMEM sin SFB por 16 h para sincronizar su ciclo celular. La herida se realizó con una punta de pipeta de 200 μL y se lavó tres veces con PBS 1X. Posteriormente, se colocaron los medios de cultivo celular: DMEM sin SFB (Medio) como control negativo y DMEM suplementado al 5% de SFB v/v (M+SFB) control positivo, medio del co-cultivo ADSC/HeLa (M CC), medio condicionado de células HeLa (M. HeLa) y medio condicionado de células HaCaT (M HaCaT). Dado que las ADSC duplican su número a las 72 h, las imágenes microscópicas del cierre de herida de todas las condiciones se capturaron en los tiempos 0, 12, 24 y 48 h para su análisis. El área libre de células se calculó con el programa ImageJ (https://imagej.net/). Para el ensayo se realizaron tres replicas independientes con sus correspondientes triplicados técnicos.

6.12 Actividad de ALDH

Las poblaciones celulares ADSC monocultivo y ADSC co-cultivo se lavaron y despegaron utilizando tripsina-EDTA (0.05% tripsina y 0.02% EDTA g/L) La actividad de ALDH se evaluó con el reactivo ALDEFLUOR (StemCell Technologies, Cat. 01700), de acuerdo con las instrucciones del fabricante. Se resuspendieron $1x10^6$ células en 1 mL de buffer y se

agregaron 5 µL de reactivo ALDEFLUOR. Después, se transfirieron 500 µL de la suspensión celular a un tubo con 5 µL del reactivo N,N-dietilaminobenzaldehído (DEAB), el cual es un inhibidor de la actividad de la ALDH y se usó como control negativo de la actividad enzimática para cada condición. La medición se realizó por citometría de flujo empleando el citómetro FACSCalibur, (BD Biosciences) y para el análisis de los resultados se empleó el programa FlowJo v10 (Tree Star, BD Bioscences). Para el ensayo se realizaron 3 réplicas independientes.

6.13 Ensayo de formación de esferas

Las ADSC cultivadas en monocultivo, en co-cultivo o las 3T3-L1 se despegaron, contaron y sembraron a una densidad de 1×10^4 células/mL en MammoCult Basal Medium (Cat. 05621, Stemcell Technologies) suplementado con 4 µg/mL de heparina, 0.48 µg/ml de hidrocortisona y suplemento de proliferación MammoCult (Cat. 05622, Stemcell Technologies) según las instrucciones del fabricante. Las células se cultivaron a 37°C y 5% de CO_2 durante 15 días, y el medio de cultivo se sustituyó cada 3 días. La formación de esferas se registró por fotografías a los 1, 5, 10 y 15 días. Se realizaron tres réplicas biológicas con duplicados técnicos cada una.

6.14 Ensayos de ELISA para cuantificación de citocinas

Las quimiocinas se determinaron en sobrenadantes obtenidos de monocultivos o co-cultivos de ADSC utilizando el método Enzyme-Linked Immunosorbent (ELISA). GROβ humano ELISA Kit (Cat. OKAG00021, Aviva Systems Biology), Human CXCL3 ELISA Kit (Cat. OKEH00399, Aviva Systems Biology) y Human CXCL5 ELISA kit (Cat. EHCXCL5 Thermo Scientific) se emplearon según los protocolos del fabricante. Las mediciones se realizaron por duplicado de tres experimentos independientes.

6.15 Análisis de sobrevida global asociada a la expresión de quimiocinas en pacientes con cáncer cervical

Se utilizaron las bases de datos públicas GEPIA (http://gepia.cancer-pku.cn/index.html)[68] y The Human Protein Atlas versión 23.0 (https://www.proteinatlas.org/)[69] que proporcionan datos de secuencias de RNA y datos clínicos de pacientes para analizar la expresión

diferencial de las quimiocinas tanto en tejido tumoral y tejido normal. Se introdujeron los genes diana en el cuadro de entrada de la base de datos y se procedió a su búsqueda. Se realizó un estudio pronóstico de las quimiocinas en el cáncer cervical mediante la curva de Kaplan-Meier en la base de datos GEPIA.

6.16 Inhibición de la expresión mediada por shRNAs

Las secuencias de shRNA se diseñaron para inhibir la expresión de lnc-CXCL3 a partir de la secuencia de referencia anotada en LNCipedia (https://lncipedia.org/). Las secuencias de shRNAs (Anexo 12.5) se alinearon utilizando la metodología propuesta en Knockout RNAi Systems (laboratorios Clontech Inc.). Las secuencias se insertaron en un plásmido pSIREN-RetroQ a través de extremos creados con EcoRI y BamHI, utilizando el kit de ligación rápida de DNA (Rapid DNA Ligation Kit Cat. K1422, Thermo Fisher Scientific) acorde al procedimiento descrito por el fabricante.

6.17 Transfección de plásmidos

5×10^5 células HeLa o 2.5×10^5 células 3T3-L1 se transfectaron con 4 μg del plásmido pSIREN-RetroQ-shRNA o pGFP-V-RS (plásmido control) utilizando Xfect (Cat. 631.317, Clontech). La eficacia de la inhibición transitoria se evaluó mediante la cuantificación de los niveles de expresión relativa por RT-qPCR.

6.18 Selección de clonas knockdown estables

Tras la transfección de shRNAs, se seleccionaron células HeLa y células 3T3-L1 utilizando 0.7 μg/mL y 2 μg/mL de puromicina, respectivamente. La inhibición estable se validó mediante RT-qPCR.

6.19 Ensayo de migración celular

La migración celular se determinó con el sistema transwell (inserto de 6.5 mm, placa de 24 pozos con membrana de policarbonato de 8.0 μm Corning, Costar Cat. 3422 Reino Unido). Se sembraron 1.5×10^4 células HeLa en 200 μL de medio libre de SFB en el compartimento superior de la placa de la cámara transwell. El medio suplementado con 5% de SFB se usó como quimioatrayente en el compartimiento inferior y las células se incubaron durante 24 h.

Posteriormente, las células que migraron se fijaron con paraformaldehido al 4% y se tiñeron con solución de cristal violeta y se tomaron fotos al microscopio con un aumento de 10x. Los experimentos se realizaron por triplicado biológico, con 4 réplicas técnicas cada uno.

6.20 Análisis estadístico

Todos los valores graficados representan la media y su error estándar (SEM). Los valores promedio se calcularon a partir de tres experimentos independientes utilizando la herramienta GraphPad PRISM6. Los datos se analizaron mediante ANOVA o la prueba t de Student. Un valor de $p < 0.05$ se consideró estadísticamente significativo.

7. RESULTADOS

7.1 Caracterización del transcriptoma codificante y no codificante de ADSC en co-cultivo con células HeLa

Un mecanismo que relaciona la obesidad con cáncer es la comunicación que se establece entre las ADSC y las células tumorales. Actualmente, el cáncer cervical es el segundo de mayor incidencia entre la población mexicana, por lo que se eligió a las células HeLa como modelo de línea celular proveniente de este tipo de cáncer.

La comunicación entre las ADSC con las células tumorales conlleva a cambios en procesos celulares tanto en las células tumorales como en las ADSC, por lo que fue de nuestro interés determinar el transcriptoma de ADSC en presencia de células HeLa.

Las ADSC provenientes de pacientes se sembraron en co-cultivo con células HeLa y como grupo control ADSC en ausencia de células HeLa. Se mantuvieron en medio sin SFB durante 24 h y se extrajo el RNA de cada población celular de estudio (ADSC co-cultivo y ADSC monocultivo) para secuenciar el transcriptoma completo por RNAseq y comparar los transcriptomas de ambas condiciones (Figura 18).

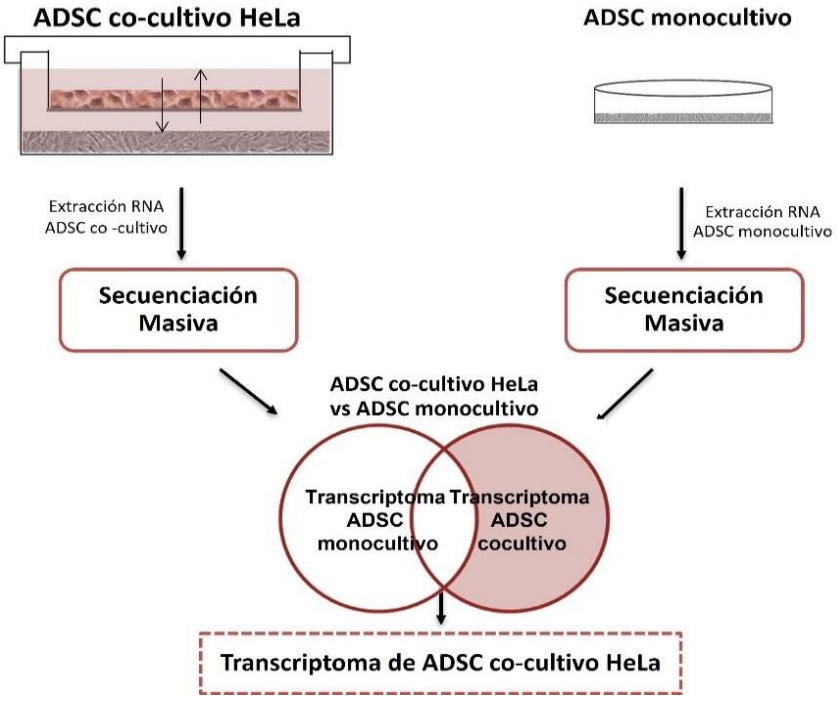

Figura 18. Ensayo de co-cultivo para el análisis del transcriptoma de ADSC. El ensayo se realizó en 24 h en ausencia de SFB. El transcriptoma de ADSC en co-cultivo con células HeLa se comparó con el transcriptoma de ADSC en monocultivo.

Una vez realizada la secuenciación del transcriptoma de ambas condiciones de cultivo y toda vez que se cumplieron los parámetros de calidad, la comparación de los transcriptomas estableció que ADSC en co-cultivo presentó 761 moléculas diferencialmente expresadas, de las cuales 687 correspondieron a RNAs codificantes y 74 ncRNAs (Figura 19a). Dentro del grupo de RNAs codificantes o RNAs mensajeros (mRNAs), 618 moléculas aumentaron su expresión y 69 disminuyeron posterior al co-cultivo. Se muestran los 10 genes con mayor aumento y decremento en su expresión (Figura 19b).

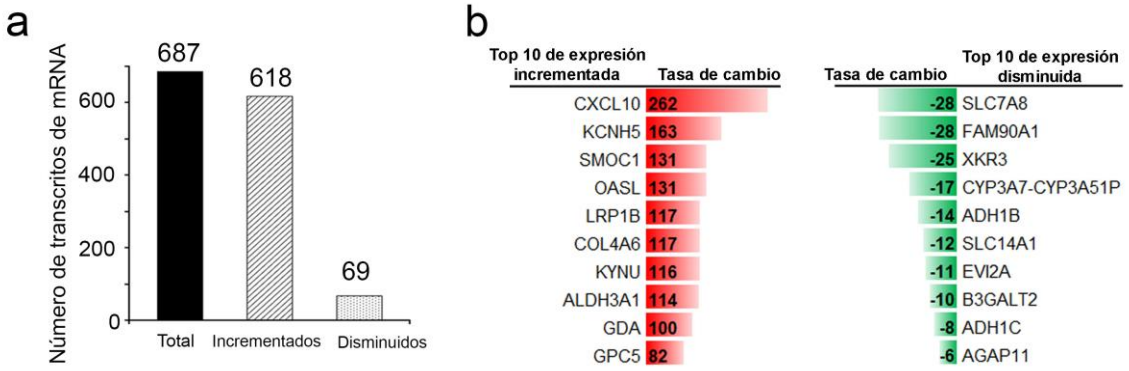

Figura 19. Transcriptoma codificante diferencialmente expresado de ADSC en co-cultivo con células HeLa. a) Número de transcritos de mRNAs expresados diferencialmente (incrementaron o disminuyeron su expresión) en las ADSC co-cultivo en comparación con las ADSC monocultivo a partir del análisis de transcripción. b) los 10 primeros mRNAs con un incremento en su expresión (en rojo) y los 10 con una mayor disminución de expresión (en verde).

Por otra parte, se analizó el transcriptoma no codificante de ADSC en co-cultivo. De las 74 moléculas con una expresión diferencial, 59 aumentaron y 15 disminuyeron su expresión (Figura 20a). Según su clasificación, se identificaron 43 lncRNA intergénicos, 20 lncRNAs intragénicos, 6 pseudogenes y 5 miRNAs (Figura 20b).

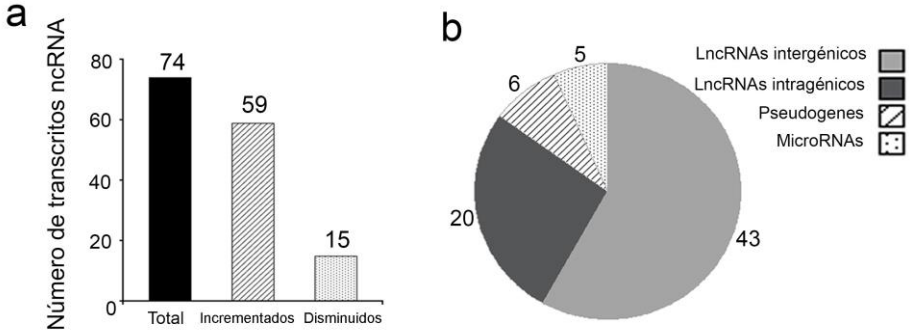

Figura 20. Transcriptoma no codificante diferencialmente expresado de ADSC en co-cultivo con células HeLa. a) Número de transcritos RNAs no codificantes expresados diferencialmente (incrementados o disminuyeron su expresión) en ADSC co-cultivo comparadas con ADSC monocultivo. b) Clasificación de los RNAs no codificantes expresados diferencialmente en ADSCs co-cultivo con células HeLa.

En la siguiente figura, se muestran las 10 moléculas no codificantes con mayor incremento o disminución en su expresión en ADSC en co-cultivo (Figura 21a), así como los miRNAs (Figura 21b) y los pseudogenes identificados (Figura 21c).

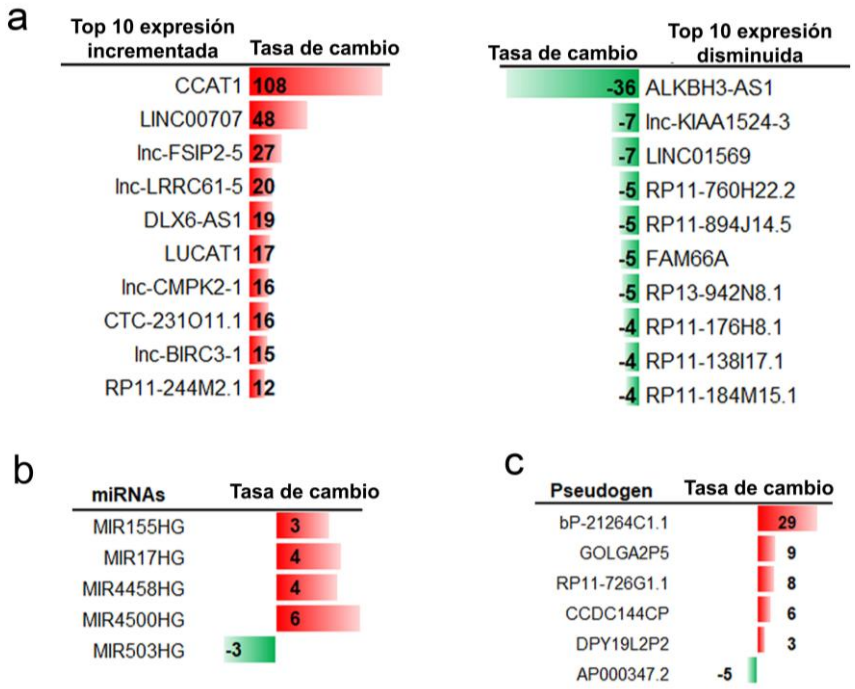

Figura 21. Moléculas no codificantes en ADSC co-cultivo. a) Los 10 primeros con expresión incrementada (en rojo) o disminuida (en verde) en ADSC durante el co-cultivo con células HeLa. b) miRNAs y c) pseudogenes diferencialmente expresados en ADSC durante el co-cultivo con células HeLa.

Entre los lncRNAs diferencialmente expresados en ADSC co-cultivo, se identificaron 20 lncRNAs intragénicos que comparten la región genómica con un gen codificante. Por ejemplo, el lnc-CXCL3, el cual recibe su nombre por localizarse dentro de la secuencia codificante del gen CXCL3 (Figura 22).

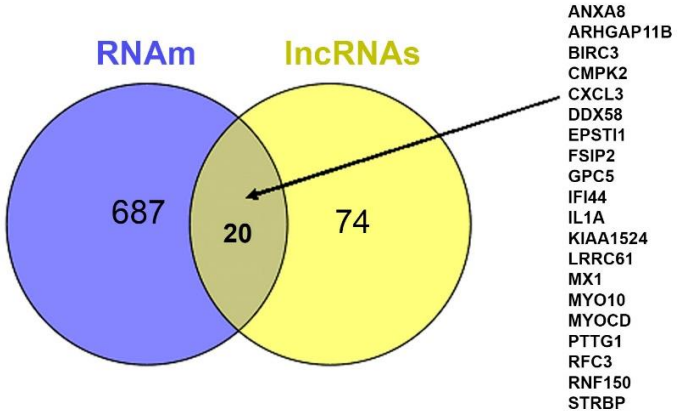

Figura 22. LncRNAs intragénicos en ADSC co-cultivo. Diagrama de Venn Euler muestra en azul el número mRNAs y en amarillo el número de lncRNA diferencialmente expresados en ADSC. La intersección corresponde a los lncRNAs intergénicos, cuyos mensajeros se encuentra enlistados. Creado con VENNY 2.1 (https://bioinfogp.cnb.csic.es/tools/venny)

Para caracterizar el modelo de estudio, se evaluó el potencial de diferenciación adipogénica de ADSCs provenientes de pacientes, mediante la inducción adipogénica (coctel de dexametasona, indometacina, insulina y tiazolidona) e identificando la acumulación de triglicéridos con el colorante rojo-oleoso. Se observó la formación de vacuolas lipídicas teñidas de rojo después de dos semanas de inducción adipogénica, a diferencia del grupo control donde no se detectaron (Figura 23).

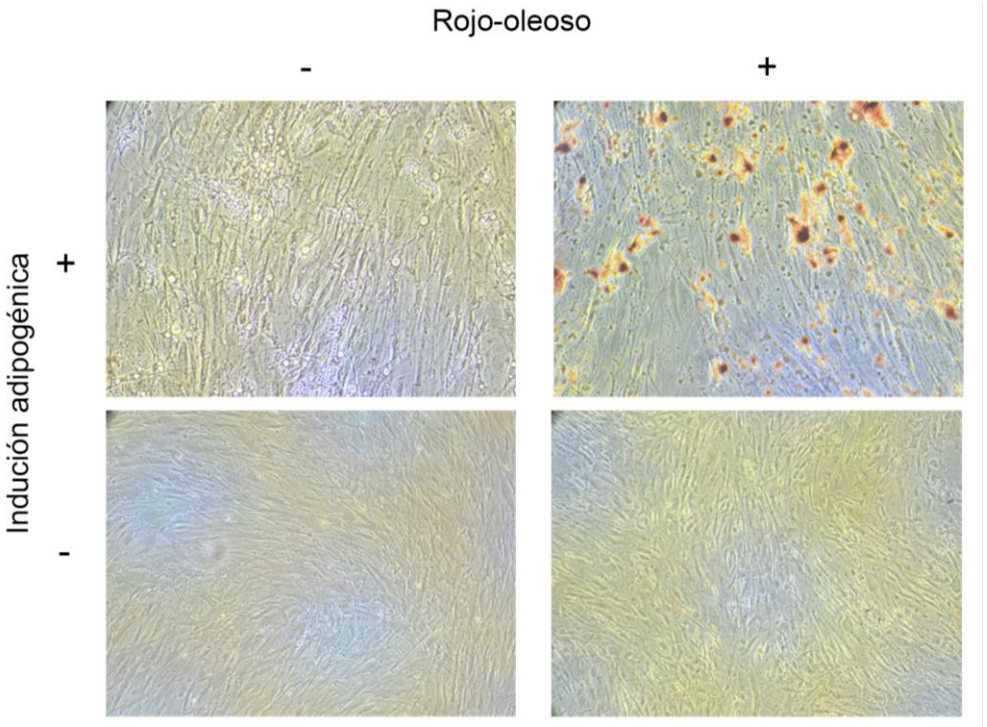

Figura 23. Inducción adipogénica en ADSC de pacientes posterior al periodo de congelación en nitrógeno líquido. Imágenes representativas de la monocapa de ADSC observada bajo el microscopio óptico, microscopía de campo claro con el objetivo de 40x. En rojo los depósitos de lípidos.

Posteriormente, se replicó el co-cultivo de ADSC con células HeLa, realizando la extracción del RNA total de ADSC en co-cultivo y de ADSC en monocultivo. Se analizó la expresión relativa RT-qPCR de: 4 RNAS codificantes y 6 lncRNAs. Los resultados mostraron que todas las moléculas presentaron un patrón de expresión similar al obtenido por RNAseq con ADSC de pacientes (Tabla 4, Figura 24).

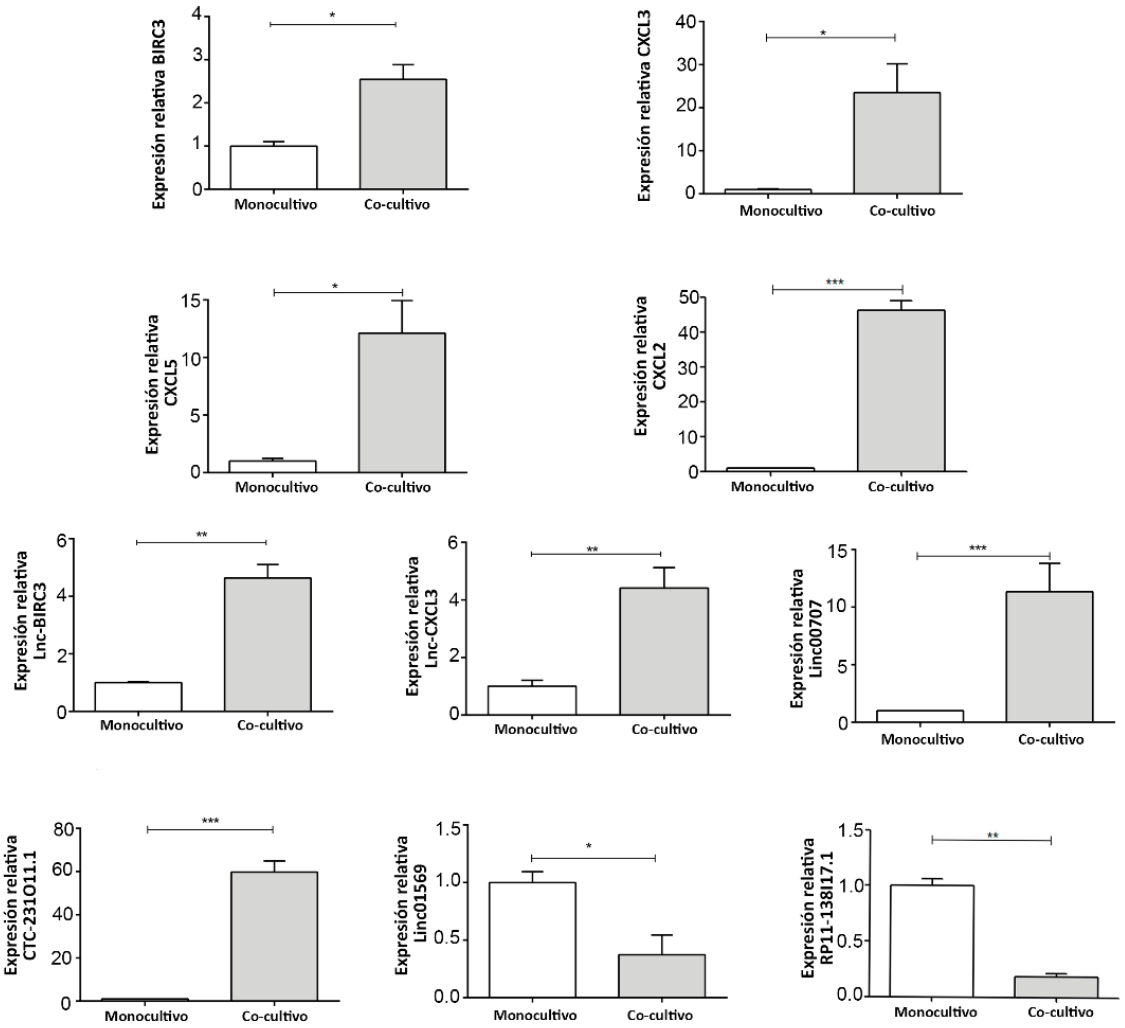

Figura 24. Validación por RT-qPCR de la expresión relativa de moléculas en ADSC de pacientes posterior al co-cultivo con células HeLa. Las barras representan el promedio ±SEM de tres experimentos independientes. El análisis estadístico se realizó con una prueba t-Student no pareada, considerando *p<0.05, **p<0.01 y ***p<0.001

Tabla 4. Expresión relativa de moléculas en ADSC de pacientes posterior al co-cultivo por RNAseq y RT-qPCR.

Molécula	ADSC Pacientes co–cultivo/HeLa	
	RNAseq	RT-qPCR
mRNAs		
BIRC3	6	2.5*
CXCL3	14	23.5*
CXCL2	16	46.1**
CXCL5	12	12.1*
LncRNAs		
Lnc-BIRC3	15	4.6**
Lnc-CXCL3	11	6.7**
Linc00707	48	11.3***
CTC-231O11.1	15.7	59.7***
Linc01569	-7	-2.7*
RP11-138I17.1	-4	-5.3**

Comparación de los resultados obtenidos del RNAseq y RT-qPCR. ±SEM de tres experimentos independientes. *p<0.05, **p<0.01 y ***p<0.001

De las moléculas seleccionadas para su validación, se eligieron dos mRNAs (BIRC3 y CXCL3) y dos lncRNAs intragénicos (lnc-BIRC3 y lnc-CXCL3). Tanto los mRNAs como los lncRNAs aumentaron su nivel de expresión, lo cual siguiere que los lncRNAs podrían tener un efecto regulatorio en *cis* sobre los mRNAs (Figura 22).

7.2 La expresión diferencial de quimiocinas en ADSC posterior al co-cultivo con células HeLa, es similar a lo observado en co-cultivo con células Ca Ski o SiHa

Para evaluar si los genes diferencialmente expresados en ADSC co-cultivadas con células HeLa presentan cambios similares en co-cultivo con otras líneas celulares de cáncer cervical, se analizaron los niveles de expresión de 1 lncRNA y 4 mRNAs (con un aumento su expresión en ADSC/HeLa: lnc-CXCL3, CXCL2, CXCL3, CXCL5 y CXCL10) en ADSC co-cultivadas con células Ca Ski o SiHa. Se determinó que las ADSC co-cultivadas con Ca Ski mostraron mayores niveles de estos RNAs, de manera similar a lo observado en el co-cultivo ADSC/HeLa (Figura 25). En el caso del co-cultivo de ADSC con células Ca Ski, la expresión del lnc-CXCL3 aumento (Figura 25a). Para los co-cultivos de ADSC con células SiHa, aumentó la expresión de CXCL5 y CXCL10 (Figura 25d y e) mientras que disminuyó la expresión de CXCL2 y CXCL3 (Figura 25b y c).

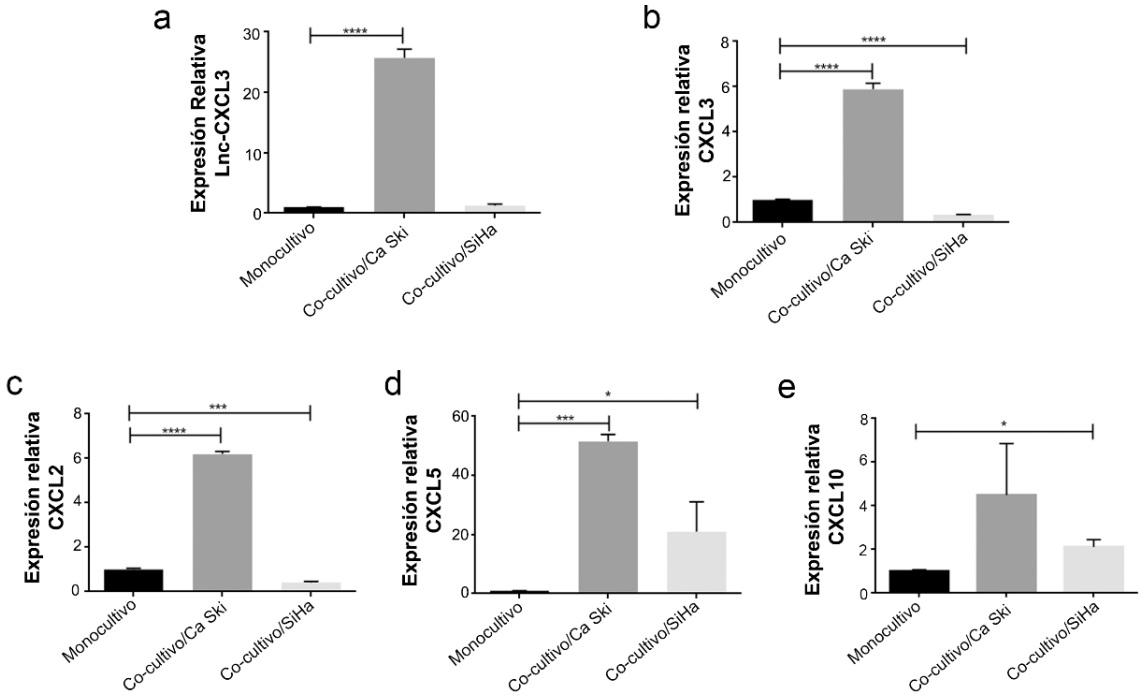

Figura 25. Expresión relativa de quimiocinas de ADSC en co-cultivo con células Ca Ski y en co-cultivo con células SiHa. Las barras representan el promedio ±SEM de tres experimentos independientes. El análisis estadístico se realizó con una prueba t-Student no pareada, considerando *p<0.05, ***p<0.01 y ****p<0.0001

7.3 El análisis del transcriptoma de ADSC posterior al co-cultivo con células HeLa, mostró cambios en vías que están relacionadas a procesos celulares relevantes

El gran número de moléculas que cambian su expresión en ADSC en presencia de células HeLa, sugiere un efecto a nivel funcional, por lo que se realizó el análisis integral del transcriptoma diferencial en ADSC en co-cultivo utilizando las herramientas Ingenuity Pathways Analysis (IPA), Gene Set Enrichment Analysis (GSEA) y Key Pathway Advisor (KPA). Estos análisis infieren cambios en procesos celulares, a partir de los cambios de expresión de mRNAs, que se alteran en la condición de co-cultivo. Como se muestra en la tabla 5, la regulación del ciclo celular, la respuesta inflamatoria y la reparación del DNA se identificaron como procesos celulares modificados en ADSC en co-cultivo, posiblemente en consecuencia de la comunicación intercelular. Cabe destacar que, algunos procesos celulares se predijeron por una sola herramienta informática, como la muerte celular por IPA; el desarrollo celular y el matrisoma por GSEA; y la angiogénesis y la troncalidad por KPA (Tabla 5).

Tabla 5. Procesos y funciones modificados en ADSC posterior al co-cultivo.

	IPA	GSEA	KPA
	No de moléculas	NES	P-value
Ciclo celular	109		1.14E-46
Citocinas y Sistema Inmune		3.2	5.25E-15
Replicación, recombinación y reparación del DNA	88		
Procesos del desarrollo			8.04E-21
Ensamble y organización celular	151		
Muerte y sobrevivencia celular	175		2.84E-06
Movilidad celular	125		1.14E-11
Reactoma de citocinas		2.6	1.15E-15
Matrisoma		2.03	
Proliferación			4.42E-27
Angiogenesis			0.004865

IPA: Ingenuity Pathways Analysis. GSEA: Gene Set Enrichment Analysis. KPA Key Pathway Advisor. NES: Normalized Enrichment Score.

Para confirmar los resultados inferidos por el análisis de procesos, se realizaron ensayos funcionales *in vitro.* Dado que las ADSC de pacientes, por ser un cultivo primario tiene un número limitado de pases antes de su diferenciación, optamos por utilizar la línea celular comercial de ADSC de ATCC (PC-500-011), aislada de tejido adiposo blanco de una mujer caucásica sana de 52 años con un IMC de 30.2 (obesidad). Esta línea celular muestra crecimiento adherente con morfología fibroblástica (Figura 26), con multipotencialidad hacia los linajes adipogénico, osteogénico y condrogénico.

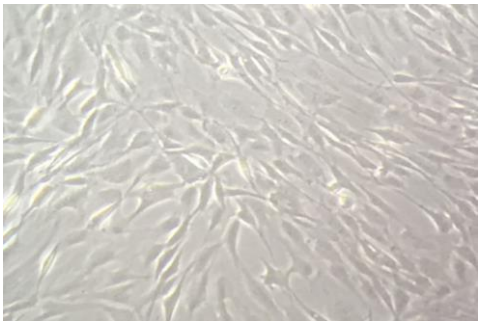

Figura 26. Morfología de la línea celular comercial de ADSC. Imagen representativa al 100% de confluencia. Microscopía óptica de campo claro, objetivo 40x.

Como primer paso, para evaluar si la línea celular ADSC de ATCC tenía un comportamiento similar al observado en las ADSC aisladas de pacientes con obesidad mórbida, se replicó el ensayo de co-cultivo con las ADSC de la línea comercial y las células HeLa bajo las mismas condiciones de experimentación. Posterior a la extracción de RNA, se evaluó en ambos grupos (ADSC monocultivo y ADSC co-cultivo con células HeLa) la expresión de las 10 moléculas anteriormente estudiadas para la validación. El análisis mostró que todos los RNAs evaluados presentaron una tendencia similar en los perfiles de expresión al compararse entre grupos (Tabla 6).

Tabla 6. Comparación de la expresión de 10 moléculas en ADSC de pacientes y ADSC de línea comercial, posterior al co-cultivo con HeLa.

Molécula	$ADSC_{Pacientes}$ Co–cultivo HeLa Tasa de cambio RNAseq	$ADSC_{ATCC}$ Co-cultivo HeLa Expresión relativa RT-qPCR
mRNAs		
BIRC3	6 ↑	7.4*** ↑
CXCL3	14 ↑	5.2 ↑
CXCL2	16 ↑	11.7↑
CXCL5	12 ↑	4.9** ↑
LncRNAs		
Lnc-BIRC3	15 ↑	17.8** ↑
Lnc-CXCL3	11 ↑	7.5** ↑
Linc00707	48 ↑	13.6* ↑
CTC-231º11.1	15.7 ↑	26.0*** ↑
Linc01569	-7 ↓	-2.5↓
RP11-138I17.1	-4 ↓	-0.9↓

±SEM de tres experimentos independientes. *p<0.05, **p<0.01 y ***p<0.001

Por lo tanto, los resultados demostraron que la línea celular comercial ADSC mostró un comportamiento similar a las ADSC de pacientes, por lo que se decidió utilizar esta para los ensayos funcionales.

7.4 El ciclo celular de ADSC no se afecta por la presencia de células HeLa durante el co-cultivo

Los cambios observados en el patrón de expresión de 109 moléculas de RNAs a través de las herramientas de análisis, sugirieron cambios en la regulación del ciclo celular (Tabla 5). Para comprobar esta predicción, se realizó un análisis de progresión del ciclo celular empleando BrdU, un análogo de la timina que determina de manera indirecta la población celular en cada fase del ciclo celular por citometría de flujo. Los resultados en ADSC co-cultivo y monocultivo indicaron que no existió diferencia significativa entre las poblaciones ($p>0.05$), ya que el 60.11% de ADSC en monocultivo y el 60.47% de ADSC en co-cultivo se encontraron en fase G0/G1 (Figura 27). Así mismo, fue interesante que ninguna de las dos condiciones favoreció la fase de proliferación S, que representó un 21.64% en monocultivo y un 20.7% en co-cultivo (Figura 27). La fase del ciclo celular G2/M mostró una población cercana al 18% en ambas condiciones de estudio (Figura 27). Esto sugiere que la presencia de células HeLa no afectó la progresión del ciclo celular.

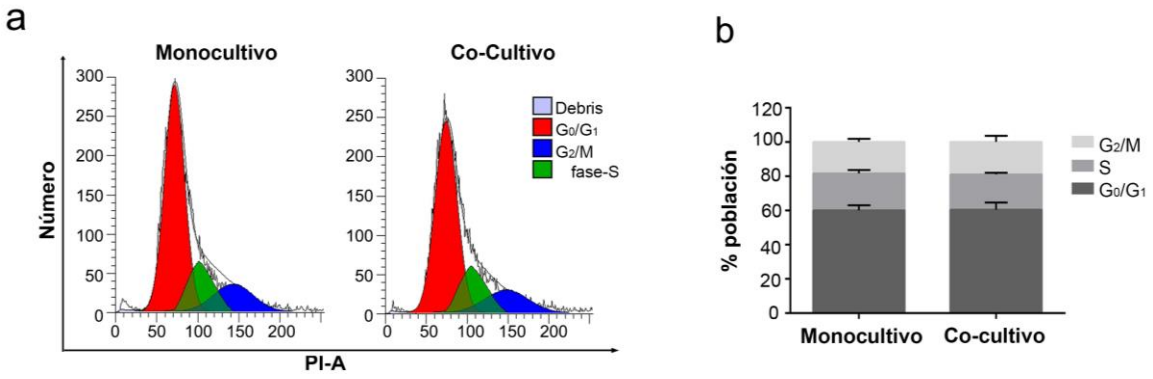

Figura 27. Cuantificación del porcentaje de las subpoblaciones de ADSC en las etapas del ciclo celular. a) Histograma con perfiles del ciclo celular de ADSC en monocultivo o co-cultivo. b) cuantificación de las subpoblaciones de ADSC en las fases del ciclo celular G0-G1, S, y G2-M

El cambio en los procesos celulares es la suma de la activación e inhibición de vías de transducción de señales que están cambiando a nivel celular. El análisis con KPA reveló el enriquecimiento de diversas vías de señalización relacionadas con proliferación celular (Tabla 5). Por un lado, se promovió la replicación del DNA a través de la activación de NF-κB (Anexo 12.6)[70], IL-6 (Anexo 12.7)[71] y AP-1 (Anexo 12.8)[72]; pero, por otro lado, se favoreció la actividad de STAT1 (Anexo 12.9) y CDK1 (Anexo 12.10), los cuales pueden

inhibir la proliferación[73,74] que podría conllevar a un efecto compensatorio y, por tanto, una respuesta neta neutral.

7.5 La presencia de células tumorales no afecta la apoptosis en ADSC

De acuerdo con el análisis del transcriptoma, la apoptosis es un proceso celular que se predijo estar alterado en ADSC en presencia de células HeLa, con 175 moléculas involucradas (Tabla 5). Para corroborar cambios en este proceso, posterior al co-cultivo se realizó un ensayo de TUNEL el cual permite identificar las células en apoptosis. El análisis señaló un bajo porcentaje de células en apoptosis en ambas condiciones con 1.5% en monocultivo y 3% en co-cultivo, sin presentar diferencias significativas entre ambas condiciones ($p>0.05$), debido posiblemente a la ausencia de un estímulo apoptótico (Figura 28).

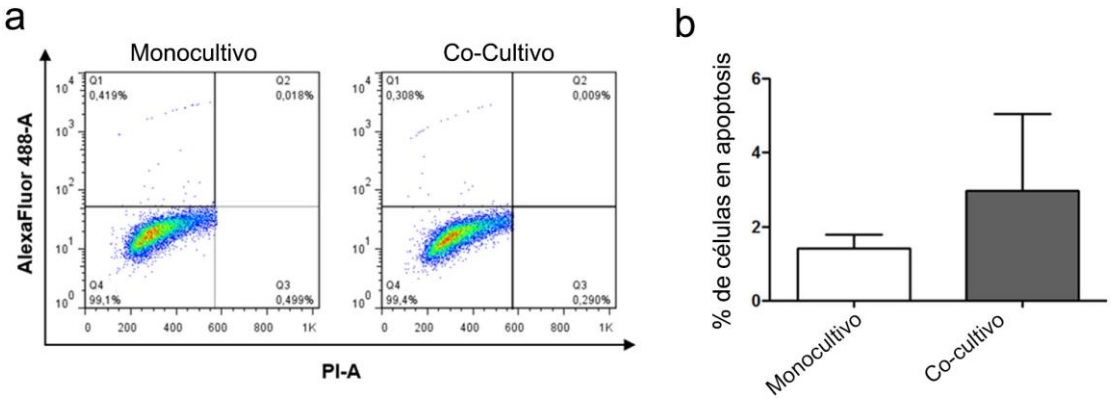

Figura 28. Apoptosis en ADSC posterior al co-cultivo con células HeLa. Ensayo TUNEL a) Gráficos de densidad de la subpoblación de ADSC en apoptosis (Q) posterior al monocultivo y co-cultivo respectivamente. b) Cuantificación de la población en apoptosis. Las barras representan el promedio ±SEM de tres experimentos independientes.

7.6 La capacidad de migración de las ADSC aumenta en co-cultivo con células HeLa

A través del análisis del transcriptoma, los datos identificaron a la migración como uno de los procesos celulares con mayor cambio en ADSC después de co-cultivarse con células de cáncer (Tabla 5). Para comprobarlo, se realizó el ensayo de cierre de herida en una monocapa de ADSC con alta confluencia. Se evaluó el área al cierre en distintas condiciones: medio condicionado de células HeLa (para determinar el cierre en presencia de los factores solubles propios de estas células), medio del co-cultivo ADSC/HeLa (para evaluar el cierre en presencia de los factores solubles propios de la comunicación y retroalimentación entre ambas líneas celulares), y medio condicionado de células HaCat, (para corroborar si el efecto

fue específico de las células tumorales). El área libre de células se determinó a las 12, 24 y 48 h; y se comparó con el área al cierre en presencia de medio suplementado con o sin SFB como control positivo y negativo, respectivamente (Figura 29).

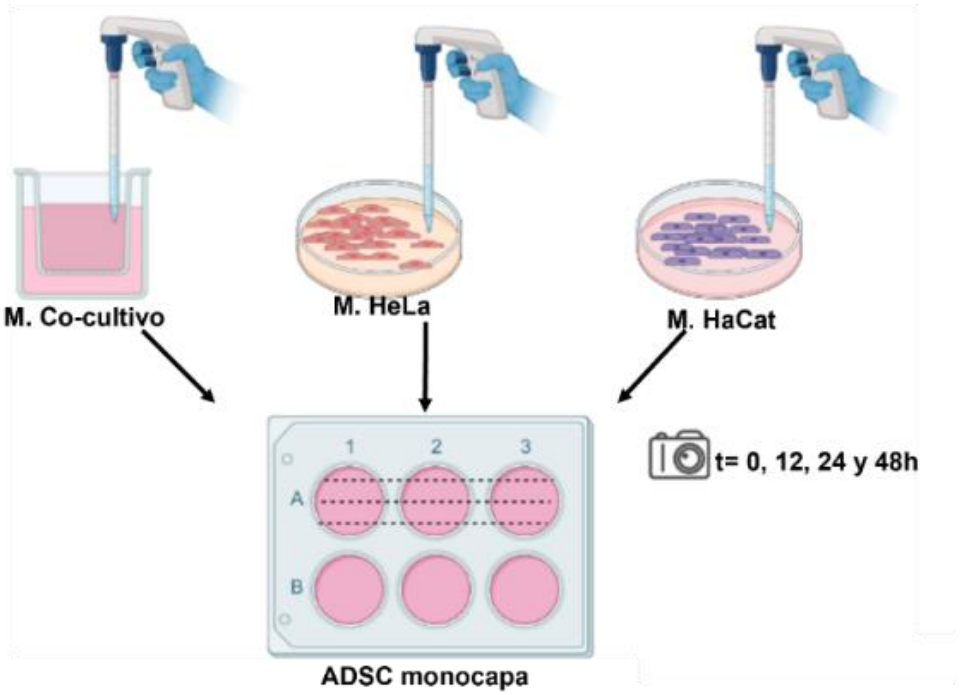

Figura 29. Ensayo del cierre de herida. *M. Co-cultivo* es el medio que compartieron las células ADSC/HeLa durante el co-cultivo de 24h. *M. HeLa* es el medio de mantenimiento de HeLa en monocultivo durante 24h en ausencia de SFB; M. HaCat es el medio de mantenimiento de HaCat en monocultivo durante 24h en ausencia de SFB. Una vez completados los tiempos de crecimiento, los medios fueron colectados y empleados en el ensayo del cierre de herida Creado con BioRender.com

Tanto el medio condicionado de células HeLa como el medio de co-cultivo ADSC/HeLa, aumentaron la capacidad de migración de las ADSC, alcanzando su máximo a las 24 y 48 h (Figura 30). El efecto en el cierre de herida fue similar al control positivo (medio suplementado con 5% SFB). En contraste, este efecto no se observó en las ADSC suplementadas con medio condicionado de células HaCaT (Figura 30).

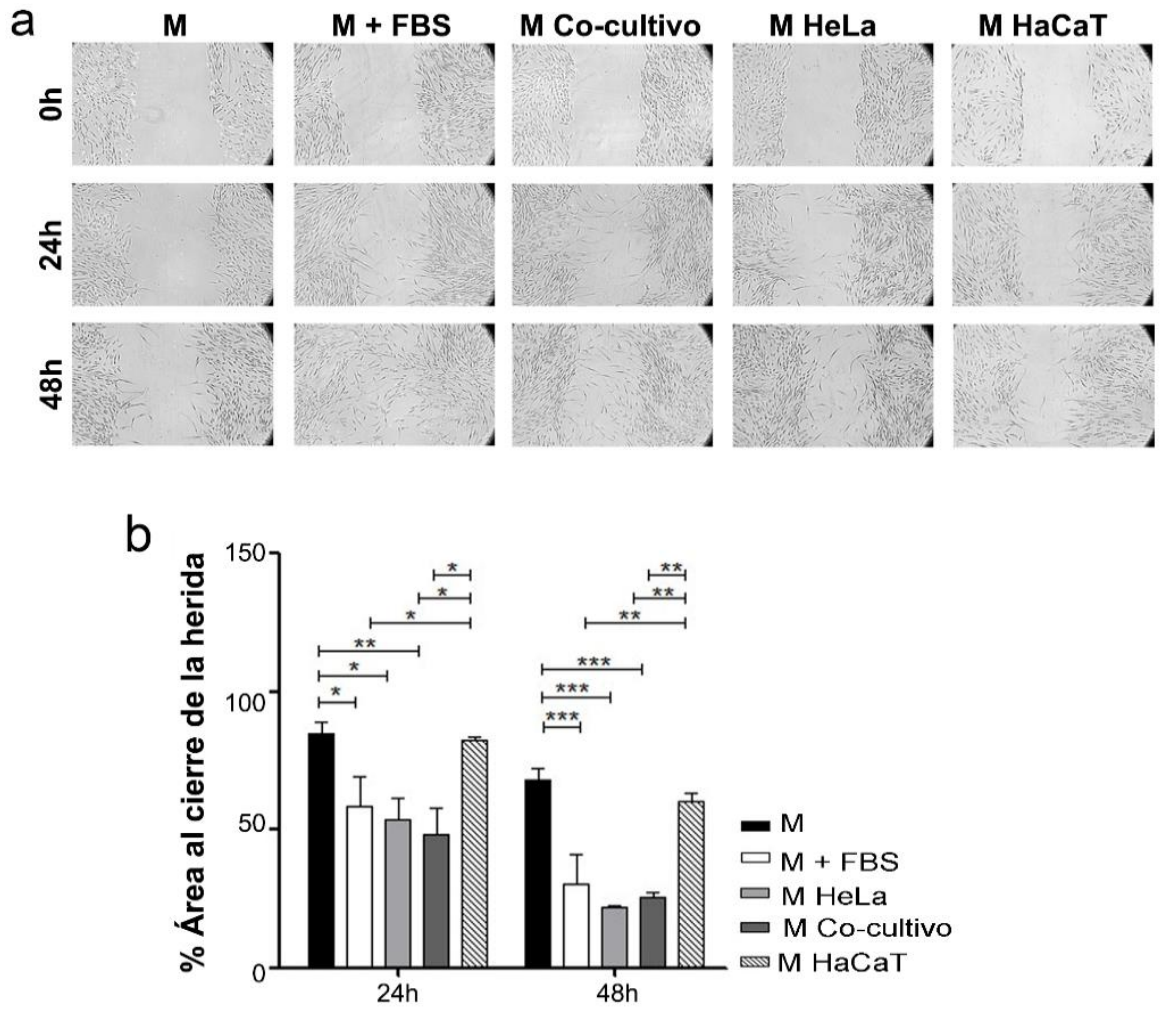

Figura 30. Área al cierre de la herida. a)Imágenes representativas del cierre de herida a las 24 y 48h en condiciones de medio libre de SFB (M), medio con 5% de SFB (M+FBS), medio condicionado de células HeLa (M HeLa),medio de co-cultivo ADSC/HeLa (M Co-cultivo), y medio condicionado de HaCaT (M HaCaT). B) Área normalizada al cierre de la herida. Las barras representan el promedio ±SEM de tres experimentos independientes. El análisis estadístico se realizó con una ANOVA de dos vías, considerando *p<0.05, **p<0.01 y ***p<0.001

Estos resultados concuerdan con los análisis de vías de transducción de señales inferidos a partir de los datos de RNAseq, los cuales demostraron un incremento en la expresión de los genes IL8/IRAKs/NF-κB e IL8/IRAKs/cSRC/FOS/AP-1, que participan en la capacidad de migración celular (Anexos 12.6 y 12.8).

7.7 El inmunofenotipo troncal en ADSC se mantiene posterior al co-cultivo con células HeLa

Dado que las ADSC expuestas a factores solubles derivados de células HeLa presentaron una mayor capacidad de migración, se decidió evaluar la troncalidad de ADSC.

Como primera aproximación, se comparó el inmunofenotipo de las ADSC en co-cultivo y monocultivo, a través de la expresión de las proteínas de superficie CD31, CD44, CD45 y CD90. Aunque se observó un discreto aumento en la población de ADSCs que expresó CD31, no hubo una diferencia significativa ($p>0.05$) en ninguno de los marcadores entre las poblaciones, por lo que el inmunofenotipo troncal se mantuvo como CD31-, CD44+, CD45-, CD90+ después del co-cultivo de 24h (Figura 31).

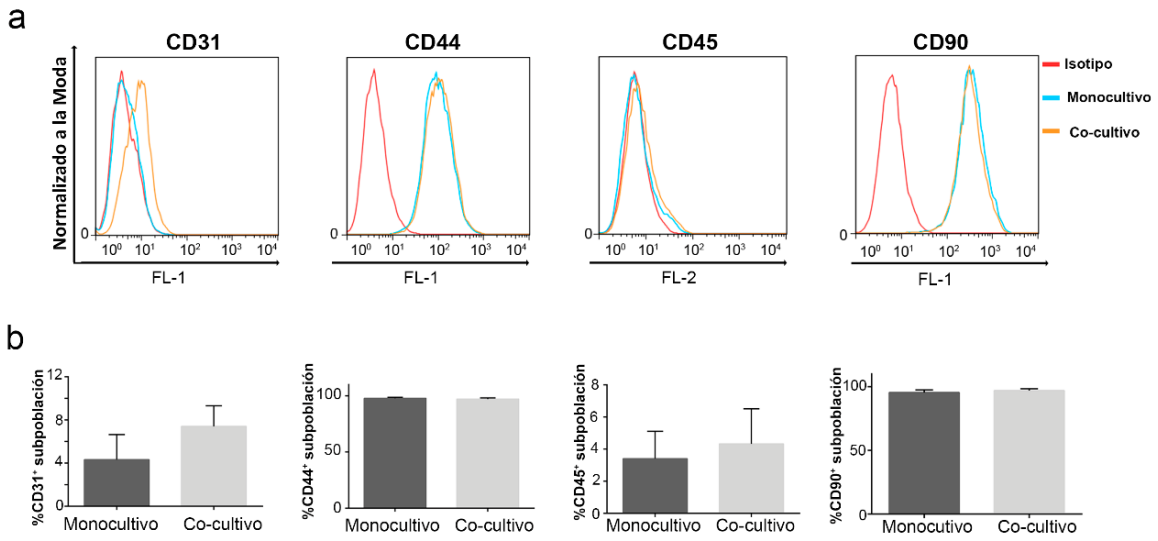

Figura 31. Caracterización del inmunofenotipo de ADSC en monocultivo y co-cultivo con células HeLa. a) Histogramas representativos del análisis por citometría de ADSC en monocultivo (azul) y co-cultivo (naranja). El isotipo se muestra en rojo. b) Cuantificación de células positivas CD31, CD44, CD45 y CD90 de ADSC en monocultivo y co-cultivo. Las barras representan el promedio ±SEM de tres experimentos independientes. El análisis estadístico se realizó con una prueba t-Student no pareada

7.8 Las células ALDH^{high} aumentan en las ADSC durante el co-cultivo con células HeLa

La alta actividad de la enzima ALDH (ALDH^{high}) es considerada un marcador de diversos tipos de células troncales, tanto normales como tumorales, por lo que se utiliza para identificar esta población[75,76]. Como resultado del análisis del transcriptoma de ADSC en co-cultivo, los 4 genes ALDH (ALDH1B1, ALDH3A1, ALDH3A2, ALDH3B1), presentaron un aumento en sus niveles de expresión, especialmente ALDH3A1 con una razón de cambio

de 113, por lo que se analizó este marcador en el modelo de co-cultivo ADSC/HeLa (Figura 32a).

Los resultados mostraron un incremento en el número de células ALDH^{high} (2.5%) en ADSC en co-cultivo, casi al doble en comparación a ADSC en monocultivo (1.4%), siendo constante a través de las réplicas y estadísticamente significativo (p>0.05) (Figura 32b y c).

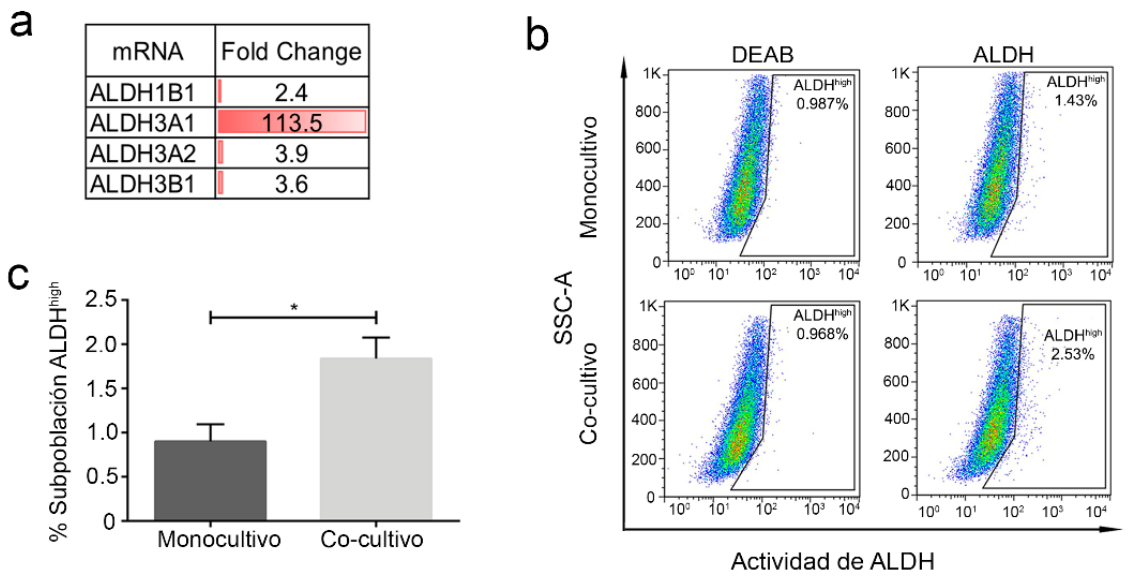

Figura 32. Evaluación de la población ALDH^{high} en ADSC posterior al co-cultivo con células HeLa. a) Incremento en la expresión de las isoformas de ALDH en ADSC después del co-cultivo. b) Gráficos de densidad de la subpoblación ALDH^{high} en ADSC en monocultivo y co-cultivo. DEAB (N,N-dietil aminobenzaldehido), inhibidor de la actividad de ALDH c) Análisis de la subpoblación ALDH^{high} en ADSC en monocultivo y co-cultivo. Las barras representan el promedio ±SEM de tres experimentos independientes. El análisis estadístico se realizó con una prueba t-Student no pareada, considerando *p<0.05

Aunque la diferencia en el porcentaje de la población ALDH^{high} fue pequeño al comparar ADSC co-cultivo con respecto al monocultivo, el potencial de esta población para producir cambios biológicamente significativos en la totalidad de la población celular puede ser considerable. Para comprobar las implicaciones biológicas del cambio en los niveles de ALDH, se evaluó la capacidad de formación de esferas de ADSC en co-cultivo con células HeLa. Las ADSC se cultivaron en presencia de células HeLa durante 24 h para posteriormente someterlas a condiciones no adherentes durante 15 días. Se observó que las ADSC posterior al co-cultivo produjeron un número similar de esferas que las ADSC en monocultivo. Sin embargo, las esferas provenientes de ADSC en co-cultivo, presentaron diámetros significativamente mayores con respecto al grupo control (p<0.01) (Figura 33).

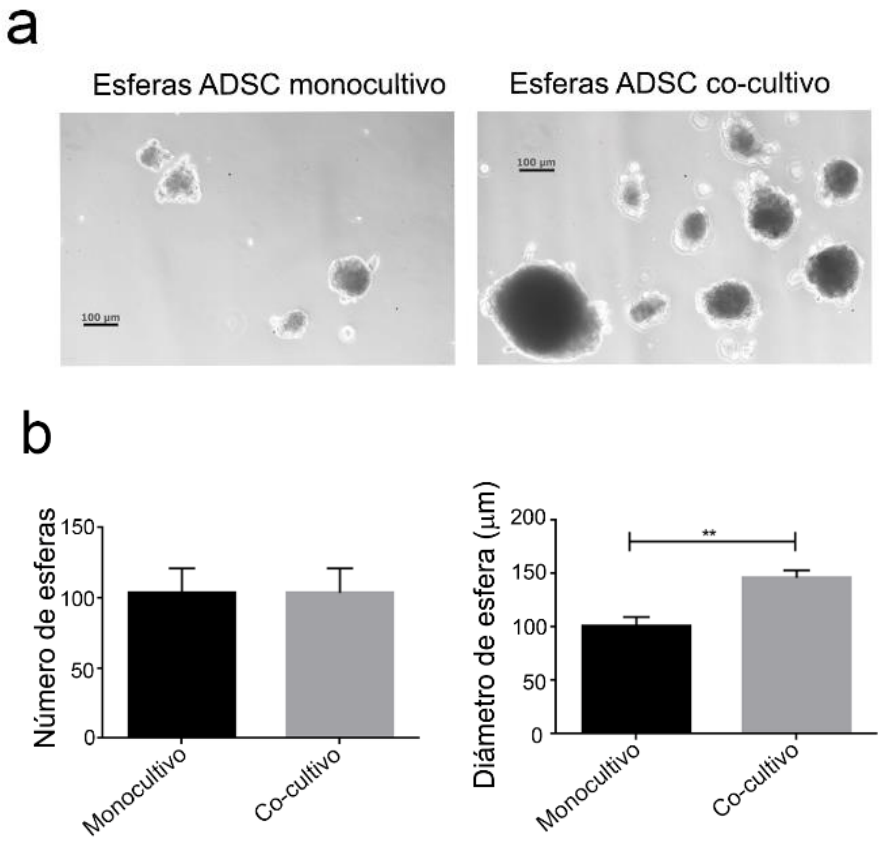

Figura 33. Ensayo de formación de esferas de ADSC posterior al co-cultivo con células HeLa. a)fotografías representativas de esferas de ADSC formadas al día 15 posterior al monocultivo o co-cultivo con células HeLa. Microscopio óptico, microscopía de campo claro, objetivo 10x, barra de escala = 10µm. b) Cuantificación del número y tamaño de esferas de ADSC posterior al monocultivo o co-cultivo con HeLa. Las barras representan el promedio ±SEM de tres experimentos independientes. El análisis estadístico se realizó con una prueba t-Student no pareada, considerando **p<0.01

7.9 La comunicación intercelular ADSC/HeLa está mediada por quimiocinas

Los factores solubles son mediadores de la comunicación intercelular en ausencia de contacto directo. El análisis del transcriptoma de ADSC en co-cultivo con células HeLa mostró una expresión diferencial de 31 citocinas y quimiocinas que funcionan como señales de comunicación intercelular (Figura 34).

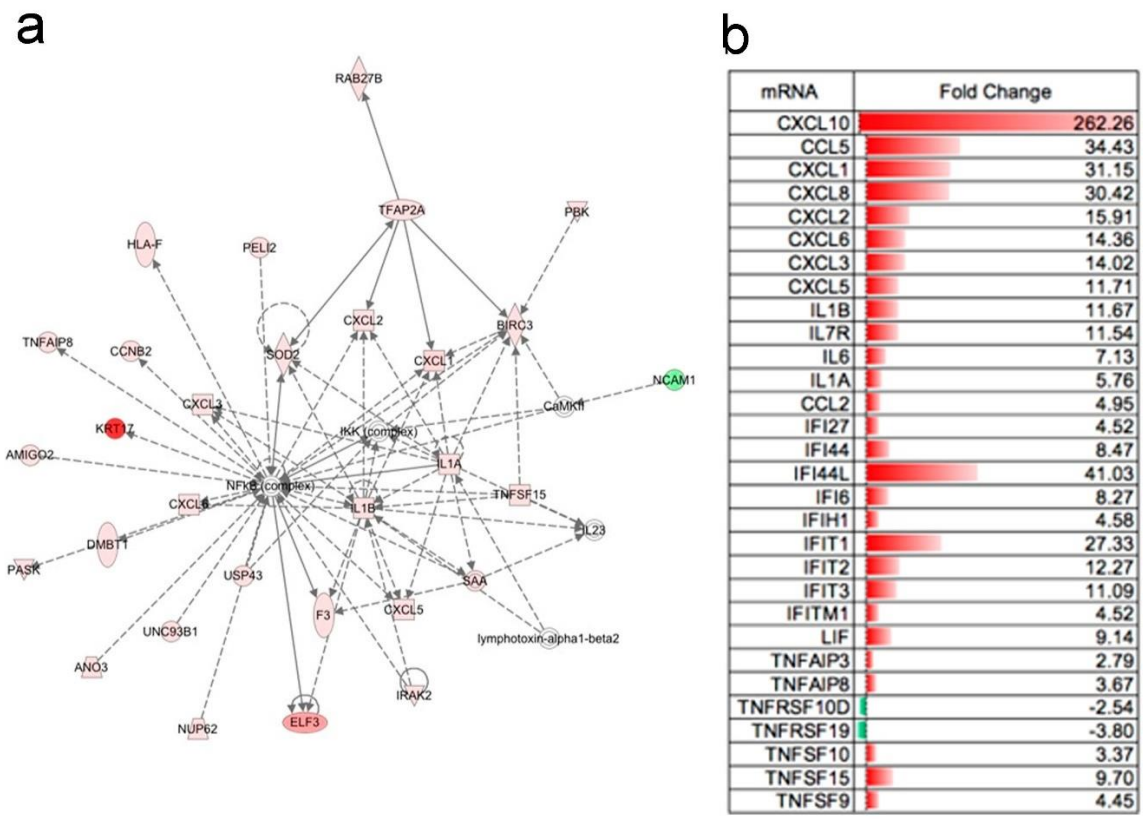

mRNA	Fold Change
CXCL10	262.26
CCL5	34.43
CXCL1	31.15
CXCL8	30.42
CXCL2	15.91
CXCL6	14.36
CXCL3	14.02
CXCL5	11.71
IL1B	11.67
IL7R	11.54
IL6	7.13
IL1A	5.76
CCL2	4.95
IFI27	4.52
IFI44	8.47
IFI44L	41.03
IFI6	8.27
IFIH1	4.58
IFIT1	27.33
IFIT2	12.27
IFIT3	11.09
IFITM1	4.52
LIF	9.14
TNFAIP3	2.79
TNFAIP8	3.67
TNFRSF10D	-2.54
TNFRSF19	-3.80
TNFSF10	3.37
TNFSF15	9.70
TNFSF9	4.45

Figura 34. **Expresión de citocinas y quimiocinas en ADSC durante el co-cultivo con células HeLa.** a) Moléculas diferencialmente expresadas en ADSC en co-cultivo con células HeLa relacionadas con la vía NF-κB. En rojo, incremento de su expresión; en verde, disminución de su expresión. B)Tasa de cambio de citocinas y quimiocinas en ADSC en co-cultivo con células HeLa.

Por lo tanto, se validaron las quimiocinas CXCL2, CXCL3 y CXCL5 en los medios obtenido de co-cultivos o monocultivos. Acorde a lo esperado, CXCL2 y CXCL3 aumentaron en los medios de cultivo provenientes de co-cultivos de ADSC (Figura 35a y b), lo que correlaciona con el aumento de los niveles de mRNAs observados por RT-qPCR. Por su parte, CXCL5 presentó un aumento discreto no significativo en estas condiciones ($p>0.05$) (Figura 35c). Además, de manera interesante se ha reportado que la expresión de CXCL2 ($p = 0.046$), CXCL3 ($p = 0.017$) y CXCL5 ($p = 0.011$) puede asociarse a un peor pronóstico en pacientes con cáncer cervical, ya sea de células escamosas o adenocarcinoma[77] (Figura 35a, b y c). De igual modo, se corroboró el aumento en la expresión de la quimiocina CXCL10 en ADSC posterior al co-cultivo con células HeLa, la cual se asocia a un menor porcentaje de sobrevida ($p = 0.16$) posterior a los 4 años de enfermedad (Figura 35d).

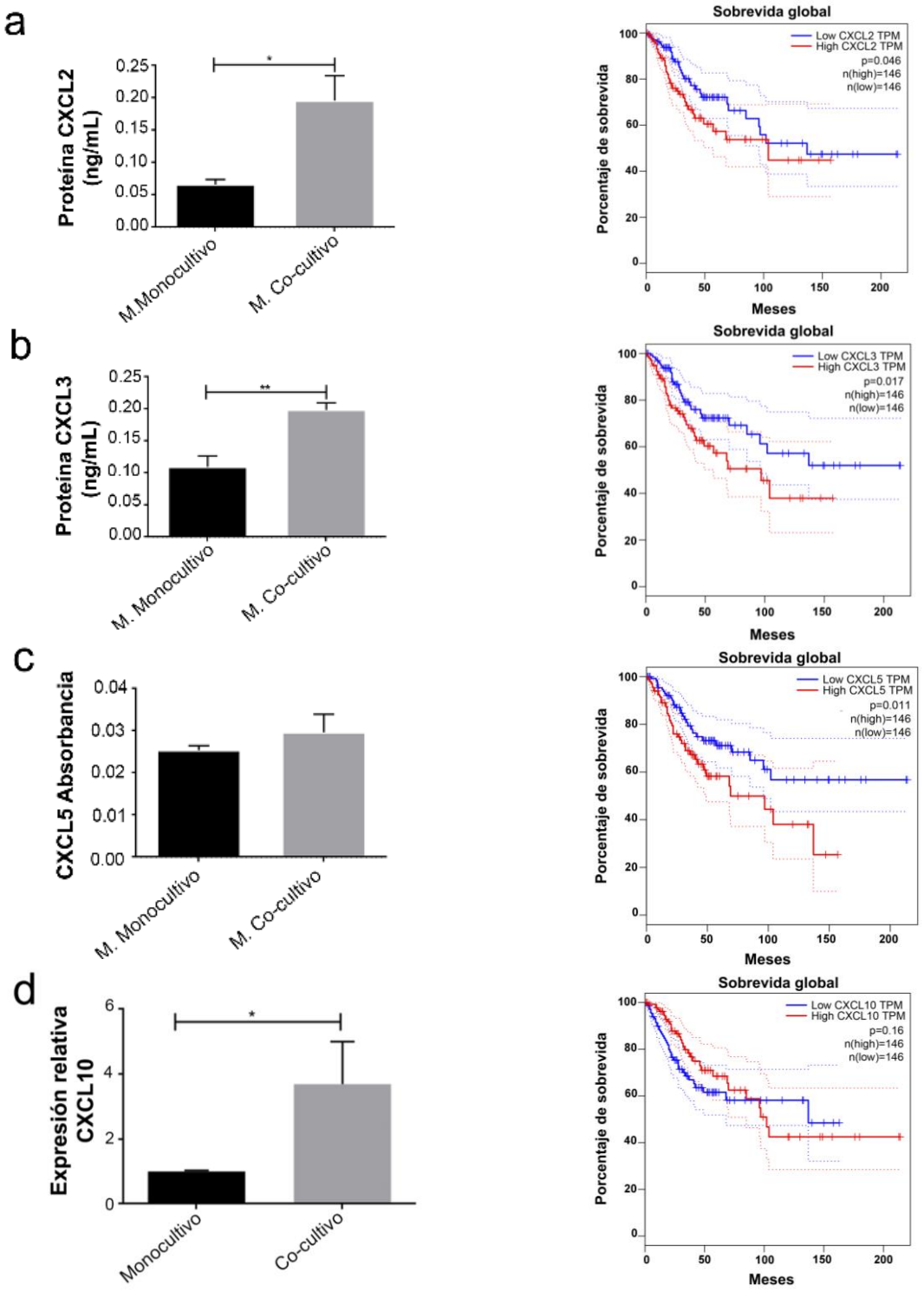

Figura 35. **Cuantificación de quimiocinas presentes en el medio posterior al co-cultivo y su relación con la sobrevida global de pacientes con cáncer cervical.** Cuantificación por ELISA de quimiocinas presentes en el medio de monocultivo de ADSC ó co-cultivo ADSC/HeLa y su asociación con la sobrevida global de pacientes con cáncer cervical para a) CXCL2, b) CXCL3, c) CXCL5 y d) CXCL10. Las barras representan el promedio ±SEM de tres experimentos independientes. Se realizó con una prueba t-Student no pareada, considerando *p<0.05 y **p<0.01. GEPIA. Tomada y modificada de *W. Kong et al.* [77]

7.10 La expresión del lnc-CXCL3 tiene un efecto en las características de troncalidad de las células semejantes a ADSC

Las quimiocinas con un aumento en su expresión en ADSC co-cultivo se asociaron a un peor pronóstico de cáncer cervical (Figura 35). Entre estas destaca CXCL3 por presentar el lncRNA intragénico lnc-CXCL3 (Figura 22) también con un aumento en su expresión bajo la misma condición. Debido a que los lncRNAs pueden regular procesos celulares a distintos niveles, fue de interés evaluar la participación del lnc-CXCL3 en el fenotipo troncal.

Para evaluarlo, se inhibió de manera estable la expresión del lnc-CXCL3 en 3T3-L1, una línea celular de fibroblastos aislada de ratón y en sustitución de las ADSC ya que las ADSC fueron de difícil transfección. Las células 3T3-L1 tienen una alta capacidad de diferenciación a adipocitos, por lo que se han utilizado ampliamente en investigación como modelo de células tipo ADSC[78].

La inhibición de lnc-CXCL3 en 3T3-L1 se corroboró por RT-qPCR empleando el shRNAs sh-lncCXCL3-1 previamente diseñado (Anexo 12.5), con una evidente inhibición de los niveles del lncRNA (Figura 36a). Posteriormente, la expresión de CXCL3 se detectó en células 3T3-L1 transfectadas con el plásmido control, pero no tras el knockdown de lnc-CXCL3 lo que sugiere que la inhibición del lncRNA llevó a la expresión de CXCL3 a niveles no detectados (dato no mostrado).

Como siguiente paso, se estudió el efecto de la inhibición de lnc-CXCL3 sobre características relacionadas a la troncalidad en células 3T3-L1. Se observó que la inhibición de lnc-CXCL3 disminuyó el tamaño de esferas, aproximadamente en un 20% (Figura 36c y d); así como el número de esferas aproximadamente en un 50%, al comparar con las células transfectadas con el plásmido control (Figura 36c y e).

Finalmente, la formación de esferas está estrechamente relacionada con la troncalidad celular y con la población de células $ALDH^{high}$. En específico, ALDH1A3 es un importante regulador de este fenotipo, tanto en las células inmortalizadas como en células precursoras[79,80]. En el presente estudio, se observó que la expresión de ALDH1A3 disminuyó drásticamente tras la inhibición de lnc-CXCL3 (Figura 36b), por lo que, en conjunto, estos resultados demuestran que lnc-CXCL3 está implicado en la regulación de las características funcionales y moleculares de las células troncales 3T3-L1.

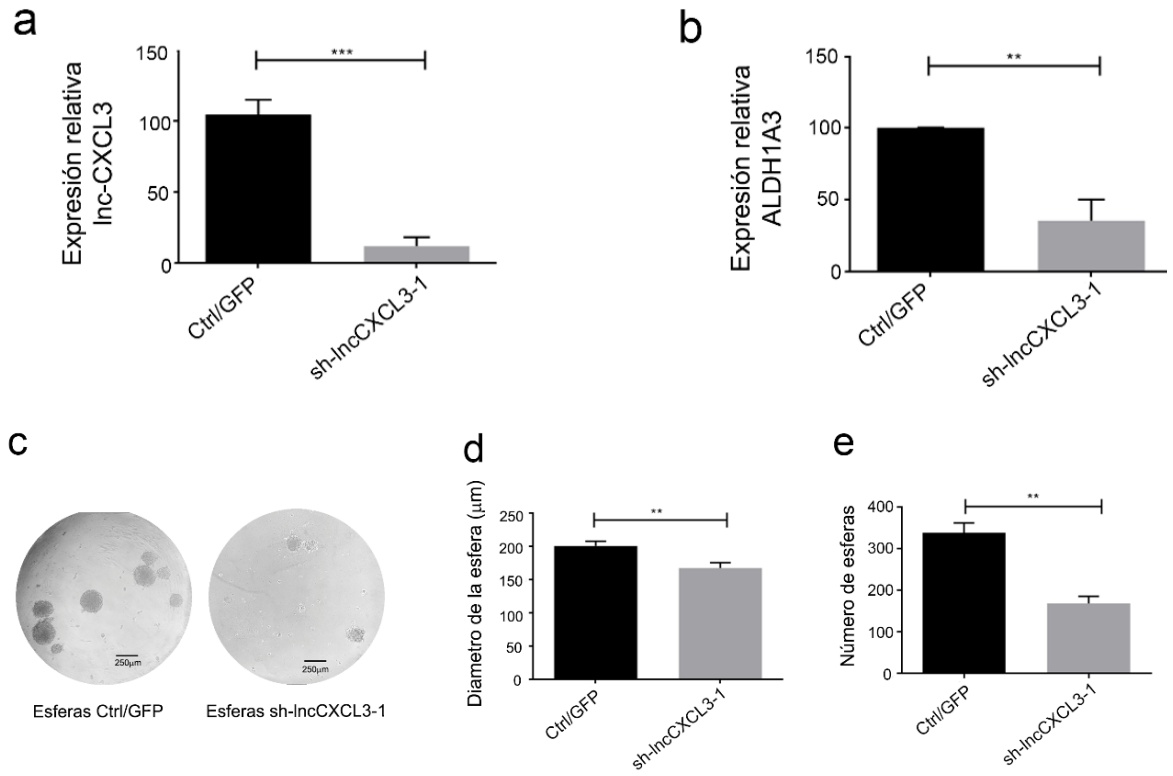

Figura 36. La inhibición de lnc-CXCL3 en 3T3-L1 afecta a las características de troncalidad. Transfección estable de los plásmidos pSIRENT-RetroQ con el sh-lncCXCL3-1 ó el plásmido control pGFP-V-RS en 3T3-L1. Evaluación por RT-qPCR de la expresión del lnc-CXCL3 posterior a la transfección. b) Evaluación por RT-qPCR de la expresión del ALDH1A3 posterior a la transfección. c) Fotografías representativas de las esferas de 3T3-L1 al día 15 posterior a la transfección. Magnificación con el objetivo 10x, barra de escala = 250µM. d) cuantificación del tamaño de las esferas. e) cuantificación del número de esferas. Las barras representan el promedio ±SEM de tres experimentos independientes. El análisis estadístico se realizó con una prueba t-Student no pareada, considerando **p<0.01 y ***p<0.001

7.11 La inhibición de la expresión del lnc-CXCL3 afecta la migración de células HeLa

Una vez que se determinó que la inhibición del lnc-CXCL3 disminuyó las características de troncalidad en células 3T3-L1, se analizó el efecto de esta inhibición en HeLa para determinar si también este lncRNA regula características en las células tumorales. En específico, se evaluó la migración, dado que esta capacidad se favoreció en ADSC co-cultivo con células HeLa.

Empleando los shRNAs sh-lncCXCL3-1 y sh-lncCXCL3-2 previamente diseñados (Anexo 12.5), se inhibió de manera estable la expresión del lnc-CXCL3 en células HeLa, el cual se confirmó por RT-qPCR (Figura 37a).

Posteriormente, se evaluó su capacidad de migración mediante un sistema transwell. Se observó que el número de células que migró a través de la membrana disminuyó significativamente ($p<0.001$) cuando se silenció la expresión de lnc-CXCL3 (Figura 37b y

c). Esto demostró que lnc-CXCL3 favorece la capacidad de migración de las células de cáncer cervical.

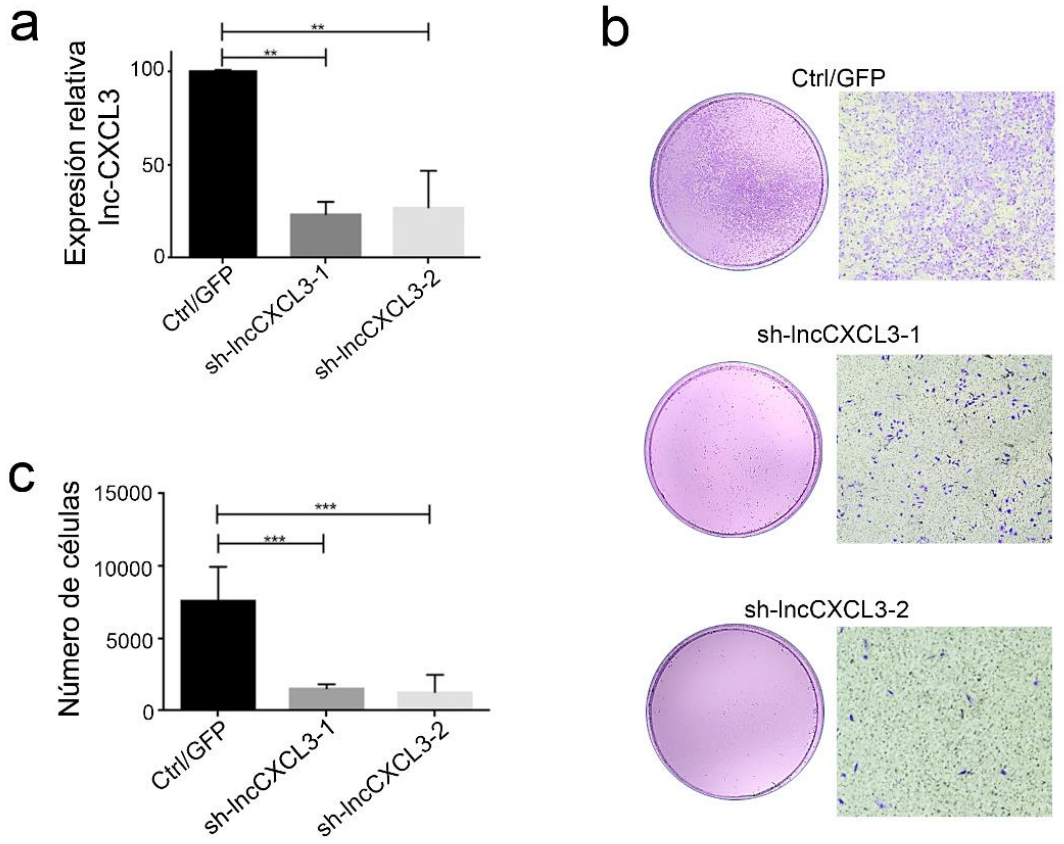

Figura 37. **La inhibición de lnc-CXCL3 afecta la capacidad de migración de células HeLa.** Las células HeLa fueron transfectadas transitoriamente empleando pSIREN-RetroQ o pGFP-V-RS como plásmido control. a) confirmación de la inhibición evaluando la expresión relativa de lnc-CXCL3 por RT-qPCR. b) La migración en células HeLa (inhibido lnc-CXCL3) fue evaluada con sistema transwell. Imágenes representativas a las 24 h y magnificadas 10x. c) cuantificación de células HeLa que migran posterior a la inhibición del lnc-CXCL3. Las barras representan el promedio ±SEM de tres experimentos independientes. El análisis estadístico se realizó con una ANOVA de dos vías seguida de Dunnett para comparaciones múltiples, considerando **p<0.01 y ***p<0.001

7.12 La expresión de quimiocinas es regulada por el lnc-CXCL3

Los lncRNAs pueden desempeñar un papel clave en la regulación transcripcional de genes cercanos. De manera particular, los mRNAs puede coexpresarse con su correspondientes lncRNAs intragénicos. Dado que los resultados de RNAseq indicaron que tanto CXCL3 como su lncRNA intragénico lnc-CXCL3 están modificados (Figura 22), fue de interés conocer si existía una coexpresión.

El gen CXCL3 se localiza en brazo q del cromosoma 4, dentro de la región 74.902.786-74.904.524 (GRCh37/h19) (Figura 38a), produciendo un transcrito maduro de 1641 pb de tamaño. En la región genómica adyacente a este gen, se localiza CXCL2 y CXCL5, a 37 912 y 43 047 bases respectivamente, con respecto a CXCL3 (con base en la secuencia de referencia GRch38.p14) (Figura 38b)

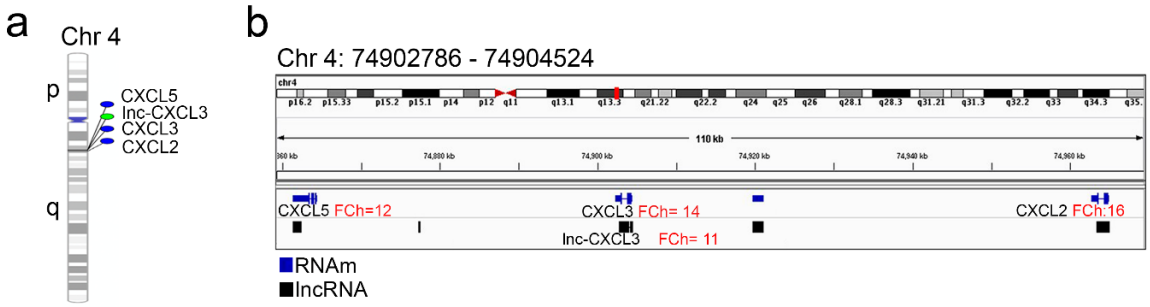

Figura 38. Localización genómica de los genes CXCL2, CXCL3, CXCL5 y el lncRNA intragénico lnc-CXCL3. a) Fenograma que muestra la ubicación génica de las moléculas interés dentro del brazo q del cromosoma 4. b) representación esquemática del locus 74902786-74904524 del cromosoma 4 donde se identifica la posición de los genes de las moléculas interés; las cajas en azul representan los transcritos codificantes y las cajas en negro los transcritos no codificantes.

Para evaluar la coexpresión de las quimiocinas CXCL2, CXCL3, CXCL5 con el lnc-CXCL3, se inhibió la expresión del lncRNA a partir de las transfecciones transitorias en células HeLa con sh-lncCXCL3-1 y sh-lncCXCL3-2 (Anexo 12.5). Se observó que ambas moléculas fueron capaces de silenciar la expresión de lnc-CXCL3 (Figura 39a). Posteriormente, se evaluó el efecto de la inhibición de lnc-CXCL3 sobre el nivel de expresión de CXCL3, CXCL2 y CXCL5. Los resultados mostraron que el silenciamiento de lnc-CXCL3 indujo la disminución concordante con la expresión de CXCL3 y CXCL2 (Figura 39b y c), mientras que para CXCL5 no fue estadísticamente significativa ($p>0.05$) (Figura 39d). Esto sugiere que lnc-CXCL3 es capaz de regular la expresión de al menos dos de los mRNAs de su vecindad genómica (CXCL2 y CXCL3).

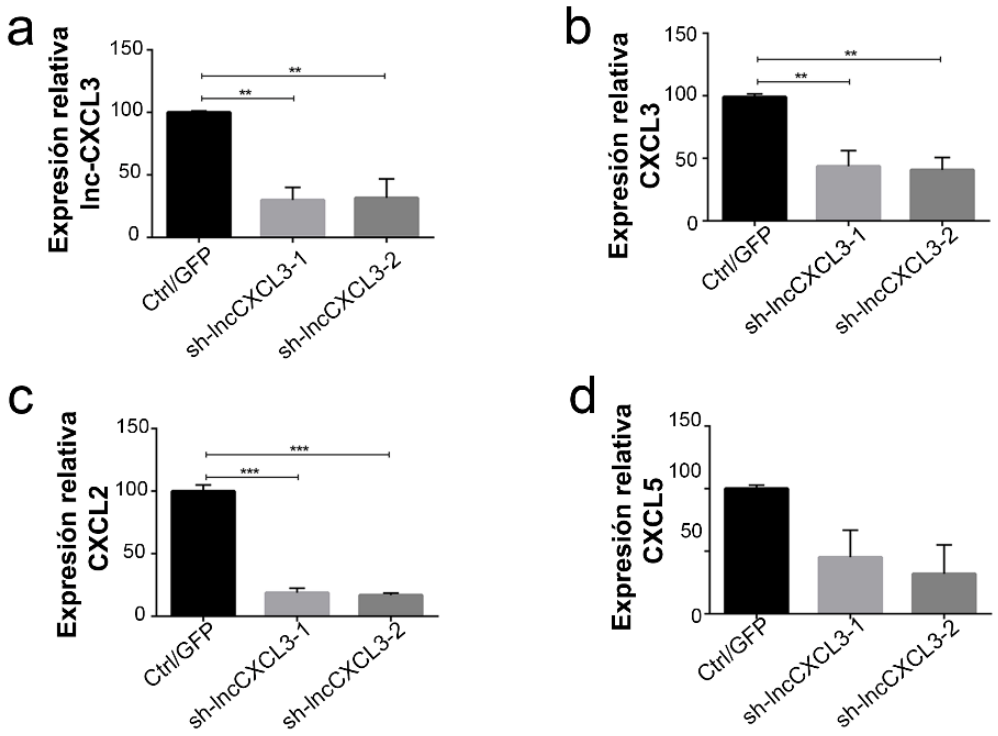

Figura 39. La inhibición de la expresión de lnc-CXCL3 en HeLa y su efecto en la expresión relativa de sus transcritos vecinos. a) expresión relativa de lnc-CXCL3 tras la inhibición con las moléculas sh-lncCXCL3-1 y sh-lncCXCL3-2. b) Expresión relativa de CXCL3 posterior a la inhibición de lnc-CXCL3. c) Expresión relativa de CXCL2 posterior a la inhibición de lnc-CXCL3. d) Expresión relativa de CXCL5 posterior a la inhibición de lnc-CXCL3. La expresión relativa se evaluó por RT-qPCR. Las barras representan el promedio ±SEM de tres experimentos independientes. El análisis estadístico se realizó con una ANOVA de dos vías, seguida de Dunnett para comparaciones múltiples, considerando **$p<0.01$ y ***$p<0.001$

8. DISCUSIÓN

La comorbilidad de enfermedades afecta la calidad y expectativa de vida en la población mundial, donde el financiamiento en investigación y tratamientos para su estudio genera una demanda económica con mayor impacto en países en vías de desarrollo.

La obesidad, junto con las enfermedades del corazón y la diabetes, son consideradas un problema de salud en México, dado su aumento y prevalencia en la población en los últimos años. Esta condición se relaciona con un mayor riesgo de padecer ciertos tipos de cáncer e incluso con un peor pronóstico de la enfermedad.

En este sentido, el estudio y el reconocimiento del tejido adiposo como agente etiológico de la obesidad, adquiere un mayor interés entre la comunidad científica, con la intención de comprender como este tejido puede orquestar fenómenos moleculares que afectan al proceso oncológico. En particular, un gran esfuerzo se ha dirigido para analizar su composición celular y su participación específica, dentro la cual se describe a la población troncal del tejido adiposo denominada ADSC.

En los últimos años, el estudio de las ADSC ha generado interés debido a sus potenciales aplicaciones clínicas e implicaciones en varias enfermedades, incluido el cáncer. Una característica importante de las ADSC es que, generalmente están ausentes en la sangre de individuos sanos, pero pueden incrementar su presencia tras estímulos patológicos como la hipoxia y la inflamación, lo que conlleva a su movilización y migración desde su nicho original[81].

La obesidad es un estado inflamatorio que favorece la movilidad de las ADSC, por lo que, los individuos obesos frecuentemente presentan un mayor número de estas células circulantes en comparación con individuos de talla normal. La movilización de ADSC también se favorece en individuos no obesos diagnosticados con cáncer, lo que indica que el desarrollo tumoral estimula la movilización de ADSC. Por lo tanto, esto explica porque en individuos obesos con cáncer aumentan aún más el número de ADSC circulantes[43].

Dado que las células tumorales no pueden sostener y llevar a cabo el crecimiento tumoral de manera autónoma, se sabe que reclutan células mesenquimales que permiten construir y dar soporte a su microambiente tumoral[82]. En varios trabajos se ha analizado como las ADSC participan en la promoción y la progresión del cáncer a través de su

establecimiento en el microambiente tumoral, donde producen y secretan diversos factores extracelulares. Sin embargo, poco se sabe sobre los cambios moleculares y celulares que experimentan las ADSC en este contexto. Como resultado de la comunicación intercelular a partir de factores solubles, las células tumorales regulan cambios a nivel transcripcional en ADSC y a su vez, las ADSC generan una respuesta a esta señalización en una amplia comunicación entre ambas poblaciones.

En el presente trabajo, las ADSC se aislaron de tejido adiposo visceral de pacientes con obesidad mórbida, que si bien, posee el mismo patrón de secreción de quimiocinas, citocinas y factores de crecimiento que el tejido adiposo subcutáneo, los niveles de expresión varían, siendo mayor en el visceral[83,84]. Estas células demostraron tener un fenotipo característico de células mesenquimales al ser adherentes y con morfología fibroblastoide, además de la expresión de moléculas de superficie y su capacidad de diferenciación (Figura 15, 16 y 23).

Teniendo en cuenta la comunicación bidireccional entre las ADSC y las células tumorales dentro del microambiente tumoral, en este trabajo se analizaron los cambios en el transcriptoma de las ADSC co-cultivadas con células de cáncer cervical utilizando un sistema transwell. En este modelo una membrana permeable permite la comunicación mediante el libre tránsito de factores solubles y exosomas derivados de ambos tipos celulares (Figura 17). De este modo, las ADSC pueden evaluarse sin riesgo de contaminación con células tumorales. El RNA total de las ADSC co-cultivadas se utilizó para el análisis masivo del transcriptoma (Figura 18), lo cual reveló cambios importantes en el perfil de expresión, incluyendo transcritos codificantes y no codificantes, al compararse con el transcriptoma de ADSC en monocultivo (Figura 19 y 20).

Al realizar la caracterización del transcriptoma diferencialmente expresado en ADSC en co-cultivo, el 90% de las moléculas pertenecieron a RNAs codificantes y solo el 10% a ncRNAs. Esto puede deberse a que los ncRNAs actúan como reguladores a distintos niveles, interaccionando con varios blancos simultáneamente. Tal es el caso de los lncRNAs, donde un discreto cambio en sus niveles de expresión puede generar una respuesta amplificada en la regulación de procesos importantes[64].

Al analizar el transcriptoma codificante de ADSC en co-cultivo, un gran número de transcritos aumentaron su expresión en esta condición. Posteriormente, a partir de los cambios en el transcriptoma, se identificaron los posibles procesos celulares y vías de

transducción de señales modificadas (Tabla 5). El análisis bioinformático por enriquecimiento demostró que procesos como el ensamblaje, la organización, la movilidad, el ciclo celular, la muerte y la sobrevivencia celular se modificaron en la condición de ADSC en co-cultivo, por tal motivo se decidió estudiarlos.

A pesar de que varios genes asociados a la regulación del ciclo y la proliferación se modificaron en las ADSC tras el co-cultivo con células de cáncer cervical, al analizar las poblaciones en las distintas etapas del ciclo celular, se determinó que las células se encontraban principalmente en fase G0/G1 (Figura 27). Lo anterior corresponde a un estado celular no proliferativo, es decir, la condición de co-cultivo no favoreció la capacidad de proliferación, y no existió una diferencia significativa en comparación con el grupo control. A pesar de que se activaron vías de señalización relacionadas con la proliferación (NF-κB, IL-6 y AP1), también aumentaron los niveles de STAT1 y CDK1, lo que posiblemente contrarrestó el efecto proliferativo y dio como resultado un proceso celular sin cambios (Anexo 12.6-12.10). Esto es similar a lo que se reportó en MSC expuestas a medio condicionado de FaDu (línea celular de carcinoma hipofaríngeo) en donde posterior a 5 días bajo esta condición, se observó un arresto en G0/G1 de la población y una disminución de la fase G2/M[85]. Estos resultados reiteran la importancia de considerar no solo los cambios en las vías de señalización, sino también la interacción entre estas y su impacto en el proceso celular.

Por otro lado, el análisis transcripcional de ADSC en co-cultivo predijo la muerte y sobrevivencia celular como procesos alterados (Tabla 5). En relación a esto, las ADSC confieren un efecto protector anti-apoptótico a fibroblastos de piel bajo condiciones de estrés (envejecimiento), en parte por moléculas secretadas que, a su vez, pueden actuar sobre las mismas ADSC en un circuito de retroalimentación[86]. Existen estudios que señalan que el efecto protector contra apoptosis inducido por peróxido en células ADSC es mediado por la activación de la vía PI3K/AKT[87]. A partir del análisis del transcriptoma, los resultados de expresión sugieren la existencia de la activación de esta vía, sin embargo, esto no se evaluó funcionalmente.

Como anteriormente se mencionó, los análisis de vías y redes de interacción sugirieron cambios en el ensamblaje del citoesqueleto y la migración celular. Los ensayos funcionales revelaron que la capacidad de migración de las ADSC aumentó tras ser

suplementadas con medio condicionado de células HeLa o con medio de co-cultivo. Esto evidencia los efectos quimiotácticos de las ADSC hacia el tumor (Figura 30). Cabe mencionar que, el efecto de los factores solubles en la movilización celular fue propio de las células de cáncer, ya que este fenómeno no se observó cuando se utilizó medio condicionado de queratinocitos inmortalizados. Debe tenerse en cuenta que, el medio condicionado careció de SFB, por lo que los efectos observados dependieron únicamente de los factores secretados por las células HeLa en condiciones de co-cultivo. Es importante considerar los tiempos largos de duplicación de las ADSC que pueden ser de hasta 72 h[88,89], por lo cual no existió un sesgo en los tiempos utilizados para el ensayo de migración. Se realizó la inspección del área al cierre de herida a las 48 h, incluso en el transcurso de la evaluación del cierre se observó la apertura de espacios posterior a la célula después de su movilización, por lo tanto, los resultados observados fueron independientes de la proliferación celular. Una de las principales citocinas producida por el tejido adiposo y que contribuye al estado pro-inflamatorio en la obesidad es la IL-6[90]. Ésta molécula modula la vía JAK/STAT para promover la proliferación de las células cancerosas, la sobrevida la angiogénesis, y cuyos niveles plasmáticos se ha correlacionado con un mal pronóstico en distintos tipos de cancer[90]. Además, se ha descrito que las células tumorales secretan IL-6 para reclutar células mesenquimales en el microambiente tumoral[91]. Sin embargo, IL-6 también actúa sobre las células tumorales de forma autocrina para producir mayores cantidades de esta misma citocina por un mecanismo de retroalimentación positiva[92]. El aumento en la expresión de IL-6 en las ADSC sugiere que, a través del mecanismo descrito, IL-6 secretada por las células HeLa en co-cultivo estimula la producción de IL-6 en ADSC (Anexo 12.7). Los análisis de vías de señalización infieren que NF-κB, AP-1/FOS (Anexo 12.8) e interleucinas se activan y, por tanto, pudieran ser responsables del cambio en la capacidad de migración de las ADSC al ser co-cultivadas con células de cáncer cervical. En particular, se ha observado que la vía NF-κB se activa en las células mesenquimales cuando son cultivadas con MDA231, células de cáncer de mama metastásico, y éstas a su vez secretan IL1β, por lo que resulta interesante comprender las implicaciones funcionales de la vía NF-κB en las ADSC en co-cultivo con células tumorales[93].

Existen reportes de que las ADSC del tejido adiposo se reclutan cerca o dentro del tejido tumoral, pero aún se desconoce si sufren algún cambio en su fenotipo[42]. Diversos

estudios sugieren que la población celular troncal en la periferia del tumor, puede cambiar a un fenotipo semejante a fibroblastos asociados a tumor (CAFs)[94], o comenzar a expresar marcadores propios de células endoteliales[44,95]. Por tal motivo se evaluó el inmunofenotipo troncal de ADSC posterior al co-cultivo con células HeLa y se determinó un aumento discreto en la población que expresó de CD31, marcador de endotelio vascular; y de CD45, marcador de células hematopoyéticas (Figura 32). Si bien, el aumento no fue significativo, la angiogénesis fue un proceso que se infirió modificado en este estudio (Tabla 5).

Por otro parte, la alta actividad de ALDH (ALDH^{high}), puede atribuirse a las células troncales y se ha utilizado como un marcador en la identificación de células trocales cancerosas[75,76]. En el año 2017 el grupo de Itoh demostró una subpoblación de ADSC positivas a ALDH con un mayor potencial de diferenciación, lo que indica que dentro de las células troncales de los tejidos existen una heterogeneidad celular[96]. En este estudio, fue interesante identificar un bajo porcentaje de población ADSC-ALDH^{high}, comparable con lo reportado previamente, donde esta población representó alrededor del 2% del total de las ADSC obtenidas de donadores[97]. Pese a que la población con alta actividad de esta enzima es muy pequeña, la condición de co-cultivo por 24 h fue suficiente para que esta población se duplicara en cantidad. En este sentido, se ha demostrado que la interacción entre células troncales y células tumorales produce un aumento en la población ALDH^{high} [98], similar a lo observado en células de cáncer de mama[91]. El incremento de la población de ADSC-ALDH^{high} desempeña un papel importante en el desarrollo tumoral, ya que estudios *in vitro* demostraron que células de ratón ALDH^{high} poseen un mayor potencial adipogénico y condrogénico, características que confieren ventajas a las células tumorales[99]. Con relación a esto, el análisis de RNAseq reveló que los genes ALDH modificaron su expresión, incluyendo ALDH3A1. De manera sobresaliente, ratones deficientes en ALDH3A1 y ALDH1A1 presentan un número reducido de células troncales hematopoyéticas (HSC)[100]. Conforme a los resultados, se propone que el enriquecimiento en la expresión de ALDH, que identifica una subpoblación de ADSC con posible potencial más troncal, es la causa de un mayor tamaño de esferas de ADSC tras el co-cultivo con células HeLa. Por su parte, ALDH1A3 se ha relacionado con células que muestran una alta actividad de ALDH[79,80]. Nuestros datos demostraron que la expresión de ALDH1A3 disminuyo tras la inhibición del

lnc-CXCL3 en 3T3-L1. Acorde a esto, el knockdown del lnc-CXCL3 redujo el tamaño de las esferas en estas células (Figura 36).

Un gran número de quimiocinas y citocinas aumentaron su expresión en ADSC en co-cultivo con células HeLa, lo que concuerda con la expresión diferencial de varias quimiocinas en co-cultivos de ADSC y células A431 de cáncer de vulva, tales como IL-6, IL-1A, CXCL2, CXCL5, CXCL3 y CXCL10[101]. La molécula CXCL10 (proteína de 10 kDa inducible por interferón-γ) fue la quimiocina con un mayor cambio en su expresión. Esta proteína se une al receptor CXCR3 y participa en la quimiotaxis, la apoptosis, el crecimiento celular y la angiogénesis. También, CXCL10 se ha reportado estar presente en células de cáncer cervical[102], tal y como se corroboró al replicar el co-cultivo de ADSC con células Ca Ski y SiHa, con un aumento estadísticamente significativo en esta última línea (Figura 25). Curiosamente, los datos obtenidos de GEPIA[68] revelaron que una expresión elevada de CXCL10 se asocia con un mal pronóstico en carcinoma cervical de células escamosas, e incluso se le considera como marcador de mal pronóstico en cáncer renal y cáncer pancreático (disponible en https://www.proteinatlas.org/ENSG00000169245-CXCL10/pathology).

En los hallazgos obtenidos a partir de este estudio, resultó interesante que la familia CXCL fue una de las más expresadas en ADSC co-cultivo, ya que diversos miembros como CXCL2, CXCL3, CXCL5 y CXCL10, tuvieron un aumento en su expresión bajo esta condición. Dentro del transcriptoma no codificante, en específico los lncRNAs, se observó que algunas combinaciones de lncRNA/mRNA resultaron estar modificadas en su regulación. En específico, llamó la atención el aumento en la expresión de lnc-CXCL3, por ser intragénico a CXCL3 y vecino de los genes CXCL2 y CXCL5 (Figura 38). Al evaluar la expresión de estas quimiocinas se encontró que, bajo las condiciones experimentales, existe un mecanismo de coexpresión entre lnc-CXCL3 y las quimiocinas CXCL2 y CXCL3 (Figura 39). De forma notable, el aumento de las proteínas CXCL2 y CXCL3 correlacionan con una menor tasa de sobrevida en pacientes con carcinoma cervical y adenocarcinoma endocervical (Figura 35). En conjunto, estos hallazgos indican que, lnc-CXCL3 regula la expresión de genes blanco contiguos importantes en el desarrollo del cáncer cervical, participando en la regulación de la capacidad de migración de estas células.

Hasta el momento, el presente trabajo es uno de los primeros en evaluar el transcriptoma completo de ADSC en co-cultivo con células de cáncer cervical, así como el

papel del lnc-CXCL3 en la regulación de la expresión de sus quimiocinas blanco y su efecto en el fenotipo troncal de las ADSC, que tiene consecuencias en la comunicación intercelular.

9. CONCLUSIONES

La obesidad, un problema de salud creciente en todo el mundo, se ha relacionado con el desarrollo, la progresión y el mal pronóstico de algunos tipos de cáncer. La evidencia sugiere que el tejido adiposo genera condiciones favorables para el microambiente tumoral. Una forma es a través del reclutamiento de las ADSC por células tumorales para contribuir en varios procesos que dan sostén a el tumor. Las células tumorales han atraído un gran interés en el campo de la investigación, mientras que las ADSC han sido menos estudiadas. En este sentido, el presente trabajo es uno de los primeros en evaluar a las ADSC en co-cultivo con células de cáncer, en específico de cáncer cervical.

- Se analizaron los cambios en el perfil de expresión de RNAs codificantes y no codificantes durante la comunicación de las ADSC con células de cáncer cervical.

- Se reveló la expresión diferencial de lncRNAs, miRNAs y pseudogenes en ADSC en co-cultivo.

- Se describieron cambios en el transcriptoma codificante de ADSC que correlacionaron con diversos procesos celulares modificados durante el co-cultivo con células de cáncer cervical.

- Se identificó un grupo importante de quimiocinas y citocinas con expresión diferencial en ADSC en co-cultivo con células de cáncer cervical.

- Se demostró el incremento en la capacidad de migración, en la subpoblación troncal $ALDH^{high}$ y en la capacidad de formación de esferas de mayor tamaño en ADSC en presencia de células de cáncer cervical.

- Se demostró el papel del lnc-CXCL3 en la regulación de la expresión de sus quimiocinas blanco (CXCL2 y CXCL3), así como su efecto en el fenotipo troncal de ADSC y la migración celular, como consecuencia de la comunicación con células de cáncer cervical.

Por lo tanto, los hallazgos del presente trabajo permiten comprender, en una manera más global, los cambios en las ADSC y su participación en el proceso tumoral. Además, abre el panorama para estudiar nuevos RNAs, codificantes y no codificantes que, por su expresión diferencial, pudiesen ser relevantes en las ADSC para la interrelación entre la obesidad y el cáncer.

10. PERSPECTIVAS

Con base en los resultados obtenidos y observaciones realizadas en el presente trabajo, se plantean las siguientes perspectivas:

En la metodología empleada, el co-cultivo de ADSC/HeLa se mantuvo durante 24h, por lo que es importante conocer el perfil transcripcional codificante y no codificante en tiempos de mayor interacción intercelular.

Dado que los resultados obtenidos partieron de ADSC de pacientes con obesidad, resultará interesante comparar con el perfil transcripcional de ADSC obtenidas de personas con talla normal, para determinar diferencias y similitudes.

En este trabajo se evaluó el co-cultivo de ADSC con células de cáncer cervical, sin embargo, queda por analizar los cambios en ADSC con células de otros tipos de cánceres asociados a obesidad, para conocer cuáles son diferentes y cuales son comunes.

Con respecto a los cambios observados en ADSC, será interesante determinar la posible adquisición de un fenotipo tipo endotelio vascular o incluso establecer los factores secretados por las ADSC que pueden favorecen la formación de nuevos vasos sanguíneos en el microambiente tumoral.

En cuanto al lnc-CXCL3, es de interés elucidar el mecanismo por el cual este lncRNA regula la expresión de las quimiocinas CXCL3 y CXCL2, determinando su función ya sea como molécula de andamio, guía o señuelo.

Para evaluar de forma global los cambios transcripcionales tras la inhibición del lnc-CXCL3, será de relevancia realizar un microarreglo que sugiera posibles blancos a distintos niveles de regulación, tanto en 3T3-L1 como HeLa, y así establecer similitudes y diferencias entre ambos tipos celulares.

La sobreexpresión del lnc-CXCL3 en el modelo empleado en este trabajo, proporcionará evidencia complementaria sobre su papel en el mantenimiento de características de troncalidad.

Finalmente, el efecto de la inhibición del lnc-CXCL3 en células tumorales transplantadas *in vivo* aportará mayor conocimiento sobre el papel de esta molécula no codificante, ya sea en la formación de tumores o favoreciendo fenotipos más agresivo.

11. REFERENCIAS BIBLIOGÁFICAS

1. Pan, J., Yin, J., Gan, L. & Xue, J. Two-sided roles of adipose tissue: Rethinking the obesity paradox in various human diseases from a new perspective. *Obes. Rev.* **24**, e13521 (2023).
2. Madden, A. M. & Smith, S. Body composition and morphological assessment of nutritional status in adults: a review of anthropometric variables. *J. Hum. Nutr. Diet.* **29**, 7–25 (2016).
3. Blue, M. N. M., Tinsley, G. M., Ryan, E. D. & Smith-Ryan, A. E. Validity of Body-Composition Methods across Racial and Ethnic Populations. *Adv. Nutr.* **12**, 1854–1862 (2021).
4. Organización Mundial de la Salud. Obesidad y sobrepeso. *Organización Mundial de la Salud* 1 https://www.who.int/es/news-room/fact-sheets/detail/obesity-and-overweight (2021).
5. González-Block, M. A. *et al.* Retos a la Encuesta Nacional de Salud y Nutrición 2017. *Salud Publica Mex.* **59**, 126 (2017).
6. Albala, C., & Reyes, M. Evolución natural y riesgos de la obesidad. *Cirugía Bariátrica. Santiago Editor. Mediterráneo* (2011).
7. Calle, E. E. & Kaaks, R. Overweight, obesity and cancer: epidemiological evidence and proposed mechanisms. *Nat. Rev. Cancer* **4**, 579–91 (2004).
8. International Agency for Research on Cancer. Cancer Attributable to Obesity. *World Health Organization* 1 https://gco.iarc.fr/causes/obesity/tools-pie (2017).
9. Lauby-Secretan, B. *et al.* Body Fatness and Cancer--Viewpoint of the IARC Working Group. *N. Engl. J. Med.* **375**, 794–8 (2016).
10. Instituto Nacional del Cáncer. Obesidad y cancer. https://www.cancer.gov/espanol/cancer/causas-prevencion/riesgo/obesidad/hoja-informativa-obesidad (2017).
11. Hursting, S. D., Nunez, N. P., Varticovski, L. & Vinson, C. The obesity-cancer link: lessons learned from a fatless mouse. *Cancer Res.* **67**, 2391–3 (2007).
12. van Kruijsdijk, R. C. M., van der Wall, E. & Visseren, F. L. J. Obesity and cancer: the role of dysfunctional adipose tissue. *Cancer Epidemiol. Biomarkers Prev.* **18**, 2569–

78 (2009).

13. Khandekar, M. J., Cohen, P. & Spiegelman, B. M. Molecular mechanisms of cancer development in obesity. *Nat. Rev. Cancer* **11**, 886–95 (2011).
14. Park, J., Morley, T. S., Kim, M., Clegg, D. J. & Scherer, P. E. Obesity and cancer--mechanisms underlying tumour progression and recurrence. *Nat. Rev. Endocrinol.* **10**, 455–465 (2014).
15. Gregor, M. F. & Hotamisligil, G. S. Inflammatory Mechanisms in Obesity. *Annu. Rev. Immunol.* **29**, 415–445 (2011).
16. Deng, T., Lyon, C. J., Bergin, S., Caligiuri, M. A. & Hsueh, W. A. Obesity, Inflammation, and Cancer. *Annu. Rev. Pathol.* **11**, 421–49 (2016).
17. Colotta, F., Allavena, P., Sica, A., Garlanda, C. & Mantovani, A. Cancer-related inflammation, the seventh hallmark of cancer: links to genetic instability. *Carcinogenesis* **30**, 1073–81 (2009).
18. Pollak, M. Insulin and insulin-like growth factor signalling in neoplasia. *Nat. Rev. Cancer* **8**, 915–28 (2008).
19. Park, J., Sarode, V. R., Euhus, D., Kittler, R. & Scherer, P. E. Neuregulin 1-HER axis as a key mediator of hyperglycemic memory effects in breast cancer. *Proc. Natl. Acad. Sci.* **109**, 21058–21063 (2012).
20. Gallagher, E. J. & LeRoith, D. Obesity and Diabetes: The Increased Risk of Cancer and Cancer-Related Mortality. *Physiol. Rev.* **95**, 727–48 (2015).
21. Goodwin, P. J. & Stambolic, V. Impact of the obesity epidemic on cancer. *Annu. Rev. Med.* **66**, 281–96 (2015).
22. Fagan, H. B., Wender, R., Myers, R. E. & Petrelli, N. Obesity and Cancer Screening according to Race and Gender. *J. Obes.* **2011**, 218250 (2011).
23. Hijazi, H. *et al.* Features of cancer management in obese patients. *Crit. Rev. Oncol. Hematol.* **85**, 193–205 (2013).
24. Choi, M. *et al.* Effect of body mass index on shifts in ultrasound-based image-guided intensity-modulated radiation therapy for abdominal malignancies. *Radiother. Oncol.* **91**, 114–9 (2009).
25. Mullen, J. T. *et al.* Impact of body mass index on perioperative outcomes in patients undergoing major intra-abdominal cancer surgery. *Ann. Surg. Oncol.* **15**, 2164–72

(2008).

26. Sung, H. *et al.* Global Cancer Statistics 2020: GLOBOCAN Estimates of Incidence and Mortality Worldwide for 36 Cancers in 185 Countries. *CA. Cancer J. Clin.* **71**, 209–249 (2021).
27. International Agency for Research on Cancer. Estimated age-standardized incidence rates (World) in 2020, World, females, all ages (excl. NMSC). 2020 https://gco.iarc.fr/today/home (2020).
28. International Agency for Research on Cancer (IARC). Estimated age-standardized incidence and mortality rates (World) in 2020, Mexico, females, all ages. *Glob. Cancer Obs. (GCO). GLOBOCAN* 2020 (2020).
29. Szymonowicz, K. A. & Chen, J. Biological and clinical aspects of HPV-related cancers. *Cancer Biol. Med.* **17**, 864–878 (2020).
30. Bhaskaran, K. *et al.* Body-mass index and risk of 22 specific cancers: a population-based cohort study of 5·24 million UK adults. *Lancet* **384**, 755–765 (2014).
31. Calle, E. E., Rodriguez, C., Walker-Thurmond, K. & Thun, M. J. Overweight, obesity, and mortality from cancer in a prospectively studied cohort of U.S. adults. *N. Engl. J. Med.* **348**, 1625–38 (2003).
32. Frigolet, M. E. & Gutiérrez-Aguilar, R. The colors of adipose tissue. *Gac. Med. Mex.* **156**, 142–149 (2020).
33. Mozo, J., Emre, Y., Bouillaud, F., Ricquier, D. & Criscuolo, F. Thermoregulation: what role for UCPs in mammals and birds? *Biosci. Rep.* **25**, 227–49 (2005).
34. Esteve Ràfols, M. Adipose tissue: cell heterogeneity and functional diversity. *Endocrinol. Nutr.* **61**, 100–12 (2014).
35. Cannon, B. & Nedergaard, J. Brown adipose tissue: function and physiological significance. *Physiol. Rev.* **84**, 277–359 (2004).
36. Mathieu, P., Poirier, P., Pibarot, P., Lemieux, I. & Després, J.-P. Visceral obesity: the link among inflammation, hypertension, and cardiovascular disease. *Hypertens. (Dallas, Tex. 1979)* **53**, 577–84 (2009).
37. Bourgeois, C. *et al.* Specific Biological Features of Adipose Tissue, and Their Impact on HIV Persistence. *Front. Microbiol.* **10**, 2837 (2019).
38. Sylvester, K. G. & Longaker, M. T. Stem cells: review and update. *Arch. Surg.* **139**,

93–9 (2004).

39. Bunnell, B. A., Flaat, M., Gagliardi, C., Patel, B. & Ripoll, C. Adipose-derived stem cells: isolation, expansion and differentiation. *Methods* **45**, 115–20 (2008).
40. Dominici, M. *et al.* Minimal criteria for defining multipotent mesenchymal stromal cells. The International Society for Cellular Therapy position statement. *Cytotherapy* **8**, 315–7 (2006).
41. Lazennec, G. & Lam, P. Y. Recent discoveries concerning the tumor - mesenchymal stem cell interactions. *Biochim. Biophys. Acta* **1866**, 290–299 (2016).
42. Senst, C. *et al.* Prospective dual role of mesenchymal stem cells in breast tumor microenvironment. *Breast Cancer Res. Treat.* **137**, 69–79 (2013).
43. Zhang, Y., Bellows, C. F. & Kolonin, M. G. Adipose tissue-derived progenitor cells and cancer. *World J. Stem Cells* **2**, 103–13 (2010).
44. Zhang, Y. *et al.* White Adipose Tissue Cells Are Recruited by Experimental Tumors and Promote Cancer Progression in Mouse Models. *Cancer Res.* **69**, 5259–5266 (2009).
45. Lin, G. *et al.* Effects of transplantation of adipose tissue-derived stem cells on prostate tumor. *Prostate* **70**, 1066–73 (2010).
46. Zhao, B.-C., Zhao, B., Han, J.-G., Ma, H.-C. & Wang, Z.-J. Adipose-derived stem cells promote gastric cancer cell growth, migration and invasion through SDF-1/CXCR4 axis. *Hepatogastroenterology.* **57**, 1382–9 (2010).
47. Alexander, R. P., Fang, G., Rozowsky, J., Snyder, M. & Gerstein, M. B. Annotating non-coding regions of the genome. *Nat. Rev. Genet.* **11**, 559–571 (2010).
48. Deniz, E. & Erman, B. Long noncoding RNA (lincRNA), a new paradigm in gene expression control. *Funct. Integr. Genomics* **17**, 135–143 (2017).
49. Harrow, J. *et al.* GENCODE: The reference human genome annotation for The ENCODE Project. *Genome Res.* **22**, 1760–1774 (2012).
50. Hon, C.-C. *et al.* An atlas of human long non-coding RNAs with accurate 5’ ends. *Nature* **543**, 199–204 (2017).
51. Cheng, J. *et al.* Transcriptional maps of 10 human chromosomes at 5-nucleotide resolution. *Science* **308**, 1149–54 (2005).
52. Niemczyk, M. *et al.* Imprinted chromatin around DIRAS3 regulates alternative

splicing of GNG12-AS1, a long noncoding RNA. *Am. J. Hum. Genet.* **93**, 224–35 (2013).

53. Quinn, J. J. & Chang, H. Y. Unique features of long non-coding RNA biogenesis and function. *Nat. Rev. Genet.* **17**, 47–62 (2016).
54. Ziegler, C. & Kretz, M. The More the Merrier-Complexity in Long Non-Coding RNA Loci. *Front. Endocrinol. (Lausanne).* **8**, 90 (2017).
55. Kapusta, A. *et al.* Transposable elements are major contributors to the origin, diversification, and regulation of vertebrate long noncoding RNAs. *PLoS Genet.* **9**, e1003470 (2013).
56. De la Fuente-Hernandez, M. A., Sarabia-Sanchez, M. A., Melendez-Zajgla, J. & Maldonado-Lagunas, V. lncRNAs in mesenchymal differentiation. *Am. J. Physiol. Cell Physiol.* **322**, C421–C460 (2022).
57. Qureshi, I. A. & Mehler, M. F. Emerging roles of non-coding RNAs in brain evolution, development, plasticity and disease. *Nat. Rev. Neurosci.* **13**, 528–41 (2012).
58. Knoll, M., Lodish, H. F. & Sun, L. Long non-coding RNAs as regulators of the endocrine system. *Nat. Rev. Endocrinol.* **11**, 151–60 (2015).
59. Kotake, Y. *et al.* Long non-coding RNA ANRIL is required for the PRC2 recruitment to and silencing of p15(INK4B) tumor suppressor gene. *Oncogene* **30**, 1956–62 (2011).
60. Hung, T. *et al.* Extensive and coordinated transcription of noncoding RNAs within cell-cycle promoters. *Nat. Genet.* **43**, 621–629 (2011).
61. Wang, K. C. & Chang, H. Y. Molecular mechanisms of long noncoding RNAs. *Mol. Cell* **43**, 904–14 (2011).
62. Rinn, J. L. & Chang, H. Y. Genome Regulation by Long Noncoding RNAs. *Annu. Rev. Biochem.* **81**, 145–166 (2012).
63. Tano, K. *et al.* MALAT-1 enhances cell motility of lung adenocarcinoma cells by influencing the expression of motility-related genes. *FEBS Lett.* **584**, 4575–80 (2010).
64. Hu, W., Alvarez-Dominguez, J. R. & Lodish, H. F. Regulation of mammalian cell differentiation by long non-coding RNAs. *EMBO Rep.* **13**, 971–83 (2012).
65. Zuk, P. A. *et al.* Multilineage cells from human adipose tissue: implications for cell-based therapies. *Tissue Eng.* **7**, 211–28 (2001).

66. Thiagarajan, P. S. & Reizes, O. Adipose Tissue-Derived Stem Cells in Regenerative Medicine and Impact on Cancer. in *Cancer Stem Cells* 411–438 (Elsevier, 2016). doi:10.1016/B978-0-12-803892-5.00016-4.
67. Livak, K. J. & Schmittgen, T. D. Analysis of relative gene expression data using real-time quantitative PCR and the 2(-Delta Delta C(T)) Method. *Methods* **25**, 402–8 (2001).
68. Tang, Z. *et al.* GEPIA: a web server for cancer and normal gene expression profiling and interactive analyses. *Nucleic Acids Res.* **45**, W98–W102 (2017).
69. Uhlen, M. *et al.* A pathology atlas of the human cancer transcriptome. *Science* **357**, (2017).
70. Livak, K. J. & Schmittgen, T. D. Analysis of relative gene expression data using real-time quantitative PCR and the 2(-Delta Delta C(T)) Method. *Methods* **25**, 402–8 (2001).
71. Huang, B., Lang, X. & Li, X. The role of IL-6/JAK2/STAT3 signaling pathway in cancers. *Front. Oncol.* **12**, 1023177 (2022).
72. Shaulian, E. & Karin, M. AP-1 in cell proliferation and survival. *Oncogene* **20**, 2390–2400 (2001).
73. Zhang, X., Li, X., Tan, F., Yu, N. & Pei, H. STAT1 Inhibits MiR-181a Expression to Suppress Colorectal Cancer Cell Proliferation Through PTEN/Akt. *J. Cell. Biochem.* **118**, 3435–3443 (2017).
74. Wang, Q., Bode, A. M. & Zhang, T. Targeting CDK1 in cancer: mechanisms and implications. *NPJ Precis. Oncol.* **7**, 58 (2023).
75. Tirino, V. *et al.* Cancer stem cells in solid tumors: an overview and new approaches for their isolation and characterization. *FASEB J.* **27**, 13–24 (2013).
76. Mele, L., Liccardo, D. & Tirino, V. Evaluation and Isolation of Cancer Stem Cells Using ALDH Activity Assay. in 43–48 (2018). doi:10.1007/978-1-4939-7401-6_4.
77. Kong, W. *et al.* Analysis of therapeutic targets and prognostic biomarkers of CXC chemokines in cervical cancer microenvironment. *Cancer Cell Int.* **21**, 399 (2021).
78. Poulos, S. P., Dodson, M. V & Hausman, G. J. Cell line models for differentiation: preadipocytes and adipocytes. *Exp. Biol. Med.* **235**, 1185–1193 (2010).
79. Puttini, S. *et al.* ALDH1A3 Is the Key Isoform That Contributes to Aldehyde

Dehydrogenase Activity and Affects in Vitro Proliferation in Cardiac Atrial Appendage Progenitor Cells. *Front. Cardiovasc. Med.* **5**, 90 (2018).

80. Zhou, L. *et al.* Identification of cancer-type specific expression patterns for active aldehyde dehydrogenase (ALDH) isoforms in ALDEFLUOR assay. *Cell Biol. Toxicol.* **35**, 161–177 (2019).
81. He, Q., Wan, C. & Li, G. Concise review: multipotent mesenchymal stromal cells in blood. *Stem Cells* **25**, 69–77 (2007).
82. Hanahan, D. & Coussens, L. M. Accessories to the crime: functions of cells recruited to the tumor microenvironment. *Cancer Cell* **21**, 309–22 (2012).
83. Chau, Y.-Y. *et al.* Visceral and subcutaneous fat have different origins and evidence supports a mesothelial source. *Nat. Cell Biol.* **16**, 367–75 (2014).
84. Ritter, A. *et al.* Characterization of adipose-derived stem cells from subcutaneous and visceral adipose tissues and their function in breast cancer cells. *Oncotarget* **6**, 34475–93 (2015).
85. Al-toub, M. *et al.* Pleiotropic effects of cancer cells' secreted factors on human stromal (mesenchymal) stem cells. *Stem Cell Res. Ther.* **4**, 114 (2013).
86. Wang, T., Guo, S., Liu, X., Xv, N. & Zhang, S. Protective effects of adipose-derived stem cells secretome on human dermal fibroblasts from ageing damages. *Int. J. Clin. Exp. Pathol.* **8**, 15739–48 (2015).
87. Chen, H. *et al.* Protective effect of gigantol against hydrogen peroxide-induced apoptosis in rat bone marrow mesenchymal stem cells through the PI3K/Akt pathway. *Mol. Med. Rep.* **17**, 3267–3273 (2018).
88. Chen, H.-T. *et al.* Proliferation and differentiation potential of human adipose-derived mesenchymal stem cells isolated from elderly patients with osteoporotic fractures. *J. Cell. Mol. Med.* **16**, 582–93 (2012).
89. Legzdina, D., Romanauska, A., Nikulshin, S., Kozlovska, T. & Berzins, U. Characterization of Senescence of Culture-expanded Human Adipose-derived Mesenchymal Stem Cells. *Int. J. stem cells* **9**, 124–36 (2016).
90. Ghosh, S. & Ashcraft, K. An IL-6 link between obesity and cancer. *Front. Biosci. (Elite Ed).* **5**, 461–78 (2013).
91. Liu, S. *et al.* Breast cancer stem cells are regulated by mesenchymal stem cells through

cytokine networks. *Cancer Res.* **71**, 614–24 (2011).

92. Wei, H.-J. *et al.* Adipose-derived stem cells promote tumor initiation and accelerate tumor growth by interleukin-6 production. *Oncotarget* **6**, 7713–26 (2015).
93. Escobar, P. *et al.* IL-1β produced by aggressive breast cancer cells is one of the factors that dictate their interactions with mesenchymal stem cells through chemokine production. *Oncotarget* **6**, 29034–47 (2015).
94. Inagaki, Y. *et al.* Abstract 171: Adipose-derived mesenchymal stem cell (ADSC) has the differentiation capacity toward cancer associated fibroblast (CAF) and reproduce the morphology of the clinical tumor stroma. *Cancer Res.* **74**, 171–171 (2014).
95. Deng, M. *et al.* Endothelial Differentiation of Human Adipose-Derived Stem Cells on Polyglycolic Acid/Polylactic Acid Mesh. *Stem Cells Int.* **2015**, 1–11 (2015).
96. Itoh, H. *et al.* Aldehyde dehydrogenase activity identifies a subpopulation of canine adipose-derived stem cells with higher differentiation potential. *J. Vet. Med. Sci.* **79**, 1540–1544 (2017).
97. Estes, B. T., Wu, A. W., Storms, R. W. & Guilak, F. Extended passaging, but not aldehyde dehydrogenase activity, increases the chondrogenic potential of human adipose-derived adult stem cells. *J. Cell. Physiol.* **209**, 987–95 (2006).
98. Li, H.-J., Reinhardt, F., Herschman, H. R. & Weinberg, R. A. Cancer-Stimulated Mesenchymal Stem Cells Create a Carcinoma Stem Cell Niche via Prostaglandin E2 Signaling. *Cancer Discov.* **2**, 840–855 (2012).
99. Najar, M., Crompot, E., van Grunsven, L. A., Dollé, L. & Lagneaux, L. Aldehyde Dehydrogenase Activity in Adipose Tissue: Isolation and Gene Expression Profile of Distinct Sub-population of Mesenchymal Stromal Cells. *Stem cell Rev. reports* **14**, 599–611 (2018).
100. Gasparetto, M. *et al.* Aldehyde dehydrogenases are regulators of hematopoietic stem cell numbers and B-cell development. *Exp. Hematol.* **40**, 318–29.e2 (2012).
101. Koellensperger, E. *et al.* Alterations of gene expression and protein synthesis in co-cultured adipose tissue-derived stem cells and squamous cell-carcinoma cells: consequences for clinical applications. *Stem Cell Res. Ther.* **5**, 65 (2014).
102. Liu, M., Guo, S. & Stiles, J. K. The emerging role of CXCL10 in cancer (Review). *Oncol. Lett.* **2**, 583–589 (2011).

Cellular Oncology
https://doi.org/10.1007/s13402-021-00653-6

ORIGINAL ARTICLE

Molecular changes in adipocyte-derived stem cells during their interplay with cervical cancer cells

Marcela Angelica De la Fuente-Hernandez[1,2] · Erika Claudia Alanis-Manriquez[2] · Eduardo Ferat-Osorio[3] · Arturo Rodriguez-Gonzalez[3] · Lourdes Arriaga-Pizano[4] · Karla Vazquez-Santillan[2] · Jorge Melendez-Zajgla[5] · Veronica Fragoso-Ontiveros[6] · Rosa Maria Alvarez-Gomez[6] · Vilma Maldonado Lagunas[1,2]

Accepted: 22 November 2021

Abstract

Purpose Obesity is as an important risk factor and has been associated with a worse prognosis in at least 13 distinct tumor types. This is partially due to intercellular communication between tumor cells and adipose tissue-derived stem cells (ADSCs), which are increased in obese individuals. As yet, however, little is known about the molecular changes occurring in ADSCs in these conditions. Cervical cancer has a high incidence and mortality rate in women from developing countries, particularly in those with a high body mass index (BMI).

Methods We analyzed the expression profile of ADSCs co-cultured with cervical cancer cells through massive RNA sequencing followed by evaluation of various functional alterations resulting from the modified transcriptome.

Results A total of 761 coding and non-coding dysregulated RNAs were identified in ADSCs after co-culture with HeLa cells (validation in CaSki and SiHA cells). Subsequent network analysis showed that these changes were correlated with migration, stemness, DNA repair and cytokine production. Functional experiments revealed a larger $ALDH^{high}$ subpopulation and a higher migrative capacity of ADSCs after co-culture with HeLa cells. Interestingly, CXCL3 and its intragenic long-noncoding RNA, lnc-CXCL3, were found to be co-regulated during co-culture. A loss-of-function assay revealed that lnc-CXCL3 acts as a key regulator of CXCL3 expression.

Conclusions Our results suggest that intercellular communication between ADSCs and cervical cancer cells modifies the RNA expression profile in the former, including that of lncRNAs, which in turn can regulate the expression of diverse chemokines that favor malignancy-associated capacities such as migration.

Keywords Cervical cancer · Obesity · ADSC · HeLa · Transcriptome · lncRNA · Intercellular communication

✉ Vilma Maldonado Lagunas
vmaldonado@inmegen.gob.mx

1 Facultad de Medicina, Posgrado en Ciencias Biologicas, Universidad Nacional Autonoma de Mexico (UNAM), Av. Ciudad Universitaria 3000, C.P. 04510, Coyoacan, Mexico City, Mexico

2 Epigenetics Laboratory, Instituto Nacional de Medicina Genomica (INMEGEN), Periferico Sur No. 4809, Col. Arenal Tepepan, Tlalpan, C.P, 14610 Mexico City, Mexico

3 Gastrosurgery Service, UMAE. Hospital de Especialidades Dr. Bernardo Sepulveda Gutierrez of the Centro Medico Nacional Siglo XXI, Instituto Mexicano del Seguro Social (IMSS), Av. Cuauhtemoc No 330, Col. Doctores, Cuauhtemoc, C.P., 06720 Mexico City, Mexico

4 Unidad de Investigacion Medica en Inmunoquimica. Hospital de Especialidades, Dr. Bernardo Sepulveda Gutierrez of the Centro Medico Nacional Siglo XXI, Instituto Mexicano del Seguro Social (IMSS), Av. Cuauhtemoc No 330, Col. Doctores, Cuauhtemoc, C.P., 06720 Mexico City, Mexico

5 Functional Cancer Genomics Laboratory, Instituto Nacional de Medicina Genomica (INMEGEN), Periférico Sur No. 4809, Col. Arenal Tepepan, Tlalpan, C.P., 14610 Mexico City, Mexico

6 National Cancer Institute, San Fernando 22, Seccion XVI, Tlalpan, Mexico City, Mexico

Published online: 11 January 2022

1 Introduction

Obesity is defined as an abnormal or excessive accumulation of adipose tissue in the body. In the last decades, the number of people suffering from obesity has increased and currently it represents a serious health problem worldwide. In 2016 alone, more than 650 million adults (≥ 18 years of age) were classified as obese [1]. A recent cohort study showed a significant correlation of obesity and an increased risk to develop cancer, as well as a poor prognosis of the patients involved [2]. In 2012, The International Agency for Research on Cancer (IARC) declared that ~3.6% of new cancer cases are associated with a high BMI (body mass index) [3], ~ 23.3% of which are attributable to obesity originating in the corpus uteri [4]. In 2016, 13 different types of cancer were reported to be associated with obesity by promoting cancer progression and favoring a worse prognosis. Therefore, these cancers are denoted obesity-associated cancers [5].

As yet, detailed knowledge of the molecular mechanisms by which obesity affects the incidence, progression and mortality of different types of cancer is lacking. Several mechanisms have, however, been suggested, such as adipokine production, a pro-inflammatory microenvironment, insulin resistance, hypoxia and immune cell infiltration [6–9]. The adipose tissue contains a subpopulation of mesenchymal cells known as adipose tissue-derived stem cells (ADSCs), which possess self-renewal capacity and the potential to differentiate into adipogenic, osteogenic or chondrogenic lineages [10]. In vivo studies have suggested that mesenchymal cells play a key role in the effects of obesity in cancer [11], and some reports have shown that ADSCs are attracted by tumor cells through angiogenin, GM-CSF, IL-6, GRO-alpha and IL-8 signaling [12]. Once ADSCs are established within the periphery of the tumor, they favor the formation of vascular endothelium, tumor cell proliferation, invasiveness and metastasis [13–16]. Little is currently known about the changes that are undergone by ADSCs during their exposure to cancer cells, a highly relevant issue when trying to understand the interaction between these two types of cell populations. Therefore, we set out to evaluate transcriptomic changes of ADSCs in co-culture with cervical cancer cells, a type of cancer that continues to rank second in incidence in Mexican women [17].

2 Materials and methods

2.1 Isolation and maintenance of ADSCs

Under informed consent, 3 visceral white adipose tissue samples were collected from gastric bypass surgeries of women with morbid obesity (BMI ≥ 40 kg/m^2). The samples were provided by the service of the Gastrosurgery Unit of the Specialties Hospital of the National Medical Center "Siglo XXI", IMSS. At the time of obtaining the tissue, positron emission tomography (PET) was used to corroborate that donor patients did not present any type of cancer associated with obesity. ADSCs of donor tissues were isolated following a previously reported methodology [18]. Briefly, tissue was washed twice with phosphate buffered saline (PBS 1x) and digested with 0.0075% collagenase type I (Merck Millipore Cat SCR103, CDMX, Mexico) during 40 min at 37 °C with gentle agitation. The stromal fraction containing ADSCs was collected by differential centrifugation during 8 min to 1200×g after which cells were seeded in adherent cell culture plates with DMEM medium (Dulbecco's modified Eagle Medium Cat.10–013; Corning, NY, USA) supplemented with 1x streptomycin/penicillin (ATCC, Cat. 30–2300 VA, USA) and 15% fetal bovine serum on the first day (FBS; ATCC, Cat. 30–2020, VA, USA). The FBS was gradually reduced to a concentration of 5%.

To establish primary cultures, ADSCs were incubated at 37 °C in a humidified atmosphere containing 5% CO_2, and medium was replaced every third day. All experiments were performed using early passages with a maximum of six passages. Additionally, we used ADSCs obtained from the American Type Culture Collection (ATCC) (normal, human "zero pass" organism: Human *Homo sapiens*, PCS-500-011). These ADSCs were cultured in basal medium for mesenchymal cells (PCS-500-030, ATCC VA, USA) supplemented with Mesenchymal Stem Cell Growth Kit for Adipose and Umbilical-derived MSCs-Low Serum (catalog PCS-500-040, ATCC VA, USA). The medium was replaced every 4 or 5 days. This commercial primary ADSC cell culture was used for the functional assays.

2.2 ADSC immunophenotype analysis

ADSCs obtained from patients were analyzed by flow cytometry to evaluate the presence of membranal surface markers described for this population. To this end, primary cultures in the third passage were exposed to accutase (ATCC, Cat. 30–2103, VA, USA) for 10 min at 37 °C. Next, the cells were centrifuged and washed with 1x PBS, after which 1×10^6 cells were stained with 10 µl primary antibodies coupled to fluorochromes during 30 min at 4 °C in the dark. Subsequently, the cells were washed and fixed with 4% paraformaldehyde (PFA) and, finally, resuspended in 500 µl 1x PBS. The antibodies used were anti-CD31-FITC (Merck Millipore Clone HC1/6 Temecula, CA, USA), anti-CD44-FITC (Miltenyi Biotec, Clone DB105, Bergisch, DE), anti-CD45-PE (BD Pharmingen, Clone HI30, USA), anti-CD90- FITC (Merck Millipore, Clone 5E10, Temecula, CA,

USA), mouse IgG FITC (Miltenyi Biotec, Clone IS5-21F5, Bergisch, DE) and mouse IgG1-PE (Miltenyi Biotec, Clone IS5-21F5, Bergisch, DE). Expression analysis was carried out using a BD FACSCalibur Cytometer, (BD Biosciences, CA, USA) recording at least 10,000 events for each sample, after which data analysis was performed using FlowJo V10 Software (Tree Star. Ashland, OR USA).

2.3 Adipogenic differentiation assays

Adipogenic differentiation assays were performed using an adipocyte differentiation kit for mesenchymal stem cells of adipose tissue and preadipocytes (ATCC PCS-500- 050), following the manufacturer's instructions. Adipogenic differentiation was confirmed by the formation of stable neutral lipid vacuoles and staining with 0.5% Oil-Red solution in isopropanol (Sigma-Aldrich, O1391, Saint Louis, MO, USA). Culture of ADSCs in the absence of the adipocyte differentiation kit was considered as basal adipocyte differentiation. All cells were used at the same passage and confluency and those displaying lipid vacuoles were counted using Oil-Red solution.

2.4 Cells and culture conditions

HeLa (uterine cervix adenocarcinoma) CaSki (cervix, derived from metastatic site small intestine), SiHa (cervix, derived from squamous cell carcinoma, grade II) and 3 T3-L1 (mouse embryonic fibroblast) cells were obtained from the ATCC and cultured in DMEM medium supplemented with 5% to 10% FBS at 37 °C in an atmosphere containing 5% CO2. The growth medium was replaced every two days. HaCaT (human skin keratinocyte) cells were obtained from the ATCC and cultured in DMEM/F-12 medium supplemented with 5% FBS until the time of the assay when the medium was replaced by DMEM with 5% FBS.

2.5 Co-culture assays

In order to culture ADSCs in the presence of cervix cancer cells, 75 mm transwell culture plates with 3.0 µm pore diameter polycarbonate membrane inserts were used (Corning costar, cat. 3420, NY, USA). This culture method separates both cell populations but allows intercellular communication through interactions with soluble factors. ADSCs, between the third and fifth passages, were seeded at the bottom of the plate at 90% confluence (5×10^5 cells) in DMEM supplemented with 5% FBS. Next, cervix cancer cells (HeLa, CaSki or SiHa) were seeded on the transwell membrane and kept in DMEM supplemented with 5% FBS until they reached confluence. Next, the medium in both compartments was changed to DMEM without FBS 4 h before starting the co-culture. For this, membranes with cancer cells were placed into plates where ADSCs were previously seeded. The co-culture was maintained in DMEM without FBS for 24 h. At this point, the growth media were collected, and cells were washed with PBS 1x for later studies. As a control group, ADSCs were grown as monoculture (without co-culture conditions).

2.6 RNA extraction

Total RNA from ADSCs, either as co-culture or monoculture, was extracted using TRIZOL reagent, (Invitrogen No cat. 15596026, MA, USA) following the supplier's instructions. RNA was resuspended in 30 µl MilliQ water (Millipore, MA, USA) for subsequent quantification in a Nanodrop system (260 nm–280 nm absorbance).

2.7 ADSC transcriptome sequencing

RNAs with a quality score of 8.8 to 10 RIN (RNA Integrity Number) were used. Subsequently, ribosomal RNA was depleted using a Ribominus Eukaryotic RNA Seq kit (Invitrogen cat. A10837-CA, USA). Sequencing libraries were prepared from total RNA using a TruSeq sample library prep Illumina kit and analyzed using a NextSeq500 Illumina platform. Biological triplicate samples from independent trials were sequenced and at least 20 million reads were obtained. The sequence data were analyzed using CLC Genomics Workbench (Version 7CLC Bio Cambridge), and differential expression was determined between groups using the EDGE R algorithm considering fold changes >2 and <2 with a $p \leq 0.05$. Integral analysis of the coding genome was performed using the Ingenuity Pathway Analysis (IPA) tool. The results from this analysis were compared with Key Pathway Advisor (KPA) of Metacore Clarivate Analytics and Gene Set Enrichment Analysis (GSEA). The data obtained from the sequencing were deposited as SRA data: PRJNA780960.

2.8 Real-time quantitative PCR (RT-qPCR) analysis

Isolated RNA was treated with RNase-Free DNAse RQ1 (Promega Cat. M6101, WI, USA) after which 2 µg was reverse transcribed using a Maxima First Strand cDNA synthesis Kit for RT-qPCR (Thermo Scientific Cat K1641, MA, USA). To validate the data obtained from transcriptional analyses, the relative expression of 10 genes was determined in ADSCs in co-culture and monoculture using RT-qPCR. The transcription level of each gene was determined using a SYBR Select Master Mix 2x (Applied Biosystems, CA, USA) with specific primers designed using Primer Plus software (available at http://primer3plus.com/cgi-bin/dev/primer3prefold.cgi). Thermodynamic analysis of

the oligonucleotides was performed using Beacon Designer (available at http://www.premierbiosoft.com/qOligo/Oligo.jsp?PID=1) and prediction of the secondary structures of the oligonucleotides was accomplished using UNAFold (available at https://www.idtdna.com/UNAFold) (Supplementary Table 1). TBP or 18S were used as references for quantification and normalization of the results. In all cases, dissociation curves were generated, and the specificity of the PCR reactions was confirmed. We used the ΔΔCt method for data analysis. Relative expression values are represented as $2^{-\Delta\Delta Ct}$.

2.9 Conditioned medium collection

Conditioned medium of HeLa cells (M. HeLa) was collected from confluent cultures of HeLa cells after incubation with DMEM without serum for 24 h at 37 °C, 5% CO_2. Conditioned medium of HaCaT cells (M. HaCaT) was collected from confluent cultures of HaCaT cells after incubation with DMEM without serum for 24 h at 37 °C, 5% CO_2. As co-culture medium (M. co-culture) we used medium in which ADSCs were grown in the presence of HeLa cells during 24 h. This medium is composed of DMEM without serum, with soluble factors produced by the ADSCs and HeLa cells. At the end of the incubation period, the culture medium was filtered through 0.2 µm diameter filters (Corning, Cat. 431,219, Germany) and stored at −70 °C until use.

2.10 BrdU incorporation assay

Immediately after the culture periods, cell cycle progression of ADSCs in co-culture or monoculture was analyzed through BrdU incorporation using an APO-BrdU TUNEL Assay Kit (Molecular probes Cat. A23210, OR USA) according to the supplier's protocol. The readings were performed by flow cytometry using a BD FACSCalibur cytometer (BD Biosciences, CA, USA), the results were analyzed using ModFit LT software to evaluate cell cycle progression and FlowJo (Tree Star, Ashland, OR USA) was used to analyze cell death by apoptosis. The assays were performed independently in triplicate.

2.11 Scratch wound-healing assay

To evaluate the migration capacity of ADSCs, we performed scratch wound-healing analyses [19]. In brief, ADSCs between 4 and 5 passages were cultured at high confluency in 30 mm plates. Prior to the onset of the assays, ADSCs were synchronized by keeping them in serum-free DMEM medium for 16 h. Wounds were created by scratching with a 200 µl pipette tip after which the monolayers were washed with 1x PBS three times. Subsequently, the following media were added: As a negative control DMEM without serum (Medium), DMEM supplemented with 5% FBS, considered as positive control (M + FBS), co-culture medium ADSC/HeLa (M. CC), HeLa cell-conditioned Medium (M. HeLa) and HaCaT cell-conditioned medium (M. HaCaT). Images of wound closure under all conditions were captured at 0, 12, 24 and 48 h using a light microscope and analyzed using ImageJ software. The assays were performed in independent triplicates, each with its corresponding technical replicates.

2.12 ALDH activity assay

Cells were washed and detached using trypsin after which ALDH activity was assessed using ALDEFLUOR reagent (Stem Cell Technologies, Cat. 01700, Vancouver, CAN) in accordance with the manufacturer's instructions. Briefly, 1×10^6 cells were resuspended in 1 ml buffer after which 5 µl ALDEFLUOR reagent was added. 500 µl of this cell suspension was transferred to a tube with 5 µl of the ALDH activity inhibitor N, N-diethylaminobenzaldehyde (DAEB) as a negative control for enzyme activity. Measurements were carried out by flow cytometry using a BD FACSCalibur system (BD Biosciences, CA, USA) and the results were analyzed using FlowJo V10 software (Tree Star, Ashland, OR USA). The assays were performed in triplicates.

2.13 Sphere formation assay

ADSCs grown as monoculture or as co-culture were trypsinized, counted and seeded at a density of 1×10^4 cells/ml in MammoCult Basal Medium (Cat. 05621, Stemcell Technologies) supplemented with 4 µg/ml heparin, 0.48 µg/ml hydrocortisone and MammoCult Proliferation Supplement (Cat. 05622, Stemcell Technologies) according to the manufacturer's instructions. Cells were cultured at 37 °C and 5% CO2 for 15 days, and the culture medium was replaced every 3 days. Sphere formation was monitored and photographed at 1, 5, 10 and 15 days. Three biological replicates with technical duplicates were performed.

2.14 ELISA

Chemokines were determined in supernatants obtained from monocultures or co-cultures of ADSCs using a standardized commercial solid phase sandwich Enzyme-Linked Immunosorbent Assay (ELISA) protocol. Human GROβ ELISA Kit (Cat. OKAG00021, Aviva Systems Biology), Human CXCL3 ELISA Kit (Cat. OKEH00399, Aviva Systems Biology) and Human CXCL5 ELISA kit (Cat. EHCXCL5 Thermo Scientific) were employed according to manufacturer's protocols. Measurements were conducted in duplicate from three independent experiments.

2.15 ShRNA-mediated expression inhibition

ShRNA sequences were designed to inhibit lnc-CXCL3 expression from the reference sequence annotated in LNCipedia [20]. The shRNAs sequences were aligned using the proposed methodology in Knockout RNAi Systems (Clontech Inc. laboratories) and later inserted into a pSIREN-RetroQ plasmid through EcoRI and BamHI-created ends using a Rapid DNA Ligation Kit (Thermo Fisher) following the procedure described by the manufacturer.

2.16 Transfection of shRNA plasmids

5×10^5 HeLa or 2.5×10^5 3 T3-L1 cells were transfected with 4 µg pSIREN- RetroQ-shRNA plasmid or pGFP-V-RS (control plasmid) using XFect (Cat. 631,317, Clontech). Transient inhibition efficiencies were evaluated by measuring the relative mRNA expression levels.

2.17 Selection of stable knockdown clones

After shRNA transfection, HeLa and 3 T3-L1 cells were selected using 0.7 µg/ml and 2 µg/ml puromycin, respectively. Stable knockdown of relevant genes was validated by RT-qPCR.

2.18 Cell migration assay

Cell migration was determined using a Transwell System (6.5 mm insert, 24-well plate with 8.0 µm polycarbonate membrane, Corning, Costar Cat. 3422 United Kingdom). 1.5×10^4 HeLa cells were seeded in 200 µl serum-free medium in the upper compartment of the transwell chamber. Complete medium with 5% FBS was used as chemoattractant in the lower compartment and cells were incubated for 24 h at 37 °C and 5% CO_2 to allow migration. Next, cells at the opposite surface of the filter membrane facing the lower compartment were fixed with 4% paraformaldehyde, stained with Crystal Violet Staining Solution, and evaluated and photographed under a microscope. All experiments were performed in biological triplicates, with 4 technical replicates.

2.19 Statistical analysis

All values are presented as mean value with the Standard Error Mean (SEM). Mean values were calculated from three independent experiments using the GraphPad PRISM6 tool. Data were analyzed by ANOVA or student's t test. A p value < 0.05 was considered statistically significant.

3 Results

3.1 The stromal cell fraction of morbidly obese patients harbors a functional population of ADSCs

To assess the effect of tumor cells on ADSCs, primary cultures were established from the stromal fraction of visceral adipose tissues of three morbidly obese cancer-free Mexican women. The clinical-pathological characteristics of the donors are specified in Fig. 1a. The immunophenotype of the isolated cells was analyzed by flow cytometry (Fig. 1b, Supplementary Fig. 1), confirming an ADSC immunophenotype ($CD31^-$, $CD44^+$, $CD45^-$, $CD90^+$) according to the Mesenchymal Stem Cell Committee of the International Society for Cellular Therapy [21]. Cells obtained from the donors also exhibited a fibroblastic morphology and an adherent capacity, both features attributed to mesenchymal cells (Fig. 1c). Finally, to analyze the ADSCs ability to differentiate, they were cultured in adipocyte-differentiation medium or in standard growth medium for 16 days. Differentiation into an adipogenic lineage was assessed using Oil-Red staining to detect triglyceride accumulation (Fig. 1d). Quantitative analysis revealed that approximately 90% of cells exhibited lipidic vacuoles (Fig. 1d, top panel) whereas the ADSCs in basal conditions exhibited no vacuoles (Fig. 1d, bottom panel). Taking together, these results indicate that the established primary ADSC cultures exhibit both a previously reported immunophenotypic and an ability to differentiate.

3.2 ADSC/HeLa co-culture as a model of intercellular communication

Communication between ADSCs and tumor cells is one of the mechanisms by which obesity can promote cancer development. Since cervical cancer is the second most important tumor in Mexican women, we conducted co-culture experiments using HeLa cells. Once ADSCs were collected and isolated from patients with morbid obesity, we evaluated their cellular and molecular changes after co-culture with HeLa cells. A transwell system was used to separate both cell populations with a permeable membrane that avoids direct contact, but allows intercellular communication through soluble factors.

3.3 Transcriptome analysis of ADSCs in co-culture

Bidirectional communication between ADSCs and tumor cells may induce molecular modifications in both cell types. Here, we analyzed transcriptomic changes in ADSCs in the presence of HeLa cells. RNA was obtained from ADSCs co-cultured with HeLa cells or monocultured (control group)

a

Characteristics Of Donors

Donor	Age	Premenopausal Status	Weight (Kg)	Size (m)	IMC (Kg/m^2)
1	26	Yes	98	1.55	40.5
2	47	No	140	1.7	48.5
3	39	Yes	130	1.57	52

b

Immunophenotype (%)

Donor	CD31-	CD44+	CD45-	CD90+
1	96	99.4	98.5	99.5
2	98.9	99.2	ND	99.2
3	98.1	99.2	99	99.7

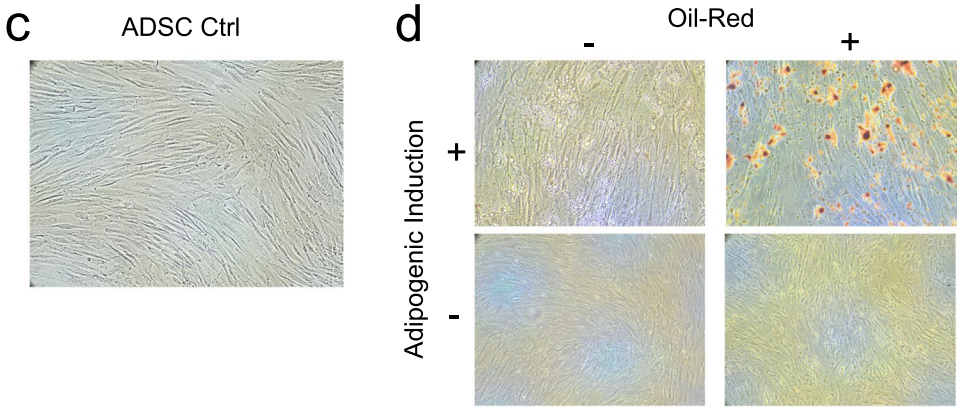

Fig. 1 Isolation and characterization of ADSCs obtained from women with morbid obesity. a Anthropometric characteristics of adipose tissue donors; **b** Immunophenotypic characterization of primary cultures isolated from each patient. The cells were stained with anti-CD31-FITC, anti-CD44- FITC, anti-CD45-PE and anti-CD90-FITC; **c** ADSC morphology of donors at 90% confluence, 10x; **d** Adipogenic induction of ADSCs. Induction$^+$ and induction$^-$ cells were stained with Oil-Red for comparison with the control group after inspection by microscopy and quantified to determine their differentiation potential

in serum-free medium for 24 h. ADSCs isolated from the 3 donors were pooled and the experiments were performed in triplicate. A comparison between both conditions revealed that co-cultured ADSCs had 761 differentially expressed RNAs with a fold change >2 or < −2 ($p < 0.05$). Among these RNAs, 687 coding RNAs were either upregulated (618) or downregulated (69) (Fig. 2a). The top upregulated (red) or downregulated (green) RNAs are shown in Fig. 2b. Interestingly, we also found 74 differentially expressed non-coding RNAs, of which 59 and 15 were up- and down-regulated, respectively (Fig. 2c). The non-coding RNAs were classified according to their locus or type of transcript, resulting in 43 intergenic and 20 intragenic lncRNAs (Fig. 2d). The top 10 non-coding RNAs that were upregulated (red) or downregulated (green) compared to the control are shown in Fig. 2e. Among the non-coding RNAs, we identified 5 miRNAs (Fig. 2f) and 6 pseudogenes (Fig. 2g).

The obtained results were validated by RT-qPCR of 4 coding RNAs and 6 lncRNAs. Both analyses showed the same significant trend (Supplementary Table 2 and Supplementary Fig. 2). To determine whether differentially expressed genes in ADSCs co-cultured with HeLa cells exhibit similar changes in other cervical cancer cell lines, we analyze 4 of 10 differentially expressed RNAs (lnc-CXCL3, CXCL2, CXCL3 and CXCL5) in ADSCs co-cultured with CaSki or SiHA cells. Interestingly, we found that ADSCs co-cultured with CaSki exhibited increased levels of these RNAs, similar to those in the ADSC/HeLa co-culture. In ADSCs co-cultured with SiHa cells only CXCL5 expression was increased, whereas the expression of both CXCL2 and CXCL3 were decreased (Supplementary Fig. 3).

4 Transcriptomic changes in ADSC/HeLa co-cultures are related to relevant cellular functions

The high numbers of differentially expressed RNAs in the ADSC/HeLa co-cultures imply a wide range of functional effects. To delve into these outcomes, we performed an integral analysis using IPA, GSEA and KPA tools. These analyses indicated that cell cycle regulation, inflammatory response and DNA repair were processes modified in ADSCs as a consequence of the intercellular communication. Remarkably, some functional processes were predicted only by a single software tool, for instance cell death and migration by IPA, cell development and matrisome by GSEA, and angiogenesis and stemness by KPA (Supplementary Fig. 4). Therefore, we also performed functional assays using a commercially available ADSC cell line (ATCC, PC-500-011). Interestingly, we found that this cell line had a similar effect as the ADSCs isolated from morbidly obese patients, showing the same expression trend of 10 selected RNA molecules (Supplementary Table 2).

4.1 The ADSCs cell cycle is not affected by HeLa cells

The observed changes in the expression pattern of 109 RNA molecules led to the notion that the proliferative capacity

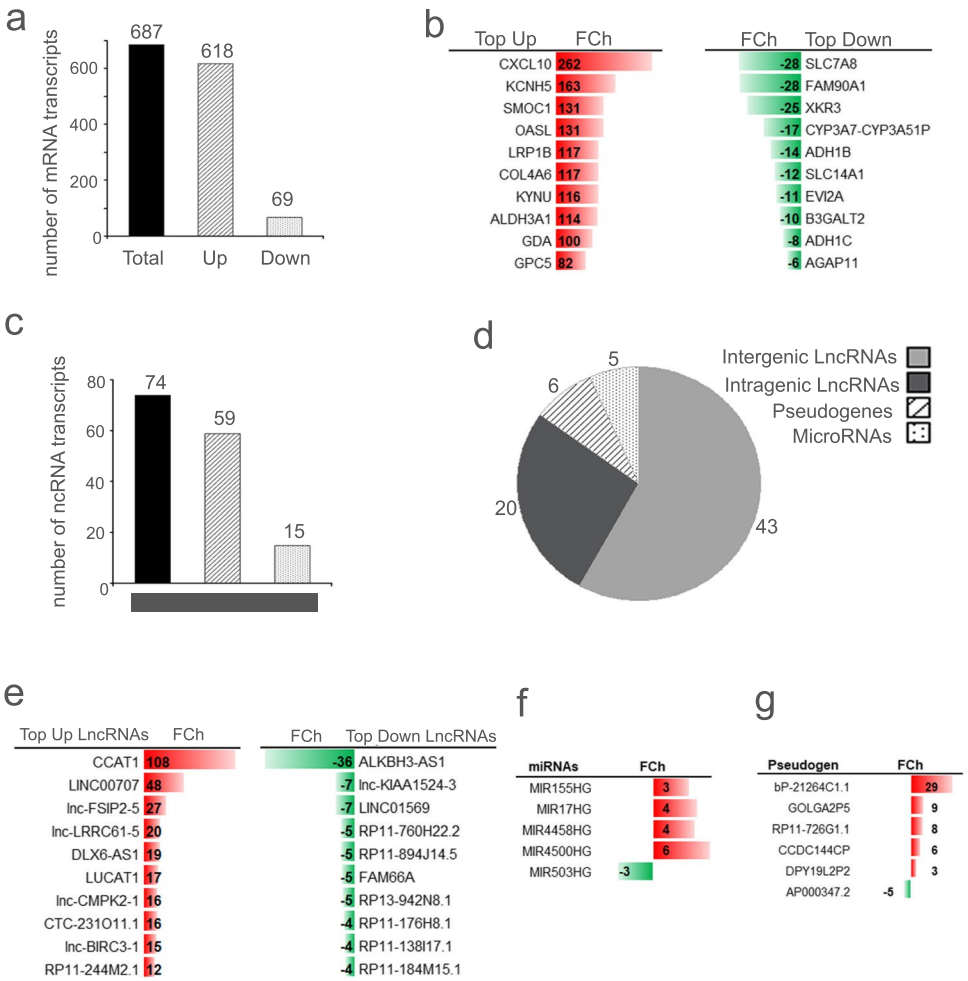

Fig. 2 Transcriptome analysis of ADSCs after co-culture. a Number of mRNA transcripts differentially expressed in co-cultured ADSCs compared to monocultured ADSCs derived from transcription analysis. **b** Top 10 upregulated mRNAs (in red) and top 10 downregulated mRNAs (in green). A fold change (FCh) ≥ 2 or ≤ −2 was considered with a $p < 0.05$. **c** Number of non-coding RNA transcripts differentially expressed in co-cultured ADSCs compared to monocultured ADSCs derived from transcription analysis. **d** Pie chart showing the classification of the different types of non-coding RNAs differentially expressed in co-cultured ADSCs. **e** Top 10 non-coding RNAs with increased (in red) or decreased (in green) expression during co-culture of ADSCs and HeLa cells. **f** miRNAs differentially expressed in co-cultured ADSCs. **g** Pseudogenes differentially expressed in co-cultured ADSCs

and cell cycle profile of ADSCs might be altered when co-cultured with HeLa cells (Supplementary Fig. 4). To test this hypothesis, we performed a cell proliferation assay using BrdU incorporation (Fig. 3a). The results obtained from ADSCs in co-culture and monoculture showed no significant differences, i.e., 60.1% of ADSCs in monoculture and 60.5% of ADSCs in co-culture were in G0/G1 phase. Different culture conditions were also tested, revealing similar S phase populations, i.e., 21.6% in monoculture and 20.7% in co-culture (Fig. 3b). Further analysis using KPA software revealed the presence of several dysregulated signaling pathways linked to proliferation, but with potential opposite effects. Whereas DNA replication through NF-κB (Supplementary Fig. 5), IL-6 (Supplementary Fig. 6) and AP-1 (Supplementary Fig. 7) may be induced, the regulation of additional pathways may inhibit proliferation by inducing changes in STAT1 (Supplementary Fig. 8) and CDK1 (Supplementary Fig. 9), likely resulting in a final neutral balance.

4.2 The migratory capacity of ADSCs increases after co-culture with HeLa cells

It has been reported that ADSCs favor cancer growth by being recruited to the tumor mass through signaling molecules secreted by cancer cells [22]. Through transcriptome analysis, we found that migrative capacity was one of the main dysregulated functions in co-cultured ADSCs (Supplementary Fig. 4). This observation was corroborated through a scratch wound-healing assay where a monolayer of ADSCs was supplemented with conditioned medium from HeLa cells, conditioned medium from ADSC/HeLa co-cultured cells, medium supplemented with FBS (positive control) or serum-free medium (negative control). Cell-free areas ('wounds') were evaluated at 0, 12, 24 and 48 h after supplementing the conditioned media. In addition, conditioned medium from HaCaT keratinocytes was used to confirm that the effects observed in ADSCs were specifically induced by cervical cancer cells. Both the conditioned media from

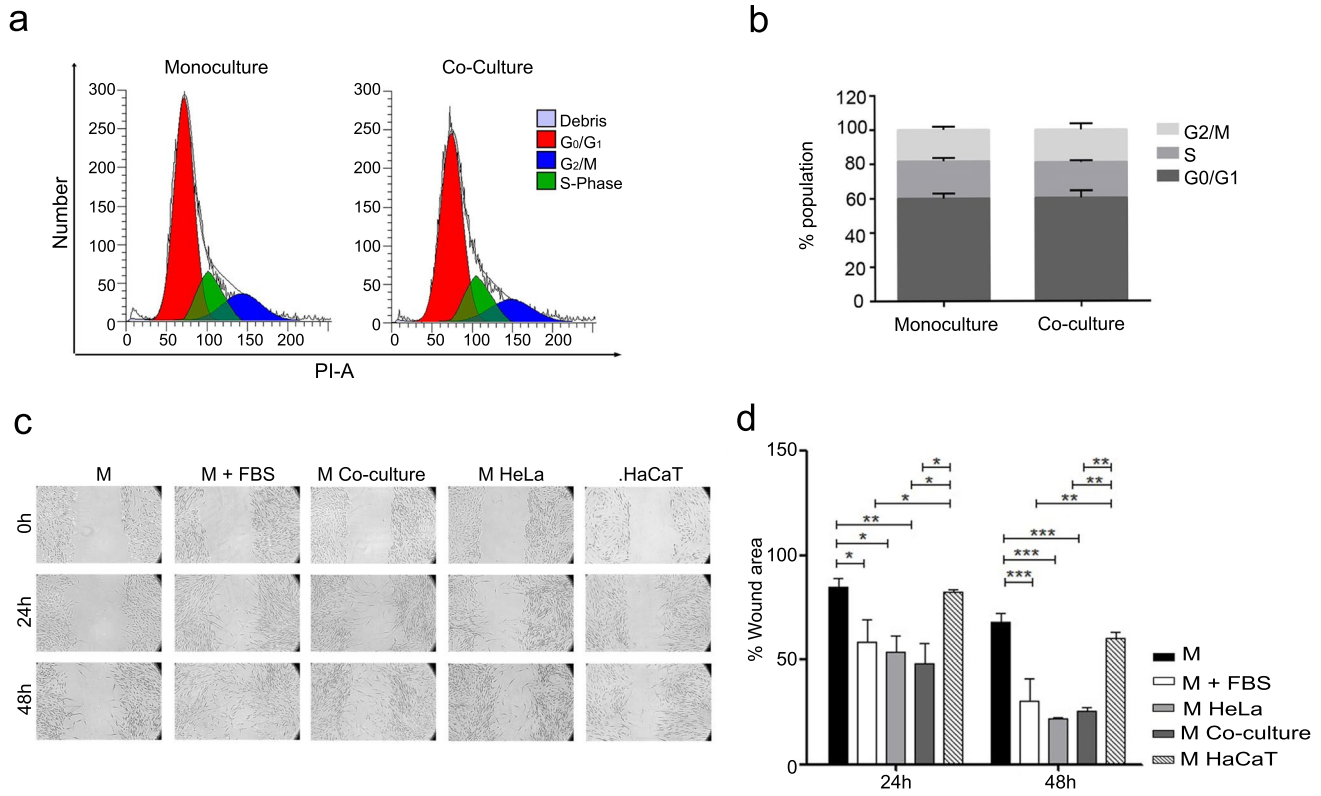

Fig. 3 Unaltered cell cycle and induced ADSC migration upon co-culture with cervical cancer cells. a Histogram showing cell cycle profiles of monocultured and co-cultured ADSCs. **b** Quantification of G0/G1, S and G2/M cell cycle populations. **c** Representative images of wound-healing closure at 0, 24 and 48 h under conditions of serum-free medium (M.), medium with 5% serum (M. + FBS), ADSC/HeLa co-culture medium (M. Co-culture), conditioned medium of HeLa (M. HeLa) and conditioned medium of HaCaT (M. HaCaT) cells. **d** Normalized area of scratch wounds at different times with DMEM medium (M.), DMEM medium supplemented with 5% FBS (M. + FBS), HeLa medium (M. HeLa), ADSC/HeLa co-culture medium (M. Co-culture) and HaCaT medium (M. HaCaT). The horizontal bars represent the means ± SEM of three independent experiments. For statistical analysis, two-way ANOVA was performed for each time, considering $p < 0.05$ *, $p < 0.01$ ** and $p < 0.001$ ***

HeLa cells and ADSC/HeLa co-cultured cells increased the migrative capacity of ADSCs, which peaked at 24 and 48 h. The wound-healing effect was comparable to that of the positive control (Fig. 3c) with a similar progression in time (Fig. 3d). Strikingly, this effect was not observed in ADSCs supplemented with HaCaT conditioned medium (Fig. 3c and d). These results are consistent with the RNAseq data (KPA software) suggesting an association of the IL8/IRAKs/NF-κB and IL8/IRAKs/cSRC/FOS/AP-1 modules with an enhanced migrative ability (Supplementary Fig. 7 and Supplementary Fig. 10).

4.3 ALDHhigh cells are increased in ADSCs after co-culture with HeLa cells

Since ADSCs exposed to soluble cancer-derived factors exhibit a higher migrative ability and a dysregulated expression of DNA repair-associated genes, we sought to assess whether the stemness of these cells was affected. Firstly, the immunophenotypes of ADSCs in co-culture and monoculture were compared (Fig. 4a). We did not find any significant difference in expression of the surface markers CD31, CD44, CD45 and CD90 (Fig. 4b). A recent study reported that a subpopulation of ADSCs with a high aldehyde dehydrogenase activity ($ALDH^{high}$) possesses adipogenic and osteogenic potentials [23]. Since $ALDH^{high}$ activity has been used to identify normal and cancer stem cells [24, 25], we decided to evaluate this marker in our model. It is important to note that several ALDH genes, especially ALDH3A1, were found to be deregulated in the RNAseq analysis (Fig. 4c). In fact, we found an increased number of $ALDH^{high}$ cells, doubling from 1.4% to 2.5%, in the ADSC/HeLa co-cultures (Fig. 4d). The increment of $ALDH^{high}$ cells remained constant throughout replicates and was statistically significant (Fig. 4e). Although changes in the stem cell subpopulations were small, they still have the capacity to produce biologically significant changes in the total cell population. To substantiate this result, we performed tridimensional spheroid assays of ADSs co-cultured with HeLa cells. The ADSCs were

grown in the presence of HeLa cells for 24 h and subjected to non-adherent conditions for 15 days. We found that ADSCs in co-culture conditions produced a similar number of spheres compared to ADSCs in monoculture conditions (Fig. 4g). However, the spheres from the ADSCs previously grown in co-culture conditions showed significantly larger diameters compared with spheres from control ADSCs (Fig. 4f).

4.4 ADSC/HeLa intercellular communication is mediated by chemokines

Soluble factors are mediators of intercellular communication in the absence of intercellular contact. Transcriptome analysis of ADSCs co-cultured with HeLa cells showed differential expression of 31 cytokines and chemokines (Fig. 5a) that function as intercellular communication signals, such as CXCL2, CXCL3 and CXCL5. Therefore, we set out to measure these chemokines in culture medium either obtained from co-cultures or monocultures. As expected, CXCL2 (Fig. 5b) and CXCL3 (Fig. 5c) were increased in culture media derived from ADSC co-cultures, which correlated with the increased mRNA levels observed by RT-qPCR. CXCL5 only showed a small non-significant increase under these conditions (Fig. 5d). Noteworthy, it has previously been reported that expression of CXCL2 (Fig. 5e), CXCL3 (Fig. 5f) and CXCL5 (Fig. 5g) may be associated with a worse prognosis in patients with cervical squamous cell carcinoma and endocervical adenocarcinoma [26].

4.5 CXCL3 expression is co-regulated by its intragenic lncRNA

Several lncRNAs are known to play key roles in the transcriptional regulation of nearby genes. In particular, mRNAs are often co-expressed with their corresponding intragenic lncRNAs. Since our data indicate that both CXCL3 and its intragenic lncRNA lnc-CXCL3 are dysregulated, we sought to delve into a possible co-regulation mechanism. The CXCL3 gene is located on chromosome 4q (Fig. 6a) within the 74,902,786–74,904,524 region (GRCh37/h19), producing a mature transcript of 1641 bp in size (Fig. 6b). To assess their putative interaction, HeLa cells were transiently transfected with two distinct shRNA constructs targeting lnc-CXCL3, referred to as sh-lncCXCL3–1 and sh-lncCXCL3–2. We found that both shRNAs were able to silence the expression of lnc-CXCL3 (Fig. 6c). Next, the effect of lnc-CXCL3 on the expression level of CXCL3 and the non-overlapping nearby genes *in cis*, CXCL2 and CXCL5, was evaluated (Fig. 6b). We found that lnc-CXCL3 silencing induced a concordant decrease in CXCL3 (Fig. 6d) and CXCL2 (Fig. 6e) expression, but a non-significant decrease in CXCL5 (Fig. 6f) expression, suggesting that lnc-CXCL3 is able to regulate the expression of at least some mRNAs in its genomic vicinity.

4.6 Inhibition of lnc-CXCL3 expression impairs the migration of HeLa cells

Since our bioinformatic analyses predicted that migration is one of the most altered functions in ADSCs co-cultured with HeLa cells, we sought to analyze whether lnc-CXCL3 could mediate this function. Therefore, we stably knocked down this non-coding RNA in HeLa cells, which was confirmed by RT-qPCR (Fig. 6g). Next, we evaluated the migrative ability of these cells using a transwell system (Fig. 6h). We found that the number of cells that migrated through the membrane decreased significatively when lnc-CXCL3 expression was silenced using two different shRNAs (Fig. 6i). This suggests that lnc-CXCL3 not only regulates the expression of chemokines such as CXCL2 and CXCL3, but also affects the migrative ability of cervical cancer cells.

4.7 Inhibition of lnc-CXCL3 expression impairs stemness characteristics in 3 T3-L1 cells

To determine whether the role of lnc-CXCL3 observed in HeLa cells is similar in ADSC-like cells, a stable knockdown of lnc-CXCL3 was established in 3 T3-L1 cells. These cells are known to be able to give rise to adipocytes, so they have been widely used as ADSC-like cells [27]. The knockdown of lnc-CXCL3 was validated by RT-qPCR (Fig.7a) and the expression levels of CXCL3 and CXCL2 were measured. CXCL3 expression could be detected in 3 T3-L1 cells transfected with the control plasmid, but not after lnc-CXCL3 knockdown (data not shown). Based on what was observed in HeLa cells, these results suggest that lnc-CXCL3 inhibition leads to downregulation of CXCL3 to undetectable levels. CXCL2 expression could not be detected in 3 T3-L1 cells transfected with the control plasmid nor with shRNAs targeting lnc-CXCL3 (data not shown).

Subsequently, the functional impact of lnc-CXCL3 knockdown on stemness-related features in 3 T3-L1 cells was analyzed. We found that inhibition of lnc-CXCL3 decreased both the size (Fig. 7d) and the number (Fig. 7e) of spheres compared to those of cells transfected with the control plasmid (Fig. 7c). Sphere formation has been reported to be closely associated with increases in $ALDH^{high}$ cells, which may result from expression upregulation of different members of the ALDH family. ALDH1A3, one of them, is an important regulator of this phenotype in both immortalized and precursor cells [28, 29]. We found that ALDH1A3 expression decreased after lnc-CXCL3 inhibition (Fig. 7b). Together these results indicate that lnc-CXCL3 is involved

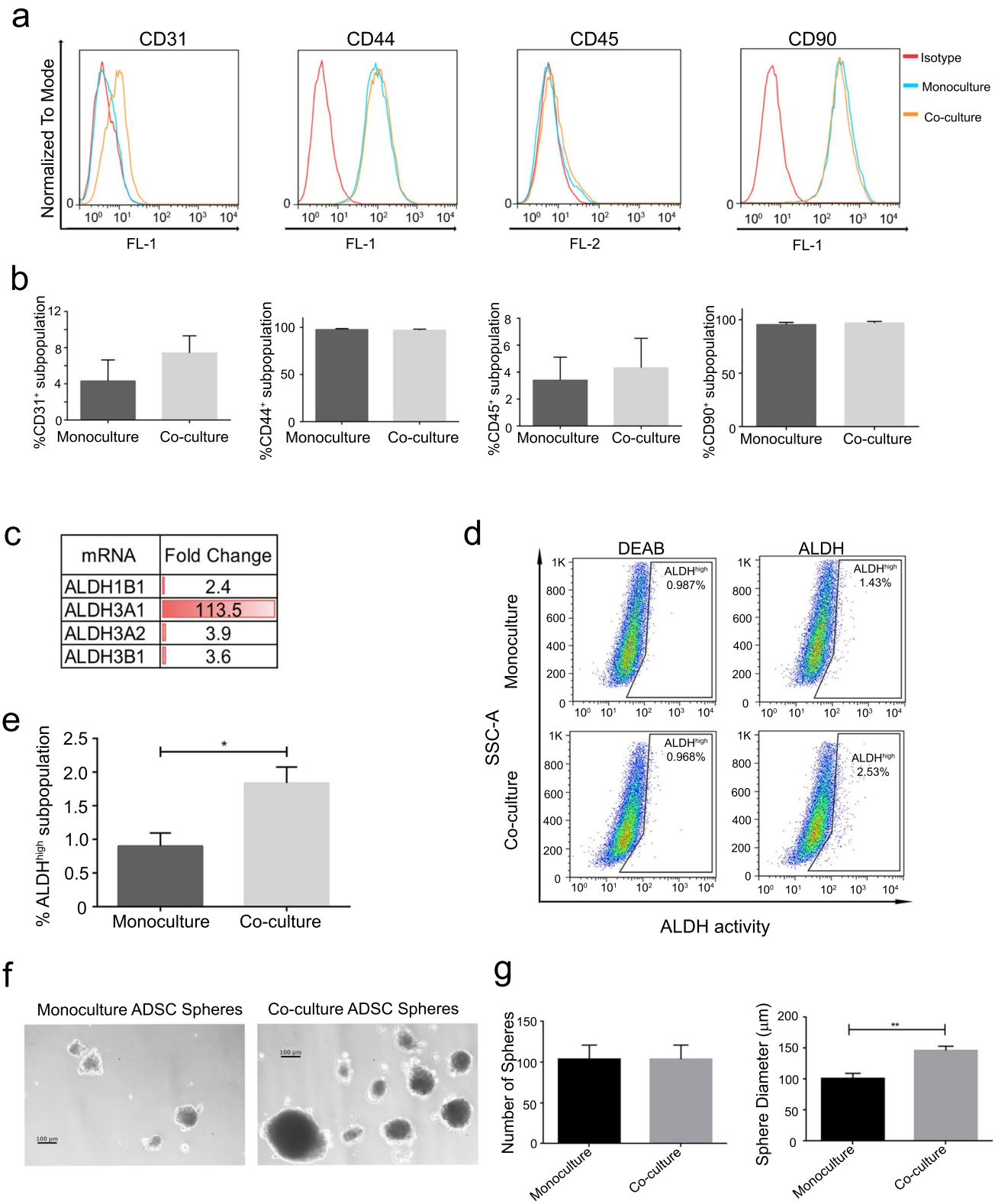

in the regulation of functional and molecular characteristics of stem-like cells.

5 Discussion

In recent years ADSCs have been gaining interest due to their emerging clinical applications and their involvement

◂**Fig. 4 ADSC stem phenotype is maintained after co-culture with HeLa. a** Histograms representing cytometric analyses of monocultured (blue) and co-cultured (orange) ADSCs. Isotype signal (red). **b** CD31, CD44, CD45 or CD90 positive cells in monocultured and co-cultured ADSCs using biological replicates. **d** Density plot with the ALDH high population in monocultured and co-cultured ADSCs. DEAB (N, N-diethylaminobenzaldehyde). **c** Increases in ALDH isoform transcripts in ADSCs after co-culture. **e** Analysis of the ALDH high population in monocultured and co-cultured ADSCs using biologic replicates. **f** Representative photographs of spheres formed after 15 days from ADSCs previously growth in monoculture or co- culture conditions. Magnification 10x. Scale bars = 100 µm. **g** Quantification of numbers and sizes of spheres obtained of ADSCs taken from ADSC monoculture or ADSC/HeLa co-culture. The bars represent the means ± SEM of three independent experiments. For the statistical analysis, the paired t test was performed with a $p < 0.05$ *, $p < 0.01$ ** and $p < 0.001$ ***

in several diseases, including cancer. An important feature of ADSCs is that they are mostly absent in blood of healthy individuals, but readily increase after pathologic stimuli such as hypoxia and inflammation, which trigger their mobilization and migration from their original niche [30]. Obesity is an inflammatory condition that favors ADSC mobilization and, therefore, obese individuals usually present a larger number of circulating ADSCs compared to non-obese individuals. ADSC mobilization may also occur in non-obese individuals diagnosed with cancer, which indicates that tumor development may also stimulate the mobilization of ADSCs, but particularly in obese individuals with cancer [14].

Cancer cells are known to recruit mesenchymal cells, which allows them to build a suitable tumor microenvironment [22]. Several studies have addressed the question how ADSCs may participate in the development and progression of cancer through their establishment in the tumor microenvironment where they produce and secrete several extracellular factors. As yet, however, little is known about the molecular and cellular changes that ADSCs undergo in this context. In the present study, ADSCs were isolated from visceral adipose tissues derived from morbidly obese patients. These ADSCs possessed a phenotype characteristic of mesenchymal cells, including an adherent capacity, a fibroblastic morphology, the expression of stem markers and adipogenic differentiation abilities (Fig. 1).

Considering the bidirectional communication between ADSCs and cancer cells within the tumor microenvironment, we analyzed transcriptomic changes in ADSCs co-cultured with cervical cancer cells using a transwell system. In this model, a permeable membrane allows communication between both cell types through a free transit of soluble factors and exosomes. These ADSCs can thus be evaluated without the risk of contamination with cancer cells. RNA from the co-cultured ADSCs was used for whole-genome RNA analysis, revealing important changes in the expression profile of these cells, including coding and non-coding transcripts. Recently, several deregulated chemokines were reported in co-cultured ADSC and A431 vulvar cancer cells, i.e., IL-6, IL-1A, CXCL2, CXCL5, CXCL3 and CXCL10 [31], an observation that is consistent with our results. In our experiments, the last chemokine was only found to be upregulated in co-cultures with HeLa cells. Interferon-γ inducible protein 10 kDa (CXCL10) binds to the CXCR3 receptor and is involved in chemotaxis, apoptosis, cell growth and angiogenesis. In addition, CXCL10 has been found to be upregulated in cervical cancer cells [32] and to be involved in the suppression of angiogenesis in advanced cancer [33]. Our RNAseq analyses showed that this chemokine exhibited a significant expression change in ADSCs co-cultured with HeLa cells, which was corroborated by RT-qPCR. In addition, we found that the expression level of CXCL10 increased in ADSC/CaSki and ADSC/SiHa co-cultures, although statistically significant only for SiHa (Supplementary Fig. 11). Interestingly, data obtained from GEPIA [26] revealed that a high CXCL10 expression is related to a poor prognosis in cervical squamous cell carcinoma and endocervical adenocarcinoma. Finally, CXCL10 may serve as an unfavorable prognostic marker in renal and pancreatic cancer (data consulted in porteinatlas.org).

Network analyses showed that several processes such as cytoskeleton assembly, cell migration, cell cycle regulation, cell death and survival were among the most altered ones in ADSC/HeLa co-cultures. As expected by these results, functional assays showed that the migrative capacity of ADSCs increased after being supplemented with conditioned medium from either HeLa or ADSC/HeLa cultures. This may reflect the reported chemotactic effects of ADSCs towards a tumor. It should be mentioned that the effect of soluble factors in cellular mobilization was inherent to cancer cells only, since this phenomenon was not observed when conditioned medium from HaCaT cells was used. It should also be noted that the conditioned medium was serum-free, so the observed effects were solely dependent on the factors secreted by HeLa cells under either single or co-culture conditions. Moreover, ADSCs have long doubling times of up to 72 h [34, 35]. Therefore, the scratch wound-healing assay lasting only 48 h rules out the possibility that the observed results are due to changes in cell proliferation. On the other hand, it has been reported that cancer cells secrete IL-6 to recruit mesenchymal cells into the tumor microenvironment, thus favoring the production of CXCL7 [36]. However, IL-6 can also act on cancer cells in an autocrine manner to produce higher amounts of this cytokine [37]. The increased expression of IL-6 in ADSCs suggests an unknown mechanism by which cancer cell-secreted IL-6 leads to its increased production in ADSCs. Bioinformatic analyses of these processes and pathways suggest that NF-κB, AP-1/FOS and interleukins could become activated and, therefore, affect ADSC migration. In particular, NF- κB

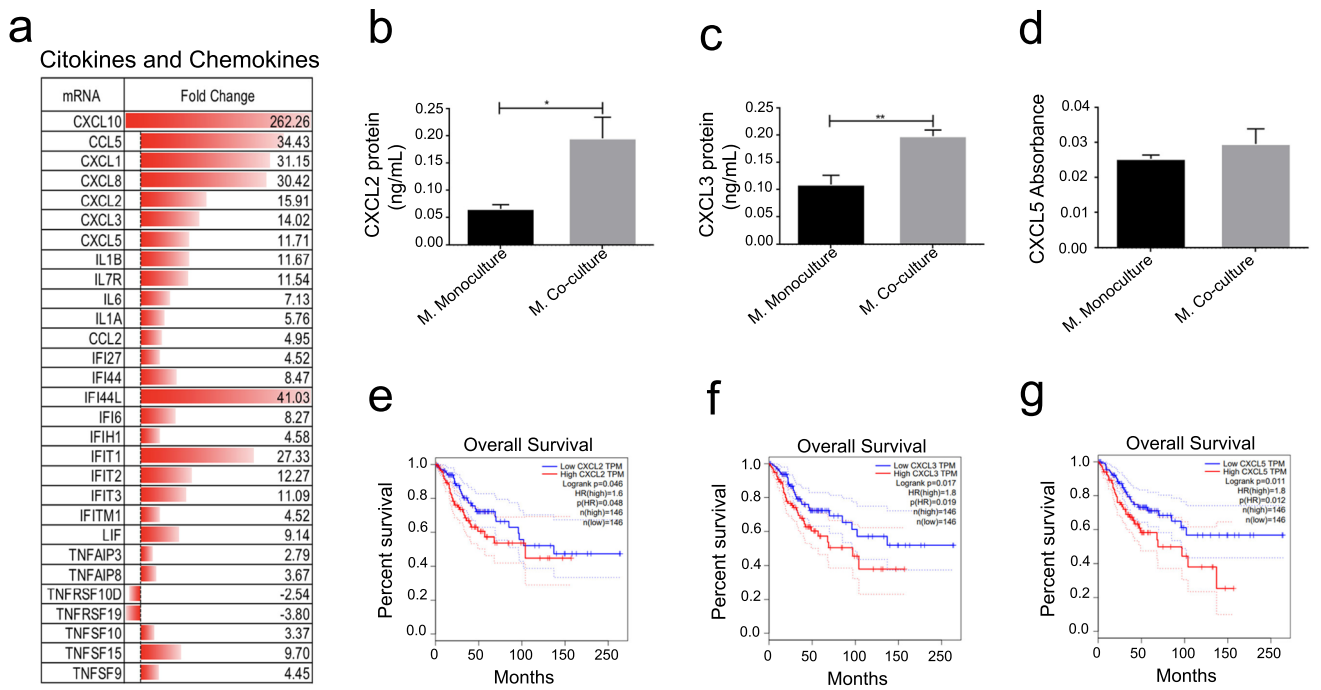

Fig. 5 Increased expression of CXCL2 and CXCL3 mRNA in ADSCs in the presence of HeLa cells correlates with their elevated levels detected in extracellular co-culture medium. a Increased cytokine and chemokine transcripts in ADSCs after co-culture. **b**, **c** Concentrations of CXCL2 (**b**) and CXCL3 (**c**) evaluated by ELISA in conditioned media obtained from ADSC monoculture or ADSC/HeLa co-culture. **d** Absorbance measurements of CXCL5 in conditioned media of monocultured or co-cultured ADSCs. **e**–**g** Overall survival plots of CXCL2 (**e**), CXCL3 (**f**) and CXCL5 (**g**) in cervical squamous cell carcinoma and endocervical adenocarcinoma obtained from the GEPIA database. The horizontal bars represent the means ± SEM of three independent experiments. For the statistical analysis, the paired t test was performed with a $p < 0.05$ *, $p < 0.01$ **

has been reported to be activated in mesenchymal cells, so it would be interesting to unravel the functional implications of this pathway in ADSCs co-cultured whit cancer cells [38].

Although several genes associated with cell cycle regulation and proliferation were deregulated in ADSCs after co-culture with cervical cancer cells, we did not observe differences in these processes, possibly because even when proliferation-related pathways such as NF-κB, IL-6 and AP1 were activated, inhibitory signaling such as STAT1 and CDK1 could be hampering their effect. These data highlight the importance of considering not only the changes in signaling pathways, but also the direction of these changes. Furthermore, the observed changes in proliferation capacity could be dependent on the type of MSCs, since it was previously reported that MSCs exposed to conditioned medium from FaDu cells (hypopharyngeal carcinoma) lead to G0/G1 arrest and a decreased G2/M population after 5 days [39].

Several studies have suggested that ADSCs recruited to the periphery of a tumor can switch into a cancer-associated fibroblast (CAF)-like phenotype [40] or start expressing endothelial cell markers allowing them to become part of the growth-favorable tumor microenvironment [13, 41]. Importantly, additional studies have suggested that the recruitment of ADSCs to the periphery of a tumor may give rise to adipocytes that provide energy to the tumor cells through lipolysis, favoring metastasis [42]. In the present study, we observed a small increase of the expression of CD31, a vascular endothelium cell marker, and CD45, a hematopoietic cell marker, in co-cultured ADSCs. Although not significant, it could be taken as a starting point to a trend that suggests promotion of the angiogenic processes in a subpopulation of the culture. These data are consistent with the transcriptome analysis, where this same process seems to be altered (data not shown). Additional experiments are required to corroborate this notion.

High ALDH activity ($ALDH^{high}$) is a well-known stemness characteristic that is widely used as a marker of both normal and cancer stem cells [24, 25]. It was indeed interesting to find an $ALDH^{high}$ cell subpopulation in ADSCs, and although this subpopulation was rather small, it is consistent with several reports showing that they constitute ~2% of the total ADSC population isolated from patients [43]. Interestingly, we found that upon co-culture with HeLa cells, $ALDH^{high}$ cells doubled their number. Supporting this, previous reports have demonstrated that the interaction between mesenchymal and cancer cells leads to an increased percentage of $ALDH^{high}$ cells [44], an effect that has also been observed in breast cancer [36]. These

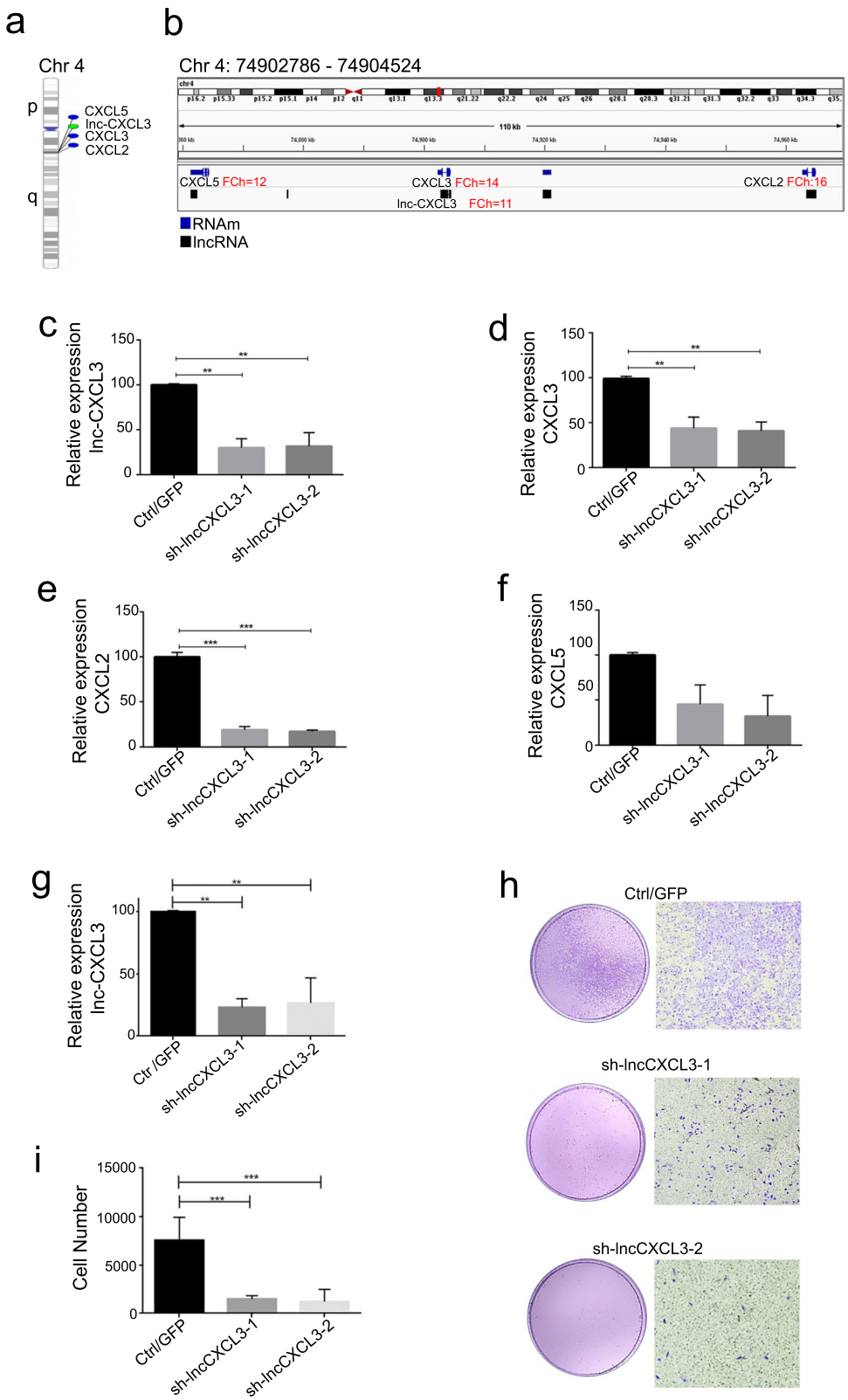

Fig. 6 Lnc-CXCL3 knockdown decreases the migratory capacity of HeLa cells. a Phenogram showing the location of lnc-CXCL3 on the q-arm of chromosome 4. **b** Scheme of the chromosome 4 locus where lnc-CXCL3 and CXCL3 are located (black FCh = 11 and blue FCh = 14, respectively). Localization of CXCL5 adjacent to the left side (Fch = 12) and CXCL2 adjacent to the right side (FCh = 16). Fold Change (FCh) was determined by RNAseq. **c**-**f** HeLa cells were transiently transfected with pGFP-V-RS (plasmid control) or pSIREN-RetroQ to knockdown lnc-CXCL3 after which the relative expression of lnc-CXCL3 (**c**), CXCL3 mRNA (**d**), CXCL2 mRNA (**e**) and CXCL5 mRNA (**f**) were measured by RT-qPCR. **g** shRNA-mediated knockdown of lnc-CXCL3 in HeLa cells stably transfected with pSIREN-RetroQ or pGFP-V-RS (plasmid control) confirmed by RT-qPCR. **h** HeLa cells with lnc-CXCL3 knockdown were seeded in a transwell system and allowed to migrate for 24 h. Representative photographs of the lower membranes are shown, and 10x magnification images are presented in the right panels. **i** Quantification of migratory HeLa cells with shRNA-mediated lnc-CXCL3 knockdown evaluated using a transwell system. The bars represent the means ± SEM of three independent experiments. Statistical analyses were performed using one-way ANOVA with a Dunnett's multiple comparisons test. $p < 0.05$ *, $p < 0.01$ ** and $p < 0.001$ ***

increased ADSC-ALDH^{high} subpopulations may play a significant role in tumor development since in vitro studies have shown that murine ALDH^{high} cells exhibit a greater potential for adipogenic and chondrogenic differentiation [45]. Therefore, it is plausible that these cells display some characteristics that are advantageous for cancer cells. Furthermore,

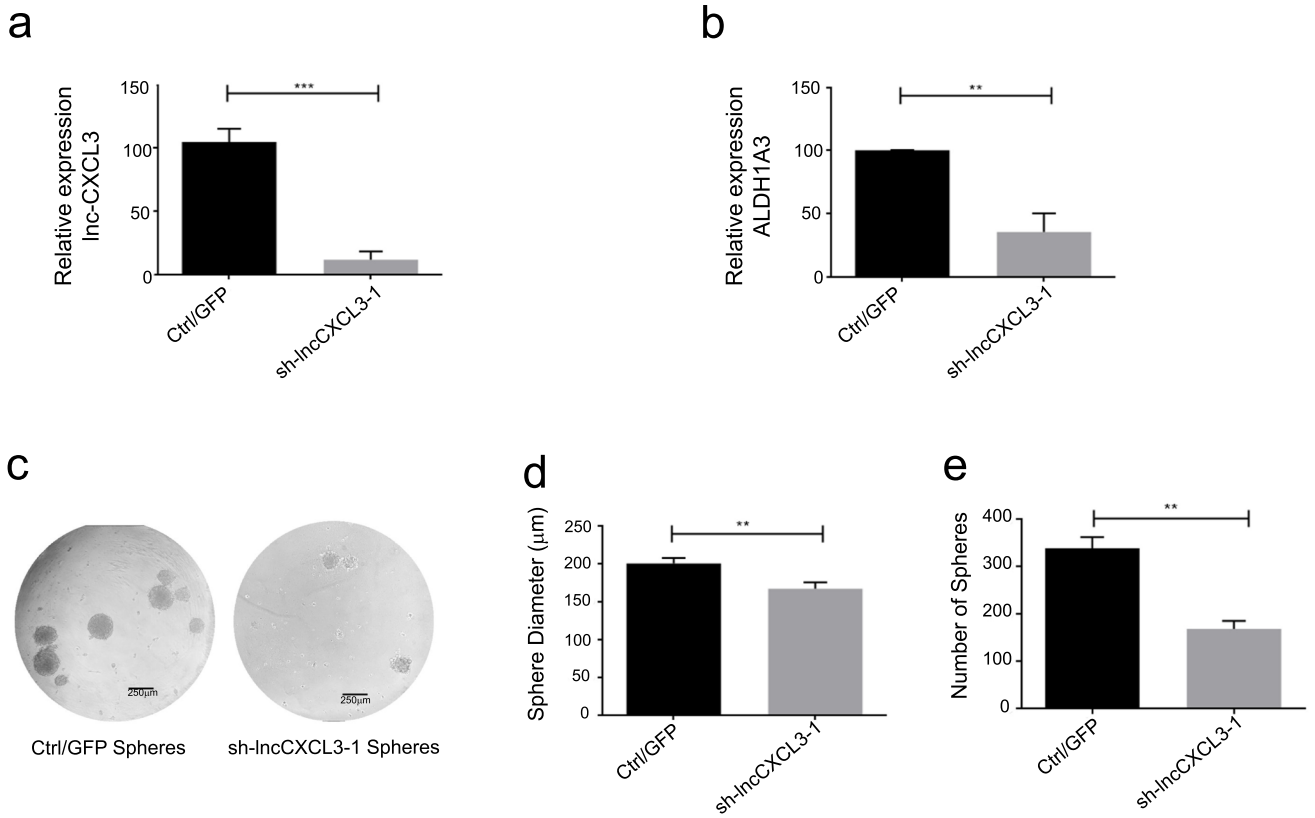

Fig. 7 Lnc-CXCL3 knockdown decreases ALDH1A3 expression and the capacity to form spheres in 3 T3-L1 cells. a Plasmids pSIREN-RetroQ with shRNA against lncCXCL3 (sh-lncCXCL3–1) or pGFP-V-RS (Ctrl/GFP) were stably transfected in 3 T3-L1 cells. The relative expression of lnc-CXCL3 was evaluated by RT-qPCR. **b** Relative expression of ALDH1A3 in 3 T3-L1 cells transfected with pSIREN-RetroQ or pGFP-V-RS (Ctrl/GFP). **c** Representative photographs of spheres formed after 15 days from 3 T3-L1 cells transfected with pSIREN-RetroQ or pGFP-V-RS (Ctrl/GFP). Magnification 10x. Scale bars = 250 µm. **d**, **e** Quantification of sizes (**d**) and numbers of spheres (**e**) from 3 T3-L1 cells transfected with pSIREN-RetroQ or pGFP-V-RS (Ctrl/GFP). The bars represent the means ± SEM of three independent experiments. For statistical analysis the paired t test was performed with $p < 0.05$ *, $p < 0.01$ ** and $p < 0.001$ ***

our RNAseq analyses revealed several dysregulated ALDH genes, including ALDH3A1. Interestingly, it has been reported that ALDH3A1 and ALDH1A1 deficient mice have lower numbers of hematopoietic stem cells (HSCs), in addition to an aberrant cell cycle distribution, higher ROS levels, p38 MAPK activation and a decreased resistance to DNA damage [46]. In our results, the enrichment of ALDH may have been one of the reasons for the increased spheroid sizes observed after ADSC/HeLa co-culture. Noteworthy, a decreased expression of ALDH1A3, a family member related to cellular characteristic of high ALDH activity [28, 29], was related to reduction in the number and sizes of 3 T3-L1 spheres after ln-CXCL3 silencing.

Since brown to white adipose tissue conversion has been found in preclinical models and patients with cancer [47, 48] we were interested in assessing the expression of genes involved in brown adipocyte development [49]. We found that PPARGC1A (FC = 23) which codes for a co-activator protein that regulates genes involved in early stages of brown adipocyte differentiation was the only differentially expressed gene in ADSCs co-culture with HeLa (Supplementary Fig. 12).

In our study, 687 RNAs were found to be dysregulated, 90% of which represented coding RNAs and 10% non-coding RNAs, including 63 lncRNAs. It has been reported that lncRNAs are able to regulate the expression of neighboring genes [50], as was also observed for some lnRNA/mRNA combinations in our study. We found that a cluster of three CXCL members (CXCL2, CXCL3 and CXCL5) and the corresponding lnc-CXCL3 showed modified expression levels, suggesting a co-regulatory module. Interestingly, increases in CXCL2 and CXCL3 proteins correlated with a lower survival rate in patients with cervical squamous cell carcinoma and endocervical adenocarcinoma. This finding indicates that lnc-CXCL3 may drive the expression of at

least some contiguous target genes important in cervical cancer development.

6 Conclusions

Obesity, a globally rising health problem, has been linked to the development, progression and poor prognosis of some types of cancer. It has been suggested that adipose tissues can generate favorable conditions that support the tumor microenvironment. Furthermore, ADSCs are known to be recruited by tumor cells and to contribute to several processes that are advantageous to the tumor. Yet, little attention has been devoted to changes elicited by tumor cells in the ADSCs. Here, we report important major RNA changes that correlate with an increased subpopulation of $ALDH^{high}$ cells, a higher migrative capacity, bigger spheres, and a deregulated expression of DNA repair related genes. The dysregulated ncRNAs found in this study may play a key role in regulating the expression of chemokines such as CXCL2 and CXCL3. This was supported by the effect of lnc-CXCL3 knockdown on cell migration. Detailed knowledge on the processes that are affected during the communication between stem and tumor cells will allow a better understanding of the phenomena observed in ADSCs. Complementary studies are needed to determine whether these phenomena are exclusive of ADSCs from obese individuals, allowing the identification of key mechanisms linking obesity to cancer.

Supplementary Information The online version contains supplementary material available at https://doi.org/10.1007/s13402-021-00653-6.

Acknowledgements This work was part of the PhD thesis of Marcela Angelica De la Fuente Hernandez (CVU: 441075) from the Programa de Doctorado en Ciencias Biológicas, Universidad Nacional Autónoma de México (UNAM). The work was supported by a Consejo Nacional de Ciencia y Tecnologia (CONACyT) fellowship (Registry number 270150). We thank Dr. Alfredo Mendoza for his help in transcriptome sequencing (Unit of Sequencing Genomics, Instituto Nacional de Medicina Genomica, Mexico City), M.C. Linda Nelly Patiño for her help in the cytometry experiments (Unit of Citometry, Instituto Nacional de Medicina Genómica, Mexico City), M.C. Miguel Angel Sarabia Sanchez for his help in the cytometry experiments in the Laboratorio Nacional de Citometría de Flujo (LabNalCit), Mexico City and Dr. Daniel Díaz for his kind assistance in proofreading this manuscript.

Authors'contributions **MDH**: substantial contributions to the conception and design of the study; substantial contributions to data acquisition and analysis and drafting the article. **EAM**: established the primary culture. **EFO**: contributed to the selection and enrollment of patients for obtaining visceral adipose tissue. **ARG**: contributed to the selection and enrollment of patients for obtaining visceral adipose tissue. **LAP**: contributed to the revision of the manuscript. **KVS**: contributed to the GSEA analysis of the RNAseq data. **JMZ**: made substantial contributions to the analysis and interpretation of sequencing data. **VFO**: contributed to the revision of the manuscript. **RMAG**: Contributed to the revision of the manuscript. **VML**: made substantial contributions to the conception and design of the study, coordinated the work, analyzed the data and contributed to the manuscript draft.

Funding Marcela Angelica De la Fuente Hernandez is a doctoral student from Programa de Doctorado en Ciencias Biologicas, Universidad Nacional Autonoma de México (UNAM) and received a fellowship 270150 from CONACyT. This work was supported by grant A1-S-33543 CONACyT to Vilma Maldonado.

Data availability The data obtained from the sequencing were deposited: SRA data: PRJNA780960.

Declarations

Ethical approval and consent to participate All procedures performed in studies involving human participants were in accordance with the ethical standards of the institutional research committee and with the 1964 Helsinki declaration and its later amendments or comparable ethical standards and consent to participate.

Consent for publication Not applicable. Inthe manuscript, no data is handled that puts the identity or privacy of the donor at risk.

Competing interests The authors declare that there is no conflict of interest.

Research involving human participants Morbidly obese women undergoing gastric bypass donor visceral adipose tissue.

Informed consent Informed consent was obtained from all individual participants included in the study.

References

1. https://www.who.int/es/news-room/fact-sheets/detail/obesity-and-overweight [Internet] Accessed 9 jun 2021
2. E.E. Calle, R. Kaaks, Overweight, obesity and cancer: Epidemiological evidence and proposed mechanisms. Nat Rev Cancer **4**, 579–591 (2004)
3. M. Arnold, N. Pandeya, G. Byrnes, P.A.G. Renehan, G.A. Stevens, P.M. Ezzati, J. Ferlay, J.J. Miranda, I. Romieu, R. Dikshit, D. Forman, I. Soerjomataram, Global burden of cancer attributable to high body-mass index in 2012: A population-based study. Lancet Oncol **16**, 36–46 (2015)
4. https://gco.iarc.fr/causes/obesity/tools-pie. https://gco.iarc.fr/causes/obesity/tools-pie [Internet] Accessed 9 jun 2021
5. B. Lauby-Secretan, C. Scoccianti, D. Loomis, Y. Grosse, F. Bianchini, K. Straif, Body fatness and Cancer--viewpoint of the IARC working group. N Engl J Med **375**, 794–798 (2016)
6. R.C.M. van Kruijsdijk, E. van der Wall, F.L.J. Visseren, Obesity and cancer: The role of dysfunctional adipose tissue. Cancer Epidemiol Biomark Prev **18**, 2569–2578 (2009)
7. S.D. Hursting, N.P. Nunez, L. Varticovski, C. Vinson, The obesity-cancer link: Lessons learned from a fatless mouse. Cancer Res **67**, 2391–2393 (2007)
8. M.J. Khandekar, P. Cohen, B.M. Spiegelman, Molecular mechanisms of cancer development in obesity. Nat Rev Cancer **11**, 886–895 (2011)
9. J. Park, T.S. Morley, M. Kim, D.J. Clegg, P.E. Scherer, Obesity and cancer-mechanisms underlying tumour progression and recurrence. Nat Rev Endocrinol **10**, 455–465 (2014)

10. B.A. Bunnell, M. Flaat, C. Gagliardi, B. Patel, C. Ripoll, Adipose-derived stem cells: Isolation, expansion and differentiation. Methods **45**, 115–120 (2008)
11. G. Lazennec, P.Y.P. Lam, Recent discoveries concerning the tumor - mesenchymal stem cell interactions. Biochim Biophys Acta **1866**, 290–299 (2016)
12. C. Senst, T. Nazari-Shafti, S. Kruger, K.H.Z. Bentrup, C.L. Dupin, A.E. Chaffin, S.K. Srivastav, P.M. Worner, A.B. Abdel-Mageed, E.U. Alt, R. Izadpanah, Prospective dual role of mesenchymal stem cells in breast tumor microenvironment. Breast Cancer Res Treat **137**, 69–79 (2013)
13. Y. Zhang, A. Daquinag, D.O. Traktuev, F. Amaya-Manzanares, P.J. Simmons, K.L. March, R. Pasqualini, W. Arap, M.G. Kolonin, White adipose tissue cells are recruited by experimental tumors and promote cancer progression in mouse models. Cancer Res **69**, 5259–5266 (2009)
14. Y. Zhang, C.F. Bellows, M.G. Kolonin, Adipose tissue-derived progenitor cells and cancer. World J Stem Cells **2**, 103–113 (2010)
15. B.-C. Zhao, B. Zhao, J.-G. Han, H.-C. Ma, Z.-J. Wang, Adipose-derived stem cells promote gastric cancer cell growth, migration and invasion through SDF-1/CXCR4 axis. Hepatogastroenterology **57**, 1382–1389 (2010)
16. G. Lin, R. Yang, L. Banie, G. Wang, H. Ning, L.-C. Li, T.F. Lue, C.-S. Lin, Effects of transplantation of adipose tissue-derived stem cells on prostate tumor. Prostate **70**, 1066–1073 (2010)
17. The global cancer observatory https://gco.iarc.fr/today/data/factsheets/populations/484-mexico-fact-sheets.pdf [Internet] Accessed 9 jun 2021
18. P. A. Zuk, M. Zhu, H. Mizuno, J. Huang, J. W. Futrell, A. J. Katz, P. Benhaim, H. P. Lorenz, M.H, Hedrick, Multilineage cells from human adipose tissue: implications for cell-based therapies. Tissue Eng **7**, 211–228 (2001)
19. C.C. Liang, A.Y. Park, J.L. Guan, In vitro scratch assay: A convenient and inexpensive method for analysis of cell migration in vitro. Nat Protoc **2**, 329–333 (2007)
20. P.-J. Volders, J. Anckaert, K. Verheggen, J. Nuytens, L. Martens, P. Mestdagh, J. Vandesompele, LNCipedia 5: Towards a reference set of human long non-coding RNAs. Nucleic Acids Res **47**, D135–D139 (2019)
21. M. Dominici, K. Le Blanc, I. Mueller, I. Slaper-Cortenbach, F.C. Marini, D.S. Krause, R.J. Deans, A. Keating, D.J. Prockop, E.M. Horwitz, Minimal criteria for defining multipotent mesenchymal stromal cells. The International Society for Cellular Therapy position statement Cytotherapy **8**, 315–317 (2006)
22. D. Hanahan, L.M. Coussens, Accessories to the crime: Functions of cells recruited to the tumor microenvironment. Cancer Cell **21**, 309–322 (2012)
23. H. Itoh, S. Nishikawa, T. Haraguchi, Y. Arikawa, S. Eto, M. Hiyama, T. Iseri, Y. Itoh, M. Nakaichi, Y. Sakai, K. Tani, Y. Taura, K. Itamoto, Aldehyde dehydrogenase activity helps identify a subpopulation of murine adipose-derived stem cells with enhanced adipogenic and osteogenic differentiation potential. World J Stem Cells **9**, 179–186 (2017)
24. V. Tirino, V. Desiderio, F. Paino, A. De Rosa, F. Papaccio, M. La Noce, L. Laino, F. De Francesco, G. Papaccio, Cancer stem cells in solid tumors: An overview and new approaches for their isolation and characterization. FASEB J **27**, 13–24 (2013)
25. L. Mele, D. Liccardo, V. Tirino, Evaluation and isolation of cancer stem cells using ALDH activity assay. Methods Mol Biol **1692**, 43–48 (2018)
26. C. Tang, B. Li, G. Kang, C. Gao, Z. Li, Zhang, GEPIA: A web server for cancer and normal gene expression profiling and interactive analyses. Nucleic Acids Res **45**, W98–W102 (2017)
27. S. P. Poulos, M. V Dodson, G. J. Hausman, Cell line models for differentiation: Preadipocytes and adipocytes. Exp Biol Med (Maywood) 235, 1185–1193 (2010)
28. L. Zhou, D. Sheng, D. Wang, W. Ma, Q. Deng, L. Deng, S. Liu, Identification of cancer-type specific expression patterns for active aldehyde dehydrogenase (ALDH) isoforms in ALDEFLUOR assay. Cell Biol Toxicol **35**, 161–177 (2019)
29. S. Puttini, I. Plaisance, L. Barile, E. Cervio, G. Milano, P. Marcato, T. Pedrazzini, G. Vassalli, ALDH1A3 is the key isoform that contributes to aldehyde dehydrogenase activity and affects in vitro proliferation in cardiac atrial appendage progenitor cells. Front Cardiovasc Med **5**, 1–15 (2018)
30. Q. He, C. Wan, G. Li, Concise review: Multipotent mesenchymal stromal cells in blood. Stem Cells **25**, 69–77 (2007)
31. E. Koellensperger, F. Gramley, F. Preisner, U. Leimer, G. Germann, V. Dexheimer, Alterations of gene expression and protein synthesis in co-cultured adipose tissue-derived stem cells and squamous cell-carcinoma cells: Consequences for clinical applications. Stem Cell Res Ther **5**, 65 (2014)
32. M.L. Liu, S.C. Guo, J.K. Stiles, The emerging role of CXCL10 in cancer (review). Oncol Lett **2**, 583–589 (2011)
33. E. Sato, J. Fujimoto, T. Tamaya, Expression of interferon-gamma-inducible protein 10 related to angiogenesis in uterine endometrial cancers. Oncology **73**, 246–251 (2007)
34. H.-T. Chen, M.-J. Lee, C.-H. Chen, S.-C. Chuang, L.-F. Chang, M.-L. Ho, S.-H. Hung, Y.-C. Fu, Y.-H. Wang, H.-I. Wang, G.-J. Wang, L. Kang, J.-K, Proliferation and differentiation potential of human adipose-derived mesenchymal stem cells isolated from elderly patients with osteoporotic fractures. J Cell Mol Med **16**, 582–593 (2012)
35. D. Legzdina, A. Romanauska, S. Nikulshin, T. Kozloyska, U. Berzins, Characterization of senescence of culture-expanded human adipose-derived mesenchymal stem cells. Int J Stem Cells **9**, 124–136 (2016)
36. S. Liu, C. Ginestier, S.J. Ou, S.G. Clouthier, S.H. Patel, F. Monville, Breast cancer stem cells are regulated by mesenchymal stem cells through cytokine networks. Cancer Res **71**, 614–624 (2011)
37. H.J. Wei, R. Zeng, J.H. Lu, W.F.T. Lai, W.H. Chen, H.Y. Liu, Y.T. Chang, W.P. Deng, Adipose-derived stem cells promote tumor initiation and accelerate tumor growth by interleukin-6 production. Oncotarget **6**, 7713–7726 (2015)
38. P. Escobar, C. Bouclier, J. Serret, I. Bieche, M. Brigitte, A. Caicedo, E. Sanchez, S. Vacher, M.L. Vignais, P. Bourin, D. Genevieve, F. Molina, C. Jorgensen, G. Lazennec, IL-1β produced by aggressive breast cancer cells is one of the factors that dictate their interactions with mesenchymal stem cells through chemokine production. Oncotarget **6**, 29034–29047 (2015)
39. M. Al-toub, A. Almusa, M. Almajed, M. Al-Nbaheen, M. Kassem, A. Aldahmash, N.M. Alajez, Pleiotropic effects of cancer cells' secreted factors on human stromal (mesenchymal) stem cells. Stem Cell Res Ther **4**, 114 (2013)
40. Y. Inagaki, T. Oda, T. Kurokawa, R. Miyamoto, Y. Kida, N. Ohkohchi, Abstract 171: Adipose-derived mesenchymal stem cell (ADSC) has the differentiation capacity toward cancer associated fibroblast (CAF) and reproduce the morphology of the clinical tumor stroma. In 105th Annual Meeting of the American Association for Cancer Research. Cancer Res **74**, 171 (2014)
41. M. Deng, Y.P. Gu, Z.J. Liu, Y. Qi, G.E. Ma, N. Kang, Endothelial differentiation of human adipose-derived stem cells on polyglycolic acid/polylactic acid mesh. Stem Cells Int **2015**, 350718 (2015)
42. K. M. Nieman, H. A. Kenny, C. V Penicka, A. Ladanyi, R. Buell-Gutbrod, M. R. Zillhardt, I. L. Romero, M. S. Carey, G. B. Mills, G. S. Hotamisligil, S. D. Yamada, M. E. Peter, K. Gwin, E. Lengyel, Adipocytes promote ovarian cancer metastasis and provide energy for rapid tumor growth. Nat Med 17, 1498–1503 (2011)

43. B.T. Estes, A.W. Wu, R.W. Storms, F. Guilak, Extended passaging, but not aldehyde dehydrogenase activity, increases the chondrogenic potential of human adipose-derived adult stem cells. J Cell Physiol **209**, 987–995 (2006)
44. H.-J. Li, F. Reinhardt, H.R. Herschman, R.A. Weinberg, Cancer-stimulated mesenchymal stem cells create a carcinoma stem cell niche via prostaglandin E2 signaling. Cancer Discov **2**, 840–855 (2012)
45. M. Najar, E. Crompot, L.A. van Grunsven, L. Dolle, L. Lagneaux, Aldehyde dehydrogenase activity in adipose tissue: Isolation and gene expression profile of distinct sub-population of mesenchymal stromal cells. Stem Cell Rev Reports **14**, 599–611 (2018)
46. M. Gasparetto, S. Sekulovic, C. Brocker, P. Tang, A. Zakaryan, P. Xiang, F. Kuchenbauer, M. Wen, K. Kasaian, M.F. Witty, P. Rosten, Y. Chen, S. Imren, G. Duester, D.C. Thompson, R.K. Humphries, V. Vasiliou, C. Smith, Aldehyde dehydrogenases are regulators of hematopoietic stem cell numbers and B-cell development. Exp Hematol **40**, 318–329 (2012)
47. M. Petruzzelli, M. Schweiger, R. Schreiber, R. Campos-Olivas, M. Tsoli, J. Allen, M. Swarbrick, S. Rose-John, M. Rincon, G. Robertson, R. Zechner, E.F. Wagner, A switch from white to brown fat increases energy expenditure in cancer-associated cachexia. Cell Metab **20**, 433–447 (2014)
48. S. Kir, J.P. White, S. Kleiner, L. Kazak, P. Cohen, V.E. Baracos, B.M. Spiegelman, Tumour-derived PTH-related protein triggers adipose tissue browning and cancer cachexia. Nature **513**, 100–104 (2014)
49. A.S. Antonopoulos, D. Tousoulis, The molecular mechanisms of obesity paradox. Cardiovasc Res **113**, 1074–1086 (2017)
50. W.Q. Hu, J.R. Alvarez-Dominguez, H.F. Lodish, Regulation of mammalian cell differentiation by long non-coding RNAs. EMBO Rep **13**, 971–983 (2012)

american physiological society
AMERICAN JOURNAL OF PHYSIOLOGY
CELL PHYSIOLOGY

Am J Physiol Cell Physiol 322: C421–C460, 2022.
First published January 26, 2022; doi:10.1152/ajpcell.00364.2021

REVIEW

Epigenetic Regulation of Cell Signaling

lncRNAs in mesenchymal differentiation

Marcela Angelica De la Fuente-Hernandez,[1,4]* Miguel Angel Sarabia-Sanchez,[2]* Jorge Melendez-Zajgla,[3] and Vilma Maldonado-Lagunas[4]

[1]*Posgrado en Ciencias Biológicas, Facultad de Medicina, Universidad Nacional Autónoma de México, Mexico City, Mexico;*
[2]*Posgrado en Ciencias Bioquímicas, Facultad de Medicina, Universidad Nacional Autónoma de México, Mexico City, Mexico;*
[3]*Laboratorio de Genómica Funcional del Cáncer, Instituto Nacional de Medicina Genómica, Mexico City, Mexico; and*
[4]*Laboratorio de Epigenética, Instituto Nacional de Medicina Genómica, Mexico City, Mexico*

Abstract

In recent years, technological advances have revealed a large potential number of long noncoding RNAs (lncRNAs). Findings recognize lncRNAs as orchestrating molecules in a wide range of processes, at the transcriptional and posttranscriptional levels, although fewer studies address function. For differentiation, which consists of rearrangements in the gene expression profile and activation of stage- and cell type-dependent signaling mechanisms, the relevance of lncRNAs becomes crucial. The relationship between lncRNAs and key molecular factors in differentiation is strengthening; therefore the present review aims to comprehensively explain the role of lncRNAs in the signaling network involved in the main types of mesenchymal differentiation: adipogenesis, chondrogenesis, myogenesis, and osteogenesis. Notably, a step toward the integration of lncRNAs in the field of cell differentiation promises an exceptional impact.

adipogenesis; chondrogenesis; lncRNA; myogenesis; osteogenesis

BACKGROUND

Currently, findings support that 75% of the human genome is actively transcribed but only 2% is translated into a protein, according to databases such as ENCODE (Encyclopedia of DNA Elements) (1). The development of high-throughput sequencing technologies, computational methods for genome assembly, and biological models has led to the realization of the importance of the previously unconsidered noncoding fraction of the genome. Along with this, noncoding RNAs (ncRNAs) have been shown to be epigenetic, transcriptional, and posttranscriptional regulators in a large number of cellular processes (2). Within the group of ncRNAs, long noncoding RNAs (lncRNAs) represent a fascinating field of study, given the functional versatility in their mode of action on their molecular targets. In recent years, there has been an interest in learning about lncRNAs in differentiation. The aim of this review is to address the signaling mechanisms where lncRNAs are involved, emphasizing their role in either stimulating or inhibiting the transition to differentiated cells. Specifically, the main types of mesenchymal tissue differentiation are discussed: myogenesis, osteogenesis, adipogenesis, and chondrogenesis. The increasing description of new lncRNAs reinforces their role as players in the well-studied field of differentiation, allowing a step toward a better understanding of their biology and their potential application in the clinic.

THE LONG NONCODING RNA: ONE MAN'S TRASH IS ANOTHER MAN'S TREASURE

Most recent reports frequently recall the time when the utility of noncoding RNAs (ncRNAs) was doubted and thus, despite being so abundant, they were placed under the shadow of the term "trash." In contrast, now even the diversity of noncoding RNAs has led to their categorization. Generally, function or structure is used to establish classifications. In terms of function, ncRNAs are divided into two subclasses: regulated ncRNAs and housekeeper ncRNAs [rRNA, tRNA, small nuclear RNA (snRNA), and small nucleolar RNA (snoRNA)] (3). However, a very common way to classify noncoding RNAs is based on their length. Noncoding RNAs shorter than 200 nt are considered small RNAs, which include siRNAs, microRNAs (miRNAs), and piwi-interacting RNAs (piRNAs) (4). When the length exceeds 200 nt up to several kilobases, they are named long noncoding RNAs (5).

The number of genes for lncRNAs has been estimated in a range from 20,000 to over 100,000 in humans (6, 7). For

* M. A. De la Fuente-Hernandez and M. A. Sarabia-Sanchez contributed equally to this work.
Correspondence: V. Maldonado-Lagunas (vilmaml@gmail.com).
Submitted 1 October 2021 / Revised 21 January 2022 / Accepted 22 January 2022

instance, 15,787 lncRNAs were identified in the ENCODE database (version 26), but Hon and collaborators (8) reported 27,919 lncRNAs in 2017.

lncRNAs are synthesized by the RNA polymerase II and most can be affected by polyadenylation (9, 10). In addition to the fact that many lncRNAs have poly(A) tails, they are also modified by alternative splicing (11), so diversification from the same molecule due to the presence of isoforms is foreseeable (12). Furthermore, the level of methylation at the transcriptional start site of lncRNAs is generally higher than mRNAs; therefore lncRNAs exhibit low expression and, relevant to this review, are enriched in specific tissues (13). It is worth noting that a small group of lncRNAs may encode peptides, despite being part of the ncRNAs, working independently of each other, but the factors leading to translation of these lncRNAs are still unclear (14, 15).

Different types of lncRNAs have been distinguished by their location in the genome relative to protein-coding genes. Intronic lncRNAs are encoded within introns of protein-coding genes as opposed to intragenic lncRNAs that overlap with the exons of genes. Some lncRNAs are encoded entirely within the intergenic genomic space, between protein-coding loci, and are known as intergenic lncRNAs, although when the latter are derived as a by-product of transcription in enhancer regions, they are called enhancer lncRNAs. The direction of transcription also contributes to the way in which lncRNAs can be characterized. Sense lncRNAs are transcripts occurring in the same orientation as the protein-coding genes, whereas antisense lncRNAs originate from the reverse direction. Intriguingly, the same promoter can mediate transcription of both the protein-coding gene and the lncRNA, despite transcribing in the opposite direction, which justifies that these lncRNAs are also called divergent lncRNAs (16, 17) (Fig. 1).

The intracellular localization of lncRNAs may play an additional regulatory mechanism affecting function, whereby cytoplasmic and nuclear lncRNAs are described, although in many cases the distribution is not limited to a single compartment (18) or may vary under certain stimuli.

Functionally, lncRNAs can be regulatory molecules of the local chromatin structure in *cis* or in *trans* manner, being independent of their own transcription site. The existence of specific lncRNAs capable of operating both in *cis* and in *trans* has even been ascertained (9). Moreover, lncRNAs are able to bind with biomolecules such as RNA, DNA, and protein, giving lncRNAs a position with multiple interactions and therefore the mechanisms employed becoming very numerous (4).

lncRNAs can also act as molecular guides by recruiting chromatin-modifying complexes that favor opening (euchromatin) or closing (heterochromatin) conformation, as occurs with ANRIL (Antisense noncoding RNA in the INK4 locus), a lncRNA that directly interacts with PRC1/2 (Polycomb Repressive Complex 1 and 2, respectively) to silence genes (19).

In addition, lncRNAs also operate as decoys for transcription factors, preventing transcription of their target genes. For instance, PANDA (p21-Associated ncRNA DNA Damage-Activated) is a lncRNA associated with NF-YA (Nuclear transcription factor Y subunit alpha) to prevent p53-mediated apoptosis (20).

At the posttranscriptional level, lncRNA can serve as a miRNA sponge, through direct complementary base-pairing to attenuate miRNA function and thus rescue the stability and translation of mRNA that is hijacked and inhibited by miRNA. Possibly, this mechanism is the most described in elucidating the mode of action of lncRNAs (4, 21), as observed in the differentiation of mesenchymal stem cells (MSCs) described in this review. Distinctly, the relationship between lncRNAs and miRNAs could be more complex than simple competition for mRNA binding, as there are few lncRNAs that, after processing, could give rise to primary miRNAs as precursors to mature miRNAs (22, 23).

The involvement of lncRNAs in mRNA processing by modulation of their translation, splicing, or degradation has been highlighted. Malat1 (noncoding metastasis-associated lung

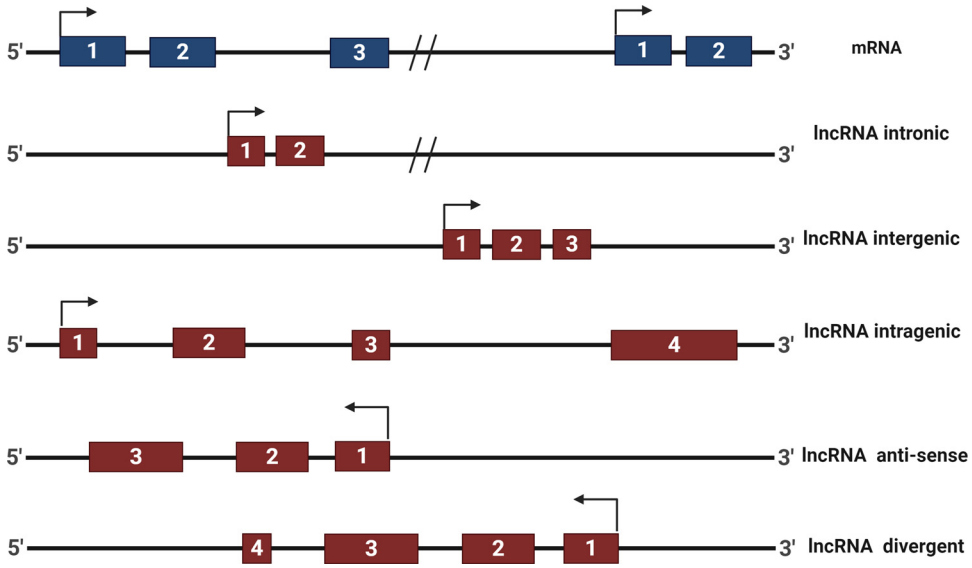

Figure 1. Classification of lncRNAs. The location and orientation of lncRNA (red boxes) in relation to protein-coding genes (blue boxes) establishes the type of lncRNA. The exons are numbered, and the direction of transcription is indicated for each case. See GLOSSARY for abbreviations.

adenocarcinoma transcript 1) is an example of a lncRNA that affects the expression of genes related to the cytoskeleton and extracellular matrix through the control of alternative splicing. This is achieved by influencing the activity and distribution of SR (serine- and arginine-rich) proteins, which compose the splicing complex (24).

The assembly of various multiprotein complexes is also promoted by lncRNAs that help as scaffolds to facilitate proximity and interaction (21). A case is observed with HOTAIR (HOX transcript antisense intergenic RNA), which can simultaneously bind both PRC2 and LSD1 (Lysine-Specific Demethylase 1), forming a complex with CoREST to ensure H3K27 methylation and H3K4 demethylation, corresponding to gene silencing (25).

A great deal of information has been directed toward identifying the nucleotide sequence of lncRNAs and their cellular location to address their function; however, recognition of direct targets leads to a better understanding of lncRNAs, because the modes of action discussed above are not mutually exclusive (Fig. 2).

lncRNAs are not only molecular regulators at different levels but also participate in different cellular processes, including tissue-specific cell differentiation. lncRNAs are involved in the differentiation of neuronal, epidermal, hematopoietic, and adipocyte cells, among others (25, 26). The differentiation is accompanied by changes ranging from morphology to functionality, mainly through modifications in genetic expression. Differentiation also implies commitment to a specific lineage, where the specialized cells are capable of choosing between lineages. Thus, the degree of potentiality is dependent on the types of cells. Since lncRNAs are known to collaborate in reaching the threshold for activation of specific genes necessary to drive toward a differentiated cell during cellular decision-making (27), the explanation of cellular differentiation taking lncRNAs into account is striking.

MULTIPLE ORIGINS, SAME DESTINY: TERMINALLY DIFFERENTIATED CELLULAR STATE

The cellular potential for differentiation is indispensable in the development of living beings. Cells with the capacity to give rise to terminally differentiated cells are recognized as progenitor cells, which reside within multiple tissues. Differentiation has attracted attention, especially in clinical treatments, because of the possibility of obtaining a specific cell type (28). The stromal cells isolated from bone marrow (BM) drew attention because of their ability to differentiate into cells with mesenchymal phenotype and were called mesenchymal stem cells (MSCs) (29). Since then, many cells obtained from different anatomical sites have been categorized under the acronym MSC. Although not all MSCs have the same differentiation potential (30), they have served as precursor cells to assess differentiation. Considering that the biological characteristics depend on the site from which the cells are purified, the present review mentions the origin of MSCs in each report. It should be noted that we focus on mesenchymal differentiation because of the knowledge that has spread since the description of MSCs, specifically adipogenic, chondrogenic, myogenic, and osteogenic differentiation. However, it has also been possible to learn about mesenchymal differentiation by using non-MSC cells that, in addition to being in a less differentiated stage, are committed to a mesenchymal cell type, such as the progenitor cells mentioned above. MSC and endogenous progenitor cells share characteristics, so it is often confusing to refer to one or the other. For example, adventitial progenitors express MSC-related markers (31). In addition, adipose-derived stem cells (ADSCs) and MSCs have in common the presence of surface markers CD29 and Sca-1, whereas CD45 is absent (32). Even as endogenous progenitor cells, MSC clones can differentiate into mesenchymal cells (29). However, a widely

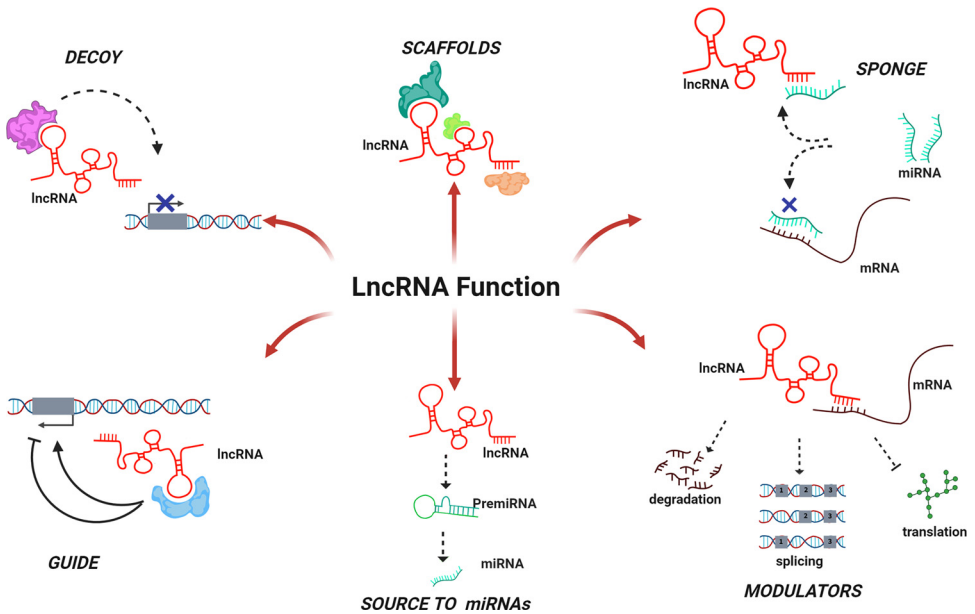

Figure 2. Functions of lncRNAs. Scheme of the main forms of action of lncRNAs, through interactions with DNA, RNA, and protein. Functional diversification of lncRNAs allows them to positively or negatively regulate transcriptional or post-transcriptional mechanisms. See GLOSSARY for abbreviations.

supported distinction between MSCs and endogenous progenitor cells is that MSCs do not necessarily differentiate under in vivo conditions after being transplanted, and, in the event that they do, this occurs in low percentages (30).

MESENCHYMAL DIFFERENTIATION AND lncRNA: A PROMISING RELATIONSHIP

Understanding differentiation allows progenitor cells to be stimulated more efficiently and, in the case of multipotent progenitors, to be targeted to a specific cell type (33). For MSCs, one of the challenges comes from cellular heterogeneity; however, single-cell RNA sequencing has made it possible to complement what is described in total cell populations. For example, cellular functional differences have been recognized in primary MSCs from Wharton's jelly (34). This technology, targeted beyond gene expression, gives the advantage of predicting transcripts and thus potential new lncRNAs. Moreover, the use of single-cell RNA sequencing has led to the identification of unique expression profiles of lncRNAs, allowing the identity of MSCs to be distinguished from other cells, including stem cells and differentiated cells (35). As for the differentiation process, new details have begun to be revealed, as demonstrated by the identification of a fibroblastic stage in mesenchymal progenitors before chondrogenesis (36).

In this review, not only are molecular mechanisms explained but biological models are mentioned for a better understanding of precursor cells. In fact, biological models are not only a representative tool of the biological phenomenon of interest but also a simplified context that can be analyzed. Therefore, clarification of the cellular system used in the reports reveals the scope and limitations of the findings. It is important to note that each type of differentiation addressed in this review has its singularities, so differentiation should not be considered as a unique phenomenon, but it is notable that lncRNAs are recurrently present.

MYOGENESIS: UNITY IS STRENGTH

The skeletal muscle in adulthood requires cell turnover during normal growth and after injury. The presence of mesenchymal cells called fibro-adipogenic progenitors (FAPs) has been identified as a source of signals to improve regeneration of muscle after injury or aging. Expansion of progenitor cells derived of satellite cells (SCs) is one of the ways in which FAPs achieve this (37). SCs express PAX7 (Paired Box 7) protein, which acts upstream of myogenic regulatory factors (MRFs). MRFs are transcription factors involved in coordinating the process of myogenesis, in which MYF5 (myogenic factor 5), MYOD (Myoblast Determination), MYOG (Myogenin), and MRF4 (also called MYF6) proteins are recognized. The minority of SCs in muscle are capable of self-renewal, in addition to lacking MRF expression. Meanwhile, the majority of SCs are characterized by MYF5 mRNA expression, but with the myogenic program inactive. Nevertheless, MYF5 transcript evidences commitment to the myogenic lineage of these SCs, and therefore they are referred to as myogenic progenitors (38). The myoblasts are derived from SCs, and myoblast cell lines such as C2C12 have been established. Although myoblasts are immature differentiated cells, their use in most studies has made it possible to elucidate the stages before the formation of myotubes (39).

Promyogenic stimuli activate myogenic progenitors to proliferate, concomitant with an increase in MYF5 and MYOD protein levels and giving rise to myoblasts at this stage. Upregulation of MYF5 and MYOD expression occurs through PAX7, which binds directly to DNA, specifically to the *MYF5* gene enhancer and the *MYOD* gene promoter. Furthermore, MYOD protein expression is supported at the posttranscriptional level, as the mRNA is targeted by miR-672, which prevents translation of the mRNA, but lncMUMA (mechanical unloading-induced muscle atrophy-related lncRNA) allows mRNA release by binding to miR-675 (40).

Transcriptional control of MYOD expression involves three DNA sequences upstream of the *MYOD* gene that act as regulatory elements: PRR (Proximal Regulatory Region), DRR (Distal Regulatory Region), and CE (Core Enhancer). CE encodes the lncRNA named CERNA, and it favors chromatin access and POLII binding to *MYOD* loci (41). Moreover, DRR encodes the lncRNA DRR, subsequently called MUNC (MyoD upstream noncoding), which is not limited to acting in *cis* on the MYOD gene but also increases the levels of MYOG and MyHC3 (Myosin Heavy Chain 3) mRNAs, muscle-specific components, by *trans* modulation independent of MYOD and dependent on the spliced form of MUNC (42, 43).

The importance of growth factors for myoblast cell cycle entry has been described, such as IGF1 and IGF2, which also exert functions during differentiation. After birth, IGF2 expression decreases whereas IGF1 increases; however, there has been a greater interest in IGF2 as it acts in an autocrine and paracrine manner to promote differentiation under in vitro conditions (44). IGF2 mRNA is driven to degradation by the action of miR-125b but is evaded when lncRNAs lnc-mg (myogenesis-associated lncRNA) and linc-smad7 (long intergenic noncoding RNA smad7) perform as a miR-125b sponge, thus favoring IGF2 mRNA stabilization and translation (45, 46). Additionally, lnc-mg is able to reduce miR-351-5p levels, which stimulates cell cycle gene expression; thus the role of lnc-mg requires further investigation to explain these seemingly opposite functions (47). It is well known that IGF2 mRNA can bind to members of the IMP (Igf2 mRNA-binding protein) family. It is possible that the effect of IMPs (IMP1, IMP2, and IMP3) on IGF2 mRNA is cell context specific and dependent on accessory molecules. For example, the transcriptional coregulator HMGA2 (high-mobility group AT-hook 2) binds IMP2 and promotes translation of IGF2 mRNA and other mRNAs such as Myc, Sp1, and Igf1r, all of which are involved in myoblast proliferation. When cells exit the cell cycle, MYOD promotes the expression of lncRNA lncMyoD (lncRNA upstream of MYOD1 gene), which interacts with IMP2 to competitively displace mRNAs, including IGF2 mRNA (48). The mechanisms responsible for regulation of IGF2 are versatile inasmuch as it also participates in differentiation. One of these is the inhibition of IGF2 mRNA by IMP1, where lncRNA H19 contributes to IMP1 function by acting as a sponge for let-7, a miRNA that decreases IMP1 mRNA levels (49). It is worth mentioning that the H19 gene belongs to the imprinted gene cluster containing the IGF2 gene and, apparently contrary to this evidence, H19 has also been proposed as a positive regulator of myogenic differentiation, through miR-675-3p and miR-675-

5p, both miRNAs derived from the H19 transcript; therefore, H19 processing is likely controlled by specific stages, leading to different outcomes (50).

During myoblast proliferation, cell cycle progression and repression of genes related to mature muscle cells must occur simultaneously. The SIRT1 (Sirtuin 1) protein is a deacetylase implicated in both tasks that prevents the expression of cell cycle inhibitors p21 and p27, in addition to interacting with the MYOD/PCAF complex and GCN5, a histone acetyltransferase, to silence muscle-specific enhancers (51). Importantly, the antisense lncRNA of SIRT1 mRNA, named SIRT1 AS, favors the stability and translation of SIRT1 mRNA through direct binding to form a duplex that prevents degradation mediated by miR-34a (52, 53). Another mechanism for myoblast proliferation focuses on the role of lncRNA SYISL (SYNPO2 intron sense-overlapping lncRNA), which interacts with EZH2 (Enhancer of Zeste Homolog 2) and SUZ12 (Suppressor of Zeste 12) proteins, subunits of the histone methyltransferase complex PRC2, to repress transcription of target genes. Similar to SIRT1, SYISL suppresses the expression of p21 and muscle markers (54). lncRNAs SIRT1-AS and SYISL are assumed to be inhibitors of myogenesis, as their mode of action discourages both exit from the cell cycle and entry into differentiation, but the requirement for the growth of myogenic progenitors to later become myotubes highlights the importance of these lncRNAs in muscle regeneration.

The transcription of muscle-specific genes mediated by MYOD can be repressed by mitogen-activated protein kinase kinase (MEK) that interacts directly with MYOD, although this interaction is ablated by SMAD7 (55). Negative modulation of SMAD7 mRNA is performed by miR-125b, but linc-smad7 downregulates miR-125b, leading to SMAD7 expression and thus myoblast differentiation (46). Additionally, MYOD coordinates with histone deacetylase 1(HDAC1) to repress transcription of target genes (56). In epigenetic silencing, Malat1 supports the recruitment of SUV39H1, a histone methyltransferase, to MYOD-recognized promoter regions. Reports suggest diverse functions of Malat1 and may even seem contradictory, as it can be detected in transcriptionally active genes, so it is possible that the contribution of Malat1 is highly dependent on the cell stage or interacting partner (57, 58).

Prevention of premature differentiation of proliferating myoblasts is partially influenced by ID (Inhibitor of DNA binding) proteins such as ID2 and ID3, which heterodimerize with MYOD and reduce its DNA binding capacity. Interestingly, at the onset of myoblast proliferation, PAX7 binds to the promoter of the *ID3* gene to activate its transcription, establishing negative feedback from the early stages. Moreover, ID3 expression can be modulated indirectly by ROCK1 (Rho-associated coiled-coil containing protein kinase 1) protein (59). ROCK1 mRNA translation is stimulated by a ribonucleoprotein complex harboring YB-1 (Y-box binding protein 1) and lncRNA lnc-31. In this same study, lnc-31 reduced the expression of NUPR1 (Nuclear protein 1, transcriptional regulator) protein, a positive regulator of MYOD/p300 complex-dependent transcription. Therefore, lnc-31 attenuates MYOD-dependent transcription through two different ways (60, 61).

The transition from the proliferative stage to differentiation is also mediated by MYOD, hindering cell division due to increased expression of p21. The p68/72 RNA helicases and lncRNA SRA (steroid receptor RNA activator) together facilitate the expression of a subset of MYOD target genes involved in cell cycle exit. Specifically, p68/72 recruit TBP (TATA Binding Protein), POLII, and components of chromatin remodelers such as BRG-1 (Brahma-Related Gene 1) to stimulate transcription, whereas SRA serves as a coactivator of MYOD/p68 complex (62). It should be noted that the SRA gene gives rise not only to SRA but also to a transcript encoding SRA protein (SRAP). Binding between SRA and SRAP has been demonstrated, and although the downstream signaling of this interaction has not yet been described, it appears that SRAP could impede SRA-dependent MYOD activity (63).

Once cells begin to differentiate, chromatin undergoes remodeling that allows the overall genetic profile of transcription to change. MYOD plays a regulatory role in chromatin rearrangement leading to genetic expression, where lncRNAs are implicated (Fig. 3). The lncRNA linc-RAM (lincRNA Activator of Myogenesis) is found in this phenomenon, interacting with MYOD to improve the assembly of the MYOD/BAF60C/BRG1 complex, responsible for modifying chromatin to an active state and downstream expression of MYOG and nucleosome assembly-related genes (64). Dum (DPPA2 upstream binding muscle lncRNA) is upregulated by MYOD and decreases expression of the neighboring gene DPPA2 (Developmental Pluripotency Associated 2) in *cis*, because of promoter methylation by recruitment of DNA methylases such as DNMT1, DNMT3A, and DNMT3B (65). DPPA2 protein, together with DPPA4, has been associated with maintenance of an undifferentiated state in embryonic stem cells, in addition to evasion of DNA methylation in bivalent chromatin of genes that are expressed during differentiation, so it would be relevant to know whether a similar role is performed in MSC differentiation (66).

During myogenic differentiation, transcriptional activity of MYOD at target genes must be coordinated with the dissociation of genetic repressor complexes. YY1 protein accomplishes epigenetic silencing of MYOD target genes through recruitment of EZH2. The YY1/EZH2 complex is destabilized by lncRNA linc-YY1, disabling transcriptional inhibition. Meanwhile, linc-YY1 also triggers YY1/STAT3 assembly, reinforcing the promyogenic role of linc-YY1 (67). It has been suggested that YY1 function is more complicated, as it binds upstream of DNA regions encoding lncRNAs such as Yam-1 (YY1-associated muscle lncRNA 1), Yam-2, Yam-3, and Yam-4. These YY1-dependent lncRNAs modulate in favor of (Yam-2 and Yam-4) or against (Yam-1 and Yam-3) myogenesis, although how they act is not yet understood, with the exception of Yam-1, which positively regulates miR-715 to downregulate Wnt7b, thereby impairing differentiation (68).

MRFs are determining factors in myogenesis, but their action is synergized by the involvement of proteins such as the MEF2 (Myocyte Enhancer Factor 2) family. The MEF2c mRNA is repressed by miR-135, but lncRNA linc-MD1 modulating as a sponge on miR-135 permits the increase of MEF2C protein (69). Remarkably, the interaction between linc-MD1 and its target miRNAs is facilitated by HUR protein, known to interact with various noncoding RNAs and mRNAs (70). MEF2 is able to collaborate with MYOD, MYOG, or MRF4. A

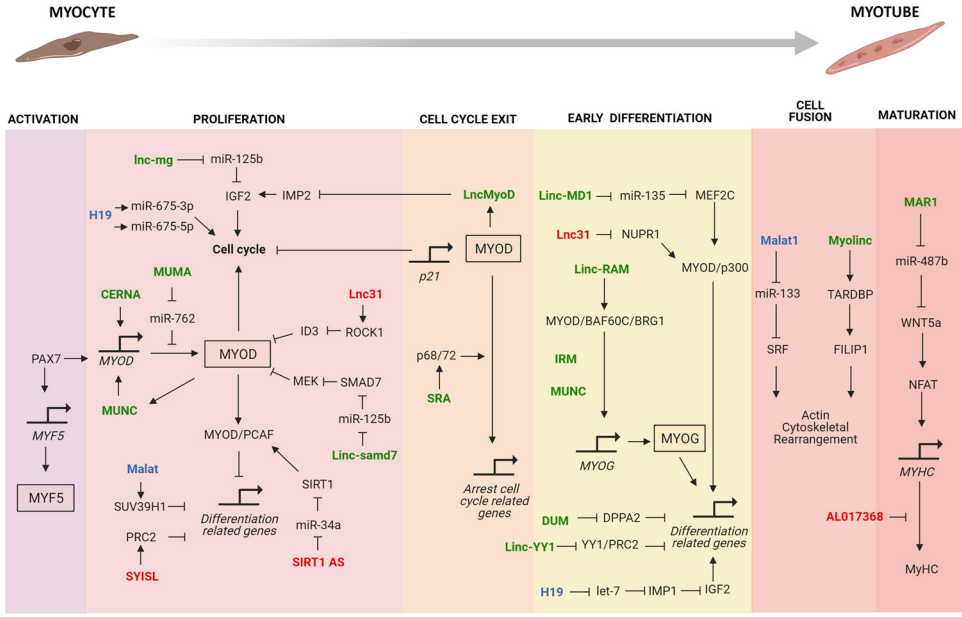

Figure 3. Myogenesis. The signaling mechanisms of myogenic program regulated by lncRNAs are shown. Key transcription factors are indicated in boxes. The figure is divided into sequential stages toward myotubes. lncRNAs favor (green) or inhibit (red) markers of differentiation. lncRNAs described in both cases are also indicated (blue). Effect of lncRNA on its targets can be direct or indirect. For more details see text. See GLOSSARY for abbreviations.

previous study argued that the binding between MEF2D and MYOD is upregulated by lncRNA Irm (imprinted RNA near Meg3/Gtl2), which functions as scaffold between MEF2D and the promoter of MYOG gene, a genomic region recognized by MYOD (71).

The myogenic program establishes a network characterized by self-regulation and cross talk modulation between MRFs, with exception of MRF4, which is dependent on other MRFs. When MYOD expresses lncRNA MUNC, a positive feedback loop is established because MUNC induces MYOD protein localization to DRR and CER, the upstream regulatory elements of *MYOD* gene. Indeed, MUNC also mediates cross-regulation between MRFs, because it favors MYOG binding to DRR and MYOD recruitment to *MYOG* gene promoter, leading to expression in both cases (69).

In advanced stages of myogenic differentiation, myoblasts fuse to form multinucleated myotubes. Myoblast fusion involves different cellular mechanisms. SMD (STAU1-mediated mRNA decay) is one of the least described but certainly important where lncRNAs play a crucial role. Recognition of the lncRNA-mRNA complex by STAU1 (Staufen Double-Stranded RNA Binding Protein 1) protein is followed by destabilization of mRNAs. Regarding SMD, lncRNAs named m1/2-sbsRNA1 (mouse 1/2-Staufen-binding site RNA 1), m1/2-sbsRNA2, and m1/2-sbsRNA3 (also known as B1, B2, and B4, respectively) are identified as regulators of specific mRNA levels to trigger differentiation, although a larger number of mRNAs are expected (72). The functions of paraspeckles have also been attributed to the transition from myoblasts to myotubes. Paraspeckles are subcompartments within the nucleus that retain genetic regulatory elements such as RNA binding proteins (RBPs) or lncRNAs. However, evidence suggests that lncRNAs might not only be controlled by the distribution within the nucleus but also actively contribute to maintaining the structural organization of paraspeckles, as evidenced in the case of lncRNA Men (multiple endocrine neoplasia) isoforms Men-β and Men-ε (73).

The actin dynamic is essential during myoblast fusion to form multinucleated cells, with regulators such as RAC1 (Rac family small GTPase 1), CDC42 (cell division control protein 42), N-WASP (neural Wiskott–Aldrich syndrome protein), and SRF (serum response factor). MRFs such as *MYOD* gene and cytoskeleton constituents such as α-actin and myosin light chain (MLC) are targets of SRF (74). However, SRF mRNA is degraded because of miR-133 until lncRNA Malat1 sponges for miR-133, thereby inhibiting its suppressive activity and increasing SRF levels (75). In a complementary manner, FILIP1 is another protein that promotes the formation of multinucleated cells, possibly by mediating the changes in actin through its interaction with FLNA (Filamin A). lncRNA Myolinc has been shown to positively regulate FILIP1 expression by favoring the recruitment of TARDBP (TAR DNA binding protein) to promoter of FILIP1 gene (76).

In myotubes, MYOD leads to the expression of MUNC, which in turn increases MYOG levels in *trans* by achieving accessible chromatin at the MYOG locus (43). Myotubes will form new myofibers (regeneration) or combine with preexisting muscle fibers (hypertrophy). Structurally, myotubes fuse to form myofibrils, and these together become myofibers, which are responsible for contractile function in muscle (77). In myofiber maturation, lncRNA Charme (chromatin architect of muscle expression) regulates in *cis* the genetic transcription of a genomic region named NCTC, which contains both CME (Core Muscle Enhancer) regulatory element and muscle-associated genes. The presence of Charme brings NCTC region closer to the Charme genomic locus, activating the transcription of nearby genes such as *IGF2* (78).

Muscle fibers are distinguished by the presence of MyHC isoforms, and MyHC expression is regulated downstream of NFAT (Nuclear factor of activated T cells), a known effector of the WNT5a/CaMKIIδ axis (79, 80). WNT5a is a protein ligand whose mRNA translation appears to be negatively regulated by miR-487b. However, it has been proposed that

lncRNA MAR1 (Muscle anabolic regulator 1) suppresses miR-487b inhibition to allow WNT5a expression and thereby activate cellular signaling. WNT5a could have implications even at early stages of myogenesis, as it also regulates MYF5, MYOD, and MYOG expression, although the mechanisms involved remain to be clarified (80, 81). However, MyHC transcription may not be sufficient, as MyHC mRNA translation is impeded by the presence of lncRNA AK017368 in proliferating myoblasts; therefore AK017368 must be repressed at the late stage of myogenesis. The effects that could occur due to AK017368 seem attractive, as it is also a sponge of miR-30c, triggering translation of TNRC6A (Trinucleotide repeat-containing 6 A) mRNA. TNRC6A is part of P bodies, compartments dedicated to mRNA processing capable of counteracting the action of muscle-specific miRNAs, so MyHC could be just one of several targets affected by AK017368 as an indirect mediator of miRNA activity (82).

The field of myogenesis has expanded enormously, but new molecules continue to be discovered. lncRNAs are part of this new group, which are essential because at every step toward the formation of mature myotubes the involvement of lncRNAs appears (Table 1). However, much remains to be learned about the mechanisms regulated and involved both at the single-cell level and in such complex processes as cell-cell interaction to give rise to multinucleated cells.

OSTEOGENESIS: GROWN TO BONE

Skeletal homeostasis is mainly based on the balance between the activities of osteoblasts, responsible for producing bone components, and osteoclasts, which reabsorb bone. The bone remodeling process occurs in response to stimuli such as fracture damage, hormonal fluctuations, and aging, among others (83). MSCs have been localized in the periosteum, endosteum, and marrow cavity, whereas osteoblasts are in direct contact with the bone surface (84). The expression of SOX9 (SRY-box transcription factor 9), a key transcription factor in skeletal development, leads MSCs to become osteoprogenitor cells, capable of generating the skeletogenic lineage: osteoblasts and chondrocytes (83). In this section we focus on osteoblasts.

Initially, the osteogenic master RUNX2 (Runt-related transcription factor 2) is repressed in osteoprogenitor cells, partially because of gene promoter methylation, which is driven by EZH2. lncRNAs HoxA-AS3 (HoxA antisense transcript 3) (85) and ANCR (antidifferentiation noncoding RNA) (86) have been shown to participate in the recruitment of EZH2 to this DNA region, which favors trimethylation of H3K27. It is worth mentioning that ANCR, also known as DANCR (differentiation-antagonizing noncoding RNA) performs several functions indicating its antiosteogenic role (87).

Expression of RUNX2 is associated with preosteoblasts, precursors of the osteoblast. RUNX2 is expressed in response to extracellular ligands, mainly those that activate bone morphogenetic protein (BMP) and WNT signaling (83). The most described BMP ligands in osteogenesis are BMP2 and BMP4; therefore regulation in the amount of these ligands allows control in osteogenic differentiation. BMP2 is maintained at low levels by the effect of the lncRNA MEG3 (maternally expressed gene 3), because MEG3 competes with BMP2 mRNA for binding to heterogeneous nuclear ribonucleoprotein I (hnRNPI). Since hnRNPI is a translational activator with function in mRNA splicing, mRNA displacement by MEG3 implies posttranscriptional downregulation of BMP2 (88). Interestingly, MEG3 promotes BMP4 expression by binding to the promoter of BMP4 gene and interacting with SOX2, a transcriptional repressor, to dissociate it from the promoter (89). Thus, MEG3 acts in favor of or against osteogenesis, probably depending on whether differentiation is already induced or not, or its role could depend on the type of BMP, which remains to be demonstrated. Even so, little is known about the regulation of MEG3 expression, where it has been suggested that DEPTOR (DEP domain-containing mTOR interacting protein) could bind to the promoter of MEG3 to repress its expression, although the role of mTOR in osteogenesis remains controversial (90).

Among the different ways in which BMP2 levels can increase, at the posttranscriptional level BMP2 mRNA is decreased by miR-106-5p, but to increase BMP2 levels lncRNA PCAT1 (prostate cancer-associated ncRNA transcript 1) functions as a molecular sponge on miR-106-5p, releasing mRNA from inhibition (91). miR-214 is another miRNA that negatively regulates BMP2 mRNA, but in this case there are two lncRNAs capable of inhibiting miR-214 activity: lncRNA LOC100506178 (92) and lncRNA KCNQ1OT1 (93), both indirectly promoting BMP2 upregulation. Intriguingly, miR-214 also targets ATF4, a relevant transcription factor in advanced stages of osteogenesis (94). On the other hand, additional tasks of KCNQ1OT1 are reported, such as impeding the repression of miR-138 on RUNX2 mRNA (95) and increasing the expression of β-catenin, a transcriptional coactivator of WNT pathway. The higher levels of β-catenin by KCNQ1OT1 are striking, because KCNQ1OT1 is a direct target of β-catenin-mediated transcription, which would imply positive feedback (96).

After expression of BMP2 or BMP4 and binding to serine/threonine kinase receptors, phosphorylation of SMAD1, SMAD5, and SMAD8 is activated. These SMADs have a common interaction partner named SMAD4, which harbors a nuclear import sequence whereby the complex is translocated to the nucleus, where gene expression is modulated. Posttranslational modification of SMADs can be subject to regulation by lncRNAs. lncRNA TUG1 (taurine upregulated gene 1) is an example, which binds to SMAD5 protein. The interaction between TUG1 and SMAD5 inhibits the phosphorylation of SMAD5, thereby repressing its effector function (97).

Furthermore, SMAD7 is a member of the inhibitory SMADs (I-SMADs) and has been associated with hindering osteogenesis (98). SMAD7 mRNA is inhibited by miR-17-5p, but miR-17-5p levels can be diminished by methylation of its promoter. This methylation is dependent on lncRNA HOTAIR, possibly through recruitment of PRC2, which confers an antiosteogenic role on HOTAIR through SMAD7 (99, 100). The role of miR-17-5p in osteogenesis seems to be complex, as it also targets SMAD5 and BMP2, which appears contradictory to this evidence, so it remains to be clarified whether miR-17-5p depends on additional factors or cellular stage (101, 102).

Notably, BMP2 not only triggers the activation of SMADs but also MAPK signaling, such as p38 and ERK1/2 (103). During osteogenesis, ANCR inhibits p38 phosphorylation

Table 1. *lncRNA in myogenesis*

lncRNA	Genomic Classification	Myogenesis Promote/Inhibit	Function	Direct Target	Biological Model	Differentiation Markers (technique, assay)	Ref.
AK017368		Inhibit	Sponge of miRNA	*miR-30c*	C2C12	MYHC, MYOG (RT-qPCR)	(82)
CERNA ENSG00000259577		Promote*			C2C12, skeletal muscle cells		(41)
Charme		Promote		CME DNA Region*	C2C12	MCK, MHC (RT-qPCR)	(78)
DRRRNA		Promote			C2C12, skeletal muscle cells	MYOD, MYOG, MYH (RT-qPCR)	(41)
Dum		Promote	Guide	Promoter of *DPPA2*	C2C12, 10T1/2	MYOG, MYHC, troponin (RT-qPCR, WB)	(65)
H19 ENSG00000130600	Intergenic	Promote	Source of miRNAs	*miR-675-3p*, *miR-675-5p*	C2C12, satellite cells	MHC, MYOG (RT-qPCR)	(50)
NR_131224.1 Gene ID: 283120	Intergenic	Inhibit	Sponge of miRNA	*let-7*	C2C12, PA-1	MHC, MYOG (RT-qPCR) Multinucleated cells (M)	(49)
Irm		Promote	Scaffold*	MEFD2, promoters of *MYOGENIN* and *miR-206* genes	C2C12, myoblasts	MYOD, MYOG (RT-qPCR) MHC (IS)	(71)
linc-MD1 ENSG00000225613	Intergenic	Promote	Sponge of miRNA	*mir-135, miR-133*	C2, myoblasts	MYOG, MHC (WB)	(69)
linc-MD1	Intergenic			HUR	C2C12		(70)
Linc-RAM NR_038041		Promote	Scaffold	MyoD	C2C12, satellite cells, C3H-10T1/2	MHC, MyoG (IF)	(64)
linc-smad7		Promote	Sponge of miRNA	miR-125b	C2C12	MYOD, MYOG, MyHC (RT-qPCR, WB)	(46)
linc-YY1 ENSMUSG00000114045 Gene ID: 102637400	Antisense	Promote	Scaffold	YY1	C2C12, satellite cells, 10T1/2	MYOG, MYHC, TNNI2, α-ACTIN (RT-qPCR)	(67)
LncMAR1		Promote		miR-487b	C2C12	MYOD, MYOG, MEF2C, MYF5 (RT-qPCR) Myotube formation (M)	(81)
lnc-mg ENSMUSG00000085348		Promote	Sponge of miRNA	*miR-125b*	C2C12, skeletal muscle cells	MYOD, MYOG(RT-qPCR) MyHC (IF)	(45)
		Promote		miR-351-5p	C2C12	MyHC (IF) Morphology (M)	(47)
lncMUMA		Promote	Sponge of miRNA	miR-762	C2C12	MyoD (WB) Myotube formation (M)	(40)
lncMyoD	Intergenic	Promote	Modulator	IMP1, IMP2	C2C12	MHC (IF)	(48)
Lnc-31 ENSG00000171889	Intronic	Inhibit			C2C12, WT-9808, DMD-9981	MYOD1, MYOG, MEF2, MYH6, CKM (WB) Fiber formation (M)	(61)
	Intronic	Inhibit	Modulator	YB-1, mRNA of Rock1	C2C12, myoblasts	MYOG(RT-qPCR)	(60)
m1/2-sbsRNA1 (B1)		Inhibit	Modulator	mRNAs of mFxn, mRnf168 or mTcea1	C2C12, NIH3T3	MYOG, MHC (WB) Cell morphology (M)	(72)
m1/2-sbsRNA2 (B2)		Inhibit	Modulator	mRNA of mTraf6	C2C12, NIH3T3	MYOG, MHC (WB) Cell morphology (M)	(72)
m1/2-sbsRNA3 (B4)		Inhibit	Modulator	mRNA of mCdc6	C2C12, NIH3T3	MYOG, MHC (WB) Cell morphology (M)	(72)
Malat1 ENSG00000251562	Intergenic	Inhibit			C2C12, satellite cells	MYOG (RT-qPCR)	(58)
NR_002819.4	Intergenic	Promote	Sponge of miRNA	*miR-133*	C2C12	MYOG, MHC (WB)	(75)
Gene ID: 378938	Intergenic	Inhibit	Guide	Suv39h1; promoters of *MYOG, TNNI2, MYHC*, and *CCND3* genes	C2C12, satellite cells, C3H/10T1/2	MYOG, MYHC, α-ACTIN, TROPONIN (RT-qPCR, WB)	(57)
Men β/ε isoform				NONO	C2C12, NIH3T3		(73)
MUNC		Promote			C2C12, C3H10T1/2, LHCN	MYOG, MHC, MyoD (RT-qPCR)	(43)
Gm45923 DRReRNA NR_131190.1 Gene ID: 105447647						MHC (IF)	
MUNC		Promote			C2C12	MYOD, MYOG, MYH3 (IF)	(42)
Myolinc ENSMUSG00000086918 Gene ID: 74633		Promote	Guide	TDP-43	C2C12, myoblasts	MYF5, MYOD, MYOG (RT-qPCR) Multinucleated cells (M)	(76)

Continued

Table 1.— *Continued*

lncRNA	Genomic Classification	Myogenesis Promote/Inhibit	Function	Direct Target	Biological Model	Differentiation Markers (technique, assay)	Ref.
Myo18, Myo77, Myo351	Intergenic (Myo18)	Promote			C2C12	MHC (IF)	(323)
Sirt1 AS Gene ID: 106633813	Antisense	Inhibit	Modulator	mRNA of Sirt1	C2C12	MYOD, MYHC, MYOG (RT-qPCR)	(52)
	Antisense	Inhibit	Modulator	mRNA of Sirt1	C2C12	MHC, MYOG (IF)	(53)
SRA Gene ID: AF092038	Intergenic	Promote		SRAP	LHCN-M2, C2C12, C3H10T1/2	MCK, MYOG(RT-qPCR)	(63)
	Intergenic	Promote	Guide	MYOD, p68	C2C12, C3H10T1/2, myoblasts	MHC (RT-qPCR) MHC (IF)	(62)
SYISLAK004418		Inhibit	Guide	EZH2, SUZ12, promoters of MYOG, P21, MYH4, MCK	C2C12,myoblasts	MYOD, MYOG, MYHC (RT-qPCR, WB)	(54)
Yam-1 Gene ID: 107161157	Antisense	Inhibit		miR-715	C2C12	MYOG, TNNI2, α-ACTIN (RT-qPCR)	(68)
Yam-2		Promote*			C2C12	MYOG, TNNI2, α-ACTIN (RT-qPCR)	(68)
Yam-3		Inhibit			C2C12	MYOG, MYHC, α-ACTIN (RT-qPCR)	(68)
Yam-4		Promote			C2C12	MYOG, MYHC, α-ACTIN (RT-qPCR)	(68)
91HNC_000011.9					C2C12	MYOG(RT-qPCR)	(338)

IF, immunofluorescence; IS, (immunostaining); M, microscopy; RT-qPCR, reverse transcription-quantitative PCR; WB, Western blot. *Suggested by the authors of the study. See GLOSSARY for other abbreviations.

(active form), although whether ANCR acts directly or indirectly is unknown (104). Members of the CXCL family, such as CXCL12, which is recognized by the CXCR4 receptor, collaborate in the upregulation of SMADs and MAPKs during the early stages of osteogenesis, particularly in response to osteogenic growth peptide (OCP) (105). Unexpectedly, lncRNA PRNCR1 (prostate cancer noncoding RNA 1) decreased osteogenic differentiation despite favoring CXCR4 expression by repressing miR-211-5p, so authors have suggested that the role of CXCR4 depends on its concentration or cellular characteristics (106). Meanwhile, CXCL13 has been implicated in the proosteogenic signaling of lncRNAs AK028326 (107) and AK141205 (108), although the mechanisms implicated are unknown.

The WNT/β-catenin pathway also promotes RUNX2 expression. In this signaling, β-catenin activates transcription of target genes when WNT ligands bind to FZD receptor and LRP5/6 coreceptor; thus the presence of WNT induces RUNX2 transcription. The expression of WNT genes can be silenced by recruitment of EZH2. MEG3 has been described to increase levels of EZH2, which increases trimethylation of H3K27 globally in the genome, enriching EZH2 at the promoters of genes such as WNT1, WNT5A, and CTNNB1 (gene encoding β-catenin) (109). However, it remains to be discovered whether this mechanism of MEG3 is tissue specific or stage dependent, as the proosteogenic role is also attributed to MEG3.

WNT synthesis can also be posttranscriptionally regulated, such as WNT2B, whose mRNA levels are decreased by miR-370-3p. Thus, inhibition of miR-370-3p by lncRNA LINC00707 leads to upregulation of WNT2B and RUNX2 (110). Also, the expression of WNTs is affected by upstream activation of TLR4 (toll-like receptor 4) in the presence of ligands such as LPS, specifically inducing WNT3a and WNT5a (111). TLR4 expression is negatively regulated by miR-145-5p, which is reversed by PCAT1, the abovementioned lncRNA capable of affecting BMP2 levels (112). The data highlight the primary importance of suppressing miR-145, because it has been shown to inhibit valuable factors such as core-binding factor subunit beta (CBFB), a non-DNA binding factor, but potentiates DNA binding of RUNX family proteins (113) and OSX, a key transcription factor in the late stages of osteogenic differentiation(114).

Regarding β-catenin expression, it can be indirectly regulated by lncRNA linc-ROR (long intergenic nonprotein coding RNA, regulator of reprogramming), acting as a sponge on miR-145 and miR-138, both involved to downregulate ZEB2 mRNA levels (115). ZEB2 is a transcription factor that improves β-catenin expression (116). At the posttranscriptional level, mRNA of β-catenin declines because of the activity of two miRNAs, miR-141 and miR-22, although lncRNA H19 acts as a molecular sponge to sequester both miRNAs to positively regulate β-catenin levels (117). Studies of H19 have provided insight into new factors around osteogenesis such as LCoR (Ligand-dependent corepressor) that have been found to have a proosteogenic role. LCoR expression is increased because of the function of H19, as H19 inhibits miR-188, repressor of Lcor mRNA, although how LCoR contributes to this differentiation is far from clarified (118).

The interaction between β-catenin and the transcription factors T cell factor (TCF) and lymphoid enhancer factor (LEF) is crucial for the downstream expression of target genes. lncRNA Crnde (colorectal neoplasia differentially expressed) favors β-catenin-dependent transcription, possibly due to higher levels of TCF7 and TCF12 mRNAs (119). In contrast, lncRNAs AK016739 and AK045490 impair this transcriptional activity, reducing TCF or LEF levels. Specifically, mRNAs of TCF7 and LEF1 are diminished by AK016739, and to counteract this Microtubule actin cross-linking factor 1 (MACF1), a cytoskeletal protein capable of aiding β-catenin-mediated transcription, diminishes AK016739 levels (120). Otherwise, AK045490 downregulates TCF1 and LEF1 mRNAs; furthermore, it has also suggested that AK045490 could improve the levels of glycogen synthase kinase 3-beta (GSK3-β, an antagonist of WNT/β-catenin pathway, by releasing its mRNA from miR-3089 suppression (121). With respect to GSK3-β, ANCR is

an additional lncRNA that posttranscriptionally upregulates GSK3-β (84). In a fascinating manner, the inactive state of GSK3-β protein is also decreased by the presence of ANCR (122), contrary to the effect of H19, which increases this inactivation (123).

Regulation of WNT/β-catenin in osteogenesis may be opposite under nonnormal conditions. For example, inhibition of β-catenin-dependent transcription stimulates osteogenic differentiation in inflammation. Furthermore, FOXO1 (Fork box transcription factor), known to impede the interaction between β-catenin and TCF4, was shown to favor osteogenic markers. FOXO1 is maintained at low levels because of the inhibition of miR-182 on its mRNA, but POIR (pPDLSC osteogenesis impairment-related lncRNA), downregulating miR-182, allows FOXO1 accumulation and thus osteogenesis (124). It has also been revealed that ANCR is able to assemble a complex with FOXO1, leading FOXO1 to degradation by S-phase kinase-associated protein 2 (SKP2) recognition in the presence of polymethylmethacrylate (PMMA) in a periprosthetic wear particle model. Therefore, the drop in FOXO1 attenuated osteogenic differentiation (125). Moreover, NOTCH2 has been described to reduce osteogenic markers, through upregulating β-catenin expression. In this study, NOTCH2 levels increased when its mRNA was derepressed from miR-758 by ANCR performance (108). Altogether, this evidence underscores the issue of addressing molecular mechanisms, considering the nonnormal cellular context.

Some authors have also considered the transforming growth factor beta (TGF-β) pathway important in osteogenesis, but it focuses on the early stage. TGF-β represses the expression of late genes such as OCN (Osteocalcin), by deacetylation of H4 at the promoter. SMAD3, a downstream effector of TGF-β, recruits histone deacetylases HDAC4/5 to DNA sequences recognized by RUNX2; however, in the progression of osteogenic differentiation, TGF-β must be inhibited. H19 is a molecule that reduces TGF-β1 mRNA, and although it is unknown how this is achieved, the involvement of miR-675, which originates downstream of H19 processing, has been proposed (126).

Once the RUNX2 gene is expressed in preosteoblasts, mainly as a consequence of activation of BMP or WNT signaling, the Runx2 transcript can be repressed by the regulation of some miRNAs. One example, miR-93-3p, is reduced by lncRNA lnc-NTF3-5, thus promoting RUNX2 expression (127). MODR (MSMSC osteogenesis differentiation-related lncRNA) performs similarly to lnc-NTF3-5, except that MODR impedes the inhibition of miR-454 on RUNX2 mRNA (128). An additional lncRNA that recovers RUNX2 transcript is TCPNS_00041960, which diminishes levels of miR204-5p, repressor of RUNX2 mRNA (129). In contrast, MEG3 contributes to the accumulation of miR-133a-3p (130), which targets RUNX2 mRNA (102), suggesting that MEG3 reduces osteogenesis, although this evidence was obtained in an ovariectomized model, so it remains to be established under normal conditions.

During osteogenesis, the function of RUNX2 depends on the interaction with partner proteins. For example, a transcriptional complex composed of RUNX2 and TAZ (Tafazzin) is assembled and activated by ABL protein. BMNCR1 (bone marrow stem cell-related lncRNA) serves as a scaffold to improve the interaction between RUNX2, TAZ, and ABL. Furthermore, BMNCR1 promotes this differentiation by increasing levels of BMP2 mRNA in addition to the phosphorylated state of SMAD1 and SMAD5 (131). In addition, the transcriptional repressor MSX2 negatively regulates RUNX2, which is hindered by DLX5 (Distal-less Homeobox 5) (132). In this respect, DLX5 mRNA is targeted by miR-141, a miRNA that prevents osteogenesis (133). Fascinatingly, the effect of miR-141 also implies downregulation of H19 (134).

Both RUNX5 and DLX5 are able to activate the transcription of SP7 (gene encoding OSTERIX, also referred as OSX), crucial in osteoblasts (135), as OSX allows transit to the mature state. Returning to extracellular factors, IGF1 upregulates OSX expression without altering RUNX2 levels, although this effect is less obvious than BMP2 stimulation. Nonetheless, IGF1 expression is hampered by miR-27a-3p, which reduces the amount of its mRNA. In this signaling axis, IGF1 is increased by the presence of MEG3, which reduces miR-27a-3p levels (136).

Epigenetic control of OSX is also mediated by an E3 ligase called FBXO25, which leads to ubiquitination of H2BK120 and trimethylation of H3K4 at the promoter of SP7 gene, enabling OSX expression. However, lncRNA ODIR1 (osteogenic differentiation inhibitory regulator 1) triggers proteasomal degradation of FBXO25 through CUL3 (Cullin 3), a possible mechanism that could maintain OSX silencing in early osteogenesis (137).

The function of RUNX2 on upregulation of OSX may be synergistically mediated by Special AT-rich sequence-binding protein 2 (SATB2), a DNA-binding protein modulated downstream of WNT (138). SATB2 mRNA may be at low levels because of the effect of miR-140-5p; however, both H19 (139) and MEG3 (140) negatively regulate miR-140-5p, enabling SATB2 expression. Thereby, upregulation of SATB2 triggers transcription of target genes, including the SP7 gene (139). It should be noted that miR-140-5p also targets BMP2, implying the role of miR-140-5p at various stages of osteogenesis (141). In regard to posttranscriptional regulation of OSX, the negative effect of miR-143 on OSX mRNA was demonstrated, but lncRNA Malat1 rescued OSX levels by inhibiting miR-143 (142).

The activity of the complex consisting of SATB2 and RUNX2 is augmented by the recruitment of ATF4, a key transcription factor in terminal differentiation of osteoblasts. ATF4 is required for the activation of BGLAP (gene encoding OCN). The promoter of BGLAP gene also has a regulatory region recognized by the transcription factor called CBFA1 (Core-binding factor subunit alpha-1), also known as RUNX2. The transcriptional repressor MSX1 (Msh homeobox 1), mentioned above in negative regulation on RUNX2, has been shown to negatively regulate OCN and CBFA1 (143). It has been suggested that lncRNA Msx1-AS (Msx1 antisense RNA) effectively reduces MSX1 levels, but the influence of this regulation on osteoblast maturation remains to be elucidated (144).

OCN is associated with osteoblast maturity since it is an extracellular protein that together with alkaline phosphatase (ALP) and type I collagen (COLI) forms part of components to form the bone structure. Furthermore, mature osteoblasts are characterized by a basophilic cytoplasm, a large Golgi apparatus, and mitochondrial abundance, due to the need to produce large amounts of protein, particularly COLI.

Regarding mitochondrial activity, it is stimulated by an RBP called LIN28A (145). The effectors of LIN28A in this process have not yet been described, but LIN28A levels increase because of interaction with TUG1, proposed to be through direct binding (146).

Osteogenesis implicates very well-defined signaling pathways, but lncRNAs have been recognized and positioned throughout this process (Fig. 4). Advancing findings are accompanied by new lncRNAs as regulators at each stage, even coincidentally modulating the same protein or affecting several targets (Table 2), which are precisely those that drive the progression in this differentiation.

ADIPOGENESIS: BEYOND AN ENERGY RESERVOIR

Actually, adipose tissue is recognized not only as a source of energy but also as a metabolic regulator at the systemic level, capable of exchanging signals with other organs to maintain homeostasis (147). Maintenance and growth of adipose tissue are controlled by adipogenesis, a complex multistep process involving the formation of adipocytes through a coordinated program of gene expression (148). Adipogenic precursor cells are distinguished from bone marrow-derived MSCs (BM-MSCs) because of the differential expression of surface markers such as CD34, CD104, and CD106 (32). Moreover, the advancement of single-cell RNA sequencing has disclosed a broad hierarchy of adipogenic precursor cell lineage (149). Nevertheless, this process can mainly be divided into two stages. In the first, the commitment leads to the restriction of the adipocyte lineage without any morphological changes, forming a preadipocyte. The preadipocyte continues with mitotic clonal expansion (MCE), including DNA replication and cell duplication (150). At this stage, the transcriptional factors CCAAT/enhancer-binding proteins (C/EBPs) and peroxisome proliferator-activated receptor-gamma (PPARγ) are expressed (150). Commitment is followed by progression of differentiation, whereby preadipocytes undergo growth arrest, lipid accumulation, and maturation into insulin-responsive adipocytes (151).

There are two main types of adipose tissues in mammals, white adipose tissue (WAT) and brown adipose tissue (BAT), with different morphologies, anatomical locations, functional characteristics, and gene expression patterns (152). WAT is composed of white adipocytes and is used by the body as an alternative source of energy, whereas brown adipocytes constitute BAT and protect against hypothermia due to the breakdown of lipids in favor of heat production, a phenomenon known as thermogenesis (152, 153). Brown and white adipocytes are generated in different manners, although both originate from adipogenic precursor cells. Briefly, the adipogenic precursor cells are capable of engendering both MYF5− white adipocytes and MYF5+ myogenic cells; the latter in turn can become brown adipocytes (151, 154, 155). A third type of adipose tissue consists of beige adipocytes (also known as brite adipocytes), which show a gene expression profile distinct from white or brown adipocytes (156). In the case of beige adipocytes, they are MYF5-inducible cells, with some features in common with brown and white adipocytes (157).

White Adipocytes, Gifted Communicators

The signaling network for mitotic clonal expansion is extensive in preadipocytes, but tyrosine phosphorylation and activation of STAT3 is one of the most described molecular events at this stage (158). The proliferation rate was higher as result of PVT1 (lncRNA homologous to plasmacytoma variant translocation gene) function, through interaction with STAT3-containing complexes. Relevantly, PVT1 also caused upregulation of genes related to

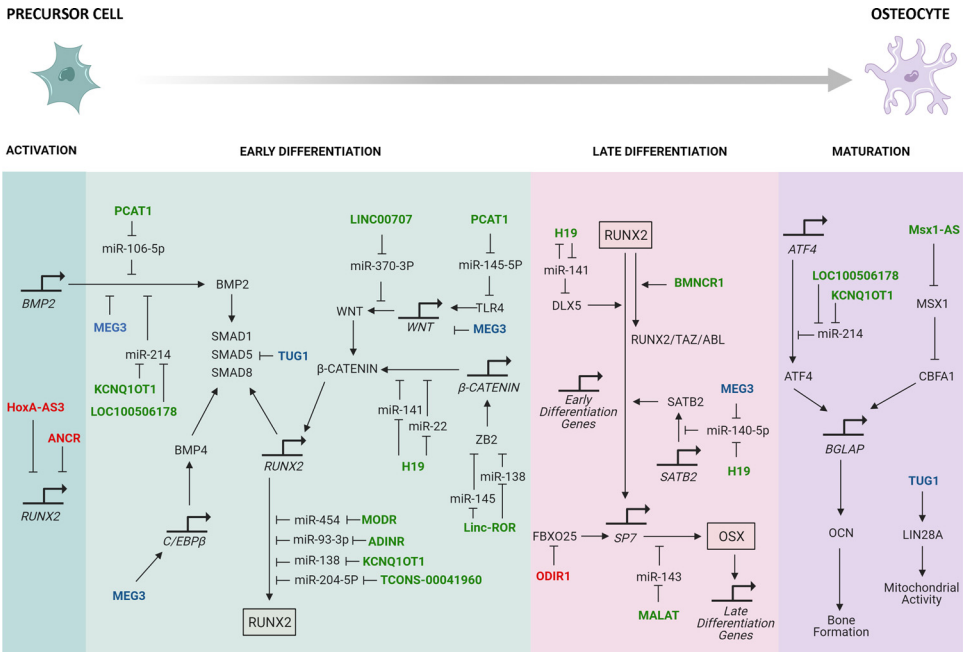

Figure 4. Osteogenesis. The signaling mechanisms of adipogenic program regulated by lncRNAs are shown. Key transcription factors are indicated in boxes. The figure is divided into sequential stages toward osteocytes. lncRNAs favor (green) or inhibit (red) markers of differentiation. lncRNAs described in both cases are also indicated (blue). Effect of lncRNA on its targets can be direct or indirect. For more details see text. See GLOSSARY for abbreviations.

Table 2. *lncRNA in osteogenesis*

lncRNA	Genomic Classification	Osteogenesis Promote/Inhibit	Function	Direct Target	Biological Model	Differentiation Markers (Technique Assay)	Ref.
AK016739 ENSMUSG00000097407 Gene ID: 74454		Inhibit			MC3T3-E1	RUNX2, ALP, COL1α1, OSX (RT-qPCR) ALP activity (APA) Calcium deposits (ARS)	(120)
AK028326 ENSMUSG00000097767 Gene ID: 330166		Promote			BMSCMC3T3-E1	RUNX2, OCN, OPN (WB) ALP activity (APA)	(107)
AK045490		Inhibit		miR-6344* miR-3089* miR-6951*	MC3T3-E1	ALP, OCN, COL1α1(RT-qPCR) ALP activity (APA) Calcium deposits (ARS)	(121)
AK141205		Promote			BMSC	RUNX2, OCN, OPN (WB)ALP activity (APA)	(108)
ANCR ENSG00000226950	Intergenic	Inhibit		EZH2	hFOB1.19	OCN (RT-qPCR) ALP activity (APA)	(86)
Gene ID: 57291 NR_145129.1	Intergenic	Inhibit			DPSC, PDLSC, SCAP	ALP, BSP, OCN (RT-qPCR) Calcium deposits (ARS)	(87)
	Intergenic	Inhibit			PDLSC	ALP, DSPP, OCN, BSP, RUNX2 (RT-qPCR) ALP activity (APA) Calcium deposits (ARS)	(84)
	Intergenic	Inhibit	Sponge of miRNA	miR-758	PDLSC	RUNX2, OSX, ALP (RT-qPCR, WB) ALP activity (APA) Calcium deposits (ARS)	(328)
DANCR	Intergenic	Inhibit			DPC	ALP activity (APA)	(122)
ENSG00000226950 NR_145129.1 Gene ID: 57291	Intergenic	Inhibit			BMSC, PTA-1058	BGLAP, COL1, RUNX2 (RT-qPCR) ALP activity (APA) Calcium deposits (ARS)	(104)
	Intergenic	Inhibit	Decoy	FOXO1	MSC		(125)
BDNF-AS ENSG00000245573 NR_033312.1 Gene ID: 497258		Inhibit	Modulator*	mRNA of BDNF*	BMSC	RUNX2, OPN (RT-qPCR, WB) ALP activity (APA) Calcium deposits (ARS)	(339)
Bmcob NONMMUT022580		Promote		SBP2	BMSC	ALP, OCN, RUNX2 (RT-qPCR, WB) Calcium deposits (ARS)	(340)
BMNCR1		Promote	Scaffold	TAZ, ABL	BMSC	ALPl, RUNX2, OSX, BGLAP (RT-qPCR) Calcium deposits (ARS)	(131)
Crnde ENSG00000245694 NR_034105.3 Gene ID: 643911	Intergenic, antisense	Promote			MC3T3-E1, osteoblasts	ALP, SPP1, COL1α1 (RT-qPCR)	(119)
HOTAIR ENSG00000228630 NR_047517.1 Gene ID: 100124700	Antisense	Inhibit	Guide*	Promoter of *miR-17-5p*	BMSC	RUNX2, COL1A1, ALP (RT-qPCR)	(99)
HoxA-AS3 ENSG00000254369 GeneID: 100133311 NR_038832.1	Antisense	Inhibit	Guide*	Promoter of *RUNX2*	BMSC	RUNX2, OSX, COL1A1, IBSP, BGLAP, SPP1 (RT-qPCR) ALP activity (APA) Calcium deposits (ARS)	(85)
	Antisense	Inhibit*	Modulator	mRNA of HOXC10	BMSC	Calcium deposits (ARS, VKS)	(341)
H19 ENSG00000130600 NR_131224.1 Gene ID: 283120	Intergenic	Promote	Sponge* of miRNA	miR-141, miR-22	BMSC	ALP, RUNX2 (RT-qPCR) ALP activity (APA) Calcium deposits (ARS)	(117)
	Intergenic	Promote	Source* of miRNAs		BMSC	RUNX2, OCN, ALP (RT-qPCR) ALP activity (APA) Calcium deposits (ARS, VKS)	(126)
	Intergenic		Sponge of miRNA	miR-188	BMSC	ALP activity (APA) Calcium deposits (ARS)	(118)
	Intergenic	Promote	Sponge of miRNA	miR140-5p	BMSC	RUNX2, OCN, OPN (WB) ALP activity (APA)	(139)
	Intergenic				hFOB1.19		(134)
	Intergenic	Promote			UMR106	RUNX2, OPG, ALP (RT-qPCR) ALP activity (APA) Calcium deposits (ARS)	(123)
	Intergenic	Promote			iMEF, iMAD	RUNX2, OSX, OPN, BSP, OCN (RT-qPCR) ALP activity (APA)	(342)

Continued

Table 2.— *Continued*

lncRNA	Genomic Classification	Osteogenesis Promote/Inhibit	Function	Direct Target	Biological Model	Differentiation Markers (Technique Assay)	Ref.
H19 ENSG00000130600 NR_131224.1 Gene ID: 283120	Intergenic	Promote	Sponge of miRNA	miR-138	BMSC	RUNX2, OPN, OCN (RT-qPCR) ALP activity (APA) Calcium deposits (ARS)	(343)
	Intergenic	Inhibit			ADSC	RUNX2, ALPL (RT-qPCR)	(344)
	Intergenic	Inhibit	Sponge of miRNA	miR-19b-3p	BMSC	RUNX2, COL1A1 (WB) ALP activity (APA)	(345)
KCNQ1OT1 ENSG00000269821 NR_002728.3 Gene ID: 10984	Antisense	Promote*		β-catenin	MSC	RUNX2, OSX, OCN (RT-qPCR) ALP activity (APA) Calcium deposits (ARS)	(96)
	Antisense	Promote	Sponge of miRNA	miR-214	BMSC	BMP2, RUNX2, OPN, OCN (RT-qPCR, WB) ALP activity (APA, AS) Calcium deposits (ARS)	(93)
		Promote	Sponge of miRNA	miR-138	TSC	RUNX2, OSX (WB) ALP activity (APA) Calcium deposits (ARS)	(95)
linc-ROR ENSG00000258609 NR_152602.1 Gene ID: 100885779	Intergenic	Promote	Sponge of miRNA	miR-145, miR-138	BMSC	OSX, OCN, ALP (RT-qPCR) ALP activity (APA) Calcium deposits (ARS)	(115)
LINC00707 ENSG00000238266 NR_038291.1 Gene ID: 100507127	Intergenic	Promote	Sponge of miRNA	miR-370-3p	BMSC	RUNX2, OSX, ALP (RT-qPCR) ALP activity (AS) Calcium deposits (ARS)	(110)
lnc-NTF3-5 ENSG00000256417 NONHSAG010263.2	Intergenic	Promote	Sponge of miRNA	miR-93-3p	MSMSC	RUNX2, OSX, ALP (RT-qPCR) Calcium deposits (ARS)	(127)
lnc RNA-MODR ENST00000447298.1		Promote	Sponge of miRNA	miR-454	MSMSC	RUNX2, OSX, ALP (RT-qPCR)	(128)
lncRNA-1		Promote			MC3T3-E1, MOB	RUNX2, SP7 (RT-qPCR)	(346)
LOC100506178 ENSG00000232759 Gene ID: 100506178	Antisense	Promote	Sponge of miRNA	miR-214-5p	BMSC	RUNX2, OSX, ALP (RT-qPCR) ALP activity (APA) Calcium deposits (ARS)	(92)
Malat1 ENSG00000251562 NR_002819.4 Gene ID: 378938	Intergenic	Promote	Sponge of miRNA	miR-143	BMSC	OCN, OPN, ALP (RT-qPCR) ALP activity (APA) Calcium deposits (ARS)	(142)
		Promote			BMSC	OCN, COL1, RUNX2 (RT-qPCR) ALP activity (APA)	(347)
MCF2L-AS1 ENSG00000235280 NR_034002.1 Gene ID: 100289410		Promote	Sponge of miRNA	miR-33a	BMSC	ALP, OCN, RUNX2 (RT-qPCR) Calcium deposits (ARS)	(348)
MEG3ENS-G00000214548 NR_046467.1 Gene ID: 55384	Intergenic	Promote	Decoy*	SOX2, promoter of *BMP4**	BMSC	RUNX2, OSX, OCN (RT-qPCR) Calcium deposits (VKS)	(89)
	Intergenic	Promote	Sponge of miRNA	miR140-5p	ADSC	RUNX2, OCN (RT-qPCR) Calcium deposits (ARS)	(140)
	Intergenic	Inhibit		ago-02	BMSC	RUNX2, OCN, OPN (WB) ALP activity (APA)	(130)
	Intergenic	Promote			BMSC	RUNX2, ALP, OCN (RT-qPCR, WB) ALP activity (APA) Calcium deposits (ARS, VKS)	(90)
	Intergenic	Inhibit*		EZH2	DFSC	RUNX2, OCN, ALP (RT-qPCR) Calcium deposits (ARS)	(109)
	Intergenic	Promote	Sponge of miRNA	miR-27a-3p	PDLSC	RUNX2, OSX, OCN, COL1α1 (WB)ALP (AS) Calcium deposits (ARS)	(136)
	Intergenic	Inhibit	Decoy to inhibit translation	hnRNPI	PDLC	RUNX2, OCN (WB)ALP activity (APA) Calcium deposits (ARS)	(88)
MIAT ENSG00000225783 NR_003491.3 Gene ID: 440823		Inhibit			ADSC	RUNX2, ALP, OCN (RT-qPCR, WB) ALP activity (APA)	(349)

Continued

Table 2.— *Continued*

lncRNA	Genomic Classification	Osteogenesis Promote/Inhibit	Function	Direct Target	Biological Model	Differentiation Markers (Technique Assay)	Ref.
MIR31HG ENSG00000171889 ID: 554202 NR_152878.1		Inhibit		IkBα	ADSC	RUNX2, OSX (RT-qPCR) ALP activity (APA) Calcium deposits (ARS, VKS)	(333)
Msx1-AS RNA	Antisense Antisense	Promote* Promote*	Modulator*	Modulator*	MO6-G3 MO6-G3	OCN (RT-qPCR)	(143) (144)
NONHSAT009968		Inhibit			BMSC	ALP activity (APA) Calcium deposits (ARS)	(350)
ODIR1 ENSG00000253746	Intergenic	Inhibit	Scaffold	CUL3, FBXO25, BARD1	QC1205	RUNX2, OSX, OPN (RT-qPCR) ALP activity (APA) Morphology (F-AS)	(137)
PCAT1 ENSG00000253438 NR_045262.2 Gene ID: 100750225	Intragenic Intragenic	Promote Promote	Sponge of miRNA Sponge of miRNA	miR-145-5p miR-106a-5p	ADSC PDLSC, BMSC,UC-MSC	RUNX2, OCN, OPN (WB) ALP activity (APA) RUNX2, OSX, ALP (RT-qPCR, WB) ALP activity (APA, AS) Calcium deposits (ARS)	(112) (91)
PGC1β-OT1		Promote	Sponge of miRNA	miR-148a-3p	BMSC, ST2, C3H10T1/2, MC3T3-E1	RUNX2, OSX, OPN, ALP (RT-qPCR) ALP activity (APA)	(334)
POIRENS-T00000446358	Intergenic	Promote	Sponge of miRNAceRNA	miR-182	PDLSC	RUNX2, COL1, ALP (RT-qPCR) ALP activity (APA) Calcium deposits (ARS)	(124)
PRNCR1 ENSG00000282961 NR_109833.1 Gene ID: 101867536	Intergenic	Inhibit	Sponge of miRNA	miR211-5p	BMSC	RUNX2, OSX, OCN (RT-qPCR) ALP activity (APA)	(106)
RMST ENSG00000255794 NR_152618.1 Gene ID: 196475		Promote	Sponge of miRNA	miR-106, miR-125a, miR-449a, miR-449b	iMAD	RUNX2, OSX, ALP, OPN, OCN, COL1A1 (RT-qPCR) ALP activity (AS)	(337)
TCONS_00041960		Promote	Sponge of miRNA	miR-204-5p, miR-125a-3p	BMSC	RUNX2, OSX, OCN (RT-qPCR) ALP activity (APA)	(129)
TUG1 ENSG00000253352 NR_152871.1 Gene ID: 55000	Intergenic Intergenic	Promote Inhibit		SMAD5	PDLSC BMSC	RUNX2, OCN, ALP (RT-qPCR) Calcium deposits (ARS) RUNX2, OSX, OCN, ALP (RT-qPCR) ALP activity (APA)	(146) (97)
XIST ENSG00000229807 NR_001564.2 Gene ID: 7503		Inhibit			BMSC	ALP, RUNX2 (RT-qPCR, WB) ALP activity (AS)	(327)
XR_111050		Promote			BMSC, PDLSC	COL1A2, OCN, OPN, BSP(RT-qPCR) Calcium deposits (ARS)	(351)

APA, alkaline phosphatase assay; ARS, Alizarin Red S staining; AS, alkaline phosphatase staining; DFSC, dental follicle stem cell; DPC, dental pulp cell; DPSC, dental pulp stem cell; F-AS, F-actin staining; MSMSC, maxillary sinus membrane stem cell; PDLC, periodontal ligament cell; PDLSC, periodontal ligament stem cell; SCAP, stem cell from apical papilla; TSC, tendon stem cell; UC-MSC, umbilical cord-derived MSC; VKS, von Kossa staining. *Suggested by the authors of the study. See GLOSSARY for other abbreviations.

synthesis and transportation of fatty acid, while the expression of genes involved in β-oxidation of fatty acid was silenced (159).

Furthermore, proliferation of preadipocytes can be synergistically driven by other lncRNAs. For example, lncRNA-Adi acts as a molecular sponge on miR-449a, a member of the miR-34 family, leading to the release of mRNA encoding Cdk6 to result in S-phase entry (160). SlincRAD (superlong intergenic noncoding RNA functioning in adipocyte differentiation) is also implicated in this step by silencing the promoter of CDKN1A, gene encoding p21, through DNA methylation by DNMT1 (DNA methyltransferase 1). Interestingly, the effect of slincRAD on a greater number of mitosis-associated genes has been suggested, because the perinuclear location of DNMT1 was depleted in the absence of slincRAD and multinucleated cells were formed at the end of differentiation in this condition (161). In fact, another study reinforced the proadipogenic role of slincRAD, but in this case proliferation was not affected, so the discrepancy on proliferation needs to be thoroughly addressed (162). The impact of slincRAD could go beyond adipogenic differentiation, as changes in glucose and lipid metabolism at the systemic level were detected by slincRAD suppression (163).

Transient expression of C/EBPβ and C/EBPδ is essential at the early stage; therefore mRNA of C/EBPβ can be repressed by miR-191, whose expression is upregulated because of transcriptional activity of PU.1 (164). Inhibition of antisense lncRNA PU.1AS on PU.1 mRNA led to diminished PU.1 levels and improved differentiation. In preadipocytes, both PU.1 mRNA and PU.1AS can be simultaneously transcribed and form a duplex, implying regulation according to the ratio of both molecules to repress PU.1 activity (165).

C/EBPβ can elicit downstream expression of PPARγ and C/EBPα (150, 166). Remarkably, PPARγ induces C/EBPα and C/EBPα in turn positively regulates PPARγ, establishing a reciprocal activation loop targeting the transcription of adipocyte-related genes (167, 168). The expression of C/EBPα and PPARγ is augmented by HuR (Hu antigen R), which is an RBP known to improve the stability of target mRNAs, although it may employ other mechanisms (169). The interaction between HuR and mRNAs of C/EBPα and PPARγ is disrupted when CAAlnc1 (cachexia-related anti-adipogenesis lncRNA 1) binds HuR, thereby reducing adipogenesis (170). Importantly, the role of HuR in this cellular process must be carefully interpreted, as a negative role of HuR has also been demonstrated, probably due to global action of HuR, beyond its effect on C/EBPα and PPARγ (171).

PPARγ expression may be restricted by the action of miR-27b (172), although lncRNA Gm15290 sponging miR-27b to increase PPARγ has been postulated (173). Interestingly, miR-27b targets lipoprotein lipase (LPL), a regulator of triglyceride levels, which also appears to participate in adipogenic differentiation, so the role of GM15290 could not affect a single downstream effector (174).

PPARγ activity is accompanied by cofactors such as NCoR (nuclear receptor corepressor) and SMRT (silencing mediator of retinoid and thyroid hormone receptors). However, SIRT1 can interact with these cofactors to decrease PPARγ-mediated transcription (175). Expression of SIRT1 is limited because its mRNA can be inhibited by miR-204. However, ADNCR (adipocyte differentiation-associated long noncoding RNA) improves SIRT1 levels by a spongelike interaction with miR-204, causing defects in adipogenesis (176). Interestingly, a relationship between SIRT1 and mobilization of fatty acids has been described, so that ADNCR could also act in differentiated adipocytes (175). miR-204-5p can also be captured by lncRNA HCGII (human leukocyte antigen complex group II), which, similar to ADNCR, impairs this differentiation (177). Otherwise, sterol regulatory element binding protein 1 (SREBP1) induces enzymatic production of PPARγ ligand or directly binds to promoter of PPARG gene, in both cases upregulating function of PPARγ. Initially, SREBP1 precursor is cleaved to release the nuclear form of SREBP1 (nSREBP1), which translocates into the nucleus to regulate gene expression. Polypyrimidine tract binding protein 1 (PTBP1) is responsible for SERBP1 cleavage; however, circular RNA designated as hsa_circH19 (originated from H19 pre-RNA) represses PTBP1 activity, causing inhibition of SREBP1 and subsequent diminished transcription of adipocyte-related genes, including PPARγ (178). Furthermore, the transcriptional activity of PPARγ can be stimulated by interaction with SRA, specifically in the presence of ciglitazone, a PPARγ agonist. Interestingly, SRA also affects cell cycle inhibitors during adipogenesis, repressing p21 and p27 during mitotic clonal expansion (MCE) but augmenting them after MCE; thus SRA plays a role in exiting the cell cycle to progress to advanced stages (179).

PPARγ1 and PPARγ2 are two protein isoforms generated by different transcription start sites and alternative splicing. In the early stages of adipogenesis, PPARγ1 is preferentially expressed compared with PPARγ2 (180). The increased transcription activity of PPARγ1 by transmembrane protein 18 (TMEM18) has recently been demonstrated (181). TMEM18 is a transmembrane protein localized in nuclear membrane, and although function as a transcription factor has been considered unlikely (182), the presence of TMEM18 was detected in the distal promoter of PPARG1 gene (181), suggesting that TMEM18 may act according to the cellular context. Expression of TMEM18 correlated with lncRNA AC092159.2 levels, so a relationship between the two molecules is possible because AC092159.2 is transcribed from the DNA region in proximity to TMEM18 gene (183). With respect to PPARγ2, lncRNA U90926 inhibited the transactivation of promoter of PPARG2 gene, although the mechanism involved has not been elucidated (184).

Interestingly, the intronic region of PPARγ is independently capable of transcribing a lncRNA named Plnc1. In this regard, Plnc1 mainly encouraged the transcriptional activity of the promoter of PPARG2 gene by reducing its methylation, whereas the absence of Plnc1 impeded adipogenic differentiation (185). Apart from that, SR proteins might be required for alternative splicing of PPARγ. In particular, SRp40 [also named SFRS5 (Serine- and Arginine-Rich Splicing Factor 5)] seems to favor splicing of PPARγ2, because both molecules are induced to a similar tendency. The activity of SRp40 in splice site selection is augmented under phosphorylation mediated by Clk1 (Cdc2-like kinase 1). Remarkably, SRp40 interacts with lncRNA NEAT1 (nuclear-enriched abundant transcript 1) for SRp40 to be phosphorylated, leading to upregulation of PPARγ2 expression (186). Moreover, it was argued that NEAT1 might have a large-scale participation in adipogenesis, because NEAT acts as scaffolding factor to form paraspeckles within the nucleus (187), with miR-140 augmenting stability of NEAT (188). With respect to paraspeckles, Paral1 (PPARγ-activator RBM14-associated lncRNA) could also be involved in regulating its structure, through interaction with RBM14 (RNA binding motif protein 14). Of particular interest, Paral1 favored the upregulation of RBM14 on transcriptional activity of PPARγ (189).

For its part, C/EBPα expression can be improved at transcriptional level through histone modifications triggered by lncRNA ADINR (adipogenic differentiation-induced noncoding RNA), which modifies the methylated state of C/EBPα locus. This is achieved because ADINR recruits PA1 (PAXIP1-associated glutamate-rich protein 1) to promoter of C/EBPα to increase and decrease the methylation of H3K4 and H3K27, respectively, as PA1 belongs to the histone methylation complex MLL3/4 (Mixed-lineage leukemia 3/4), also called the trithorax complex (190). Notably, MLL3/4 enriched trimethylation of H3K4 at the promoter of PPARγ (191), and the role of ADINR even seems to coordinate PPARγ expression, although the mechanism has not yet been described (190). Meanwhile, C/EBPα mRNA is repressed by miR-31, but lncRNA TINCR (terminal differentiation-induced ncRNA) acts as a sponge on miR-31, augmenting C/EBPα expression. In an appealing manner, C/EBPα triggers TINCR expression, thus establishing a positive feedback (192).

The transcriptional coactivator β-catenin is related to the maintenance of an undifferentiated state and prevents transcription of C/EBPβ, C/EBPα, and PPARγ; therefore, downregulation of β-catenin activity is necessary for the progression of adipogenesis (193, 194). Levels of β-catenin can

be reduced upon lnc-OAD (lncRNA associated with osteoblast and adipocyte differentiation) expression, leading to enrichment of adipogenic markers. Furthermore, the absence of lnc-OAD impairs proliferation in MCE (195). Classically, β-catenin activity is dependent on WNT ligand stimulation, which is known as the canonical WNT pathway; however, WNT can also trigger noncanonical mechanisms that repress β-catenin activity. The type of WNT ligand may dictate how downstream signaling occurs with respect to β-catenin. For example, WNT5β was observed to promote adipogenesis by inhibiting β-catenin (196). Wnt5β mRNA is diminished by miR-587, but lncRNA RP11-142A22.4 sequesters miR-587 to release mRNA and increase WNT5β expression, leading to adipogenesis (197). In addition, WNT recognition is performed by FZD receptor but is assisted by coreceptor LRP5/6, which is mainly associated with canonical signaling. Increased expression of DKK1, an antagonist of LRP5/6, was observed downstream of lncRNA AC092834.1, promoting this differentiation through decreased levels of β-catenin (198).

Adipogenic activity may be decreased as a consequence of TC1 (Thyroid cancer protein 1), because the interaction of TC1 with Chibby prevents the negative effect of Chibby on β-catenin (199, 200). TC1 mRNA is decreased by miR30a but rescued in the presence of H19, which acts as sponge on miR30a, increasing TC1 levels and thus improving β-catenin activity (201). Interestingly, miR30a belongs to the miR30 family, which is known to stimulate adipogenesis through inhibition of RUNX2, an osteogenic transcriptional factor (202). Meanwhile, the antiadipogenic role of H19 is also achieved through miR-675. In particular, miR-675 reduces mRNA and protein levels of HDAC4-6; thus H19 restrains adipogenesis-related epigenetic rearrangements, probably due to impaired histone modifications (203). Regarding this aspect, the chromatin attachment factor heterogeneous nuclear ribonucleoprotein U (HNRNPU) is responsible for performing functions related to nuclear structure. lncRNA FIRRE (functional intergenic repeating RNA element), also called RAP-1 (Regulated in Adipogenesis 1), can operate as a partner of HNRNPU (203) to mediate the architecture of chromosome interactions, building highly organized chromatin territories. However, FIRRE acted downstream of HNRNPU, because its focal localization was lost in the absence of HNRNPU (204). Therefore, HNRNPU may contribute to adipogenic progression by bringing different adipogenic loci in close proximity to coordinate their expression.

Adipogenic differentiation can also be stimulated by phosphorylation of AKT (V-akt murine thymoma viral oncogene homolog) in response to insulin. Phosphorylated AKT led to PPARγ expression in preadipocytes through mammalian target of rapamycin complex 1 (mTORC1) activity (205). lnc-ORA (obesity-related lncRNA) contributed to the activation of the phosphatidylinositol 3-kinase (PI3K)/AKT/mTOR axis, in addition to promoting S-phase entry, but apparently without altering ERK and p38 signaling (206). Lin-NFE2L3-1 (long intergenic noncoding RNA-nuclear factor, erythroid 2-like 3-1) is able to decrease insulin-induced phosphorylation of AKT; however, it occurred in mature adipocytes, without affecting adipogenic genes such as PPARγ (207). AKT can be inactivated by dephosphorylation through phosphatase and tensin homolog (PTEN) yield. One mechanism capable of repressing adipogenesis is upregulation of PTEN expression, which is achieved by inhibiting miR-21a-5p, a repressor of PTEN, through the sponge function of lncRNA GAS5 (growth arrest-specific transcript 5) (208). Interestingly, the antiadipogenic role of GAS5 involves the sponge function not only on miR-21A-5p but also on miR-18a. Downregulation of miR-18a led to connective tissue growth factor (CTGF) expression (209), which negatively modulates adipogenesis in the presence of TGF-β (210). It would be interesting to know whether these GAS5-dependent mechanisms are related to each other or represent two independent signals.

Coordination of PPARγ and C/EBPα during adipocyte maturation targets the expression of genes such as FABP4 (Fatty Acid Binding Protein 4), LPL, AGPAT2 (1-Acylglycerol-3-Phosphate O-Acyltransferase 2), PLIN (Perilipin), Adiponectin (also named AdipoQ), and LEPTIN, in relation to processes such as insulin sensitivity, lipogenesis, or lipolysis (148). Moreover, PPARγ and C/EBPα are also important for fat accumulation and size of mature adipocytes in the terminal differentiation stage (211). For LEPTIN, its expression is augmented by lnc-leptin, a lncRNA located in an enhancer region upstream of LEPTIN gene, in mature adipocytes. However, effects of lnc-leptin on adipogenesis through LEPTIN-independent mechanisms have been proposed (212).

As for FABP4, the PPARγ response element is contained in its promoter region (213), where H3 acetylation and H3K4 methylation are induced by lncRNA MIR31HG (miR-31 host gene) (214). FABP4 levels were also increased by SRA, a lncRNA mentioned above at the MCE stage. Interestingly, SRA had no effect on PPARγ and C/EBPα expression, so it would be important to know whether this regulation of SRA on FABP4 is independent of PPARγ and C/EBPα (215). Nevertheless, SRA is mainly related to roles in mature adipocytes, because SRA can function as coactivator of the steroid receptor and nonsteroidal nuclear hormone receptor (216), so SRA could participate in adipokine and cytokine secretion in terminally differentiated adipocytes in the presence of hormones such as insulin. Furthermore, SRA participates in typical adipocyte processes such as lipid metabolism by decreasing the levels of PCK1, an enzyme implicated in the balance between triglycerides and free fatty acids (217). As mentioned above, SRA1 gene encodes SRAP by alternative splicing, which can attenuate SRA activity (218). The evidence suggests that regulation of SRA should be carried out appropriately, as it would have repercussions on several aspects of adipose tissue.

Adipocytes are able to synthesize AdipoQ, a hormone engaged in control of lipid and glucose metabolism not only in adipose tissue but of the whole organism (219). Overexpression of AdipoQ led to accelerated adipogenic differentiation, in addition to detecting a more evident expression of C/EBPα and PPARγ (220). Thus, suppression of AdipoQ mRNA translation impaired progression in adipogenesis, as was demonstrated by the function of antisense lncRNA AdipoQ AS, which formed a duplex with AdipoQ mRNA to inhibit it (221).

Modulation of insulin sensitivity by adipose tissue focuses on the balance between lipid storage and mobilization. Mature adipocytes engage in lipolysis and consequently the release of free fatty acids into the circulation. In the last stage

of lipolysis, monoacylglycerol lipase (MGLL) converts monoacylglycerol to glycerol and fatty acid. Lipolysis is moderated by proteins on the surface of lipid droplet where triacylglycerol is contained, within which PLIN is defined as a blocker of lipolysis (222). ASMER-1 and ASMER-2 (adipocyte-specific metabolic-related lncRNA 1 and 2, respectively) are apparently involved in adipocyte maturation, because ASMER-1 decreased PLIN1 and MGLL expression, whereas ASMER-2 only affected MGLL (223).

At each stage on the path that leads MSCs toward the constitution of WAT, lncRNAs assert their presence (Fig. 5), where the broadening of the vision of their role goes hand in hand with the diversity of targets they have (Table 3).

Brown and Beige Adipocyte, Burning or Cooling Fat

The potential to generate heat is a common feature in brown and beige adipocytes, which is why both cell types are referred to as thermogenic fat cells. Capacity for prompt heat is mainly attributed to the presence of uncoupling protein-1 (UCP-1), which is expressed in the inner membrane of mitochondria and coordinates respiratory uncoupling reactions. UCP-1 expression is detected in brown and beige adipocytes; however, in the case of beige adipocytes, it is conditioned to external stimuli (152). For example, upon hormonal or cold exposure, Zfp516 (Zinc finger protein 516) activates UCP1 transcription by direct binding to the promoter region and interaction with the transcriptional coregulator PRDM16 (PR-domain containing protein 16) (216). lnc-dPrdm16 (also named LINC00982) is a lncRNA divergently located from PRDM16 and related to PRDM16 expression. lnc-dPrdm16 upregulates brown fat markers, but modulation of these markers in a Prdm16-independent manner has also been proposed. (225) Interestingly, Gm13133 is an intronic lncRNA in PRDM16 gene induced by cold exposure and able to increase mitochondrial biogenesis as well as expression of UCP1, phosphatidylglycerol phosphalipase alpha (PGC1α), and BMP7, the latter being a factor related to the conversion of white adipocytes to brown adipocytes, although the mode of action of Gm13133 remains to be defined (226).

UCP1 levels can be attenuated by lncRNA 2310069B03Rik, even though lncRNA 2310069B03Rik was increased upon thermogenic stimulus such as cold exposure or β-adrenergic receptor agonist. In the same study, PPARα was downregulated by lncRNA 2310069B03Rik (227). PPARα is crucial for lipolysis and thermogenic program in brown adipocytes (228). With respect to this factor, PPARα expression is augmented by two lncRNAs, nc281160 and NONMMUT024512, with the transcription site of both lncRNAs located spatially close to PPARA gene within the nucleus, whereby these molecules acted in a specific manner because other neighboring genes were not altered (229). Furthermore, PPARα mRNA can also be repressed at the translational level by interaction with IGF2BP2, but this effect is impaired when lncRNA linc-ADAL (lincRNA for adipogenesis and lipogenesis) binds IGF2BP2, releasing mRNA from negative regulation. However, other factors could be involved, because unexpectedly PPARα increased in the absence of linc-ADAL. A putative factor could be HNRNPU, with which linc-ADAL also interacted, although in this case no direct relationship with PPARα was found (230).

High concentrations of cAMP represent another stimulus capable of inducing UCP1 expression, where cyclic AMP-responsive element binding protein (CREB) directly activates the promoter of UCP1 (231). Regulation of transcriptional activity of CREB is modulated directly by CRTCs (CREB-regulated transcription coactivators) and indirectly by NONO. lncRNA LINC00473 is a molecule included in this signaling axis by stimulating the interaction between NONO and CRTCs (232). In the thermogenic context, LINC00473 increased uncoupling and lipolytic rates. It is noteworthy

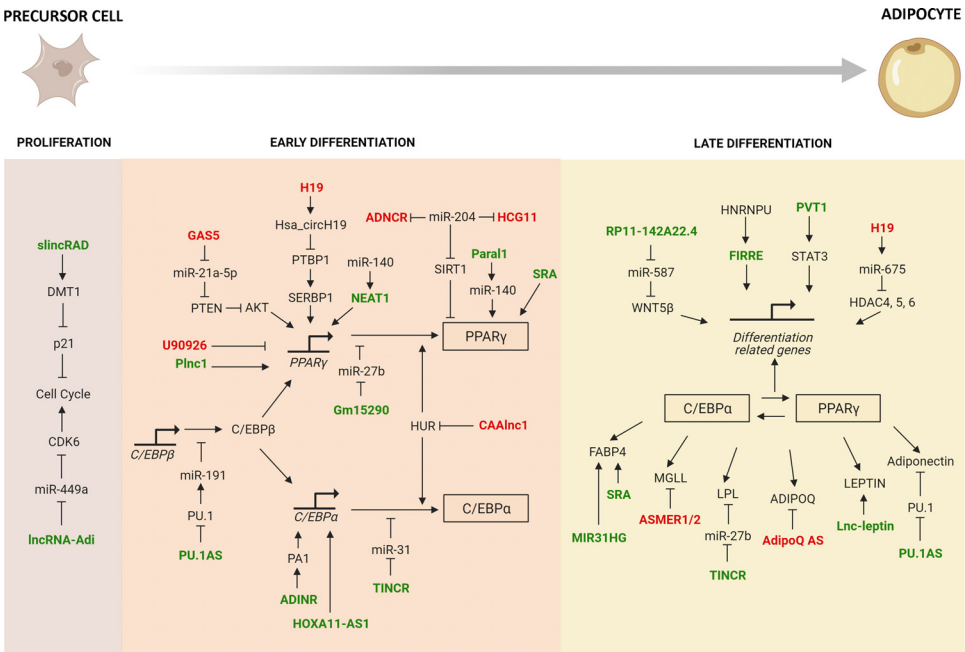

Figure 5. Adipogenesis in white adipocytes. The signaling mechanisms of adipogenic program regulated by lncRNAs are shown. Key transcription factors are indicated in boxes. The figure is divided into sequential stages toward white adipocytes. lncRNAs favor (green) or inhibit (red) markers of differentiation. lncRNAs described in both cases are also indicated (blue). Effect of lncRNA on its targets can be direct or indirect. For more details see text. See GLOSSARY for abbreviations.

Table 3. *lncRNA in white adipogenesis*

lncRNA	Genomic Classification	Adipogenesis Promote/Inhibit	Function	Direct Target	Biological Model	Differentiation Markers (Technique assay)	Ref.
AC092834.1		Promote			ADSC	C/EBPα, FABP4, PLIN, PPARγ (RT-qPCR, WB), Lipids (OROS)	(198)
ADINR ENSG00000267296 NR_026887.2 Gene ID: 80054	Bidirectional	Promote	Guide	PA1, PTIP, WDR5	ADSC	C/EBPα, FABP4, LPL, PPARγ (RT-qPCR) C/EBPα, PPARγ (WB) Lipids (OROS)	(190)
AdipoQ AS ENSG00000226482 NR_046662.2 Gene ID: 100874095	Antisense	Inhibit		mRNA of AdipoQ	3T3-L1	AdipoQ, PPARγ (RT-qPCR, WB) Lipids (OROS)	(221)
ADNCR Gene ID: 107992386		Inhibit	Sponge of miRNA	miR-204	3T3-L1	C/EBPα, FABP4, PPARγ (RT-qPCR) Lipids (OROS)	(176)
ASMER-1 ASMER-2 ENS-G00000235609.4 CATG00000111229.1		Promote			ADSC	AdipoQ, FABP4, PPARγ (RT-qPCR) Lipids (OROS)	(223)
CAAlnc1NR-015608.1		Inhibit		HuR	C3H10	AdipoQ, FAB4, LPL (RT-qPCR) Lipids (OROS)	(170)
GAS5 ENSG00000234741 NR_152521.1 Gene ID: 6067	Antisense	Inhibit	Sponge of miRNA*	miR-21a-5p	3T3-L1	FABP4, FAS, LPL, PPARγ (RT-qPCR) FABP4, PPARγ (WB)	(208)
	Antisense	Inhibit	Sponge of miRNA	miR-18a	BMSC	C/EBPα, FABP4, PPARγ (WB) Lipids (OROS)	(209)
Gm15290 ENSMUS-G00000085634 NR_151444.1 Gene ID: 102636218		Promote	Sponge of miRNA*	miR-27b	Preadipocytes of iWAT	C/EBPα, PPARγ (WB) Lipids (OROS)	(173)
H19 ENSG00000130600 NR_131224.1 Gene ID: 283120	Intergenic	Inhibit	Source of miR-675		BMSC	C/EBPα, FABP4, PPARγ (RT-qPCR, WB)	(203)
	Intergenic	Inhibit	Sponge of miRNA	miR-30a	ADSC	CEBPα, PPARγ (WB) Lipids (OROS)	(201)
	Intergenic	Inhibit	Source of has-circH19	PTBP1	ADSC	ACC-1, C/EBPα, FABP4, FAS, LPL, PPARγ, SREBP1c (RT-qPCR) Lipids (OROS, NRS)	(178)
HCG11 ENSG00000228223 NR_026790.1 Gene ID: 493812	Intergenic	Inhibit	Sponge of miRNA	miR-204-5p	ADSC	AdipoQ, C/EBPα, FABP4, LPL, PPARγ2 (RT-qPCR) Lipids (OROS) ACC, FAS (SP)	(177)
HOTAIR ENSG00000228630 NR_047517.1 Gene ID: 100124700	Antisense/ intergenic	Promote	Guide*/scaffold*		Preadipocytes of aAT or gAT	Leptin, LPL, PPARγ (RT-qPCR)	(331)
	Antisense/ intergenic	Promote		PCDH7, HOXB2 genes	BMSC	Lipids (BODIPY)	(332)
HoxA-AS3 ENSG00000254369 NR_038832.1 Gene ID: 100133311	Antisense	Promote	Guide	EZH2-dependent H3K27me3	BMSC	AdipoQ, C/EBPα, FABP4, PPARγ (RT-qPCR) Lipids (OROS)	(85)
HOXA11-AS1 ENSG00000240990 NR_002795.2 Gene ID: 745781	Antisense/ intergenic	Promote			ADSC	C/EBPα, CIDEC, DGAT2, Perilipin (RT-qPCR, WB)	(352)
linc-ADAL ENSG00000287148 Gene ID: 107986443	Intergenic	Promote	Decoy	hnRNPU, IGF2BP2	ADSC	C/EBPα, FASN, PPARγ, SREBF1 (RT-qPCR, WB) Lipids (OROS)	(230)
lnc-Leptin Gene ID: 102632876		Promote	Enhancer	Promoter of LEP*	Preadipocytes of iWAT	AdipoQ, PPARγ (RT-qPCR) Lipids (OROS)	(212)
lnc-OAD ENSMUS-G00000038408 NR_029439.1		Promote			3T3-L1	PPARγ, C/EBPα, aP2(RT-qPCR, WB) Lipids (OROS)	(195)
lnc-ORA		Promote			3T3-L1	FABP4, FASN, Leptin, PGC1-α, PPARγ (RT-qPCR) Leptin, PCG1-α (WB)	(206)
lnc-AC092159.2 ENSG00000233296 ID: 105373354	Intergenic	Promote			HPA-v	C/EBPα, C/EBPβ, FABP4, PPARγ (RT-qPCR, WB) Lipids (OROS)	(183)

Continued

Table 3.— *Continued*

lncRNA	Genomic Classification	Adipogenesis Promote/Inhibit	Function	Direct Target	Biological Model	Differentiation Markers (Technique assay)	Ref.
lncRNA-Adi ENSRNO-T00000012585		Promote	Sponge of miRNA	miR-449a	ADSC	Lipids (OROS)	(160)
lncRNA-U90926 ENSMUS-G00000029409 Gene ID: 57425		Inhibit			3T3-L1	FABP4, PPARγ (RT-qPCR, WB) Lipids (OROS)	(184)
MEG3 ENSG00000214548 NR_046467.1 Gene ID: 55384	Intergenic	Inhibit	Sponge of miRNA	miR-140-5p	ADSC	C/EBPα, PPARγ (RT-qPCR) Lipids (OROS)	(140)
MIR31HG ENSG00000171889 NR_152878.1 Gene ID: 554202	Intronic	Promote	Scaffold*	Promoter of FABP4 gene*	ADSC	C/EBPα, FABP4, PPARγ(RT-qPCR, WB)	(214)
NEAT1 ENSG00000245532	Intergenic	Promote	Sponge of miRNA	miR-140	3T3-L1	C/EBPα, PPARγ (WB) Lipids (OROS)	(188)
NR_131012.1 Gene ID: 283131	Intergenic	Promote		SRp40	3T3-L1	PPARγ1/2 (WB)	(186)
Paral1 ENSG00000243961 NR_109861.1 Gene ID: 101929371	Intronic	Promote		SFPQ, NONO, PSPC1, RBM14	3T3-L1,3T3-442A, BMSC	Lipids (OROS)	(189)
Plnc1	Intergenic	Promote	Guide*	Promoter of PPARγ gene*	ST2, 3T3-L1, C3H10T1/2	PPARγ, C/EBPα, aP2 (RT-qPCR) PPARγ 1 Y 2, C/EBPA (WB), Lipids (OROS)	(185)
PU.1 AS	Antisense	Promote	Modulator	mRNA of PU.1	3T3-L1	PPARγ (WB)Lipids (OROS)	(165)
PVT1 ENSG00000249859 NR_003367.3 Gene ID: 5820	Intergenic	Promote		STAT3-containing complexes	3T3-L1	aP2, C/EBPα, PPARγ (RT-qPCR)	(159)
RP11-142A22.4 ENSG00000272727	Intergenic	Promote	Sponge of miRNA	miR-587	Preadipocytes of VAT	C/EBPα, PPARγ (RT-qPCR, WB) Lipids (OROS)	(197)
slincRAD	Superlong intergenic	Promote			3T3-L1	C/EBPα, PPARγ (RT-qPCR), Lipids (OROS)	(162)
	Superlong intergenic	Promote	Guide	DNMT1, promoter of p21 gene	3T3-L1	C/EBPα, PPARγ (RT-qPCR)	(161)
	Superlong intergenic	Promote			3T3-L1	PPARγ, FABP4, Srebf1, Lipe (RT-qPCR) Lipids (OROS)	(163)
SRA Gene ID: AF092038	Intergenic	Promote	Coactivator	PPARγ	3T3-L1, ST2	Adiponectin, C/EBPα, FABP4, PPARγ (RT-qPCR, WB), Lipids (OROS)	(179)
	Intergenic	Promote			3T3-L1, ST2	AdipoQ, C/EBPα, FABP4, PPARγ (RT-qPCR) Lipids (OROS)	(215)
TINCR ENSG00000223573 NR_027064.3 Gene ID: 257000	Intergenic	Promote	Sponge of miRNA	miR-31	ADSC	C/EBPα, PPARγ (RT-qPCR, WB) Lipids (OROS)	(192)
TCONS_00041960		Inhibit	Sponge of miRNA	miR-204-5p, miR-125a-3p	BMSC	C/EBPα, GILZ, PPARγ (RT-qPCR, WB) Lipids (OROS)	(129)

aAT, abdominal adipose tissue; BODIPY, boron-dipyrromethene; gAT, gluteal adipose tissue; iWAT, inguinal white adipose tissue; NRS, Nile red staining; OROS, Oil Red O staining; SP, spectrophotometry; VAT (visceral adipose tissue). *Suggested by the authors of the study. See GLOSSARY for other abbreviations.

that LINC00473 localized to the interphase between lipid droplets and mitochondria, where it possibly participates in coordinating functions in both organelles (233). Activation of p38 MAP kinase pathway has also been shown as an effector of cAMP to increase UCP1 expression (234); however, lncRNA UC.417 diminished p38 phosphorylation, thus decreasing brown adipocyte-related gene expression, but without altering WAT genes (235).

There are other transcriptional regulators responsible for activating brown and beige adipocyte-related genes, including ZBTB16 (Zinc finger and BTB domain-containing protein) and EBF2 (Early B cell factor) (150, 236). Transcriptional activity of EBF2 is mediated by Blnc1 (Brown fat enriched lncRNA 1), which augments EBF2 recruitment to UCP1 and PPARα promoters (237). However, the apparent lack of RNA-binding domain in EBF2 has been argued, and the interaction between EBF2 and Blnc1 was partially promoted by HNRPU, although HNRPU was not necessary for assembly of this complex (238). Interestingly, transcription of Blnc1 is directly dependent on EBF2 activity, resulting in a feedback loop that impacts thermogenic differentiation (237). Concerning HNRPU, it improves formation of not only the EBF2/Blnc1 complex but also that constituted by ZBTB7B and Blnc1. Although ZBTB7B has been less studied than

ZBTB16 in adipose tissue, ZBTB7B has also been shown to participate considerably in the expression of thermogenic markers such as UCP1 and ELOVL3 (Elongation of very long chain fatty acids protein 3) (238). HNRNPU is even a mediator of lncBATE1 (brown adipose tissue-enriched lncRNA1) to preferentially activate BAT genes, forming a functional ribonucleoprotein complex (239). The family of lncRNA-BATEs also contains lncBATE10, another lncRNA implicated in BAT. In this case, lncBATE10 binds to CELF1 (CUGBP Elav-like family member 1) to displace and release PGC1-α mRNA. CELF1 is an RBP responsible for RNA degradation and translation repression, so the function of lncBATE10 is different but follows the same trend as lncBATE1; both molecules positively modulate this differentiation (240).

A large number of mitochondria contribute to thermogenesis, where PGC1-α participates in mitochondrial biogenesis through transcription factor A, mitochondrial (TFAM), implicated in mitochondrial DNA replication (241). Upregulation of PGC1-α by lncRNA AK079912, which is expressed in response to cold-induced browning, has been discussed (242).

The brown and beige adipocyte profile can also be acquired by processes such as inhibition of autophagy, without necessarily affecting adipocyte differentiation (242, 243, 244), and involving lncRNA FOXC2-AS1 (Forkhead Box C2 antisense RNA 1) to promote this phenomenon (245).

As an additional mechanism of epigenetic modification, H19 forms a complex with methyl-CpG binding domain protein 1 (MBD1) to exert transcriptional regulation, increasing the expression of BAT markers. MBD1 may use different mechanisms to modulate genetic expression (246), exerted through lysine methyltransferase (KMT) to augment trimethylation of H3K27. It was also observed in this same study that H19 recruited RNA-binding proteins at immature stage in contrast to association with chromatin modifiers in differentiated cells, hinting at other functions of H19 in thermogenesis, because H19 also increased upon cold exposure (247).

The characterizations of brown and beige adipocytes have not ignored the fact that there are also specific lncRNAs that are part of the process that gives rise to them (Fig. 6), which may be shared by both cell types in some cases (Table 4).

CHONDROGENESIS: MORE FLEXIBILITY, LESS FRICTION

Cartilage is a relevant connective tissue constituted by chondrocytes capable of producing abundant extracellular matrix (ECM), mainly type II collagen and proteoglycans to confer mechanical function (248). The tensile strength of cartilage is based on the fibrillar collagen structure, whereas proteoglycans produce osmotic pressure that resists compressive forces (249). In particular, articular cartilage exhibits different properties from the surface to deeper layers, of which MSC-like cells have been identified in superficial areas and nearby tissues such as synovium; however, the low capacity of these cells to regenerate cartilage, as well as their scarcity, has sometimes led to the study of chondrogenic differentiation in MSCs obtained from other anatomical areas (250).

Coordination of BMP2, a member of the TGF-β superfamily, and SOX9, a transcription factor upregulated by BMP2, drives chondrogenesis, while repressing osteogenesis (251). However, a precise regulation of BMP2 function is necessary, as BMP2 can also trigger chondrocyte progression to hypertrophy and even stimulate osteocyte formation after chondrogenic differentiation (252, 253). With respect to BMP receptors, downregulation of BMPR2 by miR-125b at the posttranscriptional level has been demonstrated, but lncRNA HOTAIRM1 (HOXA transcript antisense RNA myeloid-specific 1) acting as sponge on miR-125b improved BMPR2 expression and thus induced

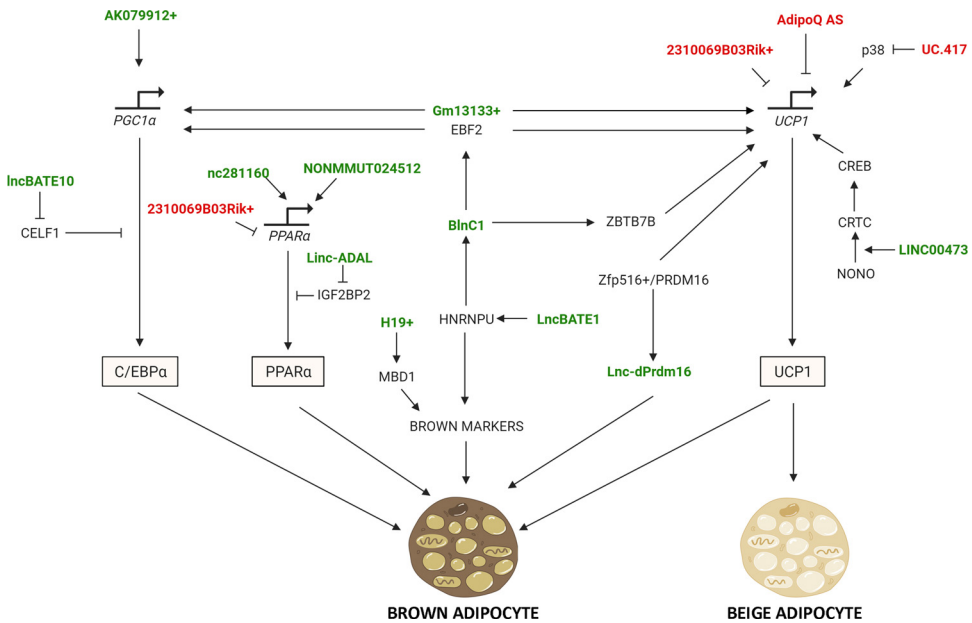

Figure 6. Adipogenesis in brown and beige adipocytes. The signaling mechanisms of adipogenic program regulated by lncRNAs are shown. Characteristic factors are indicated in boxes. The figure is divided into sequential stages toward brown or beige adipocytes. lncRNAs favor (green) or inhibit (red) markers of differentiation. lncRNAs described in both cases are also indicated (blue). Effect of lncRNA on its targets can be direct or indirect. For more details see text. See GLOSSARY for abbreviations.

Table 4. *lncRNA in brown and beige adipogenesis*

lncRNA	Genomic Classification	Adipogenesis Promote/Inhibit	Function	Direct Target	Biological Model	Differentiation Markers (technique assay)	Ref.
AK079912		Promote browning			Preadipocytes of BAT or WAT	AdipoQ, C/EBPα, Leptin, Pgc1α, PRDM16, Ucp1 (RT-qPCR), aP2, C/EBPα, Pgc1α, Ucp1 (WB) Lipids (OROS)	(242)
BATE1 ENSMUSG00000110613 Gene ID: 109215	Intergenic	Promote browning and beigeing		hnRNPU	Adipocytes of BAT, iWAT or eWAT	AdipoQ, C/EBPβ, Cidea, PPARα/γ, Pgc1α, PRDM16, Ucp1, (RT-qPCR) Pgc1α, Ucp1(WB) Lipids (OROS)	(239)
BATE10 ENSMUSG00000118229 Gene ID: 442846		Promote browning	Decoy	CELF1	Adipocytes of BAT or iWAT, 3T3-L1	AdipoQ, C/EBPα, FABP4, PPARγ (RT-qPCR) Ucp1, Pgc1α (WB) Lipids (OROS)	(240)
Blnc1 AK038898	Intergenic	Promote browning and beigeing	Scaffold	EBF2	C3H10T1/2, 3T3L1	Cox7a1, Ebf1, PPARα/γ, PRDM16, Ucp1 (RT-qPCR) FABP4, PPARγ, Ucp1 (WB) Lipids (OROS)	(237)
	Intergenic	Promote browning and beigeing		hnRNPU	C3H10T1/2	PPARγ, Ucp1 (RT-qPCR, WB) Lipids (OROS)	(353)
	Intergenic	Promote thermogenic program		hnRNPU	Brown preadipocytes	Cox7a1, Elovl3, PPARα, PPARγc1α, PRDM16, Ucp1 (RT-qPCR) ATP5A, FABP4, PPARγ, SDHB, Ucp1, UQCRC2 (WB), Lipids (OROS)	(238)
FOXC2-AS1 ENSG00000260944 NR_125795.1 Gene ID: 103752587	Antisense	Promote browning			Preadipocytes of sAT	ATGL, C/EBPα, FABP4, Ucp1, Pgc1α, PPARγ (RT-qPCR) ATGL, C/EBPα, PPARγ (WB) Lipids (OROS)	(197)
GM13133 ENSMUSG00000086565 NR_151634.1 Gene ID: 102634405	Antisense / Intronic	Promote browning			Preadipocytes of iWAT	C/EBPβ, FABP4, GLUT4, PPARγ (RT-qPCR)C/EBPβ, PPARγ2 (WB) Lipids (OROS)	(226)
H19 ENSG00000130600 NR_131224.1 Gene ID: 283120	Intergenic	Promote browning	Guide	MBD1	Brown adipocytes	AdipoQ, C/EBPα, C/EBPβ, FABP4, Leptin, PPARγ, Pgc1α (RT-qPCR) Pgc1α, Ucp1 (WB)Lipids (OROS)	(247)
LINC00473 ENSG00000112541 Gene ID: 90632	Intronic	Promote browning	Coordinate mito-chondrial fusion/ fission activity	PLIN1	Preadipocytes of scvAT or aAT	Lipids (BODIPY)	(233)
lnc-dPrdm16 (LINC00982) ENSG00000177133 NR_015440.1 Gene ID: 440556	Intergenic /divergent	Promote browning			Adipocytes of BAT, oWAT, sWAT, BWT or iWAT	AdipoQ, C/EBPβ, Cidea, Pgc1α PPARα/γ, PRDM16, Ucp1 (RT-qPCR) Pgc1α, Ucp1(WB) Lipids (OROS)	(239)
lncRN 2310069B03Rik ENSMUSG00000100291		Inhibit browning and thermogenic program			Adipocytes of iWAT	AdipoQ, FABP4, PPARγ (RT-qPCR) Lipids (OROS)	(227)
n281160, NONMMUT024512		Promote browning			Adipocyte of BAT	PPARα (RT-qPCR) Ucp1 (IF) Lipids (OROS)	(229)
uc.417		Inhibit browning			Preadipocytes of BAT	C/EBPβ, Cidea, EBF2, PPARγ2, PRDM16 (RT-qPCR) C/EBPβ, PRDM16, Ucp1 (WB)	(235)

eWAT, epididymal white adipose tissue; oWAT, omental white adipose tissue; sAT, subcutaneous adipose tissue; scvAT, supraclavicular adipose tissue) sWAT, subcutaneous white adipose tissue. See GLOSSARY for other abbreviations.

the expression of chondrocyte-related ECM components. Indirect regulation of HOTAIRM1 on BMPR2 had effects on downstream signaling proteins, including JNK, p38, and ERK (254). On the other hand, BMPR1b is also affected by lncRNAs in chondrogenesis. Specifically, corecruitment of p100 and lncRNA-HIT (HOXA transcript induced by TGF-β) to the BMPR1b locus increased its expression, through CREB binding protein (CBP), to promote H3K27 acetylation. Interestingly, not only was lncRNA-HIT identified within the HOXA locus, but lncRNA-HIT caused the expression of HOXa11 and HOXa13 (255). The Hox family is a group of key transcription factors for regulating the skeleton during development, and their involvement in adulthood has been shown (256). Since HOXa13 can regulate BMP2 and BMP7 (257), whereas HOXa11 acts upstream of RUNX2 (258), the authors have proposed lncRNA-HIT to modulate cartilage formation at early stages (255). Furthermore, increased expression of integrin α1 by HOXa13 has been demonstrated, whereby

lncRNA HOTTIP (HOXA transcript at the distal tip) is probably involved, because HOTTIP was recognized as a bidirectional transcript with HOXa13 (259). Modulation of cellular components interacting with ECM influences differentiation potential (260), so ECM may act as a modulator of chondrocyte functions (261).

Microdomains called super receptor complexes in the cell membrane are induced by BMP. These structures contain BMP receptors, repulsive guidance molecules (RGMs), and neogenin. Specifically, RGMa is expressed in chondrocytes and is recruited to lipid rafts to act as a coreceptor for BMP signaling (262). It has been predicted that RGMa mRNA can be inhibited by miR-152-3p but upregulated when lncRNA AK136902 acts as sponge on miR-152-3p. Moreover, AK136902 correlated with levels of prostaglandin F receptor (FP) (263), which is a positive regulator of BMP signaling to drive chondrocyte differentiation (264); thus the role of AK136902 is associated with modulation of BMP signaling.

SMAD5 and SMAD4, which are BMP signal transducing factors, are targets of regulation by miRNAs, where inhibition of SMAD5 and SMAD4 at the posttranscriptional level due to miRNA-145-5p and miRNA-124-3p, respectively, has been proven (265). Interestingly, it was a single lncRNA called UCA1 (urothelial cancer-associated 1) capable of repressing both miRNAs. In this report, the potential impact on several miRNAs to stimulate chondrogenesis was attributable to UCA1 (266). It is worth mentioning that UCA1 could act at an early stage of chondrogenesis, because UCA1 increased SOX9 levels (265), probably through a negative effect on miR-145, a putative target of UCA1 that directly suppresses SOX9 expression (265, 267).

SMAD4 protein abundance can also be diminished by miR-1305, but DANCR causing low levels of miR-1305 triggered SMAD4-mediated signaling. The DANCR/SMAD4 axis mainly exerted positive regulation on cell cycle genes in chondrocytes (268). In addition to SMAD4, induction of SMAD3 expression by increased stability of its corresponding mRNA as an effect of DANCR has also been demonstrated, and similarly to a previous study, DANCR improved cell proliferation, but in this case the mechanism was associated with upregulation of MYC (269). Because STAT3 mRNA was an interacting partner of DANCR and because STAT3 contributes to chondrogenic differentiation (270), SMAD3 and STAT3 were recognized as two factors mediated by DANCR to control this cellular process (269). Chondrocyte proliferation can be impaired by FGF through STAT1 signaling (271), where phosphorylation of STAT by fibroblast growth factor receptor 3 (FGFR3) has been hypothesized to induce p21 expression for cell cycle restriction (272). Nevertheless, the cellular context leading to STAT activation and the specific members involved must be known to determine its impact on differentiation. Indeed, double-stranded RNA-dependent protein kinase (PKR) was implicated in downregulation of STAT1, allowing SOX9 expression and promoting chondrogenesis (273). GRASLND (glycosaminoglycan regulatory associated long noncoding RNA) has been shown to interact with PKR, not only to increase chondrogenic markers but also to partially reverse ECM degradation in the presence of IFN-γ, probably by decreasing STAT1 and STAT2 expression (274). As for STAT2, it should be considered that, although it was detected in pathogenic conditions such as osteoarthritis (275), it might be involved downstream of H19 in promoting differentiation; thus future studies are required to corroborate it (276).

SOX9 is a key transcription factor in chondrogenesis detected during chondrocyte proliferation and differentiation (277). Long-term *cis* regulation of the SOX9 locus has been shown (278). CISTR-ACT is a DNA element classified as a *cis*-regulatory element (CRE) capable of increasing SOX9 expression, thus demonstrating spatial proximity to the chromosomal region of SOX9. CISTR-ACT encodes for lncRNA DA125942, which was proposed as an intermediate of CISTR-ACT to target protein-coding genes, because alterations in DA125942 levels led to downregulation of not only SOX9 but also parathyroid hormone-related protein (PTHrP), which is implicated in cartilage differentiation. Given that DA125942 is directly proportional to SOX9 levels in rodents but inversely related in humans, it would be interesting to elucidate the implications of DA125942 in different species (279).

A locus coding for lncRNA ROCR (regulatory of chondrogenesis RNA) was found in enhancer regions upstream of SOX9 gene, and depletion of ROCR decreased SOX9 expression. Furthermore, overexpression of ROCR had no effect on SOX9 levels, implicating *cis* regulation of SOX9 gene. Intriguingly, this same locus serves for the expression of an additional lncRNA called LINC01152, although low levels were detected in cartilage. It would be attractive to study in depth the association between these lncRNAs and how the expression of each is defined. Furthermore, SOX9-AS1 (SOX9 antisense RNA 1) was identified as another lncRNA upstream of SOX9 locus, although SOX9-AS1 appears to be involved in adipogenesis because of its induction during this process (280).

SOX5 and SOX6 are crucial factors expressed by SOX9 (281), both operating together with SOX9 to drive transcription of chondrocyte-related genes (282). Intriguingly, SOX5 and SOX6 are diminished by the action of miR-23a-3p, so the role of lncRNA SNHG5 (small nucleolar RNA host gene 5) in inhibiting miR-23a-3p is relevant to progression of differentiation, although bioinformatics analysis has postulated additional lncRNAs capable of interacting with miR-23a-3p (283).

Glucocorticoid hormones (GCs) have been one of the methods to stimulate chondrogenesis in vitro. Dexamethasone (Dex) is a synthetic GC that suppresses growth while promoting differentiation; although the mechanisms are not entirely clear, Dex has been observed to induce SCRG1 (stimulator of chondrogenesis 1) expression through activation of glucocorticoid receptor (GR), where SCRG1 acted synergistically with BMP2 downstream signaling (284). Notably, Dex can also induce differentiation into adipocytes or myoblasts, depending on specific culture conditions, but as SCRG1 prevented osteogenesis, SCRG1 does not act as a common factor in multiple differentiation (285). SCRG1 mRNA is inhibited by miR-942-5p, but lncRNA ADAMTS9-AS2 (a disintegrin and metallopeptidase with thrombospondin type 1 motif 9 antisense RNA 2) sponges on miR-942-5p, augmenting SCRG1 expression and thus improving chondrogenic markers. Moreover, miR-942-5p also reduces SOX9 levels, although it appears to be indirect, probably through SCRG1 (286).

During chondrogenic differentiation, cells are densely packed and synthesize ECM, mainly aggrecan and type II collagen, the latter accounting for ~60% of ECM. Sox9 binds

enhancer elements to activate the expression of ECM components such as COL2α1, COL11α2, and aggrecan. SOX5 and SOX6 contribute to SOX9-mediated COL2α1 transcription (281), but a role of H19 in upregulation of COL2α1 has also been demonstrated. Specifically, downstream of SOX9, the function of H19-derived miR-675 was recognized to increase COL2α1 mRNA, although the regulation of miR-675 on COL2α1 mRNA appears to be indirect (287). Remarkably, correlation between H19 and COL2α1 was observed under hypoxic conditions but not under inflammatory conditions (288).

Chondrocyte maturation and entry into chondrocyte hypertrophy is mediated by RUNX2 (289, 290). Importantly, hypertrophy is a later stage in which chondrocytes secrete type X collagen while aggrecan and type II collagen are degraded. For example, transcription of genes related to ECM degradation such as ADAMTS (A Disintegrin and Metalloproteinase with Thrombospondin Motifs) and matrix metalloproteinases (MMPs) is mediated by RUNX2 (291). H19 is able to elicit chondrogenesis while inhibiting hypertrophy mainly by downregulating RUNX2, because diminished protein levels and increased inactive form of RUNX2 protein are associated with H19 function (292), in addition to bioinformatic analysis proposing H19 as a target of SOX9 transcriptional activity (287).

On the other hand, PTHrP delays chondrocyte hypertrophy, through both RUNX2-dependent and RUNX2-independent mechanisms (293). One PTHrP function is related to cyclin-dependent kinase 1 (CDK1), which contributes to drive proliferative phase (294). Clb2 (Cyclin b2) enables CDK1 activation, but Clb2 levels are lowered by the effect of MRP, an RNase constituted by lncRNA RMRP (RNA component of mitochondrial RNA processing endoribonuclease) and protein subunits engaged in cleavage of RNA substrates, including Clb2 mRNA (295). Interestingly, RMRP may act as precursor of siRNAs such as RMRP-S1 and RMRP-S2, which seem to target skeletal development factors (296). Upregulation of RMRP upon stimulus such as BMP2 and WNT ligands has been shown to have a predominant association of RMRP with hypertrophic stage; however, not only could the role of RMRP indirectly affect cell cycle and promote SOX9 and RUNX2 expression (295) but RMRP could be involved in the maturation of ribosomal biogenesis-related rRNA for the production of extracellular matrix components in chondrocytes (297).

Evasion of chondrocyte hypertrophy depends on SOX9, as accelerated loss of function proceeds to hypertrophic cells (298). One mechanism of SOX9 to prevent hypertrophic chondrocytes is mediated by β-catenin degradation (299). WNT/β-catenin signaling not only contributes to chondrocyte hypertrophy but also promotes joint development (300, 301). The dynamic involvement of β-catenin throughout chondrogenesis is complex, where exacerbation or suppression of activity results in defects in chondrocyte formation and maturation, partially explaining the contradiction in evidence on the relationship between β-catenin and chondrogenesis (302). For example, upregulation of β-catenin by inhibiting GSK3, an antagonist of β-catenin stability, has been shown to promote chondrogenic differentiation (303). The β-catenin degradation complex includes AXIN, a scaffold protein that can be sequestered by ZEBD3 to disassemble complex and augment β-catenin levels. ZEBD3 expression appears to be increased by its antisense lncRNA ZEBD3-AS1 (ZEBD3 antisense RNA 1), because ZEBD3-AS1 increased chondrogenic markers and its effects were reversed in the presence of DKK1, a WNT pathway inhibitor, even leading to diminished SOX9 expression. In this same study, WNT3a promoted nuclear translocation of β-catenin, whereas higher levels of SOX9 were detected (304). Another report corroborated the upregulation of ZEBD3-AS1 during chondrogenesis, and an increased expression of an additional lncRNA called CTA-941F9.9 was demonstrated, although the function of both lncRNAs was not evaluated (305). Meanwhile, β-catenin can be inhibited through phosphorylation by SOX9 within the nucleus (299) and ubiquitination mediated by E3 ligases beta-transducin repeat containing E3 ubiquitin protein ligase (βTrCP), constitutive photomorphogenesis protein 1 (COP1), and SMAD ubiquitination regulatory factor 1 (Smurf1), when the contribution of TRIB2 (tribbles pseudokinase 2) has been established (306). The role of TRIB2 in chondrogenesis has been demonstrated in recent studies, although TRIB2 is widely described more in cancer cells than normal cells (305, 306). lncRNA MEG3 caused epigenetic silencing of TRIB2 gene through promoter methylation of H3K27 by EZH2 recruitment. Indeed, MEG3 impaired chondrogenic differentiation (307), and since TRIB2 has been shown to improve YAP stability, it is likely that the effect of MEG3 may affect beyond β-catenin (306).

Furthermore, DANCR acted downstream of SOX4 as a positive regulator of chondrogenesis, and because β-catenin mRNA stability due to interaction with DANCR has been observed in cancer cells, β-catenin is involved in the mechanism of DANCR (307, 308). Although several studies argue that DANCR favors chondrogenic differentiation, an opposite function has also been described. In this case, EZH2-associated DANCR results in reduced expression of chondrogenic markers including SOX9. However, the enhancement of DANCR on proliferation was consistent with other studies, but it remains to be seen whether the contrasting results on differentiation are due to cellular context or culture conditions (310).

Cartilage turnover is not only achieved because of the production of ECM components but must also be synchronized with their degradation. For example, ADAMTS-5 is engaged to cleave aggrecan, which is the major proteoglycan in articular cartilage; however, an exacerbated activity of this enzyme leads to joint damage (311). Reduced levels of ADAMTS-5 were detected during the progression of chondrogenic differentiation. To halt ADAMTS-5 expression and thus its function, miR-27b-3p reduced ADAMTS-5 mRNA, but downregulation of miR-27b-3p by lncRNA XIST (X-inactive specific transcript) was able to cause an increase in ADAMTS-5 levels, leading to impaired differentiation and increased apoptosis of chondrocytes (312). Aggrecan may also be a target for MMP13-mediated degradation (313). The mRNA and protein of MMP13 can be diminished by the action of miR-204-5p, but inhibition of miR-204-5p by UCA1 exerts a positive effect on MMP-13 to decrease levels of type II collagen and type IV collagen (314). The relationship between MMP-13 and chondrocyte-associated functions has been explored, where MMP-13 promotes SOX9 expression and stimulates proliferation. Although MMP-13 expression was reduced by miR-1275, suppression of DANCR on miR-

1275 enabled the supportive function of MMP-13 (315). Intriguingly, MMP13 is classified as a collagenase (316), but deletion of MMP13 reversed the positive regulation of DANCR on type II collagen mRNA levels, so it remains to be known what the role of MMP13 in this mechanism (315).

MMP13 is the most referenced MMP in the hypertrophic chondrocyte stage, but other members that also participate in ECM degradation have been explored (289). For example, chondrocytes impair hypertrophy and cartilage formation by overexpression of HOXc8, including diminished levels of MMP13 and MMP9 (317, 318). DLX5 was identified as a binding partner of HOXc8 to stimulate HOXc8 recruitment to promoter of lncRNA LINC01013 and repress transcription. Because LINC01013 impedes differentiation, the role of DLX5 and HOXc8 improved chondrogenic potential (319). Interestingly, DLX5 was detected in proximity to BMP2 and BMP4 loci, reinforcing the evidence for its action on BMP signaling (320). Otherwise, cartilage degradation is also induced in the presence of inflammatory stimuli such as IL-1β, which support C-C motif chemokine ligand 3 (CCL3) chemokine expression. This phenomenon was improved when CCL3 levels were augmented by lncRNA HOTTIP targeting miR-455-3p to release CCL3 mRNA (321).

The signaling mechanisms that precede chondrocytes are less divergent compared with other types of differentiation. However, it is clear that lncRNAs continue to fill the gap that remains in our understanding of this phenomenon (Fig. 7), and despite being closely related to hypertrophy, it is molecular markers of differentiation assessed in each study that could reveal the impact of each lncRNA more appropriately (Table 5).

THIS IS THE WAY: lncRNAs AS GUIDES IN CELL FATE

The function of lncRNAs has been described from early stages of differentiation, where experimental evidence supports their involvement in decision making toward one or more specific lineages, providing a guideline to discuss the findings on this topic. In general, we have mainly relied on reports addressing a single lncRNA on the induction of various types of differentiation performed in the same study, as well as mentioning different studies around the same lncRNA, even though the cells are not necessarily equivalent in the latter case but allow us to glimpse cellular commitment as a process accompanied by specific lncRNAs.

Our understanding of lncRNAs within the dynamics of cell transcriptomic changes during differentiation has been achieved by techniques such as microarrays and RNA sequencing (RNA-seq). However, data integration taking into account two or more types of differentiation is scarce. One study focused on adipogenesis, chondrogenesis, and osteogenesis, where signaling pathways and key factors were classified as shared or lineage specific (322). Nevertheless, myogenesis has also been considered, in which differentially expressed lncRNAs were identified in C2C12 and 3T3-L1 cells, cell lines recurrently used to assess myogenic and adipogenic differentiation, respectively. Remarkably, lncRNAs were organized into clusters within genomic domains, proving coregulation and designating them the name of transcription open domains (TODs). Thousands of intergenic lncRNAs were altered, but only 39 lncRNAs were common between myogenesis and adipogenesis, corroborating the existence of two classes of lncRNAs: shared or exclusive to one type of differentiation (323). Consistent with this idea, SRA is a shared lncRNA that promotes myogenesis and adipogenesis by enhancing the transcriptional activity of MYOD or PPARγ (63). Conversely, in negative regulation, SIRT1 has been reported to restrict adipogenesis and myogenesis (52). Meanwhile, Malat1 could induce another type of differentiation upon myogenesis, because Malat1 led to epigenetic repression of myogenic genes (57) and was related to OSX expression (142), but it has been claimed that Malat1 also contributes to myogenesis; therefore this role remains to be

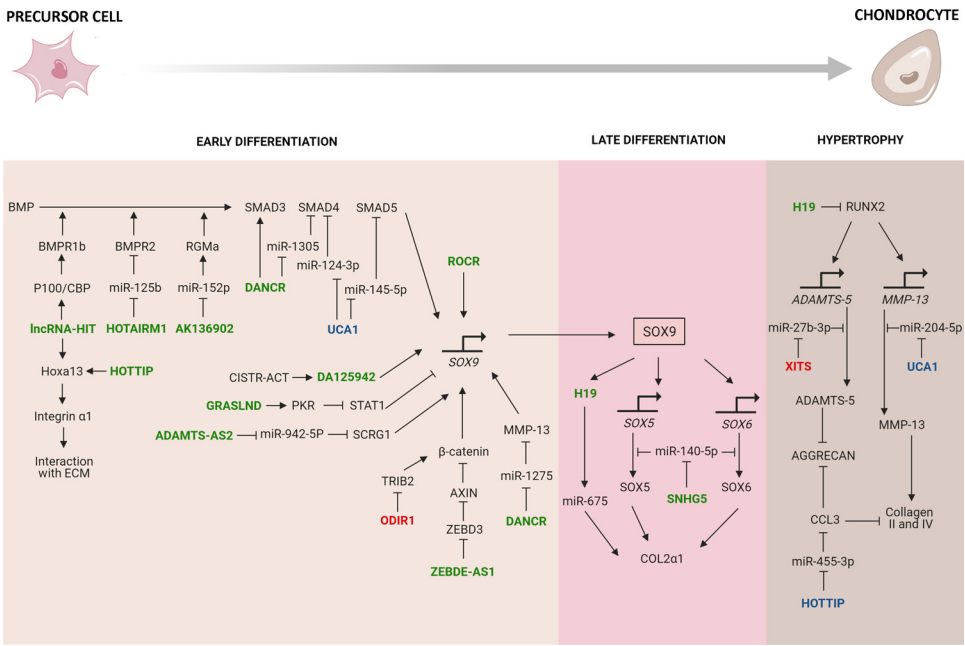

Figure 7. Chondrogenesis. The signaling mechanisms of chondrogenic program regulated by lncRNAs are shown. Key transcription factors are indicated in boxes. The figure is divided into sequential stages toward chondrocytes. lncRNAs favor (green) or inhibit (red) markers of differentiation. lncRNAs described in both cases are also indicated (blue). Effect of lncRNA on its targets can be direct or indirect. For more details see text. See GLOSSARY for abbreviations.

Table 5. *lncRNA in chondrogenesis*

lncRNA (synonym)	Genomic Classification	Chondrogenesis-Promote/Inhibit	Function	Direct Target	Biological Model	Differentiation Markers (technique assay)	Ref.
50450 +, 37692 +, 16667 +, Gm6166 + +, Gm14328 + +, Gm13998 + +		+ Promote chondrogenesis + + Promote hypertrophy			C3H10T1/2	SOX9, COL2a1, RUNX2, COL10a1 (WB) Proteoglycans (SOS, ABS)	(354)
ADAMTS9-AS2 ENSG00000241684 NR_038264.1 Gene ID: 100507098	Antisense	Promote	Sponge of miRNA	miR-942-5p	BMSC	SOX9, COL2a1 (RT-qPCR) Proteoglycans (ABS)	(286)
AK136902	Antisense	Promote			ATDC5	ACAN, COL2a1, SOX9, RUNX1, COL10a1 (RT-qPCR, WB) Proteoglycans (ABS)	(263)
ANCR ENSG00000226950 Gene ID: 57291 NR_145129.1	Intergenic	Inhibit		EZH2	LF-MSC	ACAN, COL2, SOX9 (RT-qPCR, WB) Calcium deposits (ARS, VKS) Proteoglycans (TBS) Elastic fibers (EVGS)	(310)
DA125942 ENSG00000260492 NR_104332.1 Gene ID: 102216268			Guide*	PTHLH and SOX9 locus	C28/12, ATDC5		(279)
DANCR ENSG00000226950 NR_145129.1	Intergenic	Promote			S-MSC	ACAN, SOX9, COL2 (RT-qPCR) Proteoglycans (TBS, SOS)	(309)
Gene ID: 57291	Intergenic	Promote		mRNA of MYC, STAT3 and SMAD3	S-MSC	SOX9, AGC1, COL2 (RT-qPCR)	(329)
	Intergenic	Promote	Sponge of miRNA	miR-1305	S-MSC	SOX9 (RT-qPCR)GAG content (BA)	(268)
	Intergenic	Promote	Sponge of miRNA	miR-1275	SF-MSC	S0X9, COL2 (RT-qPCR, WB) GAG (BA) Calcium deposits (ARS)	(315)
GRASLND ENSG00000228203 Gene ID: 386597	Antisense	Promote		EIF2AK2 (PKR)	BMSC, ADSC	SOX9, COL2a1, ACAN (RT-qPCR)GAG (BA) Proteoglycans (SOS)	(274)
H19 ENSG00000130600	Intergenic		Source of miR-675		HAC	ACAN, COL2a1 (RT-qPCR)	(287)
NR_131224.1 Gene ID: 283120	Intergenic	Promote			ADSC	ACAN, COL2 (RT-qPCR, WB) Cell morphology (M) Proteoglycans (ABS)Calcium deposits (ARS)	(276)
H19 ENSG00000130600	Intergenic		Source of miR-675		Chondrocytes	COL2a1 (RT-qPCR)	(288)
NR_131224.1 Gene ID: 283120	Intergenic	Promote		RUNX2	BMSC, C3H10T1/2	COL2a, ACAN, SOX9, MMP13, Adamts5, Runx2 (RT-qPCR)	(292)
HOTAIRM1 ENSG00000233429 NR_038366.1 Gene ID: 100506311	Intergenic	Promote		miR-125b	MSC	ACAN, COL2, COL10 (RT-qPCR, WB)	(254)
HOTTIP ENSG00000243766	Antisense and bidirectional*			HOXA13 gene*	Chondrocytes	Proteoglycans (ABS)	(259)
NR_037843.3 Gene ID: 100316868	Antisense andbidirectional*		Sponge of miRNA	miR-455-3p	BMSC, PHC	ACAN, CCL3, COL2a1, COL10a1, MMP3, MMP13, RUNX2, SOX9 (RT-qPCR, WB)	(321)
linc-ROR ENSG00000258609 NR_152602.1 Gene ID: 100885779	Intergenic	Promote	Sponge of miRNA	miR-138, miR-145	BMSC	COL2 (IHC) ACAN, COL2a1, SOX9 (RT-qPCR, WB) Proteoglycans (SOS, ABS)	(326)
LINC01013 ENSG00000228495 NR_038981.1 Gene ID: 100507254	Intergenic	Inhibit			SCAP	COL2, COL5, SOX9 (RT-qPCR). Collagen fibers (PSRS) Proteoglycans (ABS)	(319)
lncRNA-HIT ENSMUSG00000102373 Gene ID: 77395		Promote	Guide	p100	Limb mesenchyme tissues	COL2a1 (RT-qPCR) Proteoglycans (ABS)	(255)
MEG3 ENSG00000214548 NR_046467.1 ID: 55384	Intergenic	Inhibit	Guide	EZH2	S-MSC	ACAN, COL2a1 (WB, IF) Proteoglycans (ABS) Calcium deposits (ARS)	(307)

Continued

Table 5.— *Continued*

lncRNA (synonym)	Genomic Classification	Chondrogenesis-Promote/Inhibit	Function	Direct Target	Biological Model	Differentiation Markers (technique assay)	Ref.
RMRP ENSG00000269900 NR_003051.3 Gene ID: 6023	Bidirectional	Promote			ATDC5	ACAN, BAPX1, COL2a1, RUNX2, MEF2C, COL10a1 (RT-qPCR) Calcium deposits (ARS) ALP activity (APA)	(295)
ROCR ENSG00000228639 NR_110876.1 Gene ID: 102723505	Antisense			SOX9	BMSC, HAC	COL2a1, ACAN (RT-qPCR) Calcium deposits (ARS)	(280)
SNHG5 ENSG00000203875 NR_003038.2 Gene ID: 387066	Intergenic	Promote	Sponge of miRNA	miR-23a-3p	ADSC	ACAN, COL2a1, SOX9 (RT-qPCR, WB) Proteoglycans (ABS)	(283)
UCA1 ENSG00000214049 NR_015379.3 Gene ID: 652995	Intergenic	Promote	Sponge of miRNA	miRNA-145-5p, miRNA-124-3p	BMSC	ACAN, COL2, SOX9 (RT-qPCR, WB) Proteoglycans (ABS, TBS)	(266)
	Intergenic	Promote			BMSC, HCS-2/8, SaOS-2	ACAN, CCN, COL2a1 (RT-qPCR) Proteoglycans (SOS)	(265)
	Intergenic	Promote	Sponge of miRNA*	miR-204-5p*	C28/I2	-	(314)
XIST ENSG00000229807 NR_001564.2 Gene ID: 7503	Intergenic	Inhibit	Sponge of miRNA*	miR-27b-3p	S-MSC	ACAN, COL2a1, SOX9 (RT-qPCR, WB) Proteoglycans (ABS)	(312)
ZBED3-AS1 ENSG00000250802 NR_024398.1 Gene ID: 728723	Intronic, antisense and divergent	Promote	Modulator*	mRNA of ZBED3*	SF-MSC	SOX9, COL2 (RT-qPCR, WB) COL2 (IHS) Proteoglycans (ABS, SOS) GAG (BA)	(304)
ZBED3-AS1 ENSG00000250802 NR_024398.1 Gene ID: 728723	Divergent				BMSC	ACAN, COL2, SOX9(RT-qPCR, IHS) Proteoglycans (ABS)	(305)
CTA-941F9.9 ENSG00000238120 NR_131244.1 Gene ID: 100506737	Intronic				BMSC		

ABS, Alcian blue staining; BA, biochemical assay; EVGS, elastica van Gieson staining; HAC, human articular chondrocyte; IHC, immunohistochemistry; LF-MSC, ligament fluid-derived MSC; PHC, primary human chondrocyte; PSRS, Picro Sirius red staining; SCAP, stem cell from apical papilla; S-MSC, synovium-derived MSC; SOS, safranin O staining; TBS, toluidine blue staining. *Suggested by the authors of the study. See GLOSSARY for other abbreviations.

tested (58, 75). AK017368 is an additional candidate to encourage another type of differentiation at the expense of inhibiting myogenesis, since AK017368 proceeds as a sponge of miR-30c (82), which belongs to the miR-30 family described by downregulation of RUNX1, a positive regulator of chondrogenesis and osteogenesis; thereby AK017368, by hampering myogenesis, could trigger chondrocyte or osteocyte formation (324).

Concerning osteocytes, they can originate after chondrocytes sequentially during endochondral ossification, which could explain why certain mechanisms are shared to give rise to both cell types (325). One example is UCA1, which was relevant for both chondrogenic and osteogenic markers (265). Similarly, linc-ROR promoted the formation of osteocytes (115) and chondrocytes (326). In contrast, XIST diminished both osteogenesis (327) and chondrogenesis (312). Within lncRNAs that collaborate in one of these differentiations while inhibiting the other, ANCR is the most widely described, blocking osteogenesis by either modulating epigenetic modifiers to silence transcription of RUNX2 (86) or through signaling factors such as GSK3β (122). NOTCH (328), p38 (104), and FOXO1 (125), while stimulating chondrogenesis by upregulating SOX9 expression through SMADs (267, 328) or MMP13 (315). However, it remains to be known whether the report that ANCR functioned as a negative modulator of SOX9 was a specific feature of the tissue examined (310).

Selection for commitment between adipogenic and osteogenic lineage has received great interest because of its implications in pathological conditions (330). KCNQ1OT1 stimulates both osteogenesis and adipogenesis (95). Conversely, it has been observed that ANCR might be impeding not only the formation of osteocytes but also the emergence of adipogenic markers (84, 87); however, KCNQ1OT1 and ANCR probably have a broader role in these cellular contexts, because the progenitor cells possess mechanisms responsible for eliciting adipogenesis and evading osteogenesis after commitment, in which HoxAS-3 (85), HOTAIR (99, 330, 331), and MIR31HG are involved (213, 332). In contrast, prompting osteogenesis and restraining adipogenesis have been linked to PGC1β-OT1 (Peroxisome proliferator-activated receptor γ coactivator-1β-OT1) (334) and TCONS_00041960 (129). Particularly, TCONS_00041960 inhibited two miRNAs, miR-204-5p and miR-125a-3p, repressors of RUNX2 and GILZ expression, respectively, allowing upregulation of these positive factors of osteogenesis (129). Under the same trend, MEG3 has been shown to repress adipogenesis and trigger osteogenesis (140), which designates its involvement in cell fate targeting, albeit

MEG3 is possibly specific to the biological model employed, since MEG3 has been demonstrated to negatively regulate differentiation to osteocytes in some circumstances. (88, 109, 130).

Functional lncRNAs have been found to be enriched in genomic regions surrounding important transcription factors during development, suggesting a direct association due to position (335). Nonetheless, this phenomenon may be versatile, as exceptions have emerged. For example, SOX9 is a key factor for chondrogenic differentiation, and SOX9-AS1 variants were identified at a proximal site to the SOX9 locus. Although SOX9-AS1 levels were increased in chondrogenesis, SOX9-AS1 depletion reduced adipogenic genes, whereas it had no effect on cartilaginous disk development, so despite being located in close proximity to the SOX9 gene, the role of SOX9-AS1 is more direct to adipogenesis than chondrogenesis (280).

As outlined above, deepening our knowledge of lncRNAs has unveiled a role of "fine-tuner" of cell fate (336). However, it has also been detected that the levels of lncRNAs can be of paramount importance in activating the differentiation program, even making alteration of their levels, rendering in vitro induction by the medium dispensable (126, 178, 214, 332, 333).

The change in expression of lncRNAs does not necessarily reflect the type of control they exert throughout differentiation, so it is essential to evaluate differentiation markers to establish this. At this point, the effects of lncRNAs on multiple types of differentiation are far from being elucidated, and only a few reports have entered this less explored field. To cite one example, MEG3 overexpression was shown to stimulate osteogenesis and chondrogenesis, whereas adipogenesis was decreased and there was no effect on myogenesis (89). Another study showed that knockdown of Rmst (Rhabdomyosarcoma 2 associated transcript) reduced adipogenic, chondrogenic, and osteogenic markers (337). As research progresses, the impact of lncRNAs to drive toward a specific cell type will be elucidated, as comparing different cell contexts represents a disadvantage for certain lncRNAs. Similarly, H19 is the example that reveals the trajectory traced by the mechanisms of lncRNAs to be discovered, because H19 has been widely described in many processes, both normal and pathological, to the point of being the only one mentioned in all four types of differentiation discussed in this review. The versatile functions of H19 and the range of interacting partners associated with it show our awareness of the remaining lncRNAs as limited but at the same time promising.

CONCLUSIONS

Application of technologies of sequencing and transcriptome analysis has consolidated the lncRNAs as fundamental orchestrators of biological processes, within which differentiation is not the exception. A great deal of knowledge has been gained about the precursor cells, which has progressed in association with lncRNAs during recent years, expanding the list of identified lncRNAs. The signaling mechanisms regulated by lncRNAs lay the foundation for a field that is simultaneously complex and fascinating. Function of lncRNAs is recognized in stages throughout differentiation such as choice of cell fate, changes in expression profile, and acquisition of new functions.

It should be noted that lncRNAs are still less described than other noncoding RNAs such as miRNAs, but the influence of lncRNAs is evidently versatile in differentiating. However, progress has been made in what we know about lncRNAs, and therefore a better understanding of physiological alterations is conceivable. In addition, new proposals of their use in clinical trials can be rethought, considering the differentiation from the perspective of lncRNAs.

The description of the type of regulation of lncRNAs on the main types of mesenchymal differentiation makes it feasible to serve as a basis for other cells and other types of differentiation. It may even be harnessed for more efficient use in targeting therapies and treatments against diseases related to this process.

Finally, studies on the modes of action of lncRNAs strengthen the idea of how revolutionary these molecules have turned out to be, as the actual scenario only represents the tip of an iceberg.

GLOSSARY

aAT	Abdominal adipose tissue
ABS	Alcian blue staining
ADAMTS	A Disintegrin and Metalloproteinase with Thrombospondin Motifs
ADAMTS9-AS2	A disintegrin and metallopeptidase with thrombospondin type 1 motif 9 antisense RNA 2
ADINR	Adipogenic differentiation induced noncoding RNA
ADNCR	Adipocyte differentiation-associated long noncoding RNA
ADSC	Adipose-derived stem cell
AGPAT2	1-Acylglycerol-3-Phosphate O-Acyltransferase 2
AKT	V-akt murine thymoma viral oncogene homolog
ALP	Alkaline phosphatase
ANCR	Antidifferentiation noncoding RNA
ANRIL	Antisense noncoding RNA in the INK4 locus
APA	Alkaline phosphatase assay
ARS	Alizarin Red S staining
AS	Alkaline phosphatase staining
ASMER	Adipocyte-specific metabolic-related lncRNA
BA	Biochemical assay
BAT	Brown adipose tissue
Blnc1	Brown fat enriched lncRNA 1
BM	Bone marrow
BMNCR1	Bone marrow stem cell-related lncRNA
BMSC	Bone marrow-derived stem cells
BODIPY	Boron-dipyrromethene
BRG-1	Brahma-Related Gene 1
C/EBPC	CAAT/enhancer-binding protein
CAAlnc1	Cachexia-related antiadipogenesis lncRNA 1
CB	Perinatal cord blood
CBFA1	Core-binding factor subunit alpha-1
CBFB	core-binding factor subunit beta
CBP	CREB binding protein
CCL3	C-C motif chemokine ligand 3
CDC42	Cell division control protein 42
CDK1	Cyclin-dependent kinase 1

CE	Core Enhancer
CELF1	CUGBP Elay-like family member 1
Charme	Chromatin architect of muscle expression
Clb2	Cyclin b2
Clk1	Cdc2-like kinase 1
CME	Core Muscle Enhancer
COLI	Type I collagen
COP1	Constitutive photomorphogenesis protein 1
CRE	*cis*-regulatory element
CREB	Cyclic AMP-responsive element binding protein
Crnde	Colorectal neoplasia differentially expressed
CRTC	CREB-regulated transcription coactivator
CTGF	Connective tissue growth factor
CUL3	Cullin 3
DANCR	Differentiation-antagonizing noncoding RNA
DEPTOR	DEP domain-containing mTOR interacting protein
Dex	Dexamethasone
DFSC	Dental follicle stem cell
DLX5	Distal-less Homeobox 5
DNMT1	DNA methyltransferase 1
DPC	Dental pulp cell
DPPA2	Developmental Pluripotency Associated 2
DPSC	Dental pulp stem cell
DRR	Distal Regulatory Region
Dum	DPPA2 upstream binding muscle lncRNA
EBF2	Early B cell factor
ELOVL3	Elongation of very long chain fatty acids protein 3
ENCODE	Encyclopedia of DNA Elements
EVGS	Elastica van Gieson staining
eWAT	Epididymal white adipose tissue
EZH2	Enhancer of Zeste Homolog 2
FABP4	Fatty Acid Binding Protein 4
FAP	Fibro-adipogenic progenitor
F-AS	F-actin staining
FGFR3	Fibroblast growth factor receptor 3
FIRRE	Functional intergenic repeating RNA element
FLNA	Filamin A
FOXC2-AS1	Forkhead Box C2 antisense RNA 1
FOXO1	Fork box transcription factor
FP	Prostaglandin F receptor
GAG	Glycosaminoglycan
GAS5	Growth Arrest-Specific transcript 5
gAT	Gluteal adipose tissue
GC	Glucocorticoid hormone
GR	Glucocorticoid receptor
GRASLND	Glycosaminoglycan regulatory associated long noncoding RNA
GSK3-β	Glycogen synthase kinase 3-beta
HAC	Human articular chondrocyte
HCGII	Human leukocyte antigen complex group II
HDAC1	Histone deacetylase 1
HIT	HOXA transcript induced by TGF-β
HMGA2	High-mobility group AT-hook 2
hnRNPI	Heterogeneous nuclear ribonucleoprotein I
HNRNPU	Heterogeneous nuclear ribonucleoprotein U
HOTAIR	HOX transcript antisense intergenic RNA
HOTAIRM1	HOXA transcript antisense RNA myeloid-specific 1
HOTTIP	HOXA transcript at the distal tip
HoxA-AS3	HoxA antisense transcript 3
HuR	Hu antigen R
ID	Inhibitor of DNA binding
IF	Immunofluorescence staining
IGF	Insulin-like growth factor
IHC	Immunohistochemistry
IHS	Immunohistochemical staining
IMP	Igf2 mRNA-binding protein
IS	Immunostaining
ISCT	International Society for Cellular Therapy
iWAT	Inguinal white adipose tissue
KMT	Lysine methyltransferase
LCoR	Ligand-dependent corepressor
LEF	Lymphoid enhancer factor
LF-MSC	Ligament fluid-derived MSC
linc-ADA	LlincRNA for adipogenesis and lipogenesis
linc-RAM	linc-RNA activator of myogenesis
linc-ROR	Long intergenic nonprotein coding RNA, regulator of reprogramming
linc-smad7	Long intergenic noncoding RNA smad7
Lin-NFE2L3-1	Long intergenic noncoding RNA-nuclear factor, erythroid 2-like 3-1
lncBATE	Brown adipose tissue-enriched lncRNA
lnc-mg	Myogenesis-associated lncRNA
lncMUMA	Mechanical unloading-induced muscle atrophy-related lncRNA
lncMyoD	lncRNA upstream of Myod1 gene
lnc-OAD	lncRNA associated with osteoblast and adipocyte differentiation
lnc-ORA	Obesity-related lncRNA
lncRNA	Long noncoding RNA
lncRNA-HIT	HOXA transcript induced by TGF-β
LPL	Lipoprotein lipase
LSD1	Lysine-Specific Demethylase 1
M	Microscopy
m1/2-sbsRNA1	mouse 1/2-Staufen-binding site RNA 1
MACF	Microtubule actin cross-linking factor 1
Malat1	Noncoding metastasis-associated lung adenocarcinoma transcript 1
MAR1	Muscle anabolic regulator 1
MBD1	Methyl-CpG binding domain protein 1
MCE	Mitotic clonal expansion
MEF2	Myocyte Enhancer Factor 2
MEG3	Maternally expressed gene 3
MEK	Mitogen-activated protein kinase kinase
Men	Multiple endocrine neoplasia
MGLL	Monoacylglycerol lipase
MIR31	HGmiR-31 host gene
MLC	Myosin light chain
MLL3/4	Mixed-lineage leukemia 3/4
MMP	Matrix metalloproteinase
MOB	Mouse normal diploid osteoblast
MODRMS	MSC osteogenesis differentiation-related lncRNA
MRF	Myogenic regulatory factor
MSC	Mesenchymal stromal cell
MSMSC	Maxillary sinus membrane stem cell
MSX1	Msh homeobox 1
Msx1-AS	Msx1 antisense RNA
mTORC1	Mammalian target of rapamycin complex 1
MU	Skeletal muscle
MUNC	MyoD upstream noncoding

MYF5	Myogenic factor 5
MyHC3	Myosin heavy chain 3
MYOD	Myoblast Determination
MYOG	Myogenin
NCoR	Nuclear receptor corepressor
ncRNA	noncoding RNA
NEAT1	Nuclear-Enriched Abundant Transcript 1
NFAT	Nuclear factor of activated T cells
NF-YA	Nuclear transcription factor Y subunit alpha
NRS	Nile red staining
NUPR1	Nuclear protein 1, transcriptional regulator
N-WASP	Neural Wiskott–Aldrich syndrome protein
OCN	Osteocalcin
ODIR1	Osteogenic differentiation inhibitory regulator 1
OROS	Oil Red O staining
oWAT	Omental white adipose tissue
PA1PAXI	P1-associated glutamate-rich protein 1
PANDA	p21-Associated ncRNA DNA Damage-Activated
Paral1P	PARγ-activator RBM14-associated lncRNA
PAX7	Paired Box 7
PCAT1	Prostate cancer-associated ncRNA transcript 1
PDLC	Periodontal ligament cell
PDLSC	Periodontal ligament stem cell
PE	Periosteum
PGC1α	Phosphatidylglycerol phospholipase alpha
PGC1β-OT1	Peroxisome proliferator-activated receptor γ coactivator-1β-OT1
PHC	Primary human chondrocyte
PKR	Double-stranded RNA-dependent protein kinase
PLIN	Perilipin
PMMA	Polymethylmethacrylate
POIRp	PDLSC osteogenesis impairment-related lncRNA
PPARγ	Peroxisome proliferator-activated receptor-gamma
PRC1/2	Polycomb Repressive Complex 1 and 2
PRDM16	PR-domain containing protein 16
PRNCR1	Prostate cancer noncoding RNA 1
PRR	Proximal Regulatory Region
PSRS	Picro Sirius red staining
PTBP1	Polymyridine tract binding protein 1
PTEN	Phosphatase and tensin homolog
PTHLH	Parathyroid hormone-like hormone
PTHrP	Parathyroid hormone-related protein
PVT1lnc	RNA homologous to plasmacytoma variant translocation gene
RAC1	Rac family small GTPase 1
RAP-1	Regulated in Adipogenesis 1
RBM14	RNA binding motif protein 14
RBP	RNA binding proteins
RGM	Repulsive guidance molecule
RMRP	RNA component of mitochondrial RNA processing endoribonuclease
Rmst	Rhabdomyosarcoma 2 associated transcript
ROCK1	Rho-associated coiled-coil containing protein kinase 1
ROCR	Regulatory of chondrogenesis RNA
RT-qPCR	Reverse transcription-quantitative PCR
RUNX2	Runt-related transcription factor 2
sAT	Subcutaneous adipose tissue
SATB2	Special AT-rich sequence-binding protein 2
SCAP	Stem cell from apical papilla
SCRG1	Stimulator of chondrogenesis 1
SC	Satellite cell
scvAT	Supraclavicular adipose tissue
SF-MSC	Synovial fluid-derived MSC
SFRS5	Serine- and Arginine-Rich Splicing Factor 5
SIRT1	Sirtuin 1
SKP2	S-phase kinase-associated protein 2
slinc	Superlong intergenic noncoding
slincRAD	Superlong intergenic noncoding RNA functioning in adipocyte differentiation
SMDST	AU1-mediated mRNA decay
SMRT	Silencing mediator of retinoid and thyroid hormone receptors
S-MSC	Synovium-derived MSC
Smurf1	SMAD ubiquitination regulatory factor 1
SNHG5	Small nucleolar RNA host gene 5
SOS	Safranin O staining
SOX9	SRY-box transcription factor 9
SOX9-AS1	SOX9 antisense RNA 1
SP	Spectrophotometry
SR	Serine- and arginine-rich
SRA	Steroid receptor RNA activator
SRAP	SRA protein
SREBP1	Sterol regulatory element binding protein 1
SRF	Serum response factor
STAU1	Staufen Double-Stranded RNA Binding Protein 1
SUZ12	Suppressor of Zeste 12
sWAT	Subcutaneous white adipose tissue
SYISL	SYNPO2 intron sense-overlapping lncRNA
TARDBP	TAR DNA binding protein
TAZ	Tafazzin
TBP	TATA binding protein
TBS	Toluidine blue staining
TC1	Thyroid cancer protein 1
TCF	T-cell factor
TFAM	Transcription factor A, mitochondrial
TGF-β	Transforming growth factor beta
TINCR	Terminal differentiation-induced ncRNA
TLR4	Toll-like receptor 4
TMEM18	Transmembrane protein 18
Tnrc6a	Trinucleotide repeat-containing 6A
TOD	Transcription open domain
TRIB2	Tribbles pseudokinase 2
TSC	Tendon stem cell
TUG1	Taurine upregulated gene 1
UCA1	Urothelial cancer-associated 1
UC-MSC	Umbilical cord-derived MSC
UCP-1	Uncoupling protein-1
VAT	Visceral adipose tissue
VKS	Von Kossa staining
WAT	White adipose tissue
WB	Western blot
XIST	X-inactive specific transcript
Yam-1Y	Y1-associated muscle lncRNA 1
YB-1	Y-box binding protein 1
ZBTB16	Zinc finger and BTB domain-containing protein
ZEBD3-AS1	ZBED3 antisense RNA 1
Zfp516	Zinc finger protein 516
βTrCP	Beta-transducin repeat containing E3 ubiquitin protein ligase

GRANTS

This study was supported by Consejo Nacional de Ciencia y Tecnología [M.A.D.-H.: 270150 (CVU:441075) and M.A.S.-S. (CVU:550337)].

DISCLOSURES

No conflicts of interest, financial or otherwise, are declared by the authors.

AUTHOR CONTRIBUTIONS

M.A.D.-H., M.A.S.-S., J.M.-Z., and V.M.-L. conceived and designed research; M.A.D.-H., M.A.S.-S., and J.M.-Z. prepared figures; M.A.D.-H., M.A.S.-S., J.M.-Z., and V.M.-L. drafted manuscript; M.A.D.-H., M.A.S.-S., J.M.-Z., and V.M.-L. edited and revised manuscript; M.A.D.-H., M.A.S.-S., J.M.-Z., and V.M.-L. approved final version of manuscript.

REFERENCES

1. **Alexander RP**, **Fang G**, **Rozowsky J**, **Snyder M**, **Gerstein MB.** Annotating non-coding regions of the genome. *Nat Rev Genet* 11: 559–571, 2010. doi:10.1038/nrg2814.
2. **Deniz E**, **Erman B.** Long noncoding RNA (lincRNA), a new paradigm in gene expression control. *Funct Integr Genomics* 17: 135–143, 2017. doi:10.1007/s10142-016-0524-x.
3. **Iyer MK**, **Niknafs YS**, **Malik R**, **Singhal U**, **Sahu A**, **Hosono Y**, **Barrette TR**, **Prensner JR**, **Evans JR**, **Zhao S**, **Poliakov A**, **Cao X**, **Dhanasekaran SM**, **Wu YM**, **Robinson DR**, **Beer DG**, **Feng FY**, **Iyer HK**, **Chinnaiyan AM.** The landscape of long noncoding RNAs in the human transcriptome. *Nat Genet* 47: 199–208, 2015. doi:10.1038/ng.3192.
4. **Rinn JL**, **Chang HY.** Genome regulation by long noncoding RNAs. *Annu Rev Biochem* 81: 145–166, 2012. doi:10.1146/annurev-biochem-051410-092902.
5. **Brosnan CA**, **Voinnet O.** The long and the short of noncoding RNAs. *Curr Opin Cell Biol* 21: 416–425, 2009. doi:10.1016/j.ceb.2009.04.001.
6. **Zhao Y**, **Li H**, **Fang S**, **Kang Y**, **Wu W**, **Hao Y**, **Li Z**, **Bu D**, **Sun N**, **Zhang MQ**, **Chen R.** NONCODE 2016: an informative and valuable data source of long non-coding RNAs. *Nucleic Acids Res* 44: D203–D208, 2016. doi:10.1093/nar/gkv1252.
7. **Harrow J**, **Frankish A**, **Gonzalez JM**, **Tapanari E**, **Diekhans M**, **Kokocinski F**, et al**.** GENCODE: The reference human genome annotation for The ENCODE Project. *Genome Res* 22: 1760–1774, 2012. doi:10.1101/gr.135350.111.
8. **Hon CC**, **Ramilowski JA**, **Harshbarger J**, **Bertin N**, **Rackham OJ**, **Gough J**, et al**.** An atlas of human long non-coding RNAs with accurate 5′ ends. *Nature* 543: 199–204, 2017. doi:10.1038/nature21374.
9. **Quinn JJ**, **Chang HY.** Unique features of long non-coding RNA biogenesis and function. *Nat Rev Genet* 17: 47–62, 2016. doi:10.1038/nrg.2015.10.
10. **Cheng J**, **Kapranov P**, **Drenkow J**, **Dike S**, **Brubaker S**, **Patel S**, **Long J**, **Stern D**, **Tammana H**, **Helt G**, **Sementchenko V**, **Piccolboni A**, **Bekiranov S**, **Bailey DK**, **Ganesh M**, **Ghosh S**, **Bell I**, **Gerhard DS**, **Gingeras TR.** Transcriptional maps of 10 human chromosomes at 5-nucleotide resolution. *Science* 308: 1149–1154, 2005. doi:10.1126/science.1108625.
11. **Niemczyk M**, **Ito Y**, **Huddleston J**, **Git A**, **Abu-Amero S**, **Caldas C**, **Moore GE**, **Stojic L**, **Murrell A.** Imprinted chromatin around DIRAS3 regulates alternative splicing of GNG12-AS1, a long noncoding RNA. *Am J Hum Genet* 93: 224–235, 2013. doi:10.1016/j.ajhg.2013.06.010.
12. **Ziegler C**, **Kretz M.** The more the merrier—complexity in long noncoding RNA loci. *Front Endocrinol (Lausanne)* 8: 90, 2017. doi:10.3389/fendo.2017.00090.
13. **Kapusta A**, **Kronenberg Z**, **Lynch VJ**, **Zhuo X**, **Ramsay L**, **Bourque G**, **Yandell M**, **Feschotte C.** Transposable elements are major contributors to the origin, diversification, and regulation of vertebrate long noncoding RNAs. *PLoS Genet* 9: e1003470, 2013. doi:10.1371/journal.pgen.1003470.
14. **Anderson DM**, **Anderson KM**, **Chang CL**, **Makarewich CA**, **Nelson BR**, **McAnally JR**, **Kasaragod P**, **Shelton JM**, **Liou J**, **Bassel-Duby R**, **Olson EN.** A micropeptide encoded by a putative long noncoding RNA regulates muscle performance. *Cell* 160: 595–606, 2015. doi:10.1016/j.cell.2015.01.009.
15. **Matsumoto A**, **Pasut A**, **Matsumoto M**, **Yamashita R**, **Fung J**, **Monteleone E**, **Saghatelian A**, **Nakayama KI**, **Clohessy JG**, **Pandolfi PP.** MTORC1 and muscle regeneration are regulated by the LINC00961-encoded SPAR polypeptide. *Nature* 541: 228–232, 2017. doi:10.1038/nature21034.
16. **Knoll M**, **Lodish HF**, **Sun L.** Long non-coding RNAs as regulators of the endocrine system. *Nat Rev Endocrinol* 11: 151–160, 2015. doi:10.1038/nrendo.2014.229.
17. **Qureshi IA**, **Mehler MF.** Emerging roles of non-coding RNAs in brain evolution, development, plasticity and disease. *Nat Rev Nurosci* 13: 528–541, 2012. doi:10.1038/nrn3234.
18. **Li Z**, **Ren T**, **Li W**, **Han R.** Regulatory mechanism and application of lncRNAs in poultry. In: *Poultry—An Advanced Learning*, edited by Kamboh AA. London: IntechOpen, 2020**.**
19. **Kotake Y**, **Nakagawa T**, **Kitagawa K**, **Suzuki S**, **Liu N**, **Kitagawa M**, **Xiong Y.** Long non-coding RNA ANRIL is required for the PRC2 recruitment to and silencing of p15INK4B tumor suppressor gene. *Oncogene* 30: 1956–1962, 2011. doi:10.1038/onc.2010.568.
20. **Hung T**, **Wang Y**, **Lin MF**, **Koegel AK**, **Kotake Y**, **Grant GD**, **Horlings HM**, **Shah N**, **Umbricht C**, **Wang P**, **Wang Y**, **Kong B**, **Langerød A**, **Børresen-Dale AL**, **Kim SK**, **van de Vijver M**, **Sukumar S**, **Whitfield ML**, **Kellis M**, **Xiong Y**, **Wong DJ**, **Chang HY.** Extensive and coordinated transcription of noncoding RNAs within cell-cycle promoters. *Nat Genet* 43: 621–629, 2011. doi:10.1038/ng.848.
21. **Wang KC**, **Chang HY.** Molecular mechanisms of long noncoding RNAs. *Mol Cell* 43: 904–914, 2011. doi:10.1016/j.molcel.2011.08.018.
22. **Sweta S**, **Dudnakova T**, **Sudheer S**, **Baker AH**, **Bhushan R.** Importance of long non-coding RNAs in the development and disease of skeletal muscle and cardiovascular lineages. *Front Cell Dev Biol* 7: 228, 2019. doi:10.3389/fcell.2019.00228.
23. **Dykes IM**, **Emanueli C.** Transcriptional and post-transcriptional gene regulation by long non-coding RNA. *Genomics Proteomics Bioinformatics* 15: 177–186, 2017. doi:10.1016/j.gpb.2016.12.005.
24. **Tano K**, **Mizuno R**, **Okada T**, **Rakwal R**, **Shibato J**, **Masuo Y**, **Ijiri K**, **Akimitsu N.** MALAT-1 enhances cell motility of lung adenocarcinoma cells by influencing the expression of motility-related genes. *FEBS Lett* 584: 4575–4580, 2010. doi:10.1016/j.febslet.2010.10.008.
25. **Hu W**, **Alvarez-Dominguez JR**, **Lodish HF.** Regulation of mammalian cell differentiation by long non-coding RNAs. *EMBO Rep* 13: 971–983, 2012. doi:10.1038/embor.2012.145.
26. **Lopez-Pajares V.** Long non-coding RNA regulation of gene expression during differentiation. *Pflugers Arch* 468: 971–981, 2016. doi:10.1007/s00424-016-1809-6.
27. **Perry RB**, **Ulitsky I.** The functions of long noncoding RNAs in development and stem cells. *Development* 143: 3882–3894, 2016. doi:10.1242/dev.140962.
28. **Sheng G.** The developmental basis of mesenchymal stem/stromal cells (MSCs). *BMC Dev Biol* 15: 44, 2015. doi:10.1186/s12861-015-0094-5.
29. **Caplan AI.** Mesenchymal stem cells. *J Orthop Res* 9: 641–650, 1991. doi:10.1002/jor.1100090504.
30. **Sacchetti B**, **Funari A**, **Remoli C**, **Giannicola G**, **Kogler G**, **Liedtke S**, **Cossu G**, **Serafini M**, **Sampaolesi M**, **Tagliafico E**, **Tenedini E**, **Saggio I**, **Robey PG**, **Riminucci M**, **Bianco P.** No identical "mesenchymal stem cells" at different times and sites: human committed progenitors of distinct origin and differentiation potential are incorporated as adventitial cells in microvessels. *Stem Cell Reports* 6: 897–913, 2016. doi:10.1016/j.stemcr.2016.05.011.
31. **Corselli M**, **Chen CW**, **Sun B**, **Yap S**, **Rubin JP**, **Péault B.** The tunica adventitia of human arteries and veins as a source of mesenchymal stem cells. *Stem Cells Dev* 21: 1299–1308, 2012. doi:10.1089/scd.2011.0200.
32. **Cawthorn WP**, **Scheller EL**, **MacDougald OA.** Adipose tissue stem cells meet preadipocyte commitment: going back to the future. *J Lipid Res* 53: 227–246, 2012. doi:10.1194/jlr.R021089.

33. **Galipeau J**, **Sensébé L.** Mesenchymal stromal cells: clinical challenges and therapeutic opportunities. *Cell Stem Cell* 22: 824–833, 2018. doi:10.1016/j.stem.2018.05.004.
34. **Sun C**, **Wang L**, **Wang H**, **Huang T**, **Yao W**, **Li J**, **Zhang X.** Single-cell RNA-seq highlights heterogeneity in human primary Wharton's jelly mesenchymal stem/stromal cells cultured in vitro. *Stem Cell Res Ther* 11: 149, 2020. doi:10.1186/s13287-020-01660-4.
35. **Riquier S**, **Mathieu M**, **Bessiere C**, **Boureux A**, **Ruffle F**, **Lemaitre JM**, **Djouad F**, **Gilbert N**, **Commes T.** Long non-coding RNA exploration for mesenchymal stem cell characterisation. *BMC Genomics* 22: 412, 2021. doi:10.1186/s12864-020-07289-0.
36. **Julien A**, **Kanagalingam A**, **Martínez-Sarrà E**, **Megret J**, **Luka M**, **Ménager M**, **Relaix F**, **Colnot C.** Direct contribution of skeletal muscle mesenchymal progenitors to bone repair. *Nat Commun* 12: 2860, 2021. doi:10.1038/s41467-021-22842-5.
37. **Contreras O**, **Rossi FM**, **Theret M.** Origins, potency, and heterogeneity of skeletal muscle fibro-adipogenic progenitors—time for new definitions. *Skelet Muscle* 11: 16, 2021. doi:10.1186/s13395-021-00265-6.
38. **Pittenger MF**, **Mackay AM**, **Beck SC**, **Jaiswal RK**, **Douglas R**, **Mosca JD**, **Moorman MA**, **Simonetti DW**, **Craig S**, **Marshak DR.** Multilineage potential of adult human mesenchymal stem cells. *Science* 284: 143–147, 1999. doi:10.1126/science.284.5411.143.
39. **Wong CY**, **Al-Salami H**, **Dass CR.** C2C12 cell model: its role in understanding of insulin resistance at the molecular level and pharmaceutical development at the preclinical stage. *J Pharm Pharmacol* 72: 1667–1693, 2020. doi:10.1111/jphp.13359.
40. **Zhang ZK**, **Li J**, **Guan D**, **Liang C**, **Zhuo Z**, **Liu J**, **Lu A**, **Zhang G**, **Zhang BT.** Long noncoding RNA lncMUMA reverses established skeletal muscle atrophy following mechanical unloading. *Mol Ther* 26: 2669–2680, 2018. doi:10.1016/j.ymthe.2018.09.014.
41. **Mousavi K**, **Zare H**, **Dell'orso S**, **Grontved L**, **Gutierrez-Cruz G**, **Derfoul A**, **Hager GL**, **Sartorelli V.** eRNAs promote transcription by establishing chromatin accessibility at defined genomic loci. *Mol Cell* 51: 606–617, 2013. doi:10.1016/j.molcel.2013.07.022.
42. **Cichewicz MA**, **Kiran M**, **Przanowska RK**, **Sobierajska E**, **Shibata Y**, **Dutta A.** MUNC, an enhancer RNA upstream from the MYOD gene, induces a subgroup of myogenic transcripts in trans independently of MyoD. *Mol Cell Biol* 38: e00655-17, 2018. doi:10.1128/MCB.00655-17.
43. **Mueller AC**, **Cichewicz MA**, **Dey BK**, **Layer R**, **Reon BJ**, **Gagan JR**, **Dutta A.** MUNC, a long noncoding RNA that facilitates the function of MyoD in skeletal myogenesis. *Mol Cell Biol* 35: 498–513, 2015. doi:10.1128/MCB.01079-14.
44. **Nakae J**, **Kido Y**, **Accili D.** Distinct and overlapping functions of insulin and IGF-I receptors. *Endocr Rev* 22: 818–835, 2001. doi:10.1210/edrv.22.6.0452.
45. **Zhu M**, **Liu J**, **Xiao J**, **Yang L**, **Cai M**, **Shen H**, **Chen X**, **Ma Y**, **Hu S**, **Wang Z**, **Hong A**, **Li Y**, **Sun Y**, **Wang X.** Lnc-mg is a long non-coding RNA that promotes myogenesis. *Nat Commun* 8: 14718, 2017. doi:10.1038/ncomms14718.
46. **Song C**, **Wang J**, **Ma Y**, **Yang Z**, **Dong D**, **Li H**, **Yang J**, **Huang Y**, **Plath M**, **Ma Y**, **Chen H.** Linc-smad7 promotes myoblast differentiation and muscle regeneration via sponging miR-125b. *Epigenetics* 13: 591–604, 2018. doi:10.1080/15592294.2018.1481705.
47. **Du J**, **Zhang P**, **Zhao X**, **He J**, **Xu Y**, **Zou Q**, **Luo J**, **Shen L**, **Gu H**, **Tang Q**, **Li M**, **Jiang Y**, **Tang G**, **Bai L**, **Li X**, **Wang J**, **Zhang S**, **Zhu L.** MicroRNA-351-5p mediates skeletal myogenesis by directly targeting lactamase-β and is regulated by lnc-mg. *FASEB J* 33: 1911–1926, 2019. doi:10.1096/fj.201701394RRR.
48. **Gong C**, **Li Z**, **Ramanujan K**, **Clay I**, **Zhang Y**, **Lemire-Brachat S**, **Glass DJ.** A long non-coding RNA, LncMyoD, regulates skeletal muscle differentiation by blocking IMP2-mediated mRNA translation. *Dev Cell* 34: 181–191, 2015. doi:10.1016/j.devcel.2015.05.009.
49. **Kallen AN**, **Zhou XB**, **Xu J**, **Qiao C**, **Ma J**, **Yan L**, **Lu L**, **Liu C**, **Yi JS**, **Zhang H**, **Min W**, **Bennett AM**, **Gregory RI**, **Ding Y**, **Huang Y.** The imprinted H19 LncRNA antagonizes Let-7 microRNAs. *Mol Cell* 52: 101–112, 2013. doi:10.1016/j.molcel.2013.08.027.
50. **Dey BK**, **Pfeifer K**, **Dutta A.** The H19 long noncoding RNA gives rise to microRNAs miR-675-3p and miR-675-5p to promote skeletal muscle differentiation and regeneration. *Genes Dev* 28: 491–501, 2014. doi:10.1101/gad.234419.113.
51. **Rathbone CR**, **Booth FW**, **Lees SJ.** Sirt1 increases skeletal muscle precursor cell proliferation. *Eur J Cell Biol* 88: 35–44, 2009. doi:10.1016/j.ejcb.2008.08.003.
52. **Wang Y**, **Pang WJ**, **Wei N**, **Xiong Y**, **Wu WJ**, **Zhao CZ**, **Shen QW**, **Yang GS.** Identification, stability and expression of Sirt1 antisense long non-coding RNA. *Gene* 539: 117–124, 2014. doi:10.1016/j.gene.2014.01.037.
53. **Wang GQ**, **Wang Y**, **Xiong Y**, **Chen XC**, **Ma ML**, **Cai R**, **Gao Y**, **Sun YM**, **Yang GS**, **Pang WJ.** Sirt1 AS lncRNA interacts with its mRNA to inhibit muscle formation by attenuating function of miR-34a. *Sci Rep* 6: 21865, 2016. doi:10.1038/srep21865.
54. **Jin JJ**, **Lv W**, **Xia P**, **Xu ZY**, **Zheng AD**, **Wang XJ**, **Wang SS**, **Zeng R**, **Luo HM**, **Li GL**, **Zuo B.** Long noncoding RNA SYISL regulates myogenesis by interacting with polycomb repressive complex 2. *Proc Natl Acad Sci USA* 115: E9802–E9811, 2018. doi:10.1073/pnas.1801471115.
55. **Miyake T**, **Alli NS**, **McDermott JC.** Nuclear function of Smad7 promotes myogenesis. *Mol Cell Biol* 30: 722–735, 2010. doi:10.1128/MCB.01005-09.
56. **Mal A**, **Sturniolo M**, **Schiltz RL**, **Ghosh MK**, **Harter ML.** A role for histone deacetylase HDAC1 in modulating the transcriptional activity of MyoD: inhibition of the myogenic program. *EMBO J* 20: 1739–1753, 2001. doi:10.1093/emboj/20.7.1739.
57. **Chen X**, **He L**, **Zhao Y**, **Li Y**, **Zhang S**, **Sun K**, **So K**, **Chen F**, **Zhou L**, **Lu L**, **Wang L**, **Zhu X**, **Bao X**, **Esteban MA**, **Nakagawa S**, **Prasanth KV**, **Wu Z**, **Sun H**, **Wang H.** Malat1 regulates myogenic differentiation and muscle regeneration through modulating MyoD transcriptional activity. *Cell Discov* 3: 17002, 2017. doi:10.1038/celldisc.2017.2.
58. **Watts R**, **Johnsen VL**, **Shearer J**, **Hittel DS.** Myostatin-induced inhibition of the long noncoding RNA Malat1 is associated with decreased myogenesis. *Am J Physiol Cell Physiol* 304: C995–C1001, 2013. doi:10.1152/ajpcell.00392.2012.
59. **Iwasaki K**, **Hayashi K**, **Fujioka T**, **Sobue K.** Rho/Rho-associated kinase signal regulates myogenic differentiation via myocardin-related transcription factor-A/Smad-dependent transcription of the Id3 gene. *J Biol Chem* 283: 21230–21241, 2008. doi:10.1074/jbc.M710525200.
60. **Dimartino D**, **Colantoni A**, **Ballarino M**, **Martone J**, **Mariani D**, **Danner J**, **Bruckmann A**, **Meister G**, **Morlando M**, **Bozzoni I.** The long non-coding RNA lnc-31 interacts with Rock1 mRNA and mediates its YB-1-dependent translation. *Cell Rep* 23: 733–740, 2018. doi:10.1016/j.celrep.2018.03.101.
61. **Ballarino M**, **Cazzella V**, **D'Andrea D**, **Grassi L**, **Bisceglie L**, **Cipriano A**, **Santini T**, **Pinnarò C**, **Morlando M**, **Tramontano A**, **Bozzoni I.** Novel long noncoding RNAs (lncRNAs) in Myogenesis: a miR-31 overlapping lncRNA transcript controls myoblast differentiation. *Mol Cell Biol* 35: 728–736, 2015. [Erratum in *Mol Cell Biol* 38: e00167-18, 2018]. doi:10.1128/MCB.01394-14.
62. **Caretti G**, **Schiltz RL**, **Dilworth FJ**, **Di Padova M**, **Zhao P**, **Ogryzko V**, **Fuller-Pace FV**, **Hoffman EP**, **Tapscott SJ**, **Sartorelli V.** The RNA helicases p68/p72 and the noncoding RNA SRA are coregulators of MyoD and skeletal muscle differentiation. *Dev Cell* 11: 547–560, 2006. doi:10.1016/j.devcel.2006.08.003.
63. **Hubé F**, **Velasco G**, **Rollin J**, **Furling D**, **Francastel C.** Steroid receptor RNA activator protein binds to and counteracts SRA RNA-mediated activation of MyoD and muscle differentiation. *Nucleic Acids Res* 39: 513–525, 2011. doi:10.1093/nar/gkq833.
64. **Yu X**, **Zhang Y**, **Li T**, **Ma Z**, **Jia H**, **Chen Q**, **Zhao Y**, **Zhai L**, **Zhong R**, **Li C**, **Zou X**, **Meng J**, **Chen AK**, **Puri PL**, **Chen M**, **Zhu D.** Long noncoding RNA Linc-RAM enhances myogenic differentiation by interacting with MyoD. *Nat Commun* 8: 14016, 2017. doi:10.1038/ncomms14016.
65. **Wang L**, **Zhao Y**, **Bao X**, **Zhu X**, **Kwok YK**, **Sun K**, **Chen X**, **Huang Y**, **Jauch R**, **Esteban MA**, **Sun H**, **Wang H.** LncRNA Dum interacts with Dnmts to regulate Dppa2 expression during myogenic differentiation and muscle regeneration. *Cell Res* 25: 335–350, 2015. doi:10.1038/cr.2015.21.
66. **Eckersley-Maslin MA**, **Parry A**, **Blotenburg M**, **Krueger C**, **Ito Y**, **Franklin VN**, **Narita M**, **D'Santos CS**, **Reik W.** Epigenetic priming by Dppa2 and 4 in pluripotency facilitates multi-lineage commitment. *Nat Struct Mol Biol* 27: 696–705, 2020. doi:10.1038/s41594-020-0443-3.
67. **Zhou L**, **Sun K**, **Zhao Y**, **Zhang S**, **Wang X**, **Li Y**, **Lu L**, **Chen X**, **Chen F**, **Bao X**, **Zhu X**, **Wang L**, **Tang LY**, **Esteban MA**, **Wang CC**, **Jauch**

R, **Sun H**, **Wang H.** Linc-YY1 promotes myogenic differentiation and muscle regeneration through an interaction with the transcription factor YY1. *Nat Commun* 6: 10026, 2015. doi:10.1038/ncomms10026.
68. **Lu L**, **Sun K**, **Chen X**, **Zhao Y**, **Wang L**, **Zhou L**, **Sun H**, **Wang H.** Genome-wide survey by ChIP-seq reveals YY1 regulation of lincRNAs in skeletal myogenesis. *EMBO J* 32: 2575–2588, 2013. doi:10.1038/emboj.2013.182.
69. **Cesana M**, **Cacchiarelli D**, **Legnini I**, **Santini T**, **Sthandier O**, **Chinappi M**, **Tramontano A**, **Bozzoni I.** A long noncoding RNA controls muscle differentiation by functioning as a competing endogenous RNA. *Cell* 147: 358–369, 2011. [Erratum in *Cell* 147: 947, 2011]. doi:10.1016/j.cell.2011.09.028.
70. **Legnini I**, **Morlando M**, **Mangiavacchi A**, **Fatica A**, **Bozzoni I.** A feedforward regulatory loop between HuR and the long noncoding RNA linc-MD1 controls early phases of myogenesis. *Mol Cell* 53: 506–514, 2014. doi:10.1016/j.molcel.2013.12.012.
71. **Sui Y**, **Han Y**, **Zhao X**, **Li D**, **Li G.** Long non-coding RNA lrm enhances myogenic differentiation by interacting with MEF2D. *Cell Death Dis* 10: 181, 2019. doi:10.1038/s41419-019-1399-2.
72. **Wang J**, **Gong C**, **Maquat LE.** Control of myogenesis by rodent SINE-containing lncRNAs. *Genes Dev* 27: 793–804, 2013. doi:10.1101/gad.212639.112.
73. **Sunwoo H**, **Dinger ME**, **Wilusz JE**, **Amaral PP**, **Mattick JS**, **Spector DL.** MEN epsilon/beta nuclear-retained non-coding RNAs are up-regulated upon muscle differentiation and are essential components of paraspeckles. *Genome Res* 19: 347–359, 2009. doi:10.1101/gr.087775.108.
74. **Randrianarison-Huetz V**, **Papaefthymiou A**, **Herledan G**, **Noviello C**, **Faradova U**, **Collard L**, **Pincini A**, **Schol E**, **Decaux JF**, **Maire P**, **Vassilopoulos S**, **Sotiropoulos A.** Srf controls satellite cell fusion through the maintenance of actin architecture. *J Cell Biol* 217: 685–700, 2018. doi:10.1083/jcb.201705130.
75. **Han X**, **Yang F**, **Cao H**, **Liang Z.** Malat1 regulates serum response factor through miR-133 as a competing endogenous RNA in myogenesis. *FASEB J* 29: 3054–3064, 2015. doi:10.1096/fj.14-259952.
76. **Militello G**, **Hosen MR**, **Ponomareva Y**, **Gellert P**, **Weirick T**, **John D**, **Hindi SM**, **Mamchaoui K**, **Mouly V**, **Döring C**, **Zhang L**, **Nakamura M**, **Kumar A**, **Fukada SI**, **Dimmeler S**, **Uchida S.** A novel long noncoding RNA Myolinc regulates myogenesis through TDP-43 and Filip1. *J Mol Cell Biol* 10: 102–117, 2018. doi:10.1093/jmcb/mjy025.
77. **Endo T.** Molecular mechanisms of skeletal muscle development, regeneration, and osteogenic conversion. *Bone* 80: 2–13, 2015. doi:10.1016/j.bone.2015.02.028.
78. **Ballarino M**, **Cipriano A**, **Tita R**, **Santini T**, **Desideri F**, **Morlando M**, **Colantoni A**, **Carrieri C**, **Nicoletti C**, **Musarò A**, **Carroll DO**, **Bozzoni I.** Deficiency in the nuclear long noncoding RNA Charme causes myogenic defects and heart remodeling in mice. *EMBO J* 37: e99697, 2018. doi:10.15252/embj.201899697.
79. **Xu M**, **Chen X**, **Huang Z**, **Chen D**, **Yu B**, **Chen H**, **He J**, **Zheng P**, **Luo J**, **Yu J**, **Luo Y.** MicroRNA-139-5p suppresses myosin heavy chain I and IIa expression via inhibition of the calcineurin/NFAT signaling pathway. *Biochem Biophys Res Commun* 500: 930–936, 2018. doi:10.1016/j.bbrc.2018.04.202.
80. **Peng S**, **Song C**, **Li H**, **Cao X**, **Ma Y**, **Wang X**, **Huang Y**, **Lan X**, **Lei C**, **Chaogetu B**, **Chen H.** Circular RNA SNX29 sponges miR-744 to regulate proliferation and differentiation of myoblasts by activating the Wnt5a/Ca^{2+} signaling pathway. *Mol Ther Nucleic Acids* 16: 481–493, 2019. doi:10.1016/j.omtn.2019.03.009.
81. **Zhang ZK**, **Li J**, **Guan D**, **Liang C**, **Zhuo Z**, **Liu J**, **Lu A**, **Zhang G**, **Zhang BT.** A newly identified lncRNA MAR1 acts as a miR-487b sponge to promote skeletal muscle differentiation and regeneration. *J Cachexia Sarcopenia Muscle* 9: 613–626, 2018. doi:10.1002/jcsm.12281.
82. **Liang T**, **Zhou B**, **Shi L**, **Wang H**, **Chu Q**, **Xu F**, **Li Y**, **Chen R**, **Shen C**, **Schinckel AP.** lncRNA AK017368 promotes proliferation and suppresses differentiation of myoblasts in skeletal muscle development by attenuating the function of miR-30c. *FASEB J* 32: 377–389, 2018. doi:10.1096/fj.201700560rr.
83. **Long F.** Building strong bones: molecular regulation of the osteoblast lineage. *Nat Rev Mol Cell Biol* 13: 27–38, 2011. doi:10.1038/nrm3254.
84. **Jia Q**, **Jiang W**, **Ni L.** Down-regulated non-coding RNA (lncRNA-ANCR) promotes osteogenic differentiation of periodontal ligament stem cells. *Arch Oral Biol* 60: 234–241, 2015. doi:10.1016/j.archoralbio.2014.10.007.
85. **Zhu XX**, **Yan YW**, **Chen D**, **Ai CZ**, **Lu X**, **Xu SS**, **Jiang S**, **Zhong GS**, **Chen DB**, **Jiang YZ.** Long non-coding RNA HoxA-AS3 interacts with EZH2 to regulate lineage commitment of mesenchymal stem cells. *Oncotarget* 7: 63561–63570, 2016. doi:10.18632/oncotarget.11538.
86. **Zhu L**, **Xu PC.** Downregulated LncRNA-ANCR promotes osteoblast differentiation by targeting EZH2 and regulating Runx2 expression. *Biochem Biophys Res Commun* 432: 612–617, 2013. doi:10.1016/j.bbrc.2013.02.036.
87. **Jia Q**, **Chen X**, **Jiang W**, **Wang W**, **Guo B**, **Ni L.** The regulatory effects of long noncoding RNA-ANCR on dental tissue-derived stem cells. *Stem Cells Int* 2016: 3146805, 2016. doi:10.1155/2016/3146805.
88. **Liu Y**, **Zeng X**, **Miao J**, **Liu C**, **Wei F**, **Liu D**, **Zheng Z**, **Ting K**, **Wang C**, **Guo J.** Upregulation of long noncoding RNA MEG3 inhibits the osteogenic differentiation of periodontal ligament cells. *J Cell Physiol* 234: 4617–4626, 2019. doi:10.1002/jcp.27248.
89. **Zhuang W**, **Ge X**, **Yang S**, **Huang M**, **Zhuang W**, **Chen P**, **Zhang X**, **Fu J**, **Qu J**, **Li B.** Upregulation of lncRNA MEG3 promotes osteogenic differentiation of mesenchymal stem cells from multiple myeloma patients by targeting BMP4 transcription. *Stem Cells* 33: 1985–1997, 2015. doi:10.1002/stem.1989.
90. **Chen S**, **Jia L**, **Zhang S**, **Zheng Y**, **Zhou Y.** DEPTOR regulates osteogenic differentiation via inhibiting MEG3-mediated activation of BMP4 signaling and is involved in osteoporosis. *Stem Cell Res Ther* 9: 185, 2018. doi:10.1186/s13287-018-0935-9.
91. **Jia B**, **Qiu X**, **Chen J**, **Sun X**, **Zheng X**, **Zhao J**, **Li Q**, **Wang Z.** A feedforward regulatory network lncPCAT1/miR-106a-5p/E2F5 regulates the osteogenic differentiation of periodontal ligament stem cells. *J Cell Physiol* 234: 19523–19538, 2019. doi:10.1002/jcp.28550.
92. **Li L**, **Fang J**, **Liu Y**, **Xiao L.** LncRNA LOC100506178 promotes osteogenic differentiation via regulating miR-214-5p-BMP2 axis in human bone marrow mesenchymal stem cells. *PeerJ* 8: e8909, 2020. doi:10.7717/peerj.8909.
93. **Wang CG**, **Liao Z**, **Xiao H**, **Liu H**, **Hu YH**, **Liao QD**, **Zhong D.** LncRNA KCNQ1OT1 promoted BMP2 expression to regulate osteogenic differentiation by sponging miRNA-214. *Exp Mol Pathol* 107: 77–84, 2019. doi:10.1016/j.yexmp.2019.01.012.
94. **Wang X**, **Guo B**, **Li Q**, **Peng J**, **Yang Z**, **Wang A**, **Li D**, **Hou Z**, **Lv K**, **Kan G**, **Cao H**, **Wu H**, **Song J**, **Pan X**, **Sun Q**, **Ling S**, **Li Y**, **Zhu M**, **Zhang P**, **Peng S**, **Xie X**, **Tang T**, **Hong A**, **Bian Z**, **Bai Y**, **Lu A**, **Li Y**, **He F**, **Zhang G**, **Li Y.** miR-214 targets ATF4 to inhibit bone formation. *Nat Med* 19: 93–100, 2013. doi:10.1038/nm.3026.
95. **Yu Y**, **Chen Y**, **Zhang X**, **Lu X**, **Hong J**, **Guo X**, **Zhou D.** Knockdown of lncRNA KCNQ1OT1 suppresses the adipogenic and osteogenic differentiation of tendon stem cell via downregulating miR-138 target genes PPARγ and RUNX2. *Cell Cycle* 17: 2374–2385, 2018. doi:10.1080/15384101.2018.1534510.
96. **Gao X**, **Ge J**, **Li W**, **Zhou W**, **Xu L.** LncRNA KCNQ1OT1 promotes osteogenic differentiation to relieve osteolysis via Wnt/β-catenin activation. *Cell Biosci* 8: 19, 2018. doi:10.1186/s13578-018-0216-4.
97. **Zhang W**, **Chen L**, **Wu J**, **Li J**, **Zhang X**, **Xiang Y**, **Li F**, **Wu C**, **Xiang L**, **Ran Q**, **Li Z.** Long noncoding RNA TUG1 inhibits osteogenesis of bone marrow mesenchymal stem cells via Smad5 after irradiation. *Theranostics* 9: 2198–2208, 2019. doi:10.7150/thno.30798.
98. **Yano M**, **Inoue Y**, **Tobimatsu T**, **Hendy G**, **Canaff L**, **Sugimoto T**, **Seino S**, **Kaji H.** Smad7 inhibits differentiation and mineralization of mouse osteoblastic cells. *Endocr J* 59: 653–662, 2012. doi:10.1507/endocrj.EJ12-0022.
99. **Wei B**, **Wei W**, **Zhao B**, **Guo X**, **Liu S.** Long non-coding RNA HOTAIR inhibits miR-17-5p to regulate osteogenic differentiation and proliferation in non-traumatic osteonecrosis of femoral head. *PLoS One* 12: e0169097, 2017. doi:10.1371/journal.pone.0169097.
100. **Rinn JL**, **Kertesz M**, **Wang JK**, **Squazzo SL**, **Xu X**, **Brugmann SA**, **Goodnough LH**, **Helms JA**, **Farnham PJ**, **Segal E**, **Chang HY.** Functional demarcation of active and silent chromatin domains in human HOX loci by noncoding RNAs. *Cell* 129: 1311–1323, 2007. doi:10.1016/j.cell.2007.05.022.
101. **Fang T**, **Wu Q**, **Zhou L**, **Mu S**, **Fu Q.** miR-106b-5p and miR-17-5p suppress osteogenic differentiation by targeting Smad5 and inhibit bone formation. *Exp Cell Res* 347: 74–82, 2016. doi:10.1016/j.yexcr.2016.07.010.
102. **Li Z**, **Hassan MQ**, **Volinia S**, **van Wijnen AJ**, **Stein JL**, **Croce CM**, **Lian JB**, **Stein GS.** A microRNA signature for a BMP2-induced

osteoblast lineage commitment program. *Proc Natl Acad Sci USA* 105: 13906–13911, 2008. doi:10.1073/pnas.0804438105.

103. **Wang Y**, **Chen X**, **Yin Y**, **Li S.** Human amnion-derived mesenchymal stem cells induced osteogenesis and angiogenesis in human adipose-derived stem cells via ERK1/2 MAPK signaling pathway. *BMB Rep* 51: 194–199, 2018. doi:10.5483/BMBRep.2018.51.4.005.
104. **Zhang J**, **Tao Z**, **Wang Y.** Long non-coding RNA DANCR regulates the proliferation and osteogenic differentiation of human bone-derived marrow mesenchymal stem cells via the p38 MAPK pathway. *Int J Mol Med* 41: 213–219, 2018.
105. **Zhu W**, **Boachie-Adjei O**, **Rawlins BA**, **Frenkel B**, **Boskey AL**, **Ivashkiv LB**, **Blobel CP.** A novel regulatory role for Stromal-derived Factor-1 signaling in Bone Morphogenic Protein-2 osteogenic differentiation of mesenchymal C2C12 cells. *J Biol Chem* 282: 18676–18685, 2007. doi:10.1074/jbc.M610232200.
106. **Gong ZM**, **Tang ZY**, **Sun XL.** LncRNA PRNCR1 regulates osteogenic differentiation in osteolysis after hip replacement by targeting miR-211-5p. *Biosci Rep* 2018: BSR20180042, 2018. doi:10.1042/BSR20180042.
107. **Cao B**, **Liu N**, **Wang W.** High glucose prevents osteogenic differentiation of mesenchymal stem cells via lncRNA AK028326/CXCL13 pathway. *Biomed Pharmacother* 84: 544–551, 2016. doi:10.1016/j.biopha.2016.09.058.
108. **Li H**, **Zhang Z**, **Chen Z**, **Zhang D.** Osteogenic growth peptide promotes osteogenic differentiation of mesenchymal stem cells mediated by LncRNA AK141205-induced upregulation of CXCL13. *Biochem Biophys Res Commun* 466: 82–88, 2015. doi:10.1016/j.bbrc.2015.08.112.
109. **Deng L**, **Hong H**, **Zhang X**, **Chen D**, **Chen Z**, **Ling J**, **Wu L.** Downregulated lncRNA MEG3 promotes osteogenic differentiation of human dental follicle stem cells by epigenetically regulating Wnt pathway. *Biochem Biophys Res Commun* 503: 2061–2067, 2018. doi:10.1016/j.bbrc.2018.07.160.
110. **Jia B**, **Wang Z**, **Sun X**, **Chen J**, **Zhao J**, **Qiu X.** Long noncoding RNA LINC00707 sponges miR-370-3p to promote osteogenesis of human bone marrow-derived mesenchymal stem cells through upregulating WNT2B. *Stem Cell Res Ther* 10: 67, 2019. doi:10.1186/s13287-019-1161-9.
111. **He X**, **Wang H**, **Jin T**, **Xu Y**, **Mei L**, **Yang J.** TLR4 activation promotes bone marrow MSC proliferation and osteogenic differentiation via Wnt3a and Wnt5a signaling. *PLoS One* 11: e0149876, 2016. doi:10.1371/journal.pone.0149876.
112. **Yu L**, **Qu H**, **Yu Y**, **Li W**, **Zhao Y**, **Qiu G.** LncRNA-PCAT1 targeting miR-145-5p promotes TLR4-associated osteogenic differentiation of adipose-derived stem cells. *J Cell Mol Med* 22: 6134–6147, 2018. doi:10.1111/jcmm.13892.
113. **Fukuda T**, **Ochi H**, **Sunamura S**, **Haiden A**, **Bando W**, **Inose H**, **Okawa A**, **Asou Y**, **Takeda S.** MicroRNA-145 regulates osteoblastic differentiation by targeting the transcription factor Cbfb. *FEBS Lett* 589: 3302–3308, 2015. doi:10.1016/j.febslet.2015.09.024.
114. **Jia J**, **Tian Q**, **Ling S**, **Liu Y**, **Yang S**, **Shao Z.** miR-145 suppresses osteogenic differentiation by targeting Sp7. *FEBS Lett* 587: 3027–3031, 2013. doi:10.1016/j.febslet.2013.07.030.
115. **Feng L**, **Shi L**, **Lu YF**, **Wang B**, **Tang T**, **Fu WM**, **He W**, **Li G**, **Zhang JF.** Linc-ROR promotes osteogenic differentiation of mesenchymal stem cells by functioning as a competing endogenous RNA for miR-138 and miR-145. *Mol Ther Nucleic Acids* 11: 345–353, 2018. doi:10.1016/j.omtn.2018.03.004.
116. **Qi S**, **Song Y**, **Peng Y**, **Wang H**, **Long H**, **Yu X**, **Li Z**, **Fang L**, **Wu A**, **Luo W**, **Zhen Y**, **Zhou Y**, **Chen Y**, **Mai C**, **Liu Z**, **Fang W.** ZEB2 mediates multiple pathways regulating cell proliferation, migration, invasion, and apoptosis in glioma. *PLoS One* 7: e38842, 2012. doi:10.1371/journal.pone.0038842.
117. **Liang WC**, **Fu WM**, **Wang YB**, **Sun YX**, **Xu LL**, **Wong CW**, **Chan KM**, **Li G**, **Waye MM**, **Zhang JF.** H19 activates Wnt signaling and promotes osteoblast differentiation by functioning as a competing endogenous RNA. *Sci Rep* 6: 20121, 2016. doi:10.1038/srep20121.
118. **Wang Y**, **Liu W**, **Liu Y**, **Cui J**, **Zhao Z**, **Cao H**, **Fu Z**, **Liu B.** Long noncoding RNA H19 mediates LCoR to impact the osteogenic and adipogenic differentiation of mBMSCs in mice through sponging miR-188. *J Cell Physiol* 233: 7435–7446, 2018. doi:10.1002/jcp.26589.
119. **Mulati M**, **Kobayashi Y**, **Takahashi A**, **Numata H**, **Saito M**, **Hiraoka Y**, **Ochi H**, **Sato S**, **Ezura Y**, **Yuasa M**, **Hirai T**, **Yoshii T**, **Okawa A**, **Inose H.** The long noncoding RNA Crnde regulates osteoblast proliferation through the Wnt/β-catenin signaling pathway in mice. *Bone* 130: 115076, 2020. doi:10.1016/j.bone.2019.115076.
120. **Yin C**, **Tian Y**, **Yu Y**, **Wang H**, **Wu Z**, **Huang Z**, **Zhang Y**, **Li D**, **Yang C**, **Wang X**, **Li Y**, **Qian A.** A novel long noncoding RNA AK016739 inhibits osteoblast differentiation and bone formation. *J Cell Physiol* 234: 11524–11536, 2019. doi:10.1002/jcp.27815.
121. **Li D**, **Tian Y**, **Yin C**, **Huai Y**, **Zhao Y**, **Su P**, **Wang X**, **Pei J**, **Zhang K**, **Yang C**, **Dang K**, **Jiang S**, **Miao Z**, **Li M**, **Hao Q**, **Zhang G**, **Qian A.** Silencing of lncRNA AK045490 promotes osteoblast differentiation and bone formation via β-catenin/TCF1/Runx2 signaling axis. *Int J Mol Sci* 20: 6229–6214, 2019. doi:10.3390/ijms20246229.
122. **Chen L**, **Song Z**, **Huang S**, **Wang R**, **Qin W**, **Guo J**, **Lin Z.** lncRNA DANCR suppresses odontoblast-like differentiation of human dental pulp cells by inhibiting wnt/β-catenin pathway. *Cell Tissue Res* 364: 309–318, 2016. doi:10.1007/s00441-015-2333-2.
123. **Li B**, **Liu J**, **Zhao J**, **Ma JX**, **Jia HB**, **Zhang Y**, **Xing GS**, **Ma XL.** LncRNA-H19 modulates Wnt/β-catenin signaling by targeting Dkk4 in hindlimb unloaded rat. *Orthop Surg* 9: 319–327, 2017. doi:10.1111/os.12321.
124. **Wang L**, **Wu F**, **Song Y**, **Li X**, **Wu Q**, **Duan Y**, **Jin Z.** Long noncoding RNA related to periodontitis interacts with miR-182 to upregulate osteogenic differentiation in periodontal mesenchymal stem cells of periodontitis patients. *Cell Death Dis* 7: e2327, 2016. doi:10.1038/cddis.2016.125.
125. **Tang Z**, **Gong Z**, **Sun X.** LncRNA DANCR involved osteolysis after total hip arthroplasty by regulating FOXO1 expression to inhibit osteoblast differentiation. *J Biomed Sci* 25: 4, 2018. doi:10.1186/s12929-018-0406-8.
126. **Huang Y**, **Zheng Y**, **Jia L**, **Li W.** Long noncoding RNA H19 promotes osteoblast differentiation via TGF-β1/Smad3/HDAC signaling pathway by deriving miR-675. *Stem Cells* 33: 3481–3492, 2015. doi:10.1002/stem.2225.
127. **Peng W**, **Zhu SX**, **Wang J**, **Chen LL**, **Weng JQ**, **Chen SL.** Lnc-NTF3-5 promotes osteogenic differentiation of maxillary sinus membrane stem cells via sponging miR-93-3p. *Clin Implant Dent Relat Res* 20: 110–121, 2018. doi:10.1111/cid.12553.
128. **Weng J**, **Peng W**, **Zhu S**, **Chen S.** Long Noncoding RNA sponges miR-454 to promote osteogenic differentiation in maxillary sinus membrane stem cells. *Implant Dent* 26: 178–186, 2017. doi:10.1097/ID.0000000000000569.
129. **Shang G**, **Wang Y**, **Xu Y**, **Zhang S**, **Sun X**, **Guan H**, **Zhao X**, **Wang Y**, **Li Y**, **Zhao G.** Long non-coding RNA TCONS_00041960 enhances osteogenesis and inhibits adipogenesis of rat bone marrow mesenchymal stem cell by targeting miR-204-5p and miR-125a-3p. *J Cell Physiol* 233: 6041–6051, 2018. doi:10.1002/jcp.26424.
130. **Wang Q**, **Li Y**, **Zhang Y**, **Ma L**, **Lin L**, **Meng J**, **Jiang L**, **Wang L**, **Zhou P**, **Zhang Y.** LncRNA MEG3 inhibited osteogenic differentiation of bone marrow mesenchymal stem cells from postmenopausal osteoporosis by targeting miR-133a-3p. *Biomed Pharmacother* 89: 1178–1186, 2017. doi:10.1016/j.biopha.2017.02.090.
131. **Li C-J**, **Xiao Y**, **Yang M**, **Su T**, **Sun X**, **Guo Q**, **Huang Y**, **Luo XH.** Long noncoding RNA Bmncr regulates mesenchymal stem cell fate during skeletal aging. *J Clin Invest* 128: 5251–5266, 2018. doi:10.1172/JCI99044.
132. **Shirakabe K**, **Terasawa K**, **Miyama K**, **Shibuya H**, **Nishida E.** Regulation of the activity of the transcription factor Runx2 by two homeobox proteins, Msx2 and Dlx5. *Genes Cells* 6: 851–856, 2001. doi:10.1046/j.1365-2443.2001.00466.x.
133. **Itoh T**, **Nozawa Y**, **Akao Y.** MicroRNA-141 and -200a are involved in bone morphogenetic protein-2-induced mouse pre-osteoblast differentiation by targeting distal-less homeobox 5. *J Biol Chem* 284: 19272–19279, 2009. doi:10.1074/jbc.M109.014001.
134. **He P**, **Zhang Z**, **Huang G**, **Wang H**, **Xu D**, **Liao W**, **Kang Y.** miR-141 modulates osteoblastic cell proliferation by regulating the target gene of lncRNA H19 and lncRNA H19-derived miR-675. *Am J Transl Res* 8: 1780–1788, 2016.
135. **Sinha KM**, **Zhou X.** Genetic and molecular control of osterix in skeletal formation. *J Cell Biochem* 114: 975–984, 2013. doi:10.1002/jcb.24439.
136. **Liu Y**, **Liu C**, **Zhang A**, **Yin S**, **Wang T**, **Wang Y**, **Wang M**, **Liu Y**, **Ying Q**, **Sun J**, **Wei F**, **Liu D**, **Wang C**, **Ge S.** Down-regulation of long noncoding RNA MEG3 suppresses osteogenic differentiation of periodontal ligament stem cells (PDLSCs) through miR-27a-3p/IGF1 axis

in periodontitis. *Aging (Albany NY)* 11: 5334–5350, 2019. doi:10.18632/aging.102105.
137. **He S**, **Yang S**, **Zhang Y**, **Li X**, **Gao D**, **Zhong Y**, **Cao L**, **Ma H**, **Liu Y**, **Li G**, **Peng S**, **Shuai C.** LncRNA ODIR1 inhibits osteogenic differentiation of hUC-MSCs through the FBXO25/H2BK120ub/H3K4me3/OSX axis. *Cell Death Dis* 10: 947, 2019. doi:10.1038/s41419-019-2148-2.
138. **Zhang J**, **Tu Q**, **Grosschedl R**, **Kim MS**, **Griffin T**, **Drissi H**, **Yang P**, **Chen J.** Roles of SATB2 in osteogenic differentiation and bone regeneration. *Tissue Eng Part A* 17: 1767–1776, 2011. doi:10.1089/ten.tea.2010.0503.
139. **Bi HU**, **Wang D**, **Liu X**, **Wang G**, **Wu X.** Long non-coding RNA H19 promotes osteogenic differentiation of human bone marrow-derived mesenchymal stem cells by regulating microRNA-140-5p/SATB2 axis. *J Biosci* 45: 56, 2020. doi:10.1007/s12038-020-0024-y.
140. **Li Z**, **Jin C**, **Chen S**, **Zheng Y**, **Huang Y**, **Jia L**, **Ge W**, **Zhou Y.** Long non-coding RNA MEG3 inhibits adipogenesis and promotes osteogenesis of human adipose-derived mesenchymal stem cells via miR-140-5p. *Mol Cell Biochem* 433: 51–60, 2017. doi:10.1007/s11010-017-3015-z.
141. **Hwang S**, **Park SK**, **Lee HY**, **Kim SW**, **Lee JS**, **Choi EK**, **You D**, **Kim CS**, **Suh N.** miR-140-5p suppresses BMP2-mediated osteogenesis in undifferentiated human mesenchymal stem cells. *FEBS Lett* 588: 2957–2963, 2014. doi:10.1016/j.febslet.2014.05.048.
142. **Gao Y**, **Xiao F**, **Wang C**, **Wang C**, **Cui P**, **Zhang X**, **Chen X.** Long noncoding RNA MALAT1 promotes osterix expression to regulate osteogenic differentiation by targeting miRNA-143 in human bone marrow-derived mesenchymal stem cells. *J Cell Biochem* 119: 6986–6996, 2018. doi:10.1002/jcb.26907.
143. **Blin-Wakkach C**, **Lezot F**, **Ghoul-Mazgar S**, **Hotton D**, **Monteiro S**, **Teillaud C**, **Pibouin L**, **Orestes-Cardoso S**, **Papagerakis P**, **Macdougall M**, **Robert B**, **Berdal A.** Endogenous Msx1 antisense transcript: in vivo and in vitro evidences, structure, and potential involvement in skeleton development in mammals. *Proc Natl Acad Sci USA* 98: 7336–7341, 2001. doi:10.1073/pnas.131497098.
144. **Berdal A**, **Lezot F**, **Pibouin L**, **Hotton D**, **Ghoul-Mazgar S**, **Teillaud C**, **Robert B**, **MacDougall M**, **Blin C.** Msx1 Homeogene antisense mRNA in mouse dental and bone cells. *Connect Tissue Res* 43: 148–152, 2002. doi:10.1080/03008200290000970.
145. **Park JH**, **Park BW**, **Kang YH**, **Byun SH**, **Hwang SC**, **Kim DR**, **Woo DK**, **Byun JH.** Lin28a enhances in vitro osteoblastic differentiation of human periosteum-derived cells. *Cell Biochem Funct* 35: 497–509, 2017. doi:10.1002/cbf.3305.
146. **He Q**, **Yang S**, **Gu X**, **Li M**, **Wang C**, **Wei F.** Long noncoding RNA TUG1 facilitates osteogenic differentiation of periodontal ligament stem cells via interacting with Lin28A. *Cell Death Dis* 9: 710, 2018. doi:10.1038/s41419-018-0750-3.
147. **Min SY**, **Kady J**, **Nam M**, **Rojas-Rodriguez R**, **Berkenwald A**, **Kim JH**, **Noh HL**, **Kim JK**, **Cooper MP**, **Fitzgibbons T**, **Brehm MA**, **Corvera S.** Human "brite/beige" adipocytes develop from capillary networks, and their implantation improves metabolic homeostasis in mice. *Nat Med* 22: 312–318, 2016. doi:10.1038/nm.4031.
148. **Lowe CE**, **O'Rahilly S**, **Rochford JJ.** Adipogenesis at a glance. *J Cell Sci* 124: 2681–2686, 2011. doi:10.1242/jcs.079699.
149. **Merrick D**, **Sakers A**, **Irgebay Z**, **Okada C**, **Calvert C**, **Morley MP**, **Percec I**, **Seale P.** Identification of a mesenchymal progenitor cell hierarchy in adipose tissue. *Science* 364: eeav2501, 2019. doi:10.1126/science.aav2501.
150. **Ahmad B**, **Serpell CJ**, **Fong IL**, **Wong EH.** Molecular mechanisms of adipogenesis: the anti-adipogenic role of AMP-activated protein kinase. *Front Mol Biosci* 7: 76, 2020. doi:10.3389/fmolb.2020.00076.
151. **Ghaben AL**, **Scherer PE.** Adipogenesis and metabolic health. *Nat Rev Mol Cell Biol* 20: 242–258, 2019. doi:10.1038/s41580-018-0093-z.
152. **Park A**, **Kim WK**, **Bae KH.** Distinction of white, beige and brown adipocytes derived from mesenchymal stem cells. *World J Stem Cells* 6: 33–42, 2014. doi:10.4252/wjsc.v6.i1.33.
153. **Virtanen KA.** Adipose tissue: structure and function of brown adipose tissue. In: *Encyclopedia of Food and Health*, edited by Caballero B, Finglas PM, Toldrá F. Oxford: Academic Press, 2016, p. 30–34.
154. **Coelho M**, **Oliveira T**, **Fernandes R.** Biochemistry of adipose tissue: an endocrine organ. *Arch Med Sci* 9: 191–200, 2013. doi:10.5114/aoms.2013.33181.
155. **Timmons JA**, **Wennmalm K**, **Larsson O**, **Walden TB**, **Lassmann T**, **Petrovic N**, **Hamilton DL**, **Gimeno RE**, **Wahlestedt C**, **Baar K**, **Nedergaard J**, **Cannon B.** Myogenic gene expression signature establishes that brown and white adipocytes originate from distinct cell lineages. *Proc Natl Acad Sci USA* 104: 4401–4406, 2007. doi:10.1073/pnas.0610615104.
156. **Wu J**, **Boström P**, **Sparks LM**, **Ye L**, **Choi JH**, **Giang AH**, **Khandekar M**, **Virtanen KA**, **Nuutila P**, **Schaart G**, **Huang K**, **Tu H**, **van Marken Lichtenbelt WD**, **Hoeks J**, **Enerbäck S**, **Schrauwen P**, **Spiegelman BM.** Beige adipocytes are a distinct type of thermogenic fat cell in mouse and human. *Cell* 150: 366–376, 2012. doi:10.1016/j.cell.2012.05.016.
157. **Herz CT**, **Kiefer FW.** Adipose tissue browning in mice and humans. *J Endocrinol* 241: R97–R109, 2019. doi:10.1530/JOE-18-0598.
158. **Deng J**, **Hua K**, **Lesser SS**, **Harp JB.** Activation of signal transducer and activator of transcription-3 during proliferative phases of 3T3-L1 adipogenesis. *Endocrinology* 141: 2370–2376, 2000. doi:10.1210/endo.141.7.7551.
159. **Zhang L**, **Zhang D**, **Qin ZY**, **Li J**, **Shen ZY.** The role and possible mechanism of long noncoding RNA PVT1 in modulating 3T3-L1 preadipocyte proliferation and differentiation. *IUBMB Life* 72: 1460–1467, 2020. doi:10.1002/iub.2269.
160. **Chen Y**, **Li K**, **Zhang X**, **Chen J**, **Li M**, **Liu L.** The novel long noncoding RNA lncRNA-Adi regulates adipogenesis. *Stem Cells Transl Med* 9: 1053–1067, 2020. doi:10.1002/sctm.19-0438.
161. **Yi F**, **Zhang P**, **Wang Y**, **Xu Y**, **Zhang Z**, **Ma W**, **Xu B**, **Xia Q**, **Du Q.** Long non-coding RNA slincRAD functions in methylation regulation during the early stage of mouse adipogenesis. *RNA Biol* 16: 1401–1413, 2019. doi:10.1080/15476286.2019.1631643.
162. **Yi F**, **Yang F**, **Liu X**, **Chen H**, **Ji T**, **Jiang L**, **Wang X**, **Yang Z**, **Zhang LH**, **Ding X**, **Liang Z**, **Du Q.** RNA-seq identified a super-long intergenic transcript functioning in adipogenesis. *RNA Biol* 10: 990–1001, 2013. doi:10.4161/rna.24644.
163. **Zhang P**, **Bai H**, **Li J**, **Liu J**, **Ma W**, **Xu B**, **Xia Q**, **Wang J**, **Fan Y**, **Du Q.** Knockdown of slincRAD leads to defective adipose development in vivo. *Biochem Biophys Res Commun* 513: 983–989, 2019. doi:10.1016/j.bbrc.2019.04.035.
164. **Ji S**, **Li W**, **Bao L**, **Han P**, **Yang W**, **Ma L**, **Meng F**, **Cao B.** PU.1 promotes miR-191 to inhibit adipogenesis in 3T3-L1 preadipocytes. *Biochem Biophys Res Commun* 451: 329–333, 2014. doi:10.1016/j.bbrc.2014.07.130.
165. **Pang WJ**, **Lin LG**, **Xiong Y**, **Wei N**, **Wang Y**, **Shen QW**, **Yang GS.** Knockdown of PU.1 AS lncRNA inhibits adipogenesis through enhancing PU.1 mRNA translation. *J Cell Biochem* 114: 2500–2512, 2013. doi:10.1002/jcb.24595.
166. **Oishi Y**, **Manabe I**, **Tobe K**, **Tsushima K**, **Shindo T**, **Fujiu K**, **Nishimura G**, **Maemura K**, **Yamauchi T**, **Kubota N**, **Suzuki R**, **Kitamura T**, **Akira S**, **Kadowaki T**, **Nagai R.** Krüppel-like transcription factor KLF5 is a key regulator of adipocyte differentiation. *Cell Metab* 1: 27–39, 2005. doi:10.1016/j.cmet.2004.11.005.
167. **Zhao QH**, **Wang SG**, **Liu SX**, **Li JP**, **Zhang YX**, **Sun ZY**, **Fan QM**, **Tian JW.** PPARγ forms a bridge between DNA methylation and histone acetylation at the C/EBPα gene promoter to regulate the balance between osteogenesis and adipogenesis of bone marrow stromal cells. *FEBS J* 280: 5801–5814, 2013. doi:10.1111/febs.12500.
168. **Lefterova MI**, **Zhang Y**, **Steger DJ**, **Schupp M**, **Schug J**, **Cristancho A**, **Feng D**, **Zhuo D**, **Stoeckert CJ Jr**, **Liu XS**, **Lazar MA.** PPAR and C/EBP factors orchestrate adipocyte biology via adjacent binding on a genome-wide scale. *Genes Dev* 22: 2941–2952, 2008. doi:10.1101/gad.1709008.
169. **Hinman MN**, **Lou H.** Diverse molecular functions of Hu proteins. *Cell Mol Life Sci* 65: 3168–3181, 2008. doi:10.1007/s00018-008-8252-6.
170. **Shen L**, **Han J**, **Wang H**, **Meng Q**, **Chen L**, **Liu Y**, **Feng Y**, **Wu G.** Cachexia-related long noncoding RNA, CAAlnc1, suppresses adipogenesis by blocking the binding of HuR to adipogenic transcription factor mRNAs. *Int J Cancer* 145: 1809–1821, 2019. doi:10.1002/ijc.32236.
171. **Siang DT**, **Lim YC**, **Kyaw AM**, **Win KN**, **Chia SY**, **Degirmenci U**, **Hu X**, **Tan BC**, **Walet AC**, **Sun L**, **Xu D.** The RNA-binding protein HuR is a negative regulator in adipogenesis. *Nat Commun* 11: 213, 2020. doi:10.1038/s41467-019-14001-8.
172. **Karbiener M**, **Fischer C**, **Nowitsch S**, **Opriessnig P**, **Papak C**, **Ailhaud G**, **Dani C**, **Amri EZ**, **Scheideler M.** microRNA miR-27b impairs human adipocyte differentiation and targets PPARγ.

Biochem Biophys Res Commun 390: 247–251, 2009. doi:10.1016/j.bbrc.2009.09.098.

173. **Liu W**, **Ma C**, **Yang B**, **Yin C**, **Zhang B**, **Xiao Y.** LncRNA Gm15290 sponges miR-27b to promote PPARγ-induced fat deposition and contribute to body weight gain in mice. *Biochem Biophys Res Commun* 493: 1168–1175, 2017. doi:10.1016/j.bbrc.2017.09.114.
174. **Hu X**, **Tang J**, **Hu X**, **Bao P**, **Pan J**, **Chen Z**, **Xian J.** MiR-27b impairs adipocyte differentiation of human adipose tissue-derived mesenchymal stem cells by targeting LPL. *Cell Physiol Biochem* 47: 545–555, 2018. doi:10.1159/000489988.
175. **Picard F**, **Kurtev M**, **Chung N**, **Topark-Ngarm A**, **Senawong T**, **Machado De Oliveira R**, **Leid M**, **McBurney MW**, **Guarente L.** Sirt1 promotes fat mobilization in white adipocytes by repressing PPAR-γ. *Nature* 429: 771–776, 2004. [Erratum in *Nature* 430: 921, 2004]. doi:10.1038/nature02583.
176. **Li M**, **Sun X**, **Cai H**, **Sun Y**, **Plath M**, **Li C**, **Lan X**, **Lei C**, **Lin F**, **Bai Y**, **Chen H.** Long non-coding RNA ADNCR suppresses adipogenic differentiation by targeting miR-204. *Biochim Biophys Acta* 1859: 871–882, 2016. doi:10.1016/j.bbagrm.2016.05.003.
177. **Li D**, **Liu Y**, **Gao W**, **Han J**, **Yuan R**, **Zhang M**, **Ge Z.** LncRNA HCG11 inhibits adipocyte differentiation in human adipose-derived mesenchymal stem cells by sponging miR-204-5p to upregulate SIRT1. *Cell Transplant* 29: 963689720968090, 2020. doi:10.1177/0963689720968090.
178. **Zhu Y**, **Gui W**, **Lin X**, **Li H.** Knock-down of circular RNA H19 induces human adipose-derived stem cells adipogenic differentiation via a mechanism involving the polypyrimidine tract-binding protein 1. *Exp Cell Res* 387: 111753, 2020. doi:10.1016/j.yexcr.2019.111753.
179. **Xu B**, **Gerin I**, **Miao H**, **Vu-Phan D**, **Johnson CN**, **Xu R**, **Chen XW**, **Cawthorn WP**, **MacDougald OA**, **Koenig RJ.** Multiple roles for the non-coding RNA SRA in regulation of adipogenesis and insulin sensitivity. *PLoS One* 5: e14199, 2010. doi:10.1371/journal.pone.0014199.
180. **Cristancho AG**, **Lazar MA.** Forming functional fat: a growing understanding of adipocyte differentiation. *Nat Rev Mol Cell Biol* 12: 722–734, 2011. doi:10.1038/nrm3198.
181. **Landgraf K**, **Klöting N**, **Gericke M**, **Maixner N**, **Guiu-Jurado E**, **Scholz M**, **Witte AV**, **Beyer F**, **Schwartze JT**, **Lacher M**, **Villringer A**, **Kovacs P**, **Rudich A**, **Blüher M**, **Kiess W**, **Körner A.** The obesity-susceptibility gene TMEM18 promotes adipogenesis through activation of PPARG. *Cell Rep* 33: 108295, 2020. doi:10.1016/j.celrep.2020.108295.
182. **Larder R**, **Sim MF**, **Gulati P**, **Antrobus R**, **Tung YC**, **Rimmington D**, **Ayuso E**, **Polex-Wolf J**, **Lam BY**, **Dias C**, **Logan DW**, **Virtue S**, **Bosch F**, **Yeo GS**, **Saudek V**, **O'Rahilly S**, **Coll AP.** Obesity-associated gene TMEM18 has a role in the central control of appetite and body weight regulation. *Proc Natl Acad Sci USA* 114: 9421–9426, 2017. doi:10.1073/pnas.1707310114.
183. **Yuan Y**, **Cao X**, **Hu J**, **Li J**, **Shen D**, **You L**, **Cui X**, **Wang X**, **Zhou Y**, **Gao Y**, **Zhu L**, **Xu P**, **Ji C**, **Guo X**, **Wen J.** The role and possible mechanism of lncRNA AC092159.2 in modulating adipocyte differentiation. *J Mol Endocrinol* 62: 137–148, 2019. doi:10.1530/JME-18-0215.
184. **Chen J**, **Liu Y**, **Lu S**, **Yin L**, **Zong C**, **Cui S**, **Qin D**, **Yang Y**, **Guan Q**, **Li X**, **Wang X.** The role and possible mechanism of lncRNA U90926 in modulating 3T3-L1 preadipocyte differentiation. *Int J Obes* 41: 299–308, 2017. doi:10.1038/ijo.2016.189.
185. **Zhu E**, **Zhang J**, **Li Y**, **Yuan H**, **Zhou J**, **Wang B.** Long noncoding RNA Plnc1 controls adipocyte differentiation by regulating peroxisome proliferator-activated receptor γ. *FASEB J* 33: 2396–2408, 2019. doi:10.1096/fj.201800739RRR.
186. **Cooper D**, **Carter G**, **Li P**, **Patel R**, **Watson J**, **Patel N.** Long non-coding RNA NEAT1 associates with SRp40 to temporally regulate PPARγ2 splicing during adipogenesis in 3T3-L1 Cells. *Genes (Basel)* 5: 1050–1063, 2014. doi:10.3390/genes5041050.
187. **Naganuma T**, **Hirose T.** Paraspeckle formation during the biogenesis of long non-coding RNAs. *RNA Biol* 10: 456–461, 2013. doi:10.4161/rna.23547.
188. **Gernapudi R**, **Wolfson B**, **Zhang Y**, **Yao Y**, **Yang P**, **Asahara H**, **Zhou Q.** MicroRNA 140 promotes expression of long noncoding RNA NEAT1 in adipogenesis. *Mol Cell Biol* 36: 30–38, 2016. doi:10.1128/MCB.00702-15.
189. **Firmin FF**, **Oger F**, **Gheeraert C**, **Dubois-Chevalier J**, **Vercoutter-Edouart AS**, **Alzaid F**, **Mazuy C**, **Dehondt H**, **Alexandre J**, **Derudas B**, **Dhalluin Q**, **Ploton M**, **Berthier A**, **Woitrain E**, **Lefebvre T**, **Venteclef N**, **Pattou F**, **Staels B**, **Eeckhoute J**, **Lefebvre P.** The RBM14/CoAA-interacting, long intergenic non-coding RNA Paral1 regulates adipogenesis and coactivates the nuclear receptor PPARγ. *Sci Rep* 7: 14087, 2017. doi:10.1038/s41598-017-14570-y.
190. **Xiao T**, **Liu L**, **Li H**, **Sun Y**, **Luo H**, **Li T**, **Wang S**, **Dalton S**, **Zhao RC**, **Chen R.** Long noncoding RNA ADINR regulates adipogenesis by transcriptionally activating C/EBPα. *Stem Cell Reports* 5: 856–865, 2015. doi:10.1016/j.stemcr.2015.09.007.
191. **Sierra H**, **Cordova M**, **Chen CJ**, **Rajadhyaksha M.** Confocal imaging–guided laser ablation of basal cell carcinomas: an ex vivo study. *J Invest Dermatol* 135: 612–615, 2015. doi:10.1038/jid.2014.371.
192. **Liu Y**, **Wang Y**, **He X**, **Zhang S**, **Wang K**, **Wu H**, **Chen L.** LncRNA TINCR/miR-31-5p/C/EBP-α feedback loop modulates the adipogenic differentiation process in human adipose tissue-derived mesenchymal stem cells. *Stem Cell Res* 32: 35–42, 2018. doi:10.1016/j.scr.2018.08.016.
193. **Prestwich TC**, **Macdougald OA.** Wnt/beta-catenin signaling in adipogenesis and metabolism. *Curr Opin Cell Biol* 19: 612–617, 2007. doi:10.1016/j.ceb.2007.09.014.
194. **Jeon M**, **Rahman N**, **Kim YS.** Wnt/β-catenin signaling plays a distinct role in methyl gallate-mediated inhibition of adipogenesis. *Biochem Biophys Res Commun* 479: 22–27, 2016. doi:10.1016/j.bbrc.2016.08.178.
195. **Wang Z**, **Luo Z**, **Dai Z**, **Zhong Y**, **Liu X**, **Zuo C.** Long non-coding RNA lnc-OAD is required for adipocyte differentiation in 3T3-L1 preadipocytes. *Biochem Biophys Res Commun* 511: 753–758, 2019. doi:10.1016/j.bbrc.2019.02.133.
196. **Kanazawa A**, **Tsukada S**, **Kamiyama M**, **Yanagimoto T**, **Nakajima M**, **Maeda S.** Wnt5b partially inhibits canonical Wnt/β-catenin signaling pathway and promotes adipogenesis in 3T3-L1 preadipocytes. *Biochem Biophys Res Commun* 330: 505–510, 2005. doi:10.1016/j.bbrc.2005.03.007.
197. **Zhang T**, **Liu H**, **Mao R**, **Yang H**, **Zhang Y**, **Zhang Y**, **Guo P**, **Zhan D**, **Xiang B**, **Liu Y.** The lncRNA RP11-142A22.4 promotes adipogenesis by sponging miR-587 to modulate Wnt5β expression. *Cell Death Dis* 11: 475, 2020. doi:10.1038/s41419-020-2550-9.
198. **Fan L**, **Xu H**, **Li D**, **Li H**, **Lu D.** A novel long noncoding RNA, AC092834.1, regulates the adipogenic differentiation of human adipose-derived mesenchymal stem cells via the DKK1/Wnt/β-catenin signaling pathway. *Biochem Biophys Res Commun* 525: 747–754, 2020. doi:10.1016/j.bbrc.2020.02.140.
199. **Jang H**, **Kim M**, **Lee S**, **Kim J**, **Woo DC**, **Kim KW**, **Song K**, **Lee I.** Adipose tissue hyperplasia with enhanced adipocyte-derived stem cell activity in Tc1(C8orf4)-deleted mice. *Sci Rep* 6: 35884, 2016. doi:10.1038/srep35884.
200. **Jung Y**, **Bang S**, **Choi K**, **Kim E**, **Kim Y**, **Kim J**, **Park J**, **Koo H**, **Moon RT**, **Song K**, **Lee I.** TC1 (C8orf4) Enhances the Wnt/β-catenin pathway by relieving antagonistic activity of Chibby. *Cancer Res* 66: 723–728, 2006. doi:10.1158/0008-5472.CAN-05-3124.
201. **Li K**, **Wu Y**, **Yang H**, **Hong P**, **Fang X**, **Hu Y.** H19/miR-30a/C8orf4 axis modulates the adipogenic differentiation process in human adipose tissue-derived mesenchymal stem cells. *J Cell Physiol* 234: 20925–20934, 2019. doi:10.1002/jcp.28697.
202. **Zaragosi LE**, **Wdziekonski B**, **Brigand KL**, **Villageois P**, **Mari B**, **Waldmann R**, **Dani C**, **Barbry P.** Small RNA sequencing reveals miR-642a-3p as a novel adipocyte-specific microRNA and miR-30 as a key regulator of human adipogenesis. *Genome Biol* 12: R64, 2011. doi:10.1186/gb-2011-12-7-r64.
203. **Huang Y**, **Zheng Y**, **Jin C**, **Li X**, **Jia L**, **Li W.** Long non-coding RNA H19 inhibits adipocyte differentiation of bone marrow mesenchymal stem cells through epigenetic modulation of histone deacetylases. *Sci Rep* 6: 28897, 2016. doi:10.1038/srep28897.
204. **Hacisuleyman E**, **Goff LA**, **Trapnell C**, **Williams A**, **Henao-Mejia J**, **Sun L**, **McClanahan P**, **Hendrickson DG**, **Sauvageau M**, **Kelley DR**, **Morse M**, **Engreitz J**, **Lander ES**, **Guttman M**, **Lodish HF**, **Flavell R**, **Raj A**, **Rinn JL.** Topological organization of multichromosomal regions by the long intergenic noncoding RNA Firre. *Nat Struct Mol Biol* 21: 198–206, 2014. doi:10.1038/nsmb.2764.
205. **Zhang HH**, **Huang J**, **Düvel K**, **Boback B**, **Wu S**, **Squillace RM**, **Wu CL**, **Manning BD.** Insulin stimulates adipogenesis through the Akt-TSC2-mTORC1 pathway. *PLoS One* 4: e6189, 2009. doi:10.1371/journal.pone.0006189.
206. **Cai R**, **Tang G**, **Zhang Q**, **Yong W**, **Zhang W**, **Xiao J**, **Wei C**, **He C**, **Yang G**, **Pang W.** A novel lnc-RNA, named lnc-ORA, is identified by RNA-Seq analysis, and its knockdown inhibits adipogenesis by

regulating the PI3K/AKT/mTOR signaling pathway. *Cells* 8: 477, 2019. doi:10.3390/cells8050477.

207. **Ballantyne RL**, **Zhang X**, **Nuñez S**, **Xue C**, **Zhao W**, **Reed E**, **Salaheen D**, **Foulkes AS**, **Li M**, **Reilly MP.** Genome-wide interrogation reveals hundreds of long intergenic noncoding RNAs that associate with cardiometabolic traits. *Hum Mol Genet* 25: 3125–3141, 2016. doi:10.1093/hmg/ddw154.
208. **Liu H**, **Li H**, **Jin L**, **Li G**, **Hu S**, **Ning C**, **Guo J**, **Shuai S**, **Li X**, **Li M.** Long noncoding RNA GAS5 suppresses 3T3-L1 cells adipogenesis through miR-21a-5p/PTEN signal pathway. *DNA Cell Biol* 37: 767–777, 2018. doi:10.1089/dna.2018.4264.
209. **Li M**, **Xie Z**, **Wang P**, **Li J**, **Liu W**, **Tang S**, **Liu Z**, **Wu X**, **Wu Y**, **Shen H.** The long noncoding RNA GAS5 negatively regulates the adipogenic differentiation of MSCs by modulating the miR-18a/CTGF axis as a ceRNA. *Cell Death Dis* 9: 554, 2018. doi:10.1038/s41419-018-0627-5.
210. **Tan JT**, **McLennan SV**, **Song WW**, **Lo LW**, **Bonner JG**, **Williams PF**, **Twigg SM.** Connective tissue growth factor inhibits adipocyte differentiation. *Am J Physiol Cell Physiol* 295: C740–C751, 2008. doi:10.1152/ajpcell.00333.2007.
211. **Ambele MA**, **Dessels C**, **Durandt C**, **Pepper MS.** Genome-wide analysis of gene expression during adipogenesis in human adipose-derived stromal cells reveals novel patterns of gene expression during adipocyte differentiation. *Stem Cell Res* 16: 725–734, 2016. doi:10.1016/j.scr.2016.04.011.
212. **Lo KA**, **Huang S**, **Walet AC**, **Zhang ZC**, **Leow MK**, **Liu M**, **Sun L.** Adipocyte long-noncoding RNA transcriptome analysis of obese mice identified Lnc-Leptin, which regulates leptin. *Diabetes* 67: 1045–1056, 2018. doi:10.2337/db17-0526.
213. **Rosen ED**, **MacDougald OA.** Adipocyte differentiation from the inside out. *Nat Rev Mol Cell Biol* 7: 885–896, 2006. doi:10.1038/nrm2066.
214. **Huang Y**, **Jin C**, **Zheng Y**, **Li X**, **Zhang S**, **Zhang Y**, **Jia L**, **Li W.** Knockdown of lncRNA MIR31HG inhibits adipocyte differentiation of human adipose-derived stem cells via histone modification of FABP4. *Sci Rep* 7: 8080, 2017. doi:10.1038/s41598-017-08131-6.
215. **Liu S**, **Xu R**, **Gerin I**, **Cawthorn WP**, **Macdougald OA**, **Chen XW**, **Saltiel AR**, **Koenig RJ**, **Xu B.** SRA regulates adipogenesis by modulating p38/JNK phosphorylation and stimulating insulin receptor gene expression and downstream signaling. *PLoS One* 9: e95416, 2014. doi:10.1371/journal.pone.0095416.
216. **Dempersmier J**, **Sambeat A**, **Gulyaeva O**, **Paul SM**, **Hudak CS**, **Raposo HF**, **Kwan HY**, **Kang C**, **Wong RH**, **Sul HS.** Cold-inducible Zfp516 activates UCP1 transcription to promote browning of white fat and development of brown fat. *Mol Cell* 57: 235–246, 2015. doi:10.1016/j.molcel.2014.12.005.
217. **Liu S**, **Sheng L**, **Miao H**, **Saunders TL**, **MacDougald OA**, **Koenig RJ**, **Xu B.** SRA gene knockout protects against diet-induced obesity and improves glucose tolerance. *J Biol Chem* 289: 13000–13009, 2014. doi:10.1074/jbc.M114.564658.
218. **Kawashima H**, **Takano H**, **Sugita S**, **Takahara Y**, **Sugimura K**, **Nakatani T.** A novel steroid receptor co-activator protein (SRAP) as an alternative form of steroid receptor RNA-activator gene: expression in prostate cancer cells and enhancement of androgen receptor activity. *Biochem J* 369: 163–171, 2003. doi:10.1042/bj20020743.
219. **Stern JH**, **Rutkowski JM**, **Scherer PE.** Adiponectin, leptin, and fatty acids in the maintenance of metabolic homeostasis through adipose tissue crosstalk. *Cell Metab* 23: 770–784, 2016. doi:10.1016/j.cmet.2016.04.011.
220. **Fu Y**, **Luo N**, **Klein RL**, **Garvey WT.** Adiponectin promotes adipocyte differentiation, insulin sensitivity, and lipid accumulation. *J Lipid Res* 46: 1369–1379, 2005. doi:10.1194/jlr.M400373-JLR200.
221. **Cai R**, **Sun Y**, **Qimuge N**, **Wang G**, **Wang Y**, **Chu G**, **Yu T**, **Yang G**, **Pang W.** Adiponectin AS lncRNA inhibits adipogenesis by transferring from nucleus to cytoplasm and attenuating Adiponectin mRNA translation. *Biochim Biophys Acta Mol Cell Biol Lipids* 1863: 420–432, 2018. [doi:10.1016/j.bbalip.2018.01.005.
222. **Karczewska-Kupczewska M**, **Nikołajuk A**, **Majewski R**, **Filarski R**, **Stefanowicz M**, **Matulewicz N**, **Straôczkowski M.** Changes in adipose tissue lipolysis gene expression and insulin sensitivity after weight loss. *Endocr Connect* 9: 90–100, 2020. doi:10.1530/EC-19-0507.
223. **Gao H**, **Kerr A**, **Jiao H**, **Hon CC**, **Rydén M**, **Dahlman I**, **Arner P.** Long non-coding RNAs associated with metabolic traits in human white adipose tissue. *EBioMedicine* 30: 248–260, 2018. doi:10.1016/j.ebiom.2018.03.010.
225. **Ding C**, **Lim YC**, **Chia SY**, **Walet AC**, **Xu S**, **Lo KA**, **Zhao Y**, **Zhu D**, **Shan Z**, **Chen Q**, **Leow MK**, **Xu D**, **Sun L.** De novo reconstruction of human adipose transcriptome reveals conserved lncRNAs as regulators of brown adipogenesis. *Nat Commun* 9: 1329, 2018. doi:10.1038/s41467-018-03754-3.
226. **You L**, **Zhou Y**, **Cui X**, **Wang X**, **Sun Y**, **Gao Y**, **Wang X**, **Wen J**, **Xie K**, **Tang R**, **Ji C**, **Guo X.** GM13133 is a negative regulator in mouse white adipocytes differentiation and drives the characteristics of brown adipocytes. *J Cell Physiol* 233: 313–324, 2018. doi:10.1002/jcp.25878.
227. **Iwase M**, **Sakai S**, **Seno S**, **Yeh YS**, **Kuo T**, **Takahashi H**, **Nomura W**, **Jheng HF**, **Horton P**, **Osato N**, **Matsuda H**, **Inoue K**, **Kawada T**, **Goto T.** Long non-coding RNA 2310069B03Rik functions as a suppressor of Ucp1 expression under prolonged cold exposure in murine beige adipocytes. *Biosci Biotechnol Biochem* 84: 305–313, 2020. doi:10.1080/09168451.2019.1677451.
228. **Iizuka K**, **Wu W**, **Horikawa Y**, **Saito M**, **Takeda J.** Feedback looping between ChREBP and PPARalpha; in the regulation of lipid metabolism in brown adipose tissues. *Endocr J* 60: 1145–1153, 2013. doi:10.1507/endocrj.EJ13-0079.
229. **Feng J**, **Xu H**, **Pan F**, **Hu J**, **Wu Y**, **Lin N**, **Zhang X**, **Ji C**, **Hu Y**, **Zhong H**, **Yan L**, **Zhong T**, **Cui X.** An integrated analysis of mRNA and lncRNA expression profiles indicates their potential contribution to brown fat dysfunction with aging. *Front Endocrinol (Lausanne)* 11: 46, 2020. doi:10.3389/fendo.2020.00046.
230. **Zhang X**, **Xue C**, **Lin J**, **Ferguson JF**, **Weiner A**, **Liu W**, **Han Y**, **Hinkle C**, **Li W**, **Jiang H**, **Gosai S**, **Hachet M**, **Garcia BA**, **Gregory BD**, **Soccio RE**, **Hogenesch JB**, **Seale P**, **Li M**, **Reilly MP.** Interrogation of nonconserved human adipose lincRNAs identifies a regulatory role of linc-ADAL in adipocyte metabolism. *Sci Transl Med* 10: eaar5987, 2018. doi:10.1126/scitranslmed.aar5987.
231. **Yubero P**, **Barberá MJ**, **Alvarez R**, **Viñas O**, **Mampel T**, **Iglesias R**, **Villarroya F**, **Giralt M.** Dominant negative regulation by c-Jun of transcription of the uncoupling protein-1 gene through a proximal cAMP-regulatory element: a mechanism for repressing basal and norepinephrine-induced expression of the gene before brown adipocyte differentiation. *Mol Endocrinol* 12: 1023–1037, 1998. doi:10.1210/mend.12.7.0137.
232. **Chen Z**, **Li JL**, **Lin S**, **Cao C**, **Gimbrone NT**, **Yang R**, **Fu DA**, **Carper MB**, **Haura EB**, **Schabath MB**, **Lu J**, **Amelio AL**, **Cress WD**, **Kaye FJ**, **Wu L.** cAMP/CREB-regulated LINC00473 marks LKB1-inactivated lung cancer and mediates tumor growth. *J Clin Invest* 126: 2267–2279, 2016. doi:10.1172/JCI85250.
233. **Tran KV**, **Brown EL**, **DeSouza T**, **Jespersen NZ**, **Nandrup-Bus C**, **Yang Q**, **Yang Z**, **Desai A**, **Min SY**, **Rojas-Rodriguez R**, **Lundh M**, **Feizi A**, **Willenbrock H**, **Larsen TJ**, **Severinsen MC**, **Malka K**, **Mozzicato AM**, **Deshmukh AS**, **Emanuelli B**, **Pedersen BK**, **Fitzgibbons T**, **Scheele C**, **Corvera S**, **Nielsen S.** Human thermogenic adipocyte regulation by the long noncoding RNA LINC00473. *Nat Metab* 2: 397–412, 2020. doi:10.1038/s42255-020-0205-x.
234. **Cao W**, **Medvedev AV**, **Daniel KW**, **Collins S.** beta-Adrenergic activation of p38 MAP kinase in adipocytes: cAMP induction of the uncoupling protein 1 (UCP1) gene requires p38 MAP kinase. *J Biol Chem* 276: 27077–27082, 2001. doi:10.1074/jbc.M101049200.
235. **Cui X**, **You L**, **Li Y**, **Zhu L**, **Zhang F**, **Xie K**, **Cao Y**, **Ji C**, **Guo X.** A transcribed ultraconserved noncoding RNA, uc.417, serves as a negative regulator of brown adipose tissue thermogenesis. *FASEB J* 30: 4301–4312, 2016. doi:10.1096/fj.201600694R.
236. **Shapira SN**, **Seale P.** Transcriptional control of brown and beige fat development and function. *Obesity (Silver Spring)* 27: 13–21, 2019. doi:10.1002/oby.22334.
237. **Zhao XY**, **Li S**, **Wang GX**, **Yu Q**, **Lin JD.** A long noncoding RNA transcriptional regulatory circuit drives thermogenic adipocyte differentiation. *Mol Cell* 55: 372–382, 2014. doi:10.1016/j.molcel.2014.06.004.
238. **Mi L**, **Zhao XY**, **Li S**, **Yang G**, **Lin JD.** Conserved function of the long noncoding RNA Blnc1 in brown adipocyte differentiation. *Mol Metab* 6: 101–110, 2017. doi:10.1016/j.molmet.2016.10.010.
239. **Alvarez-Dominguez JR**, **Bai Z**, **Xu D**, **Yuan B**, **Lo KA**, **Yoon MJ**, **Lim YC**, **Knoll M**, **Slavov N**, **Chen S**, **Peng C**, **Lodish HF**, **Sun L.** De Novo Reconstruction of Adipose Tissue Transcriptomes Reveals Long Non-coding RNA Regulators of Brown Adipocyte Development. *Cell*

Metab 21: 764–776, 2015. [Erratum in *Cell Metab* 21: 918, 2015]. doi:10.1016/j.cmet.2015.04.003.

240. **Bai Z**, **Chai XR**, **Yoon MJ**, **Kim HJ**, **Lo KA**, **Zhang ZC**, **Xu D**, **Siang DT**, **Walet AC**, **Xu SH**, **Chia SY**, **Chen P**, **Yang H**, **Ghosh S**, **Sun L.** Dynamic transcriptome changes during adipose tissue energy expenditure reveal critical roles for long noncoding RNA regulators. *PLOS Biol* 15: e2002176, 2017. doi:10.1371/journal.pbio.2002176.
241. **Wu Z**, **Puigserver P**, **Andersson U**, **Zhang C**, **Adelmant G**, **Mootha V**, **Troy A**, **Cinti S**, **Lowell B**, **Scarpulla RC**, **Spiegelman BM.** Mechanisms controlling mitochondrial biogenesis and respiration through the thermogenic coactivator PGC-1. *Cell* 98: 115–124, 1999. doi:10.1016/S0092-8674(00)80611-X.
242. **Xiong Y**, **Yue F**, **Jia Z**, **Gao Y**, **Jin W**, **Hu K**, **Zhang Y**, **Zhu D**, **Yang G**, **Kuang S.** A novel brown adipocyte-enriched long non-coding RNA that is required for brown adipocyte differentiation and sufficient to drive thermogenic gene program in white adipocytes. *Biochim Biophys Acta Mol Cell Biol Lipids* 1863: 409–419, 2018. doi:10.1016/j.bbalip.2018.01.008.
243. **Armani A**, **Cinti F**, **Marzolla V**, **Morgan J**, **Cranston GA**, **Antelmi A**, **Carpinelli G**, **Canese R**, **Pagotto U**, **Quarta C**, **Malorni W**, **Matarrese P**, **Marconi M**, **Fabbri A**, **Rosano G**, **Cinti S**, **Young MJ**, **Caprio M.** Mineralocorticoid receptor antagonism induces browning of white adipose tissue through impairment of autophagy and prevents adipocyte dysfunction in high-fat-diet-fed mice. *FASEB J* 28: 3745–3757, 2014. doi:10.1096/fj.13-245415.
244. **Altshuler-Keylin S**, **Shinoda K**, **Hasegawa Y**, **Ikeda K**, **Hong H**, **Kang Q**, **Yang Y**, **Perera RM**, **Debnath J**, **Kajimura S.** Beige adipocyte maintenance is regulated by autophagy-induced mitochondrial clearance. *Cell Metab* 24: 402–419, 2016. doi:10.1016/j.cmet.2016.08.002.
245. **Wang Y**, **Hua S**, **Cui X**, **Cao Y**, **Wen J**, **Chi X**, **Pang JC**, **You L.** The effect of FOXC2-AS1 on white adipocyte browning and the possible regulatory mechanism. *Front Endocrinol (Lausanne)* 11: 565483, 2020. doi:10.3389/fendo.2020.565483.
246. **Wade PA.** Methyl CpG-binding proteins and transcriptional repression. *BioEssays* 23: 1131–1137, 2001. doi:10.1002/bies.10008.
247. **Schmidt E**, **Dhaouadi I**, **Gaziano I**, **Oliverio M**, **Klemm P**, **Awazawa M**, **Mitterer G**, **Fernandez-Rebollo E**, **Pradas-Juni M**, **Wagner W**, **Hammerschmidt P**, **Loureiro R**, **Kiefer C**, **Hansmeier NR**, **Khani S**, **Bergami M**, **Heine M**, **Ntini E**, **Frommolt P**, **Zentis P**, **Ørom UA**, **Heeren J**, **Blüher M**, **Bilban M**, **Kornfeld JW.** LincRNA H19 protects from dietary obesity by constraining expression of monoallelic genes in brown fat. *Nat Commun* 9: 3622, 2018. doi:10.1038/s41467-018-05933-8.
248. **Hollander AP**, **Dickinson SC**, **Kafienah W.** Stem cells and cartilage development: complexities of a simple tissue. *Stem Cells* 28: 1992–1996, 2010. doi:10.1002/stem.534.
249. **Poole AR**, **Kojima T**, **Yasuda T**, **Mwale F**, **Kobayashi M**, **Laverty S.** Composition and structure of articular cartilage: a template for tissue repair. *Clin Orthop Relat Res* 391: S26–S33, 2001. doi:10.1097/00003086-200110001-00004.
250. **Desai S**, **Jayasuriya CT.** Implementation of endogenous and exogenous mesenchymal progenitor cells for skeletal tissue regeneration and repair. *Bioengineering (Basel)* 7: 86, 2020. doi:10.3390/bioengineering7030086.
251. **Liao J**, **Hu N**, **Zhou N**, **Lin L**, **Zhao C**, **Yi S**, **Fan T**, **Bao W**, **Liang X**, **Chen H**, **Xu W**, **Chen C**, **Cheng Q**, **Zeng Y**, **Si W**, **Yang Z**, **Huang W.** Sox9 potentiates BMP2-induced chondrogenic differentiation and inhibits BMP2-induced osteogenic differentiation. *PLoS One* 9: e89025, 2014. doi:10.1371/journal.pone.0089025.
252. **Nasrabadi D**, **Rezaeiani S**, **Eslaminejad MB**, **Shabani A.** Improved protocol for chondrogenic differentiation of bone marrow derived mesenchymal stem cells—effect of PTHrP and FGF-2 on TGFβ1/BMP2-induced chondrocytes hypertrophy. *Stem Cell Rev Rep* 14: 755–766, 2018. doi:10.1007/s12015-018-9816-y.
253. **Zhou N**, **Li Q**, **Lin X**, **Hu N**, **Liao JY**, **Lin LB**, **Zhao C**, **Hu ZM**, **Liang X**, **Xu W**, **Chen H**, **Huang W.** BMP2 induces chondrogenic differentiation, osteogenic differentiation and endochondral ossification in stem cells. *Cell Tissue Res* 366: 101–111, 2016. doi:10.1007/s00441-016-2403-0.
254. **Xiao Y**, **Yan X**, **Yang Y**, **Ma X.** Downregulation of long noncoding RNA HOTAIRM1 variant 1 contributes to osteoarthritis via regulating miR-125b/BMPR2 axis and activating JNK/MAPK/ERK pathway. *Biomed Pharmacother* 109: 1569–1577, 2019. doi:10.1016/j.biopha.2018.10.181.
255. **Carlson HL**, **Quinn JJ**, **Yang YW**, **Thornburg CK**, **Chang HY**, **Stadler HS.** LncRNA-HIT functions as an epigenetic regulator of chondrogenesis through its recruitment of p100/CBP complexes. *PLoS Genet* 11: e1005680, 2015. doi:10.1371/journal.pgen.1005680.
256. **Rux DR**, **Song JY**, **Swinehart IT**, **Pineault KM**, **Schlientz AJ**, **Trulik KG**, **Goldstein SA**, **Kozloff KM**, **Lucas D**, **Wellik DM.** Regionally restricted Hox function in adult bone marrow multipotent mesenchymal stem/stromal cells. *Dev Cell* 39: 653–666, 2016. doi:10.1016/j.devcel.2016.11.008.
257. **Knosp WM**, **Scott V**, **Bächinger HP**, **Stadler HS.** HOXA13 regulates the expression of bone morphogenetic proteins 2 and 7 to control distal limb morphogenesis. *Development* 131: 4581–4592, 2004. doi:10.1242/dev.01327.
258. **Gross S**, **Krause Y**, **Wuelling M**, **Vortkamp A.** Hoxa11 and Hoxd11 regulate chondrocyte differentiation upstream of Runx2 and Shox2 in mice. *PLoS One* 7: e43553, 2012. doi:10.1371/journal.pone.0043553.
259. **Kim D**, **Song J**, **Han J**, **Kim Y**, **Chun CH**, **Jin EJ.** Two non-coding RNAs, MicroRNA-101 and HOTTIP contribute cartilage integrity by epigenetic and homeotic regulation of integrin-α1. *Cell Signal* 25: 2878–2887, 2013. doi:10.1016/j.cellsig.2013.08.034.
260. **Varas L**, **Ohlsson LB**, **Honeth G**, **Olsson A**, **Bengtsson T**, **Wiberg C**, **Bockermann R**, **Järnum S**, **Richter J**, **Pennington D**, **Johnstone B**, **Lundgren-Åkerlund E**, **Kjellman C.** α10 Integrin expression is upregulated on fibroblast growth factor-2-treated mesenchymal stem cells with improved chondrogenic differentiation potential. *Stem Cells Dev* 16: 965–978, 2007. doi:10.1089/scd.2007.0049.
261. **Gao Y**, **Liu S**, **Huang J**, **Guo W**, **Chen J**, **Zhang L**, **Zhao B**, **Peng J**, **Wang A**, **Wang Y**, **Xu W**, **Lu S**, **Yuan M**, **Guo Q.** The ECM-cell interaction of cartilage extracellular matrix on chondrocytes. *Biomed Res Int* 2014: 648459, 2014. doi:10.1155/2014/648459.
262. **Zhou Z**, **Xie J**, **Lee D**, **Liu Y**, **Jung J**, **Zhou L**, **Xiong S**, **Mei L**, **Xiong WC.** Neogenin regulation of BMP-induced canonical Smad signaling and endochondral bone formation. *Dev Cell* 19: 90–102, 2010. doi:10.1016/j.devcel.2010.06.016.
263. **Wang W**, **Ding Y**, **Xu Y**, **Yang H**, **Liu W**, **Wang H**, **Chen C**, **Liu R**, **Li S.** Comprehensive analysis of long noncoding RNAs and mRNAs expression profiles and functional networks during chondrogenic differentiation of murine ATDC5 cells. *Acta Biochim Biophys Sin (Shanghai)* 51: 778–790, 2019. doi:10.1093/abbs/gmz064.
264. **Kim J**, **Shim M.** Prostaglandin F2α receptor (FP) signaling regulates Bmp signaling and promotes chondrocyte differentiation. *Biochim Biophys Acta* 1853: 500–512, 2015. [doi:10.1016/j.bbamcr.2014.12.003.
265. **Ishikawa T**, **Nishida T**, **Ono M**, **Takarada T**, **Nguyen HT**, **Kurihara S**, **Furumatsu T**, **Murase Y**, **Takigawa M**, **Oohashi T**, **Kamioka H**, **Kubota S.** Physiological role of urothelial cancer-associated one long noncoding RNA in human skeletogenic cell differentiation. *J Cell Physiol* 233: 4825–4840, 2018. doi:10.1002/jcp.26285.
266. **Shu T**, **He L**, **Wang X**, **Pang M**, **Yang B**, **Feng F**, **Wu Z**, **Liu C**, **Zhang S**, **Liu B**, **Wang Q**, **Rong L.** Long noncoding RNA UCA1 promotes chondrogenic differentiation of human bone marrow mesenchymal stem cells via miRNA-145-5p/SMAD5 and miRNA-124-3p/SMAD4 axis. *Biochem Biophys Res Commun* 514: 316–322, 2019. doi:10.1016/j.bbrc.2019.04.140.
267. **Yang B**, **Guo H**, **Zhang Y**, **Chen L**, **Ying D**, **Dong S.** MicroRNA-145 regulates chondrogenic differentiation of mesenchymal stem cells by targeting Sox9. *PLoS One* 6: e21679, 2011. doi:10.1371/journal.pone.0021679.
268. **Zhang L**, **Sun X**, **Chen S**, **Yang C**, **Shi B**, **Zhou L**, **Zhao J.** Long noncoding RNA DANCR regulates miR-1305-Smad 4 axis to promote chondrogenic differentiation of human synovium-derived mesenchymal stem cells. *Biosci Rep* 37: BSR20170347, 2017. doi:10.1042/BSR20170347.
269. **Akiyama H**, **Lyons JP**, **Mori-Akiyama Y**, **Yang X**, **Zhang R**, **Zhang Z**, **Deng JM**, **Taketo MM**, **Nakamura T**, **Behringer RR**, **McCrea PD**, **de Crombrugghe B.** Interactions between Sox9 and beta-catenin control chondrocyte differentiation. *Genes Dev* 18: 1072–1087, 2004. doi:10.1101/gad.1171104.
270. **Kondo M**, **Yamaoka K**, **Sakata K**, **Sonomoto K**, **Lin L**, **Nakano K**, **Tanaka Y.** Contribution of the interleukin-6/STAT-3 signaling pathway to chondrogenic differentiation of human mesenchymal stem

cells. *Arthritis Rheumatol* 67: 1250–1260, 2015. doi:10.1002/art.39036.
271. **Sahni M**, **Ambrosetti DC**, **Mansukhani A**, **Gertner R**, **Levy D**, **Basilico C.** FGF signaling inhibits chondrocyte proliferation and regulates bone development through the STAT-1 pathway. *Genes Dev* 13: 1361–1366, 1999. doi:10.1101/gad.13.11.1361.
272. **Legeai-Mallet L**, **Benoist-Lasselin C**, **Munnich A**, **Bonaventure J.** Overexpression of FGFR3, Stat1, Stat5 and p21Cip1 correlates with phenotypic severity and defective chondrocyte differentiation in FGFR3-related chondrodysplasias. *Bone* 34: 26–36, 2004. doi:10.1016/j.bone.2003.09.002.
273. **Morimoto H**, **Baba R**, **Haneji T**, **Doi Y.** Double-stranded RNA-dependent protein kinase regulates insulin-stimulated chondrogenesis in mouse clonal chondrogenic cells, ATDC-5. *Cell Tissue Res* 351: 41–47, 2013. doi:10.1007/s00441-012-1521-6.
274. **Huynh NP**, **Gloss CC**, **Lorentz J**, **Tang R**, **Brunger JM**, **McAlinden A**, **Zhang B**, **Guilak F.** Long non-coding RNA GRASLND enhances chondrogenesis via suppression of the interferon type II signaling pathway. *Elife* 9: e49558, 2020. doi:10.7554/eLife.49558.
275. **Millward-Sadler SJ**, **Khan NS**, **Bracher MG**, **Wright MO**, **Salter DM.** Roles for the interleukin-4 receptor and associated JAK/STAT proteins in human articular chondrocyte mechanotransduction. *Osteoarthritis Cartilage* 14: 991–1001, 2006. doi:10.1016/j.joca.2006.03.013.
276. **Pang HL**, **Zhao QQ**, **Ma Y**, **Song YL**, **Min J**, **Lu JR**, **Li H**, **Zhao DQ.** Long noncoding RNA H19 participates in the regulation of adipose-derived stem cells cartilage differentiation. *Stem Cells Int* 2019: 2139814, 2019. doi:10.1155/2019/2139814.
277. **Augello A**, **De Bari C.** The regulation of differentiation in mesenchymal stem cells. *Hum Gene Ther* 21: 1226–1238, 2010. doi:10.1089/hum.2010.173.
278. **Bien-Willner GA**, **Stankiewicz P**, **Lupski JR.** SOX9cre1, a cis-acting regulatory element located 1.1 Mb upstream of SOX9, mediates its enhancement through the SHH pathway. *Hum Mol Genet* 16: 1143–1156, 2007. doi:10.1093/hmg/ddm061.
279. **Maass PG**, **Rump A**, **Schulz H**, **Stricker S**, **Schulze L**, **Platzer K**, **Aydin A**, **Tinschert S**, **Goldring MB**, **Luft FC**, **Bähring S.** A misplaced lncRNA causes brachydactyly in humans. *J Clin Invest* 122: 3990–4002, 2012. doi:10.1172/JCI65508.
280. **Barter MJ**, **Gomez R**, **Hyatt S**, **Cheung K**, **Skelton AJ**, **Xu Y**, **Clark IM**, **Young DA.** The long non-coding RNA ROCR contributes to SOX9 expression and chondrogenic differentiation of human mesenchymal stem cells. *Development* 144: 4510–4521, 2017. doi:10.1242/dev.152504.
281. **Akiyama H**, **Chaboissier MC**, **Martin JF**, **Schedl A**, **de Crombrugghe B.** The transcription factor Sox9 has essential roles in successive steps of the chondrocyte differentiation pathway and is required for expression of Sox5 and Sox6. *Genes Dev* 16: 2813–2828, 2002. doi:10.1101/gad.1017802.
282. **Smits P**, **Li P**, **Mandel J**, **Zhang Z**, **Deng JM**, **Behringer RR**, **de Crombrugghe B**, **Lefebvre V.** The transcription factors L-Sox5 and Sox6 are essential for cartilage formation. *Dev Cell* 1: 277–290, 2001. doi:10.1016/S1534-5807(01)00003-X.
283. **Yang Z**, **Ren Z**, **She R**, **Ao J**, **Wa Q**, **Sun Z**, **Li B**, **Tian X.** miR-23a-3p regulated by LncRNA SNHG5 suppresses the chondrogenic differentiation of human adipose-derived stem cells via targeting SOX6/SOX5. *Cell Tissue Res* 383: 723–733, 2021. doi:10.1007/s00441-020-03289-4.
284. **Ochi K**, **Derfoul A**, **Tuan RS.** A predominantly articular cartilage-associated gene, SCRG1, is induced by glucocorticoid and stimulates chondrogenesis in vitro. *Osteoarthritis Cartilage* 14: 30–38, 2006. doi:10.1016/j.joca.2005.07.015.
285. **Chosa N**, **Ishisaki A.** Two novel mechanisms for maintenance of stemness in mesenchymal stem cells: SCRG1/BST1 axis and cell-cell adhesion through N-cadherin. *Jpn Dent Sci Rev* 54: 37–44, 2018. doi:10.1016/j.jdsr.2017.10.001.
286. **Huang MJ**, **Zhao JY**, **Xu JJ**, **Li J**, **Zhuang YF**, **Zhang XL.** lncRNA ADAMTS9-AS2 controls human mesenchymal stem cell chondrogenic differentiation and functions as a ceRNA. *Mol Ther Nucleic Acids* 18: 533–545, 2019. doi:10.1016/j.omtn.2019.08.027.
287. **Dudek KA**, **Lafont JE**, **Martinez-Sanchez A**, **Murphy CL.** Type II collagen expression is regulated by tissue-specific miR-675 in human articular chondrocytes. *J Biol Chem* 285: 24381–24387, 2010. doi:10.1074/jbc.M110.111328.
288. **Steck E**, **Boeuf S**, **Gabler J**, **Werth N**, **Schnatzer P**, **Diederichs S**, **Richter W.** Regulation of H19 and its encoded microRNA-675 in osteoarthritis and under anabolic and catabolic in vitro conditions. *J Mol Med (Berl)* 90: 1185–1195, 2012. doi:10.1007/s00109-012-0895-y.
289. **Li F**, **Mi R**, **Fan C**, **Zhang P**, **Zhu T**, **Wang Q**, **Lu Y**, **Gu J**, **Zheng Q.** Runx2-interacting genes identified by yeast two-hybrid screening of libraries generated from hypertrophic chondrocytes. *Am J Transl Res* 8: 5465–5474, 2016.
290. **Jonason JH**, **Xiao G**, **Zhang M**, **Xing L**, **Chen D.** Post-translational regulation of Runx2 in bone and cartilage. *J Dent Res* 88: 693–703, 2009. doi:10.1177/0022034509341629.
291. **Komori T.** Molecular mechanism of Runx2-dependent bone development. *Mol Cells* 43: 168–175, 2020. doi:10.14348/molcells.2019.0244.
292. **Dai G**, **Xiao H**, **Zhao C**, **Chen H**, **Liao J**, **Huang W.** LncRNA H19 regulates BMP2-induced hypertrophic differentiation of mesenchymal stem cells by promoting Runx2 phosphorylation. *Front Cell Dev Biol* 8: 580, 2020. doi:10.3389/fcell.2020.00580.
293. **Guo J**, **Chung UI**, **Yang D**, **Karsenty G**, **Bringhurst FR**, **Kronenberg HM.** PTH/PTHrP receptor delays chondrocyte hypertrophy via both Runx2-dependent and -independent pathways. *Dev Biol* 292: 116–128, 2006. doi:10.1016/j.ydbio.2005.12.044.
294. **Saito M**, **Mulati M**, **Talib SZ**, **Kaldis P**, **Takeda S**, **Okawa A**, **Inose H.** The indispensable role of cyclin-dependent kinase 1 in skeletal development. *Sci Rep* 6: 20622, 2016. doi:10.1038/srep20622.
295. **Steinbusch MM**, **Caron MM**, **Surtel DA**, **Friedrich F**, **Lausch E**, **Pruijn GJ**, **Verhesen W**, **Schroen BL**, **van Rhijn LW**, **Zabel B**, **Welting TJ.** Expression of RMRP RNA is regulated in chondrocyte hypertrophy and determines chondrogenic differentiation. *Sci Rep* 7: 6440, 2017. doi:10.1038/s41598-017-06809-5.
296. **Rogler LE**, **Kosmyna B**, **Moskowitz D**, **Bebawee R**, **Rahimzadeh J**, **Kutchko K**, **Laederach A**, **Notarangelo LD**, **Giliani S**, **Bouhassira E**, **Frenette P**, **Roy-Chowdhury J**, **Rogler CE.** Small RNAs derived from lncRNA RNase MRP have gene-silencing activity relevant to human cartilage-hair hypoplasia. *Hum Mol Genet* 23: 368–382, 2014. doi:10.1093/hmg/ddt427.
297. **Goldfarb KC**, **Cech TR.** Targeted CRISPR disruption reveals a role for RNase MRP RNA in human preribosomal RNA processing. *Genes Dev* 31: 59–71, 2017. doi:10.1101/gad.286963.116.
298. **Bi W**, **Huang W**, **Whitworth DJ**, **Deng JM**, **Zhang Z**, **Behringer RR**, **de Crombrugghe B.** Haploinsufficiency of Sox9 results in defective cartilage primordia and premature skeletal mineralization. *Proc Natl Acad Sci USA* 98: 6698–6703, 2001. doi:10.1073/pnas.111092198.
299. **Topol L**, **Chen W**, **Song H**, **Day TF**, **Yang Y.** Sox9 inhibits Wnt signaling by promoting β-catenin phosphorylation in the nucleus. *J Biol Chem* 284: 3323–3333, 2009. doi:10.1074/jbc.M808048200.
300. **Wuelling M**, **Vortkamp A.** Chondrocyte proliferation and differentiation. *Endocr Dev* 21: 1–11, 2011. doi:10.1159/000328081.
301. **Kozhemyakina E**, **Lassar AB**, **Zelzer E.** A pathway to bone: signaling molecules and transcription factors involved in chondrocyte development and maturation. *Development* 142: 817–831, 2015. doi:10.1242/dev.105536.
302. **Wang Y**, **Fan X**, **Xing L**, **Tian F.** Wnt signaling: a promising target for osteoarthritis therapy. *Cell Commun Signal* 17: 97, 2019. doi:10.1186/s12964-019-0411-x.
303. **Tanthaisong P**, **Imsoonthornruksa S**, **Ngernsoungnern A**, **Ngernsoungnern P**, **Ketudat-Cairns M**, **Parnpai R.** Enhanced chondrogenic differentiation of human umbilical cord Wharton's jelly derived mesenchymal stem cells by GSK-3 inhibitors. *PLoS One* 12: e0168059, 2017. doi:10.1371/journal.pone.0168059.
304. **Ou F**, **Su K**, **Sun J**, **Liao W**, **Yao Y**, **Zheng Y**, **Zhang Z.** The LncRNA ZBED3-AS1 induces chondrogenesis of human synovial fluid mesenchymal stem cells. *Biochem Biophys Res Commun* 487: 457–463, 2017. doi:10.1016/j.bbrc.2017.04.090.
305. **Wang L**, **Li Z**, **Li Z**, **Yu B**, **Wang Y.** Long noncoding RNAs expression signatures in chondrogenic differentiation of human bone marrow mesenchymal stem cells. *Biochem Biophys Res Commun* 456: 459–464, 2015. doi:10.1016/j.bbrc.2014.11.106.
306. **Rowan AD**, **Litherland GJ.** Tribbles and arthritis: what are the links? *Biochem Soc Trans* 43: 1051–1056, 2015. doi:10.1042/BST20150076.
307. **You D**, **Yang C**, **Huang J**, **Gong H**, **Yan M**, **Ni J.** Long non-coding RNA MEG3 inhibits chondrogenic differentiation of synovium-derived mesenchymal stem cells by epigenetically inhibiting TRIB2 via methyltransferase EZH2. *Cell Signal* 63: 109379, 2019. doi:10.1016/j.cellsig.2019.109379.

308. **Yuan SX**, **Wang J**, **Yang F**, **Tao QF**, **Zhang J**, **Wang LL**, **Yang Y**, **Liu H**, **Wang ZG**, **Xu QG**, **Fan J**, **Liu L**, **Sun SH**, **Zhou WP.** Long noncoding RNA DANCR increases stemness features of hepatocellular carcinoma by derepression of CTNNB1. *Hepatology* 63: 499–511, 2016. doi:10.1002/hep.27893.
309. **Zhang L**, **Chen S**, **Bao N**, **Yang C**, **Ti Y**, **Zhou L**, **Zhao J.** Sox4 enhances chondrogenic differentiation and proliferation of human synovium-derived stem cell via activation of long noncoding RNA DANCR. *J Mol Histol* 46: 467–473, 2015. doi:10.1007/s10735-015-9638-z.
310. **Zhang Q**, **Wang S**, **Sheng Y**, **Zhao S**, **Jiang Y**, **Zhou D**, **Yang H.** Downregulation of antidifferentiation noncoding RNA promotes chondrogenic differentiation and calcification of ligamentum flavum-derived mesenchymal stem cells. *J Cell Biochem* 120: 3401–3414, 2019. doi:10.1002/jcb.27611.
311. **Glasson SS**, **Askew R**, **Sheppard B**, **Carito B**, **Blanchet T**, **Ma HL**, **Flannery CR**, **Peluso D**, **Kanki K**, **Yang Z**, **Majumdar MK**, **Morris EA.** Deletion of active ADAMTS5 prevents cartilage degradation in a murine model of osteoarthritis. *Nature* 434: 644–648, 2005. [Erratum in *Nature* 446: 102, 2007]. doi:10.1038/nature03369.
312. **Zhu Y**, **Li R**, **Wen LM.** Long non-coding RNA XIST regulates chondrogenic differentiation of synovium-derived mesenchymal stem cells from temporomandibular joint via miR-27b-3p/ADAMTS-5 axis. *Cytokine* 137: 155352, 2021. doi:10.1016/j.cyto.2020.155352.
313. **Takaishi H**, **Kimura T**, **Dalal S**, **Okada Y**, **D'Armiento J.** Joint diseases and matrix metalloproteinases: a role for MMP-13. *Curr Pharm Biotechnol* 9: 47–54, 2008. doi:10.2174/138920108783497659.
314. **Wang G**, **Bu X**, **Zhang Y**, **Zhao X**, **Kong Y**, **Ma L**, **Niu S**, **Wu B**, **Meng C.** LncRNA-UCA1 enhances MMP-13 expression by inhibiting miR-204-5p in human chondrocytes. *Oncotarget* 8: 91281–91290, 2017. doi:10.18632/oncotarget.20108.
315. **Fang P**, **Zhang LX**, **Hu Y**, **Zhang L**, **Zhou LW.** Long non-coding RNA DANCR induces chondrogenesis by regulating the miR-1275/MMP-13 axis in synovial fluid-derived mesenchymal stem cells. *Eur Rev Med Pharmacol Sci* 23: 10459–10469, 2019. doi:10.26355/eurrev_201912_19685.
316. **Burrage PS**, **Mix KS**, **Brinckerhoff CE.** Matrix metalloproteinases: role in arthritis. *Front Biosci* 11: 529–543, 2006. doi:10.2741/1817.
317. **Yueh YG**, **Gardner DP**, **Kappen C.** Evidence for regulation of cartilage differentiation by the homeobox gene Hoxc-8. *Proc Natl Acad Sci USA* 95: 9956–9961, 1998. doi:10.1073/pnas.95.17.9956.
318. **Kruger C**, **Kappen C.** Expression of cartilage developmental genes in Hoxc8- and Hoxd4-transgenic mice. *PLoS One* 5: e8978, 2010. doi:10.1371/journal.pone.0008978.
319. **Yang H**, **Cao Y**, **Zhang J**, **Liang Y**, **Su X**, **Zhang C**, **Liu H**, **Han X**, **Ge L**, **Fan Z.** DLX5 and HOXC8 enhance the chondrogenic differentiation potential of stem cells from apical papilla via LINC01013. *Stem Cell Res Ther* 11: 271, 2020. doi:10.1186/s13287-020-01791-8.
320. **Vieux-Rochas M**, **Bouhali K**, **Mantero S**, **Garaffo G**, **Provero P**, **Astigiano S**, **Barbieri O**, **Caratozzolo MF**, **Tullo A**, **Guerrini L**, **Lallemand Y**, **Robert B**, **Levi G**, **Merlo GR.** BMP-mediated functional cooperation between Dlx5;Dlx6 and Msx1;Msx2 during mammalian limb development. *PLoS One* 8: e51700, 2013. doi:10.1371/journal.pone.0051700.
321. **Mao G**, **Kang Y**, **Lin R**, **Hu S**, **Zhang Z**, **Li H**, **Liao W**, **Zhang Z.** Long non-coding RNA HOTTIP promotes CCL3 expression and induces cartilage degradation by sponging miR-455-3p. *Front Cell Dev Biol* 7: 161, 2019. doi:10.3389/fcell.2019.00161.
322. **Robert AW**, **Marcon BH**, **Dallagiovanna B**, **Shigunov P.** Adipogenesis, osteogenesis, and chondrogenesis of human mesenchymal stem/stromal cells: a comparative transcriptome approach. *Front cell Dev Biol* 8: 561, 2020. doi:10.3389/fcell.2020.00561.
323. **Yang Q**, **Wan Q**, **Zhang L**, **Li Y**, **Zhang P**, **Li D**, **Feng C**, **Yi F**, **Zhang L**, **Ding X**, **Li H**, **Du Q.** Analysis of LncRNA expression in cell differentiation. *RNA Biol* 15: 413–422, 2018. doi:10.1080/15476286.2018.1441665.
324. **Guess MG**, **Barthel KK**, **Harrison BC**, **Leinwand LA.** miR-30 family microRNAs regulate myogenic differentiation and provide negative feedback on the microRNA pathway. *PLoS One* 10: e0118229, 2015. doi:10.1371/journal.pone.0118229.
325. **Yang L**, **Tsang KY**, **Tang HC**, **Chan D**, **Cheah KS.** Hypertrophic chondrocytes can become osteoblasts and osteocytes in endochondral bone formation. *Proc Natl Acad Sci USA* 111: 12097–12102, 2014. doi:10.1073/pnas.1302703111.
326. **Feng L**, **Yang ZM**, **Li YC**, **Wang HX**, **Lo JH**, **Zhang XT**, **Li G.** Linc-ROR promotes mesenchymal stem cells chondrogenesis and cartilage formation via regulating SOX9 expression. *Osteoarthritis Cartilage* 29: 568–578, 2021. doi:10.1016/j.joca.2020.12.020.
327. **Chen X**, **Yang L**, **Ge D**, **Wang W**, **Yin Z**, **Yan J**, **Cao X**, **Jiang C**, **Zheng S**, **Liang B.** Long non-coding RNA XIST promotes osteoporosis through inhibiting bone marrow mesenchymal stem cell differentiation. *Exp Ther Med* 17: 803–811, 2019. doi:10.3892/etm.2018.7033.
328. **Peng W**, **Deng W**, **Zhang J**, **Pei G**, **Rong Q**, **Zhu S.** Long noncoding RNA ANCR suppresses bone formation of periodontal ligament stem cells via sponging miRNA-758. *Biochem Biophys Res Commun* 503: 815–821, 2018. doi:10.1016/j.bbrc.2018.06.081.
329. **Zhang L**, **Yang C**, **Chen S**, **Wang G**, **Shi B**, **Tao X**, **Zhou L**, **Zhao J.** Long Noncoding RNA DANCR is a positive regulator of proliferation and chondrogenic differentiation in human synovium-derived stem cells. *DNA Cell Biol* 36: 136–142, 2017. doi:10.1089/dna.2016.3544.
330. **Chen Q**, **Shou P**, **Zheng C**, **Jiang M**, **Cao G**, **Yang Q**, **Cao J**, **Xie N**, **Velletri T**, **Zhang X**, **Xu C**, **Zhang L**, **Yang H**, **Hou J**, **Wang Y**, **Shi Y.** Fate decision of mesenchymal stem cells: adipocytes or osteoblasts? *Cell Death Differ* 23: 1128–1139, 2016. doi:10.1038/cdd.2015.168.
331. **Divoux A**, **Karastergiou K**, **Xie H**, **Guo W**, **Perera RJ**, **Fried SK**, **Smith SR.** Identification of a novel lncRNA in gluteal adipose tissue and evidence for its positive effect on preadipocyte differentiation. *Obesity (Silver Spring)* 22: 1781–1785, 2014. doi:10.1002/oby.20793.
332. **Kalwa M**, **Hänzelmann S**, **Otto S**, **Kuo CC**, **Franzen J**, **Joussen S**, **Fernandez-Rebollo E**, **Rath B**, **Koch C**, **Hofmann A**, **Lee SH**, **Teschendorff AE**, **Denecke B**, **Lin Q**, **Widschwendter M**, **Weinhold E**, **Costa IG**, **Wagner W.** The lncRNA HOTAIR impacts on mesenchymal stem cells via triple helix formation. *Nucleic Acids Res* 44: 10631–10643, 2016. doi:10.1093/nar/gkw802.
333. **Jin C**, **Jia L**, **Huang Y**, **Zheng Y**, **Du N**, **Liu Y**, **Zhou Y.** Inhibition of lncRNA MIR31HG promotes osteogenic differentiation of human adipose-derived stem cells. *Stem Cells* 34: 2707–2720, 2016. doi:10.1002/stem.2439.
334. **Yuan H**, **Xu X**, **Feng X**, **Zhu E**, **Zhou J**, **Wang G**, **Tian L**, **Wang B.** A novel long noncoding RNA PGC1β-OT1 regulates adipocyte and osteoblast differentiation through antagonizing miR-148a-3p. *Cell Death Differ* 26: 2029–2045, 2019. doi:10.1038/s41418-019-0296-7.
335. **Ørom UA**, **Derrien T**, **Beringer M**, **Gumireddy K**, **Gardini A**, **Bussotti G**, **Lai F**, **Zytnicki M**, **Notredame C**, **Huang Q**, **Guigo R**, **Shiekhattar R.** Long noncoding RNAs with enhancer-like function in human cells. *Cell* 143: 46–58, 2010. doi:10.1016/j.cell.2010.09.001.
336. **Fatica A**, **Bozzoni I.** Long non-coding RNAs: new players in cell differentiation and development. *Nat Rev Genet* 15: 7–21, 2014. doi:10.1038/nrg3606.
337. **Zhang Z**, **Liu J**, **Zeng Z**, **Fan J**, **Huang S**, **Zhang L**, et al**.** lncRNA Rmst acts as an important mediator of BMP9-induced osteogenic differentiation of mesenchymal stem cells (MSCs) by antagonizing Notch-targeting microRNAs. *Aging (Albany NY)* 11: 12476–12496, 2019. doi:10.18632/aging.102583.
338. **Tran VG**, **Court F**, **Duputié A**, **Antoine E**, **Aptel N**, **Milligan L**, **Carbonell F**, **Lelay-Taha MN**, **Piette J**, **Weber M**, **Montarras D**, **Pinset C**, **Dandolo L**, **Forné T**, **Cathala G.** H19 antisense RNA can up-regulate IGF2 transcription by activation of a novel promoter in mouse myoblasts. *PLoS One* 7: e37923, 2012. doi:10.1371/journal.pone.0037923.
339. **Feng X**, **Lin T**, **Liu X**, **Yang C**, **Yang S**, **Fu D.** Long non-coding RNA BDNF-AS modulates osteogenic differentiation of bone marrow-derived mesenchymal stem cells. *Mol Cell Biochem* 445: 59–65, 2018. doi:10.1007/s11010-017-3251-2.
340. **Sun X**, **Yuan Y**, **Xiao Y**, **Lu Q**, **Yang L**, **Chen C**, **Guo Q.** Long non-coding RNA, Bmcob, regulates osteoblastic differentiation of bone marrow mesenchymal stem cells. *Biochem Biophys Res Commun* 506: 536–542, 2018. doi:10.1016/j.bbrc.2018.09.142.
341. **Li B**, **Han H**, **Song S**, **Fan G**, **Xu H**, **Zhou W**, **Qiu Y**, **Qian C**, **Wang Y**, **Yuan Z**, **Gao Y**, **Zhang Y**, **Zhuang W.** HOXC10 regulates osteogenesis of mesenchymal stromal cells through interaction with its natural antisense transcript lncHOXC-AS3. *Stem Cells* 37: 247–256, 2019. doi:10.1002/stem.2925.
342. **Liao J**, **Yu X**, **Hu X**, **Fan J**, **Wang J**, **Zhang Z**, et al**.** lncRNA H19 mediates BMP9-induced osteogenic differentiation of mesenchymal stem cells (MSCs) through Notch signaling. *Oncotarget* 8: 53581–53601, 2017. doi:10.18632/oncotarget.18655.

343. **Wu J**, **Zhao J**, **Sun L**, **Pan Y**, **Wang H**, **Zhang WB.** Long non-coding RNA H19 mediates mechanical tension-induced osteogenesis of bone marrow mesenchymal stem cells via FAK by sponging miR-138. *Bone* 108: 62–70, 2018. doi:10.1016/j.bone.2017.12.013.
344. **Huang G**, **Kang Y**, **Huang Z**, **Zhang Z**, **Meng F**, **Chen W**, **Fu M**, **Liao W**, **Zhang Z.** Identification and characterization of long non-coding RNAs in osteogenic differentiation of human adipose-derived stem cells. *Cell Physiol Biochem* 42: 1037–1050, 2017. doi:10.1159/000478751.
345. **Xiaoling G**, **Shuaibin L**, **Kailu L.** MicroRNA-19b-3p promotes cell proliferation and osteogenic differentiation of BMSCs by interacting with lncRNA H19. *BMC Med Genet* 21: 11, 2020. doi:10.1186/s12881-020-0948-y.
346. **Nardocci G**, **Carrasco ME**, **Acevedo E**, **Hodar C**, **Meneses C**, **Montecino M.** Identification of a novel long noncoding RNA that promotes osteoblast differentiation. *J Cell Biochem* 119: 7657–7666, 2018. doi:10.1002/jcb.27113.
347. **Zheng S**, **Wang YB**, **Yang YL**, **Chen BP**, **Wang CX**, **Li RH**, **Huang D.** LncRNA MALAT1 inhibits osteogenic differentiation of mesenchymal stem cells in osteoporosis rats through MAPK signaling pathway. *Eur Rev Med Pharmacol Sci* 23: 4609–4617, 2019. doi:10.26355/eurrev_201906_18038.
348. **Chen Q**, **Wang M**, **Wu S.** The lncRNA MCF2L-AS1 controls osteogenic differentiation by regulating miR-33a. *Cell Cycle* 19: 1059–1065, 2020. doi:10.1080/15384101.2020.1747776.
349. **Jin C**, **Zheng Y**, **Huang Y**, **Liu Y**, **Jia L**, **Zhou Y.** Long non-coding RNA MIAT knockdown promotes osteogenic differentiation of human adipose derived stem cells. *Cell Biol Int* 41: 33–41, 2017. doi:10.1002/cbin.10697.
350. **Cui Y**, **Lu S**, **Tan H**, **Li J**, **Zhu M**, **Xu Y.** Silencing of long non-coding RNA NONHSAT009968 ameliorates the staphylococcal protein A-inhibited osteogenic differentiation in human bone mesenchymal stem cells. *Cell Physiol Biochem* 39: 1347–1359, 2016. doi:10.1159/000447839.
351. **Zhang W**, **Dong R**, **Diao S**, **Du J**, **Fan Z**, **Wang F.** Differential long noncoding RNA/mRNA expression profiling and functional network analysis during osteogenic differentiation of human bone marrow mesenchymal stem cells. *Stem Cell Res Ther* 8: 30, 2017. doi:10.1186/s13287-017-0485-6.
352. **Nuermaimaiti N**, **Liu J**, **Liang X**, **Jiao Y**, **Zhang D**, **Liu L**, **Meng X**, **Guan Y.** Effect of lncRNA HOXA11-AS1 on adipocyte differentiation in human adipose-derived stem cells. *Biochem Biophys Res Commun* 495: 1878–1884, 2018. doi:10.1016/j.bbrc.2017.12.006.
353. **Li S**, **Mi L**, **Yu L**, **Yu Q**, **Liu T**, **Wang GX**, **Zhao XY**, **Wu J**, **Lin JD.** Zbtb7b engages the long noncoding RNA Blnc1 to drive brown and beige fat development and thermogenesis. *Proc Natl Acad Sci USA* 114: E7111–E7120, 2017. doi:10.1073/pnas.1703494114.
354. **Cao Z**, **Huang S**, **Li J**, **Bai Y**, **Dou C**, **Liu C**, **Kang F**, **Gong X**, **Ding H**, **Hou T**, **Dong S.** Long noncoding RNA expression profiles in chondrogenic and hypertrophic differentiation of mouse mesenchymal stem cells. *Funct Integr Genomics* 17: 739–749, 2017. doi:10.1007/s10142-017-0569-5.

12.3 Aprobación de Comité de Ética en Investigación

SALUD
SECRETARÍA DE SALUD

Instituto Nacional de Medicina Genómica
MÉXICO

"2013, Año de la Lealtad Institucional y Centenario del Ejército Mexicano"

EL COMITÉ DE ÉTICA EN INVESTIGACIÓN DEL INSTITUTO NACIONAL DE MEDICINA GENÓMICA,

Con fundamento en lo dispuesto por los artículos 41 Bis, 98 y 100 de la Ley General de Salud; 14 fracción VII, 98-112 del Reglamento de la Ley General de Salud en materia de Investigación para la Salud; 37 del Estatuto Orgánico del INMEGEN y de conformidad a su propio Manual de Funcionamiento, emite el presente dictamen:

Título del Proyecto:	**ANÁLISIS GENÓMICO DE LA INTERACCIÓN ENTRE CÉLULAS TRONCALES DE TEJIDO ADIPOSO ADSC Y CÉLULAS TUMORALES**
Dirigido al Investigador Responsable:	**DRA. VILMA MALDONADO LAGUNAS**
Objetivo del Proyecto:	Analizar los cambios de expresión génica (RNA codifcante y miRNAS) y metilación del ADN que provocan los co-cultivos de células ADSC y células de cáncer.
No. de Documento:	**CEI 2013/09**
Fecha de elaboración del documento:	**6 de septiembre de 2013**
Tipo de Documento:	**Dictamen Aprobatorio**

CONSIDERACIONES DE LOS INTEGRANTES DEL COMITÉ DE ÉTICA EN INVESTIGACIÓN (CEI)

Con fecha 6 de junio de 2013, el CEI-INMEGEN emitió un dictamen con algunas recomendaciones al proyecto de referencia. Mediante documento de fecha 29 de julio del mismo año, el Investigador Responsable dio respuesta formal al CEI en la que señala los cambios que hizo al proyecto de investigación tomando en consideración las recomendaciones señaladas.

Por lo antes expuesto, el CEI-INMEGEN emite el presente **Dictamen Aprobatorio**, el cual tendrá validez de un año a partir de la fecha en que es entregado al Investigador responsable, debiéndose solicitar una prorroga un mes antes de su vencimiento. El CEI-INMEGEN se reserva el derecho de hacer revisiones periódicas cuando así lo estime pertinente, para salvaguardar los derechos de los participantes.

Atentamente,

PRESIDENTE DEL COMITÉ DE ÉTICA EN INVESTIGACIÓN DEL INMEGEN

Mtra. Garbiñe Saruwatari Zavala

C.c.p.: Dra. Alessandra Carnevale Cantoni - Secretaria Ejecutiva del Comité de Investigación del INMEGEN. Presente.

Periférico Sur No. 4809, Col. Arenal Tepepan, Delegación Tlalpan, México, D.F., C.P. 14610
Tel.: 52 (55) 5350 1900, Fax: 52 (55) 5350 1950 www.inmegen.gob.mx

12.4 Oligonucleótidos para el análisis de expresión por RT-qPCR

Molécula	Secuencia 5’-3’	Amplicón (pb)
BIRC3	TCTCCATCAAATCCTGTA AAC TCC	201
	GGCAAAGCA AGCCACTCT	
CXCL10	AGTGGATGTTCTGACCCTGCTTCA	191
	CCCCTTGGGAGGATGGCAGT	
CXCL3	CGCCCAAACCGAAGTCATAG	109
	GCTCCCCTTGTTCAGTATCTTTT	
CXCL5	AAGAAGCTAGAA AACAGGCAAA	202
	TCC AAG GAG AAA TGC TAG GG	
CXCL2	CATCGAAAAGATGCTGAAAAATG	77
	TTCAGGAACAGCCACCAATA	
lnc-BIRC3	ATT TCCACAAATATATGCCTTG	112
	TCC AGC TAC TCA GGA GAC T	
lnc-CXCL3	CTGGTTTGGGCACTTTGG	164
	ACACAACCCTATGAAATAACTACC	
LINC01569	AACATCCTCCTTCACCTTGA	100
	AAGTATTAGGCTTGTCCTGTGT	
RP11-138I17.1	TTATCAAGTCAAGCCCAGTCA	163
	GGAGATTCAGACCTATGCCC	
LINC00707	CAGGTGGATAAGACTAACACTGAA	179
	ATGGAGTAGAGGCGGGATTT	
CTC-231º11.1	GGGTGTGTTCTCTGGGTTG	153
	CGATCTCTGGTGTCGGTTG	

12.5 Diseño y análisis predictivo de sh-lnc-CXCL3

Molécula	Secuencia blanco (5´-3´)	Identidad	E Value	% de Eficiencia
sh-lncCXCL3-1	CGTTTACCTCAGTCCCTAA	100%	0.045	91.1
Sh-lncCXCL3-2	GGGAGATCATGAATGGACA	100%	0.045	77.61

12.6 Vía NFkappaB

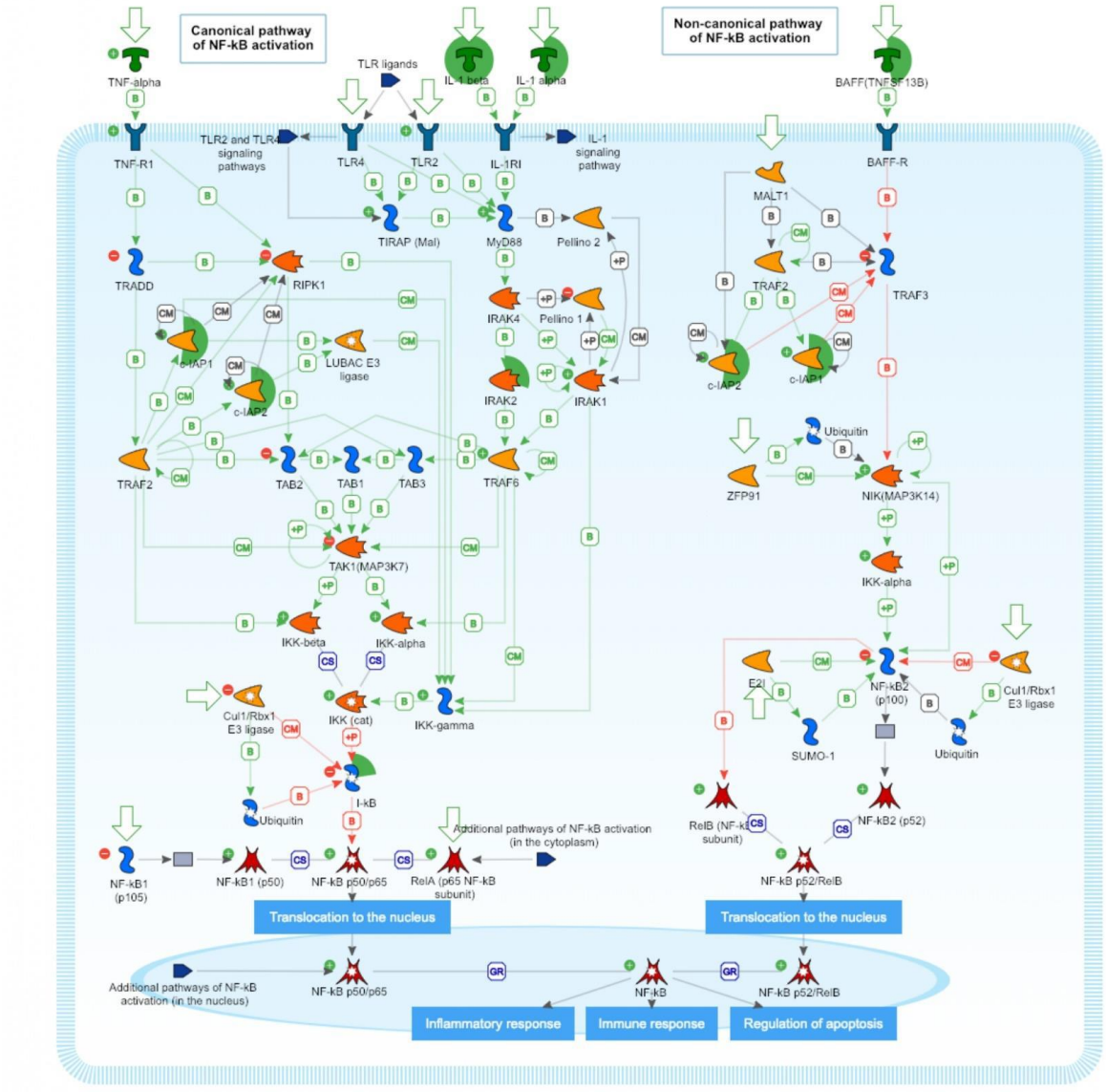

12.7 Vía de IL-6

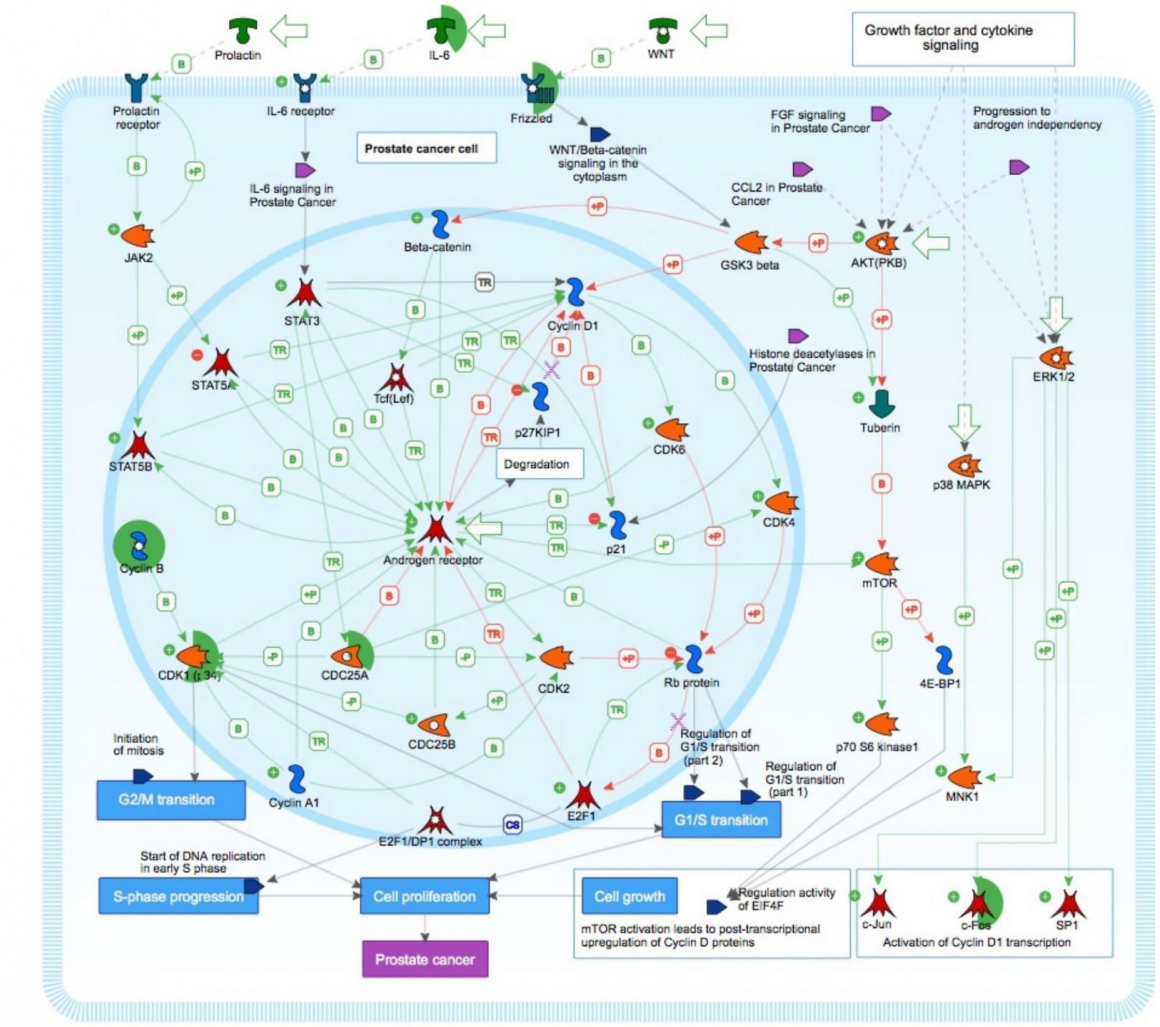

12.8 Vía ILs y AP-1

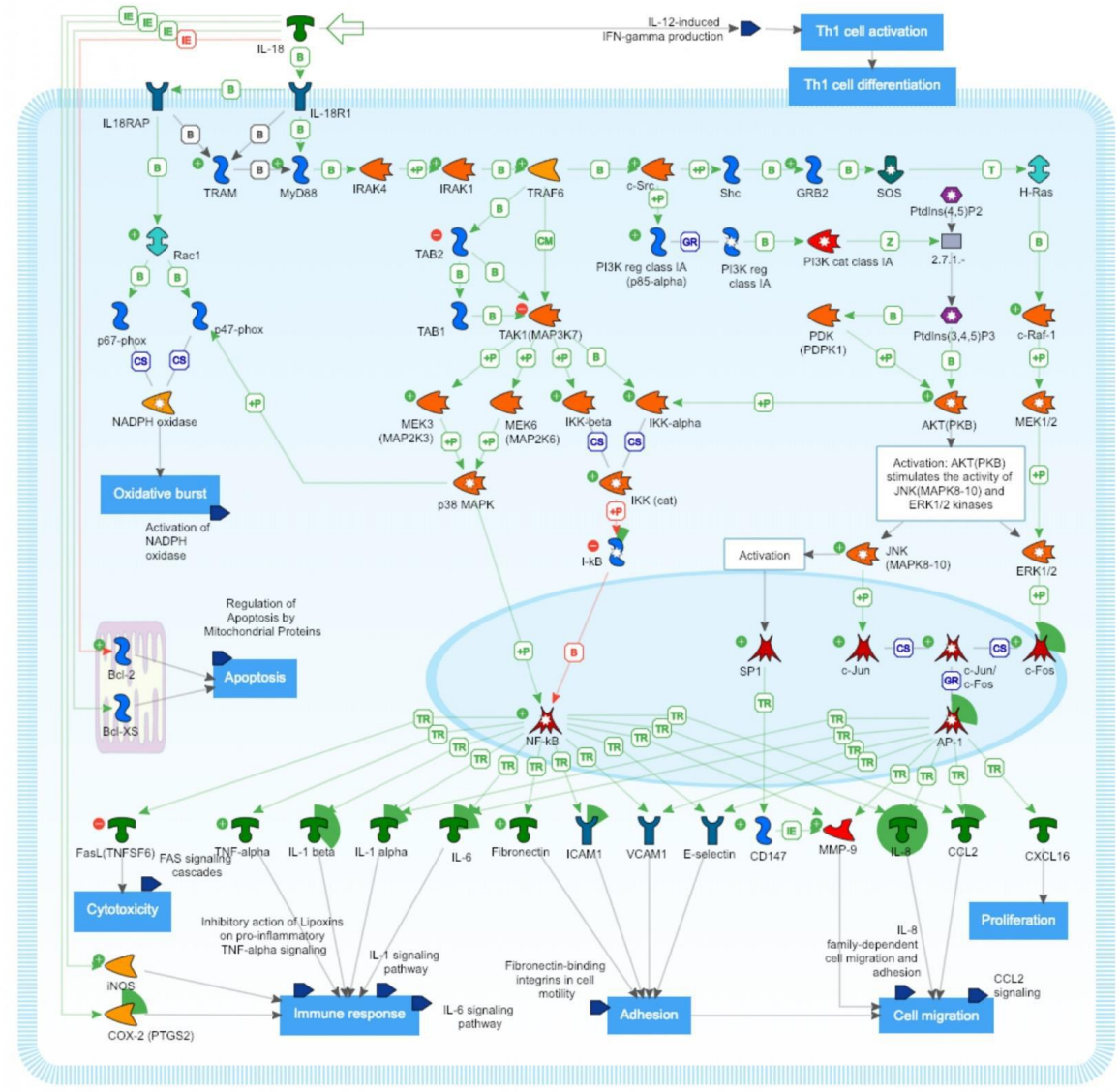

12.9 Vía STAT1

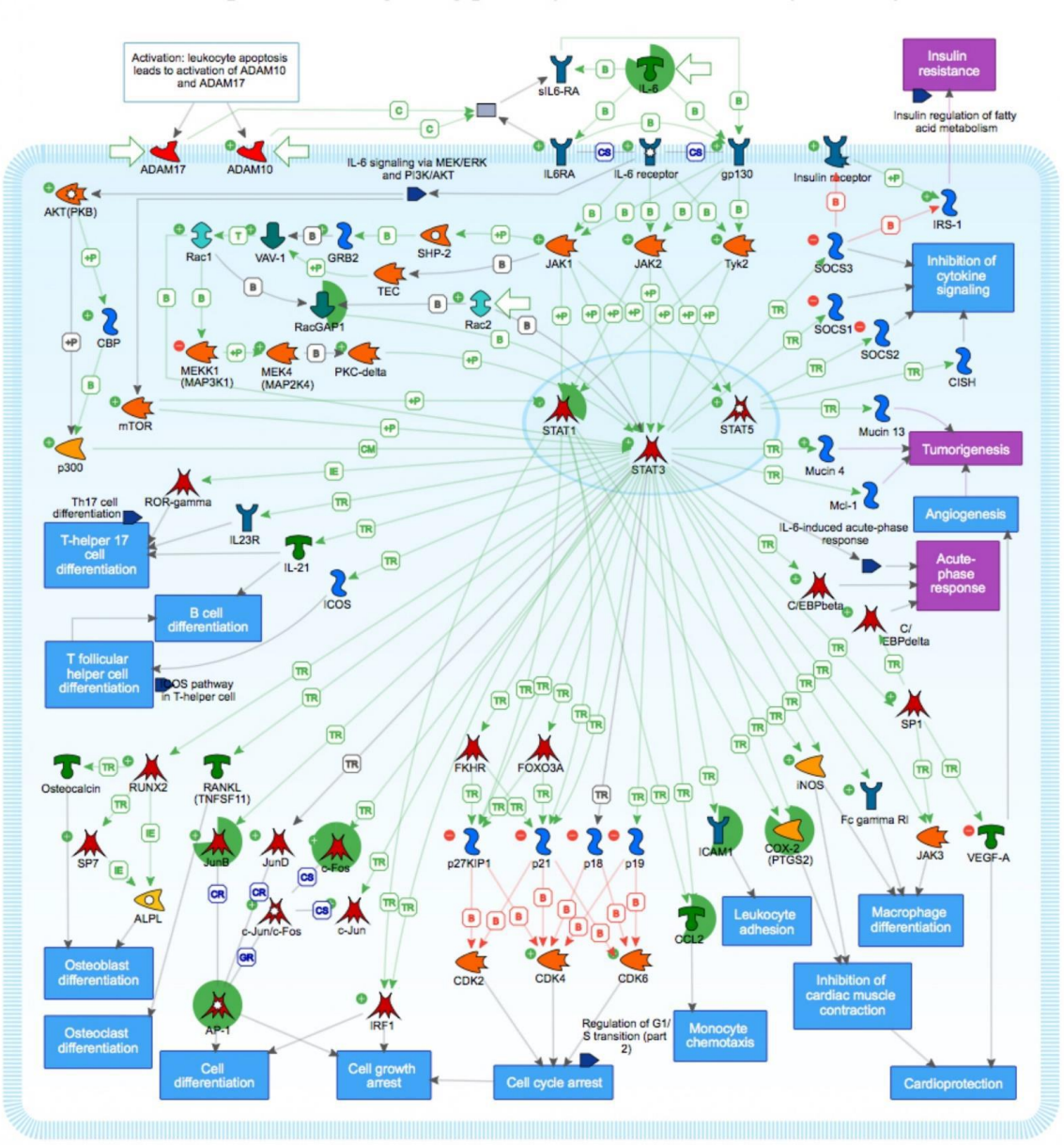

12.10 Vía CDK1

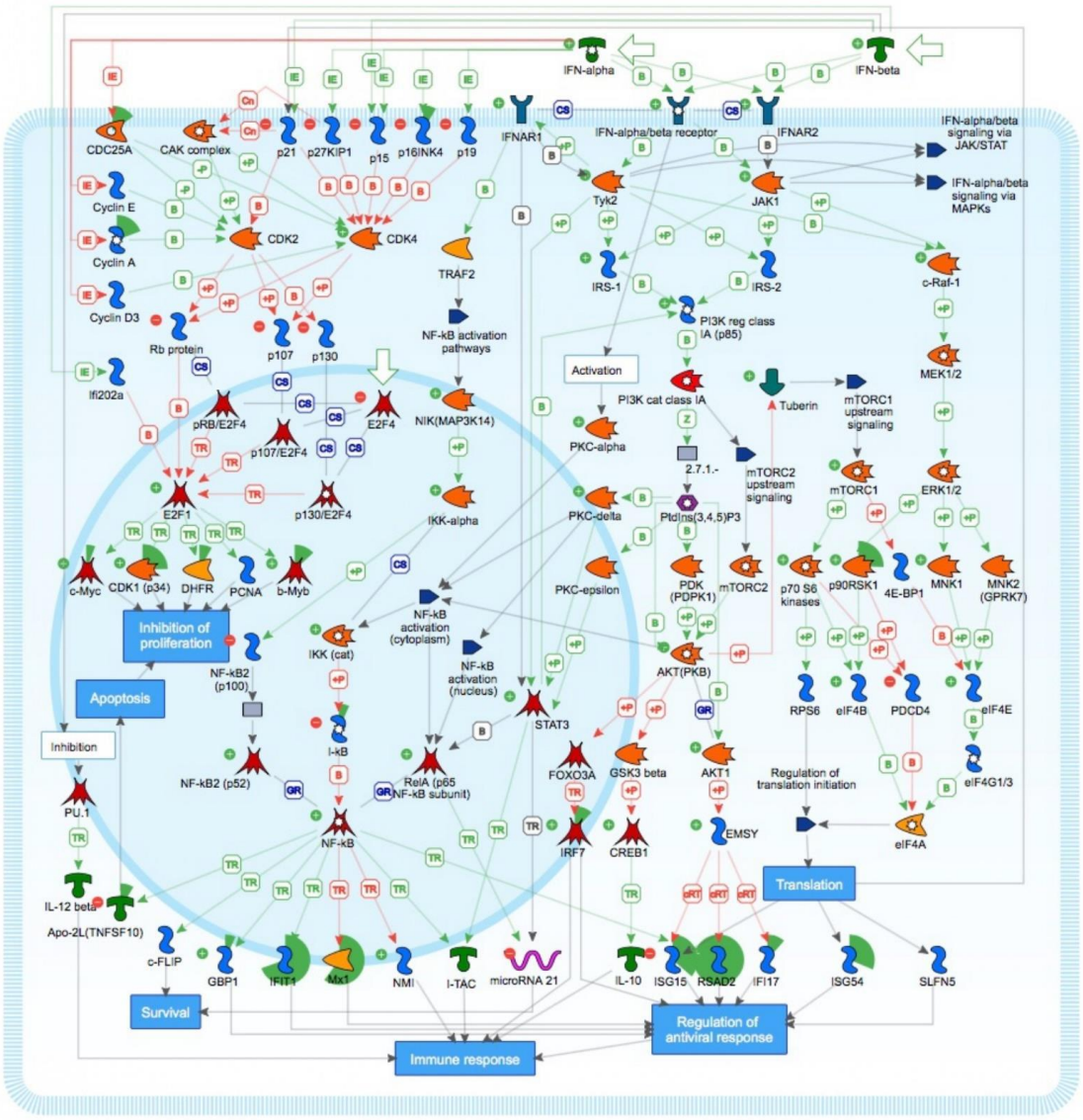

12.11 Vía IL-8

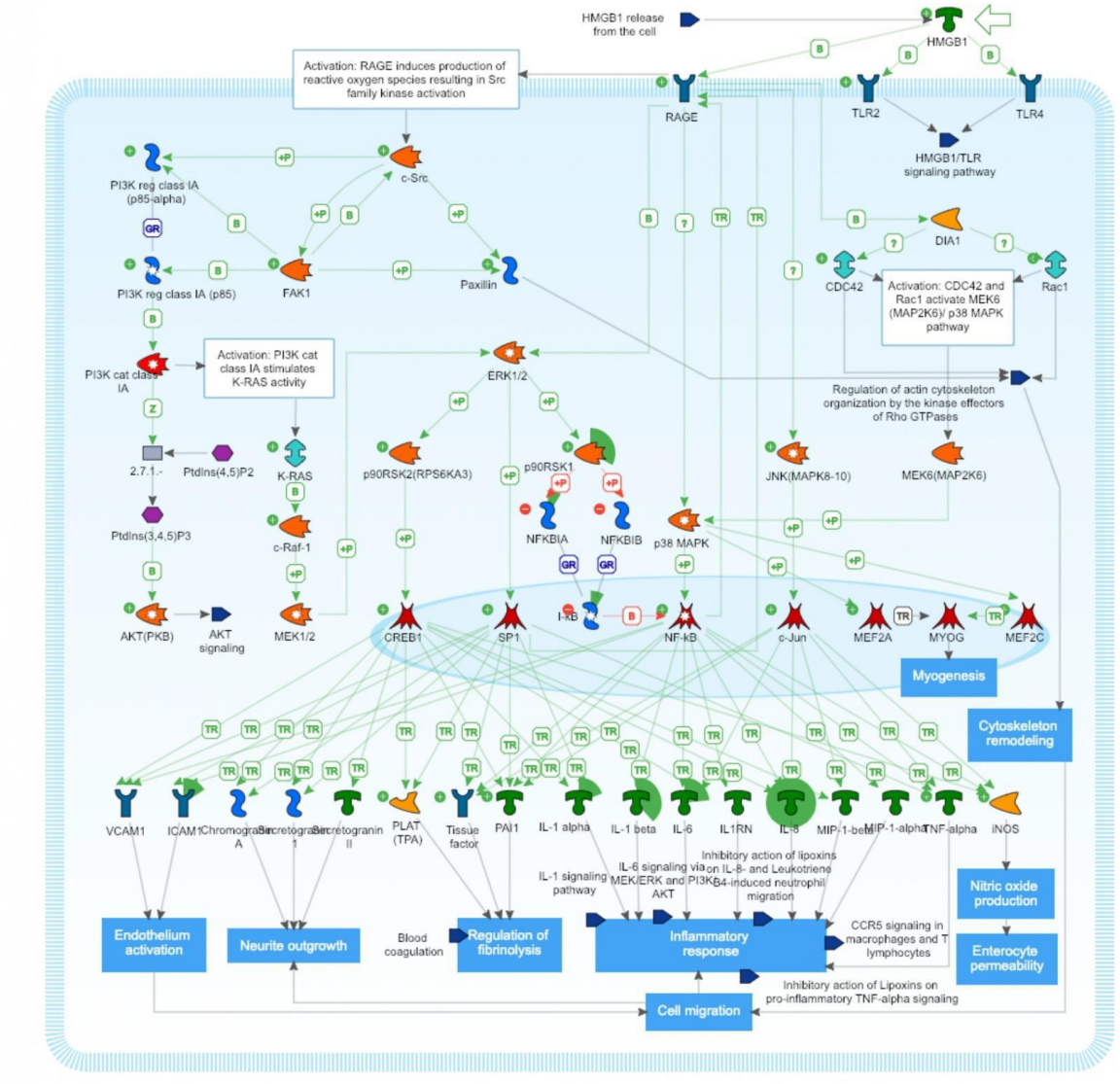
HMGB1 release from the cell
HMGB1
Activation: RAGE induces production of reactive oxygen species resulting in Src family kinase activation
RAGE
TLR2
TLR4
HMGB1/TLR signaling pathway
PI3K reg class IA (p85-alpha)
c-Src
PI3K reg class IA (p85)
FAK1
Paxillin
DIA1
CDC42
Rac1
Activation: CDC42 and Rac1 activate MEK6 (MAP2K6)/ p38 MAPK pathway
PI3K cat class IA
Activation: PI3K cat class IA stimulates K-RAS activity
ERK1/2
Regulation of actin cytoskeleton organization by the kinase effectors of Rho GTPases
2.7.1.-
PtdIns(4,5)P2
K-RAS
p90RSK2(RPS6KA3)
p90RSK1
JNK(MAPK8-10)
MEK6(MAP2K6)
PtdIns(3,4,5)P3
c-Raf-1
NFKBIA
NFKBIB
p38 MAPK
AKT(PKB)
AKT signaling
MEK1/2
CREB1
SP1
I-KB
NF-kB
c-Jun
MEF2A
MYOG
MEF2C
Myogenesis
Cytoskeleton remodeling
VCAM1
ICAM1
Chromogranin A
Secretogranin I
Secretogranin II
PLAT (TPA)
Tissue factor
PAI1
IL-1 alpha
IL-1 beta
IL-6
IL1RN
IL-8
MIP-1-beta
MIP-1-alpha
TNF-alpha
iNOS
IL-1 signaling pathway
IL-6 signaling via MEK/ERK and PI3K/AKT
Inhibitory action of lipoxins on IL-8- and Leukotriene B4-induced neutrophil migration
Nitric oxide production
Endothelium activation
Neurite outgrowth
Blood coagulation
Regulation of fibrinolysis
Inflammatory response
CCR5 signaling in macrophages and T lymphocytes
Enterocyte permeability
Inhibitory action of Lipoxins on pro-inflammatory TNF-alpha signaling
Cell migration